Advances
in Clinical and Experimental Medicine

WROCLAW
MEDICAL UNIVERSITY

Advances
in Clinical and Experimental Medicine

Editorial Policy

Advances in Clinical and Experimental Medicine (Adv Clin Exp Med) is an independent multidisciplinary forum for exchange of scientific and clinical information, publishing original research and news encompassing all aspects of medicine, including molecular biology, biochemistry, genetics, biotechnology and other areas. During the review process, the Editorial Board conforms to the "Uniform Requirements for Manuscripts Submitted to Biomedical Journals: Writing and Editing for Biomedical Publication" approved by the International Committee of Medical Journal Editors (www.ICMJE.org). The journal publishes (in English only) original papers and reviews. Short works considered original, novel and significant are given priority. Experimental studies must include a statement that the experimental protocol and informed consent procedure were in compliance with the Helsinki Convention and were approved by an ethics committee.

Contents

Research letters

Translational biomedicine-oriented exploratory research on bioactive rotifer-specific biopolymers

Zsolt Datki[1,A,B,D,F], Rita Sinka[2,A,C–E]

[1] Micro-In Vivo Research Laboratory, Interdisciplinary Research, Development and Innovation Centre of Excellence, University of Szeged, Hungary

[2] Department of Genetics, Faculty of Science and Informatics, University of Szeged, Hungary

A – research concept and design; B – collection and/or assembly of data; C – data analysis and interpretation;
D – writing the article; E – critical revision of the article; F – final approval of the article

Address for correspondence
Zsolt Datki
E-mail: datki.zsolt.laszlo@szte.hu

Abstract

There are numerous surprising discoveries in current comprehensive biopolymer research, including the description of new types of biopolymers and the extension of their applications. The discovery of a new rotifer-specific biopolymer family (Rotimers) and the exceptional ability of these micrometazoans to inactivate and catabolize human-type neurotoxic aggregates (e.g., beta-amyloids, alpha-synucleins, prions) by their exudates can be mentioned as the original work of our research group. Rotimers are exogenous and protein complex molecules with a calcium-dependent production mechanism in both bdelloid and monogonant rotifers. However, their experimental and application possibilities are still unknown; only part of the class has been explored and described. Current Rotimer-related studies present promising biodiversity and bioactivity of these biomaterials (e.g., anti- and disaggregation effects or high degrees of adhesion to other molecules). The primary objective of current research is to explore and develop their application in translational biomedicine. A key area is the design of drug candidates against neurodegeneration-related aggregates based on the molecular information provided by the composition, structure and function of Rotimers. These novel biomaterials have the potential to open new perspectives in the pharmaceutical industry and healthcare.

Key words: biopolymer, rotifer, exudate, Rotimer, biomedicine

Biopolymers as molecules of the future

Biopolymers, as organic substances that occur in large numbers and completely degrade in nature, can be applied in several disciplines, from food technologies to conservation procedures, drug carrier-related pharmacology, and in the development of different nanoparticles (e.g., in translational biomedicine).[1] Living organisms produce biopolymers from specific molecular units that can be classified based on their chemical composition, such as polymerized forms of nucleotides, saccharides and peptides, or their complexes.[2] In many cases, stabilizing metal ions, such as magnesium or calcium, are required to form the structure of polymers.[3] These biomolecules (e.g., spider silk, collagen, cellulose, chitosan, albumin, casein) have been studied in various ways, making their extended use unquestionable.[4] However, their molecular properties can vary depending on how the organisms that produce them have changed and adapted to the environment. These agents of biological origin are used in the pharmaceutical and energy industries, as well as in the natural environment.[5] The living organisms involved in biological secretion processes depend on their endemic microenvironment, which has a regulatory role in production of the agents.[6,7] According to the generally accepted theory of evolution, the origin of life is connected with water; thus, the first biopolymer molecules were produced by species living in ancient seas, such as snails, sea urchins and ammonites.[8] The abovementioned biocomposites were soft or hard (or complexes of soft and hard ones), with different protective functions for proto- and metazoa from chemical, ultraviolet and thermal influences.[9] Due to the diversity of natural habitats (e.g., oceans, lakes, rivers, streams, thermal springs, puddles, etc.), microscopic organisms have developed multifunctional biopolymers with properties such as energy and food sources, metabolism and structural constituents, and cell and tissue regeneration functions in the relevant organisms or their environment.[10] These macromolecules exist inside and outside the cells, such as in the extracellular space, cell wall, exoskeleton, or external secretions in soil and water.[1] Natural (ecological) and artificial (laboratorial) niches are extremely sensitive to physicochemical and biological parameters.[11] The formation and production of these species-specific substances can be influenced by several environmental factors, from light intensity to osmolarity, temperature, redox state, and even from dissolved gases to the presence of prey and predators.[12] The increasing utilization of natural materials, such as adapting biodegradable and renewable products, is an essential consideration in the industrial and pharmaceutical sectors, especially due to its environment-friendly approach.[13]

Human-related exceptional properties of rotifers

In several cases of scientific research, one can gain information on specific substances (e.g., organic molecules) from unexpected natural sources (e.g., plants like wheat, soybean, corn, sorghum, rubber trees; animals like sea anemones, shellfish, spiders), with possible retrospective human applications, such as in different forms of medicine.[14,15] The focus has thus shifted from micrometazoans to rotifers, a less explored and studied scientific world. These smallest animals in the world (i.e., eutelic organisms) have been long accepted models for aging, longevity and pharmaceutical studies, or relevant indicators of drug and toxic substances screening, and have even been used in space exploration.[16,17] Due to the widely used omics technologies (genomics, transcriptomics, proteomics, glycomics, and lipidomics), a new alternative model could be employed in basic research and biomedicine; therefore, these phylogenetically ancient rotifers have not yet been investigated in the context of biopolymer production and application of these products.[18] These microscopic organisms are multicellular animals that make up a significant portion of biomass globally.[19] Both bdelloid and monogonant types are found in saltwater environments as well as in freshwater ones.[20] Although their body consists of only approx. 1000 cells, they have independent and complex organs, such as reproductive, digestive and secretory units; moreover, they exhibit extreme resistance to radiation doses and cryptobiosis. In addition to the abovementioned potential, these animals are ideal and promising model systems of special metabolic pathways, thematically connected to human-type neurodegeneration.[21] Rotifer-related research (Fig. 1) presents the interdisciplinary processes in this theme. Our research team was the first to describe a unique and exceptional natural phenomenon, namely the ability of these animal models (e.g., *Philodina acuticornis* or *Adineta vaga*) to degrade and catabolize neurotoxic aggregated peptides/proteins (e.g., beta-amyloids, E46K alpha-synuclein, cellular and scrapie prion proteins), applying it as an exclusive source of material and energy. These Alzheimer's disease-, Parkinson's disease- and prion disease-related human-type toxins were consumed as food and served as special regulating factors to rotifers.[22,23] The tested toxic aggregates did not have the expected and described pathological effects on animals; on the contrary, they increased the lifespan of the treated (i.e., "fed") entities. As opposed to the above, the peptides/proteins proved to be toxic in the viability tests measured on tardigrades and nematodes. Considering the unconventional catabolic ability of rotifers (presumably an evolutionarily evolving property to break down natural debris), the question arises: By what kind of biochemical mechanism can these simple creatures execute the molecular processes described above? This inactivating phenomenon against
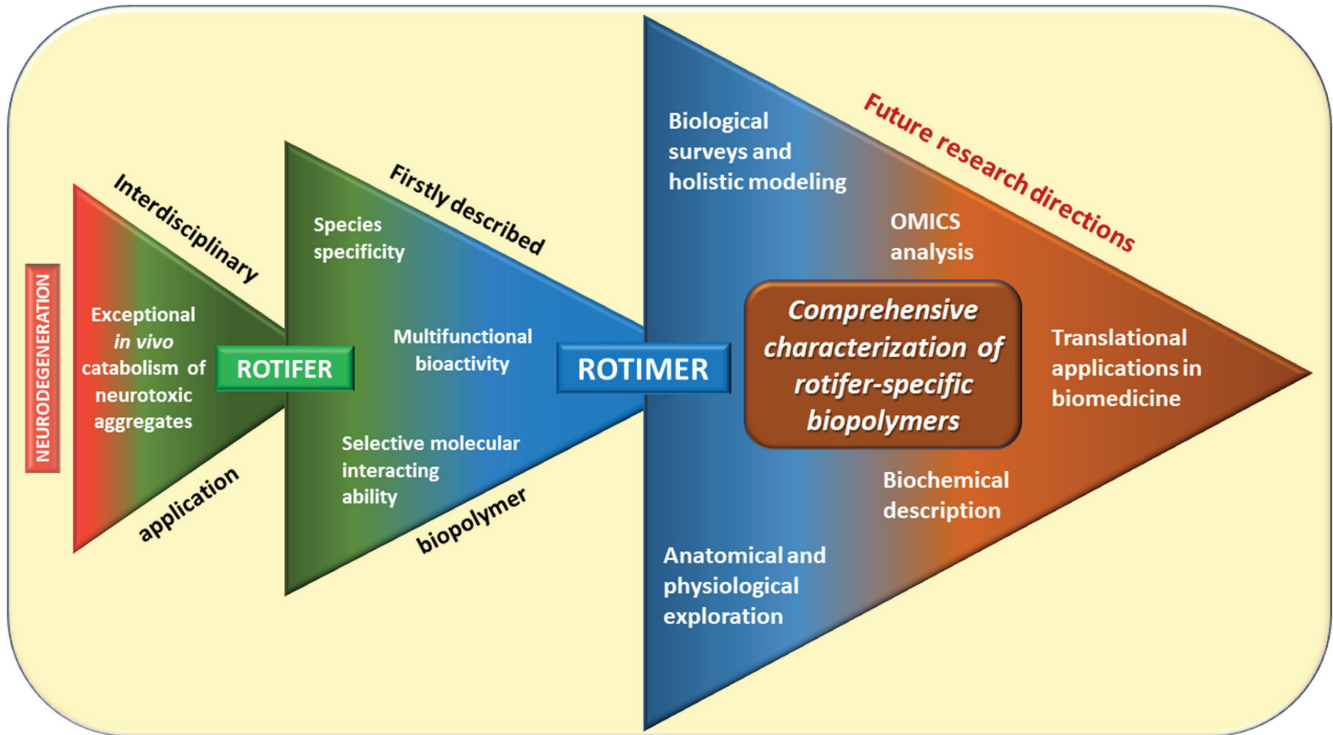
Fig. 1. Exploratory research on newly discovered bioactive Rotimers

notorious neurotoxic aggregates is also remarkable because researchers have not found a solution for neutralizing and degrading these "hard" materials under physiological conditions for several decades. Although rotifers and their species-specific exudates do not directly interact with neurotoxic aggregates in nature, an interaction with specific mechanisms can develop between them under artificial conditions. The autocatabolism–attenuator effect of beta-amyloids in these animals also demonstrates such a case.[24] A similar interdisciplinary regulatory interaction is the effect of kynurenic acid on the metabolism of rotifers.[25] Several studies have proven that this ancient molecule alone prominently and adequately represents the multifunctionality occurring in nature or specific effects on the nervous system.[26–28] However, the relevance between micrometazoa and human studies can only be applied and interpreted to a certain extent. In the innovative

intersection of seemingly independent scientific fields, including the topic of biopolymer research, interdisciplinary extensions have no limits, reaching out to physiology of aging or mental phenomena.[29–31]

The Rotimer family and recently discovered biopolymers

While studying the exceptional ability of rotifers and the abovementioned catabolic mechanism, a special exogenous secretion with relatively high tensile strength was observed in several species. The fact that rotifers can secrete filamentous and glue- or film-type bioproducts (Fig. 2) following particle-related mechanical stimulation has recently been discovered and described in the academic literature.[32] These rotifer-specific bioactive

Rotimer characteristics				Rotifers			
				Bdelloids		Monogonants	
				Philodina acuticornis	*Adineta vaga*	*Euchlanis dilatata*	*Lecane bulla*
Conglomerate form	Fibrillar	Floating	Thin	+	+	+	+
			Thick	+	+	+	+
		Fixed	Simple	?	+	+	?
			Double	?	+	+	?
	Amorphous		Gluelike	?	+	+	+
			Film-coated	+	+	?	?
Type	Proteinous		Proteaze-sensitive	+	+	+	+
Function	Bioactivity		*In vitro* (antiaggregation)	?	?	+	+
			In vivo (immobilization)	?	?	+	+

Fig. 2. Species-specific characterizations of Rotimers (+ – known; ? – unknown)
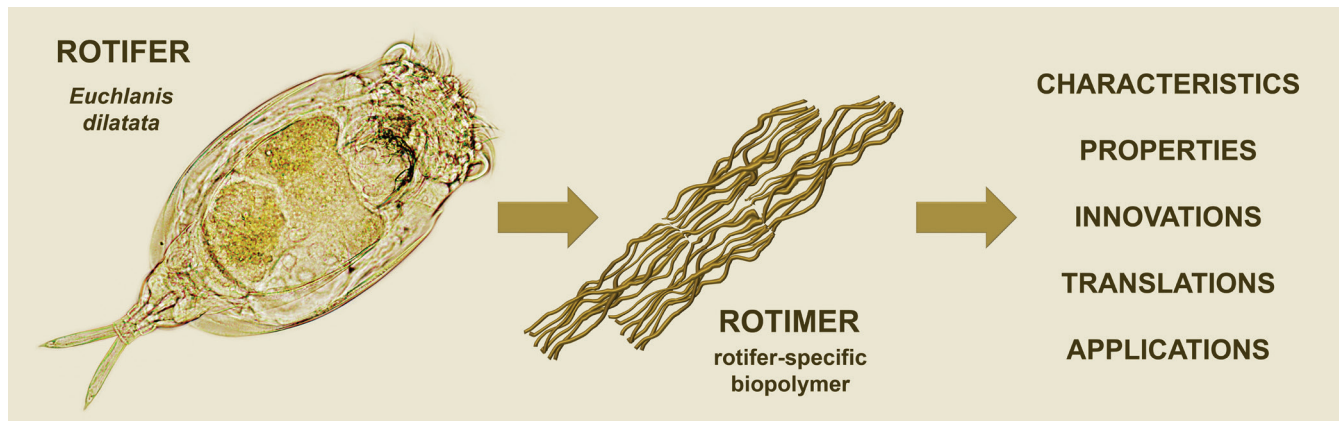
Fig. 3. The Rotifer–Rotimer system and concept

biopolymers, named Rotimers, are multifunctional molecules of these micrometazoans (Fig. 3) that are located inside and outside their bodies. From capturing particle-based food to plucking rotifer eggs (adhesive nature) and cleaning the relevant medium (antiseptic and filtration effect), these tiny creatures use their exogenic exudates in nature. It is known that numerous protozoa, plant and animal species produce polymers, similarly to rotifers. The composition, structure and molecular nature of this novel bioproduct have not yet been explored. Due to its novelty, a complex molecular family of Rotimers potentially holds several yet unknown advantageous properties. However, preliminary measurements have revealed their diverse and promising bioactivity (e.g., inhibition of cancer neuroblastoma cell proliferation and migration, high intercalation and absorption capacity, partial disinfection ability, anti- and disaggregating effects on beta-amyloid aggregates). The induction of Rotimer secretion, both under natural and laboratory conditions, can only be triggered by mechanical irritation of the cilia using different types (e.g., microcrystalline cellulose, urea or carmine crystals, sand, epoxy beads) and sizes (approx. 2–50 μm in diameter) of inert particles as inducers. The external formation of this newly discovered adhesive and protease-sensitive molecule is a calcium-dependent process that can only be observed using optical microscopy when biopolymers and particles form a Rotimer–Inductor Conglomerate (RIC) complex in a random web form. The production of entities and populations by RIC depends on their viability, energy level, and chemical (e.g., toxic agents, osmolarity, pH) and environmental (e.g., temperature) effects. By examining the RIC isolates of several rotifer species, it was found that this conglomerate is resistant to various chemical effects (e.g., detergents, acids, bases, chelators) and has cell immobilization bioactivity with low toxicity.[20] The holistic biological evidence and molecular composition/structure of this protein-type natural biopolymer are unexplored in detail but generally predictable. The use of Rotimers leads to new approaches in biotechnology, pharmaceutical research and biomedicine (e.g., dermatology, neurology).

Possibilities offered by Rotimers in biomedicine

Based on the observation that many freshwater rotifer species can produce different Rotimers, it can be assumed that this biomaterial, a type of biopolymer, is phylogenetically formed and evolutionarily ancient (presumably more than 0.5 billion years old). This proteinous multifunctional macromolecule may be a key component of the abovementioned catabolic and neurotoxic aggregate inactivation capacity.[33] Therefore, the aim of future research is to fully understand the different groups and types of Rotimers, and explore their molecular structure and possible translational and multifunctional applications. The related novel and interdisciplinary methodologies, the phenomenon of catabolism of aggregated proteins, the existence of Rotimers, and their pilot characterization were recently introduced. The research timeline and work on rotifers and their secretions have reached a stage from which forward movement can only happen after gaining knowledge on specific, holistic and molecular endpoints. Investigating the full range and potential applicability of Rotimer biomolecules can shed light on their species specificity, molecular composition and structure, and possible use as active substances. Moreover, these natural products can serve as a good starting point for amassing information about their artificial molecular design and medical applications. The full characterization of this new family of biopolymers provides an exceptional opportunity to launch new projects and to develop further application areas on countless lines. Based on the currently available data, it may be applied indirectly in chemistry (e.g., as a drug carrier) or externally in medicine (e.g., on the skin surface). These special Rotimer exudates are promising new biopolymers that may serve as raw materials for industrial production and more advanced applications, such as developing drug candidates in pharmacological research or translational medicine (e.g., regenerating tissue matrix or even as carriers of active substances).

ORCID iDs

Zsolt Datki https://orcid.org/0000-0002-2537-4741
Rita Sinka https://orcid.org/0000-0003-4040-4184

References

1. Baranwal J, Barse B, Fais A, Delogu GL, Kumar A. Biopolymer: A sustainable material for food and medical applications. *Polymers (Basel)*. 2022;14(5):983. doi:10.3390/polym14050983
2. Mohan S, Oluwafemi OS, Kalarikkal N, Thomas S, Songca SP. Biopolymers: Application in nanoscience and nanotechnology. In: Parveen FK, ed. *Recent Advances in Biopolymers*. London, UK: InTech; 2016. doi:10.5772/62225
3. Reddy N, Reddy R, Jiang Q. Crosslinking biopolymers for biomedical applications. *Trends Biotechnol*. 2015;33(6):362–369. doi:10.1016/j.tibtech.2015.03.008
4. Niaounakis M. Definitions of terms and types of biopolymers. In: *Biopolymers: Applications and Trends*. Amsterdam, the Netherlands: Elsevier; 2015:1–90. doi:10.1016/B978-0-323-35399-1.00001-6
5. Yavuz B, Chambre L, Kaplan DL. Extended release formulations using silk proteins for controlled delivery of therapeutics. *Expert Opin Drug Deliv*. 2019;16(7):741–756. doi:10.1080/17425247.2019.1635116
6. Wu CZ, Hsieh CH, Lu CH, Pei D, Chen JS, Chen YL. First-phase insulin secretion is positively correlated with alanine aminotransferase in young adults. *Adv Clin Exp Med*. 2021;30(1):35–40. doi:10.17219/acem/128229
7. Shamsuddin IM, Sani N, Adamu M, Abubakar M. Biodegradable polymers for sustainable environmental and economic development. *MOJ Biorg Org Chem*. 2018;2(4):192–194. doi:10.15406/mojboc.2018.02.00080
8. Frenkel-Pinter M, Rajaei V, Glass JB, Hud NV, Williams LD. Water and life: The medium is the message. *J Mol Evol*. 2021;89(1–2):2–11. doi:10.1007/s00239-020-09978-6
9. Ehrlich H. *Marine Biological Materials of Invertebrate Origin*. Cham, Switzerland: Springer International Publishing; 2019. doi:10.1007/978-3-319-92483-0
10. Yadav P, Yadav H, Shah VG, Shah G, Dhaka G. Biomedical biopolymers, their origin and evolution in biomedical sciences: A systematic review. *J Clin Diagn Res*. 2015;9(9):ZE21–ZE25. doi:10.7860/JCDR/2015/13907.6565
11. Balazs E, Galik-Olah Z, Galik B, Somogyvari F, Kalman J, Datki Z. External modulation of Rotimer exudate secretion in monogonant rotifers. *Ecotoxicol Environ Saf*. 2021;220:112399. doi:10.1016/j.ecoenv.2021.112399
12. Olatunji O. *Aquatic Biopolymers: Understanding Their Industrial Significance and Environmental Implications*. Cham, Switzerland: Springer International Publishing; 2020. doi:10.1007/978-3-030-34709-3
13. Lalit R, Mayank P, Ankur K. Natural fibers and biopolymers characterization: A future potential composite material. *J Mech Eng*. 2018;68(1):33–50. doi:10.2478/scjme-2018-0004
14. Sun XS. Overview of plant polymers: Resources, demands, and sustainability. In: Ebnesajjad S, ed. *Handbook of Biopolymers and Biodegradable Plastics*. Oxford, UK: Elsevier; 2013:1–10. doi:10.1016/B978-1-4557-2834-3.00001-X
15. Wankhade V. Animal-derived biopolymers in food and biomedical technology. In: Pal K, Banerjee I, Sarkar P, et al., eds. *Biopolymer-Based Formulations*. Oxford, UK: Elsevier; 2020:139–152. doi:10.1016/B978-0-12-816897-4.00006-0
16. Olah Z, Bush AI, Aleksza D, et al. Novel in vivo experimental viability assays with high sensitivity and throughput capacity using a bdelloid rotifer. *Ecotoxicol Environ Saf*. 2017;144:115–122. doi:10.1016/j.ecoenv.2017.06.005
17. Macsai L, Olah Z, Bush AI, et al. Redox modulating factors affect longevity regulation in rotifers. *J Gerontol A Biol Sci Med Sci*. 2019;74(6):811–814. doi:10.1093/gerona/gly193
18. Snell TW, Johnston RK, Matthews AB, Zhou H, Gao M, Skolnick J. Repurposed FDA-approved drugs targeting genes influencing aging can extend lifespan and healthspan in rotifers. *Biogerontology*. 2018;19(2):145–157. doi:10.1007/s10522-018-9745-9
19. Dahms HU, Hagiwara A, Lee JS. Ecotoxicology, ecophysiology, and mechanistic studies with rotifers. *Aquat Toxicol*. 2011;101(1):1–12. doi:10.1016/j.aquatox.2010.09.006
20. Snell TW, Johnston RK, Gribble KE, Mark Welch DB. Rotifers as experimental tools for investigating aging. *Invertebr Reprod Dev*. 2015;59(1):5–10. doi:10.1080/07924259.2014.925516
21. Datki Z, Olah Z, Hortobagyi T, et al. Exceptional in vivo catabolism of neurodegeneration-related aggregates. *Acta Neuropathol Commun*. 2018;6(1):6. doi:10.1186/s40478-018-0507-3
22. Chojdak-Łukasiewicz J, Małodobra-Mazur M, Zimny A, Noga L, Paradowski B. Plasma tau protein and Aβ42 level as markers of cognitive impairment in patients with Parkinson's disease. *Adv Clin Exp Med*. 2020;29(1):115–121. doi:10.17219/acem/112058
23. Datki Z, Galik-Olah Z, Janosi-Mozes E, et al. Alzheimer risk factors age and female sex induce cortical Aβ aggregation by raising extracellular zinc. *Mol Psychiatry*. 2020;25(11):2728–2741. doi:10.1038/s41380-020-0800-y
24. Balazs E, Galik-Olah Z, Galik B, Bozso Z, Kalman J, Datki Z. Neurodegeneration-related beta-amyloid as autocatabolism-attenuator in a micro-in vivo system. *IBRO Rep*. 2020;9:319–323. doi:10.1016/j.ibror.2020.10.002
25. Datki Z, Galik-Olah Z, Bohar Z, et al. Kynurenic acid and its analogs are beneficial physiologic attenuators in bdelloid rotifers. *Molecules*. 2019;24(11):2171. doi:10.3390/molecules24112171
26. Martos D, Tuka B, Tanaka M, Vécsei L, Telegdy G. Memory enhancement with kynurenic acid and its mechanisms in neurotransmission. *Biomedicines*. 2022;10(4):849. doi:10.3390/biomedicines10040849
27. Tanaka M, Vécsei L. Monitoring the kynurenine system: Concentrations, ratios or what else? *Adv Clin Exp Med*. 2021;30(8):775–778. doi:10.17219/acem/139572
28. Annus Á, Tömösi F, Rárosi F, et al. Kynurenic acid and kynurenine aminotransferase are potential biomarkers of early neurological improvement after thrombolytic therapy: A pilot study. *Adv Clin Exp Med*. 2021;30(12):1225–1232. doi:10.17219/acem/141646
29. Battaglia S, Thayer JF. Functional interplay between central and autonomic nervous systems in human fear conditioning. *Trends Neurosci*. 2022;45(7):504–506. doi:10.1016/j.tins.2022.04.003
30. Battaglia S, Garofalo S, di Pellegrino G. Context-dependent extinction of threat memories: Influences of healthy aging. *Sci Rep*. 2018;8(1):12592. doi:10.1038/s41598-018-31000-9
31. Battaglia S, Orsolini S, Borgomaneri S, Barbieri R, Diciotti S, di Pellegrino G. Characterizing cardiac autonomic dynamics of fear learning in humans. *Psychophysiology*. 2022:e14122. doi:10.1111/psyp.14122
32. Datki Z, Acs E, Balazs E, et al. Exogenic production of bioactive filamentous biopolymer by monogonant rotifers. *Ecotoxicol Environ Saf*. 2021;208:111666. doi:10.1016/j.ecoenv.2020.111666
33. Datki Z, Balazs E, Galik B, et al. The interacting rotifer-biopolymers are anti- and disaggregating agents for human-type beta-amyloid in vitro. *Int J Biol Macromol*. 2022;201:262–269. doi:10.1016/j.ijbiomac.2021.12.184

Neutrophil-to-lymphocyte ratio as a predictor of inflammatory response in patients with acute kidney injury after transcatheter aortic valve implantation

Anna Olasińska-Wiśniewska[1,A–D], Tomasz Urbanowicz[1,A–D], Kajetan Grodecki[2,A,C,D], Bartłomiej Perek[1,A,C,E,F], Marek Grygier[3,E,F], Michał Michalak[4,C], Marcin Misterski[1,B,E,F], Mateusz Puślecki[1,5,E,F], Michał Rodzki[1,B,E], Konrad Stelmark[6,B], Maciej Lesiak[3,E,F], Marek Jemielity[1,E,F]

[1] Department of Cardiac Surgery and Transplantology, Poznan University of Medical Sciences, Poland

[2] 1st Department of Cardiology, Medical University of Warsaw, Poland

[3] 1st Department of Cardiology, Poznan University of Medical Sciences, Poland

[4] Department of Computer Science and Statistics, Poznan University of Medical Sciences, Poland

[5] Department of Medical Rescue, Poznan University of Medical Sciences, Poland

[6] Student Scientific Group, English Division, Poznan University of Medical Sciences, Poland

A – research concept and design; B – collection and/or assembly of data; C – data analysis and interpretation;
D – writing the article; E – critical revision of the article; F – final approval of the article

Address for correspondence
Anna Olasińska-Wiśniewska
E-mail: annaolasinska@ump.edu.pl

Abstract

Background. Persistent inflammatory response after transcatheter aortic valve implantation (TAVI) is one of the possible causes of early and mid-term postprocedural adverse events.

Objectives. To establish the predictive role of whole blood parameters on inflammatory response characteristics within a 1-year follow-up.

Materials and methods. The study group comprised 163 consecutive patients (52.1% females), mean age 78.6 ($\pm$6.6) years ($\pm$ standard deviation (SD)) who underwent TAVI and completed 1-year follow-up on-site examinations. Patients were retrospectively divided into acute kidney injury (AKI) and non-AKI subgroups. Clinical and laboratory data were collected. In-hospital and follow-up outcomes were assessed.

Results. The clinical and procedural details did not show significant differences between AKI and non-AKI groups. Neutrophil-to-lymphocyte ratio (NLR) decreased from baseline to measurement after 1 year with a statistically significant decline in the whole study population and non-AKI subgroup (both p = 0.005). The baseline NLR cutoff value of 4.2 for the non-AKI group ((area under the curve (AUC) = 0.718, p < 0.0001; sensitivity 46.27%, specificity 92.31%) and of 3.8 for the AKI group (AUC = 0.673, p = 0.0174; sensitivity 59.25%, specificity 84%) had prognostic properties for persistent NLR elevation.

Conclusions. The NLR decreases after TAVI, and this phenomenon is more evident in patients without AKI. Furthermore, baseline NLR cutoff values may be considered predictors of persistence of inflammatory response.

Key words: acute kidney injury, heart failure, transcatheter, aortic stenosis, neutrophil-to-lymphocyte ratio

Background

Transcatheter aortic valve implantation (TAVI) has become an established method of treatment for patients with aortic stenosis. While first TAVI cohorts included only patients disqualified from surgical aortic valve replacement (SAVR), currently, a variety of subjects with low to high perioperative risk and low to severe comorbidity undergo the procedure.[1–3] The treated population is diverse; therefore, several issues should be evaluated, including the qualification process and the follow-up management, to obtain the best therapeutic results.

Chronic heart failure (chronic HF), as a common feature of the TAVI population, is associated with an inflammatory process, and circulating inflammatory cytokines can predict clinical outcomes.[4] For clinicians, simple and easily available markers of inflammation are most suitable for daily practice, while more advanced assessment of cytokines is often inaccessible, costly and time-dependent. Therefore, white blood cell (WBC) count and its subgroups are both common and most available markers of inflammation. Neutrophil-to-lymphocyte ratio (NLR) is derived from a routine complete blood count. The normal range is between 1 and 2, and higher values are warning signals of pathological state.[5] Neutrophil-to-lymphocyte ratio has been proposed as a prognostic marker of systemic inflammation in several cardiovascular and non-cardiovascular diseases, including HF, aortic stenosis and acute myocardial infarction, and in outcomes after coronary revascularization.[6–12]

Acute kidney injury (AKI) is a well-known complication after TAVI, which may impair long-term outcomes.[13,14] The NLR has been associated with the development of AKI after TAVI.[11,12] However, there are limited data concerning the role of NLR in long-term observation after the procedure.

Objectives

The aim of our study was to establish the predictive role of basic whole blood parameters on inflammatory response characteristics within a 1-year follow-up in patients with and without AKI after TAVI.

Materials and methods

Study design

Basic whole blood parameters were collected in the study population divided retrospectively into AKI and non-AKI subgroups. The NLR variations were analyzed in the whole population and in the subgroups. The risk of persistence of inflammatory response was studied.

Study patients

A total of 210 patients underwent TAVI between January 2013 and March 2017 in our hospital. All of the patients were qualified to the procedure after careful assessment of clinical history and diagnostic examinations. Patients who did not have blood test or echocardiographic examination during 1-year follow-up visit and those who presented with the signs of infection or neoplasm were excluded from the analysis. Moreover, 24 patients who died (time to death 137.5 (120.8) days (mean ± standard deviation (SD)) were not included in the study group. Five of them died due to perioperative complications and the others in course of HF and/or comorbidities/neoplasms.

Finally, the study group was selected and comprised 163 consecutive patients (85 of them females, 52.1%) with the mean (±SD) age of 78.6 (±6.6) years, who underwent TAVI and completed the 1-year follow-up (12 ±1 months) on-site examinations. Patients were divided into AKI and non-AKI subgroups according to the Valve Academic Research Consortium 3 (VARC-3) criteria[15] (increase of serum creatinine ≥1.5× within 7 days compared with baseline or increase of ≥0.3 mg/dL (≥26.4 mmol/L) within 48 h or hemofiltration) (Fig. 1).
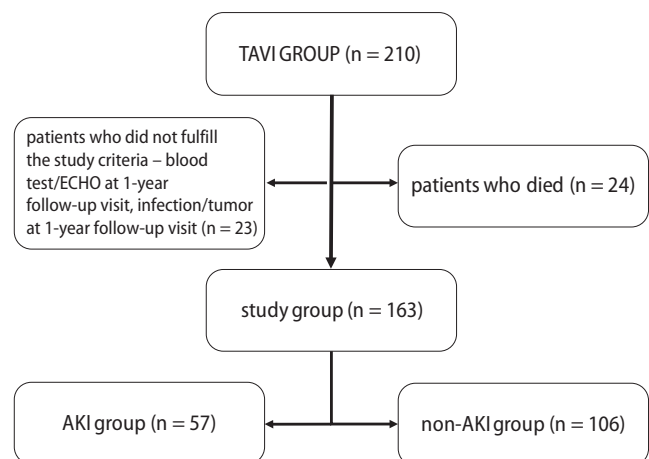
Fig. 1. Flowchart of the study inclusion and explanation of exclusion criteria

TAVI – transcatheter aortic valve implantation; AKI – acute kidney injury.

Details of TAVI

The TAVI procedures were performed in a hybrid room by the same team of cardiologists and cardiac surgeons, under fluoroscopic and echocardiographic guidance. In a majority of patients (n = 158, 96.9%), percutaneous access (using Prostar XL or Perclose ProGlide systems (both from Abbott, Chicago, USA)) was performed. General anesthesia was used in 72.4% of patients, whereas 27.6% (n = 45) had local anesthesia with sedation. In transapical access (n = 1), left anterolateral minithoracotomy was performed through the 6th intercostal space. In direct aortic

Table 1. Demographic, clinical and procedural characteristics

Variable	Whole group n = 163	AKI group n = 57	Non-AKI group n = 106	p-value[#]
Males, n	78 (47.9)	28 (49.1)	50 (47.2)	0.814
Age [years]	80 (75–83)	80 (76–83)	80 (75–83)	0.851
BMI [kg/m^2]	28 (25.35–30.85)	29.6 (26.9–31.2)	27.6 (24.6–29.7)	0.03
EuroSCORE II [%]	4.7 (2.735–9.265)	5.45 (3.13–10.12)	4.4 (2.587–8.067)	0.146
STS score [%]	5.3 (3.381–14.312)	5.06 (3.33–13.457)	5.85 (3.7–14.718)	0.278
T2DM	51 (31.3)	22 (38.6)	29 (27.4)	0.140
Hypertension	118 (72.4)	42 (73.7)	76 (71.7)	0.787
AF	54 (33.1)	17 (29.8)	37 (34.9)	0.511
COPD	33 (20.2)	10 (17.5)	23 (21.7)	0.529
MI history	56 (34.4)	23 (40.4)	33 (31.1)	0.237
Stroke or TIA history	29 (17.8)	11 (19.3)	18 (17)	0.712
eGFR [mL/min/1.73 m^2]	56 (46–67.5)	49 (40–66)	58.5 (49–69.5)	0.007
MPG [mm Hg]	57 (47–69)	56.5 (47–66)	56.5 (47.25–69)	0.640
PPG [mm Hg]	90 (78.5–109.5)	90 (78–109)	90 (80–110)	0.965
LVEF [%]	55 (45–60)	55 (45–60)	55 (45–60)	0.967
Predilatation	79 (48.5)	28 (49.1)	51 (48.1)	0.902

Prosthesis
  Medtronic CoreValve/Evolut R
  Lotus
  Symetis
	131 (80.4)
	30 (18.4)
	2 (1.2)
		49 (86)
		8 (14)
		0
			82 (77.3)
			22 (20.8)
			2 (1.9)
				0.312

Anesthesia
  general
  local
	118 (72.4)
	45 (27.6)
		43 (75.4)
		14 (24.6)
			75 (70.8)
			31 (29.3)
				0.524

Access
  femoral
  apical/direct aortic
	158 (96.9)
	5 (3.1)
		56 (98.2)
		1 (1.8)
			102 (96.2)
			4 (3.8)
				0.475

TAVI time [min]	75 (70–90)	75 (65–95)	75 (75–90)	0.290
Volume of contrast media [mL]	182.5 (150–250)	200 (150–230)	180 (150–250)	0.691
Hospitalization [days]	7 (6–9)	9 (7–13)	7 (6–8)	<0.001

Continuous variables are expressed either as the means with standard deviations (SD) (if normally distributed) or the medians (Q1–Q3) (the others), whereas categorical variables are expressed as the numbers (n) with percent (%). [#] – comparison between AKI and non-AKI subgroups; AKI – acute kidney injury; EuroSCORE II – European System for Cardiac Operative Risk Evaluation II; eGFR – estimated glomerular filtration rate; TAVI – transcatheter aortic valve implantation; TIA – transient ischemic attack; STS – Society of Thoracic Surgeons; MPG – mean pressure gradient; PPG – peak pressure gradient; BMI – body mass index; T2DM – type 2 diabetes mellitus; COPD – chronic obstructive pulmonary disease; LVEF – left ventricular ejection fraction; AF – atrial fibrillation; MI – myocardial infarction.

(n = 4) access, the ministernotomy was performed and aorta was punctured. The procedural data are presented in detail in Table 1.

Analyzed clinical and laboratory data

Demographic and clinical data were collected and analyzed. Blood samples were collected at baseline, after the procedure (on daily routine) and at the 1-year follow-up visit. The following parameters were taken into consideration: WBC count, neutrophils (NEU), lymphocytes (LYMPH), NLR, and creatinine concentration (CREA). Estimated glomerular filtration rate (eGFR) was calculated. Echocardiography was performed in all patients before and after the procedure, at discharge and at 1-year follow-up.

In-hospital and follow-up outcomes were also assessed, the latter based on hospital follow-up visit records and national database.

Statistical analyses

Continuous variables were checked for normality by means of the Shapiro–Wilk W test. These satisfying criteria of normal distribution were presented as mean ±SD and compared using the unpaired t-test or repeated measures analysis of variance (ANOVA). If continuous data were not normally distributed, they were expressed as median with interquartile range (IQR: 1st to 3rd quartile (Q1–Q3)) and compared with the use of nonparametric Mann–Whitney U test. Categorical

variables were reported as numbers (n) and percentages (%), and then compared with the use of the Fisher's exact test. The p-values less than 0.05 were considered statistically significant. The cutoff values of the baseline NLR that discriminated between patients with and without inflammation persistence were calculated using a receiver operating characteristic (ROC) curve. We performed multivariable logistic regression analysis, adjusted for total clinical parameters and echocardiographic and procedural variables, to evaluate predictors of failed decrease of NLR during 1-year follow-up. Statistical analysis was performed using JASP statistical software (https://jasp-stats.org/) and IBM SPSS v. 23 (IBM Corp., Armonk, USA).

The study was approved by the Institutional Ethics Committee of Poznan University of Medical Sciences (approval No. 971/15) and respected the principles outlined in the Declaration of Helsinki.

Results

Clinical characteristics

The clinical profile and procedural details did not show significant differences between the AKI and non-AKI groups, besides lower eGFR and body mass index (BMI) in the AKI group. Baseline characteristics are presented in Table 1. Before TAVI, 89.6% (n = 146) of patients presented symptoms of class III or IV HF, and 10.4% of class II HF according to the New York Heart Association (NYHA) classification. During the 1-year follow-up, patients presented significant and sustained clinical (97% had NYHA class I or II) and echocardiographic improvement.

NLR analysis

Median baseline NLR values related to main clinical variables are presented in Table 2. The NLR decreased from baseline to the measurement after 1 year in the whole population and subgroups; however, a statistically significant

Table 2. Median neutrophil-to-lymphocyte ratio (NLR) values in relation to the presence (1) or absence (0) of clinical variables

Variable	1	0	p-value
Gender – female	3.040 (2.215–4.343)	3.868 (2.556–4.801)	0.041
COPD	3.733 (2.433–4.558)	3.307 (2.360–4.588)	0.693
Hypertension	3.381 (2.336–4.639)	3.385 (2.458–4.558)	0.866
T2DM	4.495 (2.762–6.164)	3.051 (2.284–4.161)	0.001
Metabolic syndrome	3.506 (2.533–4.835)	3.231 (2.199–4.471)	0.097
AF	3.449 (2.516–4.703)	3.323 (2.253–4.558)	0.529
Stroke in history	2.957 (2.213–4.027)	3.534 (2.401–4.703)	0.121
MI in history	3.860 (2.961–4.888)	3.000 (2.168–4.498)	0.009
General anesthesia	3.534 (2.497–4.582)	2.709 (1.894–4.684)	0.071

Continuous variables are expressed as the medians (Q1–Q3). COPD – chronic obstructive pulmonary disease; T2DM – type 2 diabetes mellitus; MI – myocardial infarction; AF – atrial fibrillation.

Table 3. Neutrophil-to-lymphocyte ratio (NLR) levels at baseline, discharge and 1-year follow-up visit

Study group	Baseline NLR	Discharge NLR	1-year NLR	Baseline compared to 1-year p-value	Discharge compared to 1-year p-value
Whole group	3.385 (2.38–4.586)	3.741 (2.659–4.993)	2.978 (2.327–4.438)	0.005	<0.001
AKI group	3.385 (2.433–4.684)	4.451 (2.987–5.605)	3.255 (2.324–4.441)	0.328	0.003
Non-AKI group	3.404 (2.372–4.532)	3.468 (2.623–4.708)	2.891 (2.331–4.428)	0.005	0.042

Continuous variables are expressed as the medians (Q1–Q3). AKI – acute kidney injury.

Table 4. Creatinine levels at baseline, discharge and during 1-year visit

Study group	Baseline creatinine	Discharge creatinine	1-year creatinine	Baseline compared to 1-year p-value	Discharge compared to 1-year p-value
Whole group	104.4 (84.35–122.25)	101.05 (80.65–126.95)	105.95 (84.35–125.85)	0.112	0.031
AKI group	111.5 (97.2–137.7)	123.5 (93.1–138.45)	116.3 (98.2–139.2)	0.818	0.441
Non-AKI group	97.3 (80.525–112.675)	94.7 (76.35–112.3)	99.4 (82.1–117)	0.066	<0.001

Continuous variables are expressed as the medians (Q1–Q3). AKI – acute kidney injury.
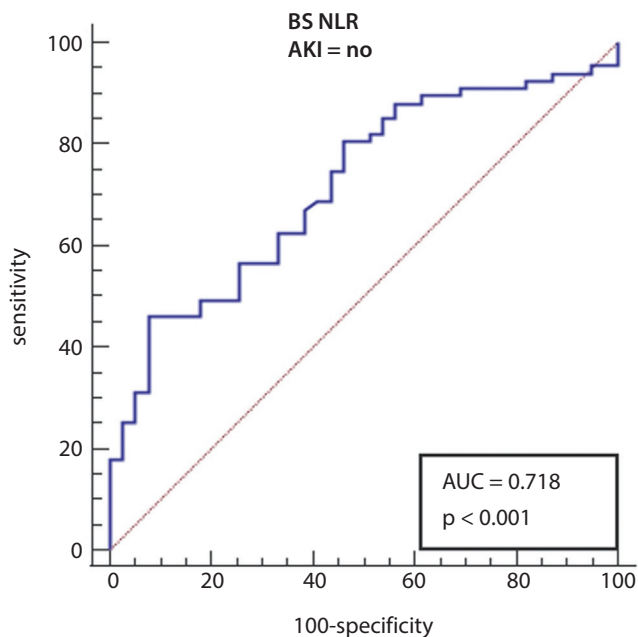
Fig. 2. The receiver operating characteristic (ROC) curve analysis of the baseline neutrophil-to-lymphocyte ratio (BS NLR) for predicting inflammatory response persistence in the non-acute kidney injury (AKI) group

AUC – area under the curve.
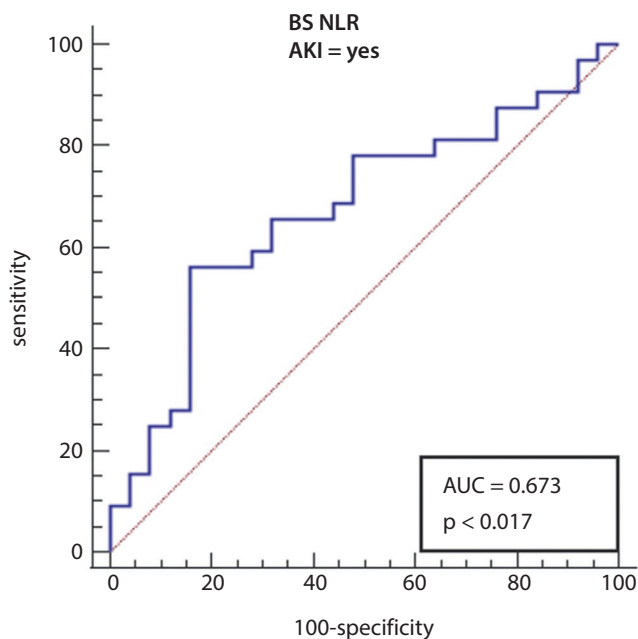
Fig. 3. The receiver operating characteristic (ROC) curve analysis of the baseline neutrophil-to-lymphocyte ratio (BS NLR) for predicting inflammatory response persistence in the acute kidney injury (AKI) group

AUC – area under the curve.

decline was noted in the whole group and in non-AKI subgroup (both p = 0.005) (Table 3). The creatinine level did not change significantly in the measurements before and 1 year after the procedure (Table 4).

In both subgroups, there were some patients characterized by continuous NLR persistence during the observation
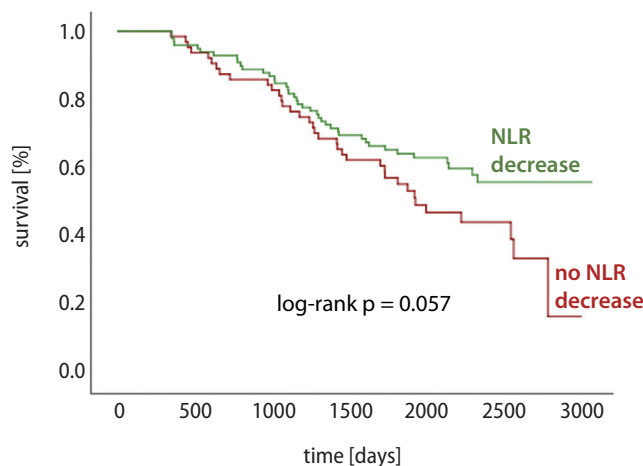
Fig. 4. All-cause mortality after 1-year follow-up in patients with and without neutrophil-to-lymphocyte ratio (NLR) decrease

time. For the non-AKI group, the ROC curve presented the baseline NLR cutoff value of 4.2 as a significant predictor for persistent NLR elevation (Fig. 2). Even more interestingly, a corresponding group of patients in AKI subgroup who presented with chronic NLR elevation were characterized by the baseline NLR cutoff value of 3.8 in ROC analysis ((area under the curve (AUC) = 0.673, p-value = 0.017, Fig. 3).

The risk of failed NLR decrease between baseline and 1-year values was evaluated based on demographic, clinical and procedural data (Fig. 4). In the multivariate logistic regression analysis, peak pressure gradient (PPG; p = 0.008) and predilatation (p = 0.028) were significant predictors of NLR decrease failure in AKI group, while in non-AKI group, only diabetes (p = 0.031) showed prognostic value (Table 5).

Echocardiographic assessment

During the 1-year follow-up echocardiographic examination, parameters of blood flow through bioprostheses were comparable to the findings in the discharge echocardiography. The transvalvular pressure gradients were: mean pressure gradient (MPG) 9.00 (±5.2) mm Hg and peak pressure gradient (PPG) 16.9 (±8.6) mm Hg in non-AKI subgroup, and MPG 9.1 (±5.0) mm Hg and PPG 17.8 (±7.7) mm Hg in AKI subset of TAVI patients (mean (±SD)).

The median (IQR) changes of pressure gradients (PGs) were as follows: MPG (−23.3% (−36.4%; 16.6%)) in non-AKI subgroup compared to −12.5% (−26.7%; 19.0%) in AKI subgroup; p = 0.12); PPG (−16.2% (−31.1%; 18.7%)) in non-AKI subgroup compared to −5.6% (−23.8%; 29.3%) in AKI subset; p = 0.21).

Of note, in some of them decrease and in the others increase in PGs have been noted. An increase in absolute values of PPG was observed in 34.5% of non-AKI patients and 44.2% of AKI patients, whereas an increase in MPG absolute values in 38.9% of non-AKI patients and

Table 5. Association of clinical, echocardiographic and procedural characteristics with the risk of failed decrease of NLR during follow-up in a multivariable* logistic regression analysis

Variable	AKI group n = 57		Non-AKI group n = 106	p-value
	OR (95% CI)	p-value	OR (95% CI)	
Males, n	–	–	–	–
Age [years]	–	–	–	–
BMI [kg/m²]	–	–	–	–
EuroSCORE II [%]	–	–	–	–
STS score [%]	–	–	–	–
T2DM, n	–	–	0.30 [0.10; 0.90]	0.031
Hypertension, n	–	–	–	–
AF, n	–	–	–	–
COPD, n	–	–	–	–
MI in history, n	–	–	–	–
Stroke or TIA in history, n	–	–	–	–
eGFR [mL/min/1.73 m²]	–	–	–	–
MPG [mm Hg]	–	–	–	–
PPG [mm Hg]	0.96 [0.92; 0.99]	0.008	–	–
LVEF [%]	–	–	–	–
Predilatation	4.25 [1.17; 15.40]	0.028	–	–
Non-femoral access	–	–	–	–
Self-expandable valve	–	–	–	–
TAVI time [min]	–	–	–	–
Volume of contrast media [mL]	–	–	–	–
Hospitalization [days]	–	–	–	–

All variables entered into multivariable logistic regression with backward stepwise selection at a Wald p-value of 0.1. The final model containing statistically significant variables is shown. OR – odds ratio; 95% CI – 95% confidence interval; AKI – acute kidney injury; eGFR – estimated glomerular filtration rate; EuroSCORE II – European System for Cardiac Operative Risk Evaluation II; TAVI – transcatheter aortic valve implantation; STS – Society of Thoracic Surgeons; MPG – mean pressure gradient; PPG – peak pressure gradient; BMI – body mass index; T2DM – type 2 diabetes mellitus; COPD – chronic obstructive pulmonary disease; TIA – transient ischemic attack; LVEF – left ventricular ejection fraction; AF – atrial fibrillation; MI – myocardial infarction.

40.5% of AKI patients was noted, but these differences were not of statistical significance (p = 0.30 and p = 0.87, respectively).

No statistical significance of echocardiographic parameters between patients with persistent NLR and without persistent NLR was found. The baseline transvalvular pressure gradients were as follows: mean (±SD) MPG of 55.2 (±16.6) mm Hg and 59.4 (±17.6) mm Hg (p = 0.142), and mean (±SD) PPG of 90.2 (±25.9) mm Hg and 94.7 (±27.3) mm Hg (p = 0.302) in patients without persistent NLR and with persistent NLR, respectively. The median (Q1–Q3) left ventricular ejection fraction (LVEF) was 60% (47.25–60%) and 55% (45–60%) (p = 0.248) in patients without persistent NLR and with persistent NLR, respectively. Similarly, echocardiographic parameters after TAVI did not differ significantly between both subgroups: median (Q1–Q3) MPG values were 8 (6.025–9.975) mm Hg and 9 (7–11.25) mm Hg (p = 0.076), median (Q1–Q3) PPG values were 16.9 (12–20) mm Hg and 18 (13.1–22.75) mm Hg (p = 0.069), while median (Q1–Q3) EF values were 60% (50–60%) and 55% (50–60%) (p = 0.112), in patients without persistent NLR and with persistent NLR, respectively. Likewise, paravalvular leak (PVL) presence did not show statistical significance (p = 0.359).

Discussion

There are 2 major findings of our study. First, inflammatory response represented by the NLR decrease after the TAVI procedure; second, the decrease is more profound and statistically significant in patients without AKI occurring as a complication of the procedure. Patients who suffered from AKI after the procedure did not achieve significant NLR reduction within a 1-year follow-up. Moreover, baseline NLR cutoff values of 4.2 for non-AKI group and of 3.8 for AKI group were found as predictors of inflammatory long-lasting persistence.

Preprocedural planning and patient selection process are crucial for optimal TAVI results. Clinical profile evaluation, echocardiography and computed tomography (CT) examination analyses play fundamental roles, enabling a precise diagnosis as well as the choice of approach and

the device type which will more likely achieve the best result.[16–20] Several cardiac and cardiosurgical scores, including the European System for Cardiac Operative Risk Evaluation II (EuroSCORE II), Society of Thoracic Surgeons (STS) score and Intermountain Risk Score,[21–23] have been used to determine the mortality risk. Simple laboratory analysis, with C-reactive protein (CRP),[24,25] leucocytes[25] as well as NLR evaluation,[11] may facilitate prediction of clinical outcomes.

The NLR was pointed out as a marker of systemic inflammation and worse prognosis in patients with HF.[7,8] Moreover, systemic inflammation has been recognized as a dominant feature of HF deterioration,[26] particularly when reduction in left ventricular function is observed.[26,27] Aortic stenosis is characterized with constant progression of HF. The pathogenesis of calcific aortic stenosis is multifactorial. Inflammation, including both innate and adaptive immune responses, is an essential process which initiates calcification and acts in progression of the disease.[28–30] Baratchi et al. used an in vitro model to investigate the effect of shear stress present in aortic stenosis on the adhesion of monocytes to endothelial cells.[31] They showed that the shear forces in aortic stenosis translate into the amplification of inflammation and further progression of valve degeneration.

The NLR as a simple marker of inflammation provides an easy and quickly available prognostic evaluation of patients with aortic stenosis and HF. Gul et al. did not find a decrease in NLR in an observation after TAVI; however, the study group was small (33 patients) and the follow-up short – only up to 4 months.[32] Conversely, Afşin et al. presented a decrease in NLR after 1 month and 6 months after the procedure.[33] We believe that our longer, 1-year observation period may reflect long-lasting results of cardiac remodelling after the procedure. Left ventricular remodelling occurs after TAVI, with reductions in left ventricular end-diastolic volume index, end-systolic volume index, left ventricular mass index, and increased LVEF.[34] Abu Khadija et al. showed that the reduction of the NLR as an inflammatory marker after TAVI in group with reduced left ventricular function caught up with the NLR in patients with preserved left ventricular function after 6 months of follow-up.[26]

Condado et al. showed that elevated NLR and platelet–lymphocyte ratio (PLR) are associated with a higher Society of Thoracic Surgeons – Predicted Risk of Mortality (STS-PROM) score.[35] Therefore, high NLR may characterize patients with higher perioperative risk. In the same analysis, baseline NLR and PLR did not predict the 1-year outcome. However, change in NLR from baseline to discharge by a level variation greater than 8 resulted in a worse 1-year clinical outcome.

We proved an NLR decrease in a long-term observation. In our analysis, NLR decreased significantly in the whole group, but particularly in non-AKI patients. This observation may reflect diminished inflammatory response

in the course of heart remodelling after TAVI, which was shown by Abu Khadija et al. in patients with HF related to aortic stenosis.[26] Simultaneously, we did not observe a decrease in creatinine level from baseline to 1-year measurement in any of the study groups. An increase was observed between the measurements at discharge and at 1 year in the whole study population and non-AKI groups; however, it reflected the return to a value approximate to the baseline one. Therefore, we did not observe an improvement in renal function, but we found insufficient NLR decrease which may suggest a persistent inflammatory response in AKI patients.

Interestingly, in both subgroups (AKI and non-AKI), we noted patients without long-lasting NLR decrease after TAVI. In the multivariate analysis, in the AKI group, PPG and predilatation (while in the non-AKI group – diabetes) were prognostic factors of NLR decrease failure. We believe that this easily available hematologic index may enable differentiation of patients with clinically silent chronic inflammatory response. In patients who survived the periprocedural period without kidney injury, baseline NLR cutoff point of 4.2 was found as statistically significant for persistent chronic inflammation as a possible ominous factor, whereas the same parameter was even lower (NLR cutoff point of 3.8) in the AKI group. Therefore, we suppose that in AKI patients, lower baseline NLR may predict worse late outcomes in terms of HF- and kidney failure-related inflammatory status. Thus, we pointed out that the NLR changes presented throughout the study period may be interfered by AKI occurrence. Patients who experienced perioperative AKI may induce inflammatory reactions leading to persistence of NLR elevation up to 1 year following the procedure. Therefore, we emphasize the importance of baseline NLR assessment.

The novelty of the results from our study is the presentation of prolonged consequences of perioperative AKI. The kidney injury seemed transient in clinical observational characteristics, but in fact it changed the inflammatory status, with possible significant implications.

We suppose that in the TAVI population, persistent inflammation may influence the long-term performance of the biological prosthesis. A faster structural bioprosthesis degeneration is observed in patients with chronic renal insufficiency,[36] mainly because the underlying disease with systemic inflammation and metabolic disturbance is still active. In our study population, patients with AKI presented lower baseline eGFR, which reflects chronic renal impairment. Moreover, a majority of patients presented some degree of renal dysfunction resulting from the advanced age of that population and impairment in body organ blood flow in the presence of aortic stenosis. Based on these insights, we decided to compare the 1-year echocardiographic assessment of bioprostheses in AKI and non-AKI groups. The median changes in PPG and MPG were not significant in the study groups. We analyzed in detail the patients in whom an increase in PGs has been noted

between discharge and the measurement after 1 year. An increase in the absolute values of PPG was observed in 34.5% of non-AKI patients and in 44.2% of AKI patients, whereas of the absolute MPG values – in 38.9% and in 40.5% of non-AKI and AKI patients, respectively. These differences were noticeable but not statistically significant (p = 0.30 and p = 0.87, respectively).

Limitations

We assume that our study presents some trend, but the study period (12 months) and the relatively low number of subjects precludes a precise estimation of this phenomenon. This issue may be treated as a study limitation, and therefore larger studies with longer observation periods seem necessary to evaluate the influence of AKI-related inflammatory response on bioprosthetic performance. The significance of that matter is of particular importance since the inflammatory process may promote both valve calcification and thrombosis. Moreover, NLR is a multifactorial value influenced not only by aortic stenosis, but also by HF, atrial fibrillation after cardiac surgery, acute myocardial infarction, infections, etc.[37–39] Patients with signs of infection were excluded from the analysis, and there were no cases of acute coronary syndrome during hospitalization or at 1-year follow-up. We believe that changes in NLR levels are relevant to changes in exaggeration of HF. Therefore, HF in means of its remission is strictly included in the observed phenomenon.

Conclusions

The NLR decreases after TAVI procedure, and this phenomenon is more profound in patients without periprocedural AKI.

ORCID iDs

Anna Olasińska-Wiśniewska https://orcid.org/0000-0002-4213-8708
Tomasz Urbanowicz https://orcid.org/0000-0001-8080-2764
Kajetan Grodecki https://orcid.org/0000-0002-0358-5679
Bartłomiej Perek https://orcid.org/0000-0003-2398-9571
Marek Grygier https://orcid.org/0000-0002-1134-7099
Michał Michalak https://orcid.org/0000-0002-2852-3984
Marcin Misterski https://orcid.org/0000-0001-5102-4094
Mateusz Puślecki https://orcid.org/0000-0003-0015-2808
Michał Rodzki https://orcid.org/0000-0003-1057-8044
Maciej Lesiak https://orcid.org/0000-0003-2630-5016
Marek Jemielity https://orcid.org/0000-0003-2442-4644

References

1. Dąbrowski M, Parma R, Huczek Z, et al. The Polish Interventional Cardiology TAVI Survey (PICTS): 10 years of transcatheter aortic valve implantation in Poland. The landscape after the first stage of Valve for Life initiative. *Pol Arch Intern Med*. 2021;131(5):413–420. doi:10.20452/pamw.15887
2. Huczek Z, Jędrzejczyk S, Jagielak D, et al. Transcatheter aortic valve-in-valve implantation for failed surgical bioprostheses: Results from Polish Transcatheter Aortic Valve-in-Valve Implantation (ViV-TAVI) Registry. *Pol Arch Intern Med*. 2022;132(2):16149. doi:10.20452/pamw.16149
3. Huczek Z, Rymuza B, Mazurek M, et al. Temporal trends of transcatheter aortic valve implantation in a high-volume academic center over 10 years. *Kardiol Pol*. 2021;79(7–8):820–826. doi:10.33963/KP.a2021.0030
4. Dick SA, Epelman S. Chronic heart failure and inflammation: What do we really know? *Circ Res*. 2016;119(1):159–176. doi:10.1161/CIRCRESAHA.116.308030
5. Zahorec R. Neutrophil-to-lymphocyte ratio, past, present and future perspectives. *Bratisl Lek Listy*. 2021;122(7):474–488. doi:10.4149/BLL_2021_078
6. Urbanowicz T, Olasińska-Wiśniewska A, Michalak M, Straburzyńska-Migaj E, Jemielity M. Neutrophil to lymphocyte ratio as noninvasive predictor of pulmonary vascular resistance increase in congestive heart failure patients: Single-center preliminary report. *Adv Clin Exp Med*. 2020;29(11):1313–1317. doi:10.17219/acem/126292
7. Khalil C, Pham M, Sawant AC, et al. Neutrophil-to-lymphocyte ratio predicts heart failure readmissions and outcomes in patients undergoing transcatheter aortic valve replacement. *Indian Heart J*. 2018; 70:S313–S318. doi:10.1016/j.ihj.2018.08.002
8. Angkananard T, Anothaisintawee T, McEvoy M, Attia J, Thakkinstian A. Neutrophil lymphocyte ratio and cardiovascular disease risk: A systematic review and meta-analysis. *BioMed Res Int*. 2018;2018:1–11. doi:10.1155/2018/2703518
9. Urbanowicz TK, Michalak M, Gąsecka A, et al. A risk score for predicting long-term mortality following off-pump coronary artery bypass grafting. *J Clin Med*. 2021;10(14):3032. doi:10.3390/jcm10143032
10. Papa A, Emdin M, Passino C, Michelassi C, Battaglia D, Cocci F. Predictive value of elevated neutrophil–lymphocyte ratio on cardiac mortality in patients with stable coronary artery disease. *Clin Chim Acta*. 2008;395(1–2):27–31. doi:10.1016/j.cca.2008.04.019
11. Olasińska-Wiśniewska A, Perek B, Grygier M, et al. Increased neutrophil-to-lymphocyte ratio is associated with higher incidence of acute kidney injury and worse survival after transcatheter aortic valve implantation [published online ahead of print on November 15, 2021]. *Cardiol J*. 2021. doi:10.5603/CJ.a2021.0149
12. Yelgeç NS, Karataş MB, Karabay CY, et al. The relationship between acute renal failure after transcatheter aortic valve replacement and preprocedural neutrophil to lymphocyte ratio. *Dicle Tıp Dergisi*. 2020; 47(1):1–9. doi:10.5798/dicletip.705532
13. Tandar A, Sharma V, Ibrahim M, et al. Preventing or minimizing acute kidney injury in patients undergoing transcatheter aortic valve replacement. *J Invasive Cardiol*. 2021;33(1):E32–E39. PMID:33385984.
14. Rodriguez R, Hasoon M, Eng M, et al. Incidence and predictors of acute kidney injury following transcatheter aortic valve replacement: Role of changing definitions of renal function and injury. *J Invasive Cardiol*. 2020;32(4):138–141. PMID:31941833.
15. VARC-3 Writing Committee, Généreux P, Piazza N, et al. Valve Academic Research Consortium 3: Updated endpoint definitions for aortic valve clinical research. *Eur Heart J*. 2021;42(19):1825–1857. doi:10.1093/eurheartj/ehaa799
16. Dąbrowski M, Pyłko A, Chmielak Z, et al. Comparison of transcatheter aortic valve implantation outcomes in patients aged <85 years and ≥85 years: A single centre study. *Pol Arch Intern Med*. 2021;131(2):145–151. doi:10.20452/pamw.15780
17. Nieznańska M, Zatorska K, Stokłosa P, et al. Computed tomography assessment of the aortic root morphology in predicting the development of paravalvular leak following transcatheter aortic valve implantation. *Pol Arch Intern Med*. 2021;131(10):16085. doi:10.20452/pamw.16085
18. Grodecki K, Tamarappoo BK, Huczek Z, et al. Non-calcific aortic tissue quantified from computed tomography angiography improves diagnosis and prognostication of patients referred for transcatheter aortic valve implantation. *Eur Heart J Cardiovasc Imaging*. 2021;22(6): 626–635. doi:10.1093/ehjci/jeaa304
19. Scisło P, Grodecki K, Rymuza B, et al. Impact of transcatheter aortic valve implantation on coexistent mitral regurgitation parameters. *Kardiol Pol*. 2021;79(2):179–184. doi:10.33963/KP.15680
20. Mangieri A, Laricchia A, Montalto C, et al. Patient selection, procedural planning and interventional guidance for transcatheter aortic valve intervention. *Minerva Cardiol Angiol*. 2021;69(6):671–683. doi:10.23736/S2724-5683.21.05573-0
21. Jemielity M. EuroSCORE is a predictor of postoperative pericardial effusion following heart transplantation. *Ann Transplant*. 2015;20: 193–197. doi:10.12659/AOT.892582

22. Taleb Bendiab T, Brusset A, Estagnasié P, Squara P, Nguyen LS. Performance of EuroSCORE II and Society of Thoracic Surgeons risk scores in elderly patients undergoing aortic valve replacement surgery. *Arch Cardiovasc Dis*. 2021;114(6–7):474–481. doi:10.1016/j.acvd.2020.12.004

23. Özdemir E, Esen Ş, Emren SV, Karaca M, Nazlı C. Association between Intermountain Risk Score and long-term mortality with the transcatheter aortic valve implantation procedure. *Kardiol Pol*. 2021;79(11): 1215–1222. doi:10.33963/KP.a2021.0120

24. Krumsdorf U, Chorianopoulos E, Pleger ST, et al. C-reactive protein kinetics and its prognostic value after transfemoral aortic valve implantation. *J Invasive Cardiol*. 2012;24(6):282–286. PMID:22684383.

25. Stähli BE, Grünenfelder J, Jacobs S, et al. Assessment of inflammatory response to transfemoral transcatheter aortic valve implantation compared to transapical and surgical procedures: A pilot study. *J Invasive Cardiol*. 2012;24(8):407–411. PMID:22865312.

26. Abu Khadija H, Gandelman G, Ayyad O, et al. Comparative analysis of the kinetic behavior of systemic inflammatory markers in patients with depressed versus preserved left ventricular function undergoing transcatheter aortic valve implantation. *J Clin Med*. 2021;10(18):4148. doi:10.3390/jcm10184148

27. Avci A, Elnur A, Göksel A, et al. The relationship between neutrophil/lymphocyte ratio and calcific aortic stenosis. *Echocardiography*. 2014;31(9):1031–1035. doi:10.1111/echo.12534

28. Coté N, Mahmut A, Bosse Y, et al. Inflammation is associated with the remodeling of calcific aortic valve disease. *Inflammation*. 2013; 36(3):573–581. doi:10.1007/s10753-012-9579-6

29. García-Rodríguez C, Parra-Izquierdo I, Castaños-Mollor I, López J, San Román JA, Sánchez Crespo M. Toll-like receptors, inflammation, and calcific aortic valve disease. *Front Physiol*. 2018;9:201. doi:10.3389/fphys.2018.00201

30. Šteiner I, Timbilla S, Stejskal V. Calcific aortic valve stenosis: Comparison of inflammatory lesions in the left, right, and non-coronary cusp. *Pathol Res Pract*. 2021;227:153636. doi:10.1016/j.prp.2021.153636

31. Baratchi S, Zaldivia MTK, Wallert M, et al. Transcatheter aortic valve implantation represents an anti-inflammatory therapy via reduction of shear stress-induced, piezo-1-mediated monocyte activation. *Circulation*. 2020;142(11):1092–1105. doi:10.1161/CIRCULATIONAHA.120.045536

32. Gul M, Uyarel H, Akgul O, et al. Hematologic and clinical parameters after transcatheter aortic valve implantation (TAVI) in patients with severe aortic stenosis. *Clin Appl Thromb Hemost*. 2014;20(3):304–310. doi:10.1177/1076029612462762

33. Afşin A, Kavalci V, Ulutaş Z, et al. The impact of transcatheter aortic valve implantation on neutrophil to lymphocyte ratio: A retrospective study. *Int J Clin Cardiol*. 2019;6(4):153. doi:10.23937/2378-2951/1410153

34. Mehdipoor G, Chen S, Chatterjee S, et al. Cardiac structural changes after transcatheter aortic valve replacement: Systematic review and meta-analysis of cardiovascular magnetic resonance studies. *J Cardiovasc Magn Reson*. 2020;22(1):41. doi:10.1186/s12968-020-00629-9

35. Condado JF, Junpaparp P, Binongo JN, et al. Neutrophil-lymphocyte ratio (NLR) and platelet-lymphocyte ratio (PLR) can risk stratify patients in transcatheter aortic-valve replacement (TAVR). *Int J Cardiol*. 2016;223:444–449. doi:10.1016/j.ijcard.2016.08.260

36. Ternacle J, Côté N, Krapf L, Nguyen A, Clavel MA, Pibarot P. Chronic kidney disease and the pathophysiology of valvular heart disease. *Can J Cardiol*. 2019;35(9):1195–1207. doi:10.1016/j.cjca.2019.05.028

37. Urbanowicz T, Olasińska-Wiśniewska A, Michalak M, et al. The prognostic significance of neutrophil to lymphocyte ratio (NLR), monocyte to lymphocyte ratio (MLR) and platelet to lymphocyte ratio (PLR) on long-term survival in off-pump coronary artery bypass grafting (OPCAB) procedures. *Biology*. 2021;11(1):34. doi:10.3390/biology11010034

38. Weedle RC, Costa MD, Veerasingam D, Soo AWS. The use of neutrophil lymphocyte ratio to predict complications post cardiac surgery. *Ann Transl Med*. 2019;7(23):778–778. doi:10.21037/atm.2019.11.17

39. Maleki M, Tajlil A, Separham A, et al. Association of neutrophil to lymphocyte ratio (NLR) with angiographic SYNTAX score in patients with non-ST-segment elevation acute coronary syndrome (NSTE-ACS). *J Cardiovasc Thorac Res*. 2021;13(3):216–221. doi:10.34172/jcvtr.2021.40

Preoperative and postoperative diagnostic efficiency of multi-inflammatory index on pain scoring of degenerated intervertebral disc

Mustafa Nevzat Firidin[1,A,B,E,F], Mehmet Emin Akyüz[2,A–D]

[1] Department of Neurosurgery, Siirt University, Turkey

[2] Department of Neurosurgery, Siirt Training and Research Hospital, Turkey

A – research concept and design; B – collection and/or assembly of data; C – data analysis and interpretation;
D – writing the article; E – critical revision of the article; F – final approval of the article

Address for correspondence
Mehmet Emin Akyüz
E-mail: mehmeteminakyuz25@gmail.com

Abstract

Background. The inflammatory index can be useful for neurosurgeons to understand and grade pain in degenerated intervertebral disc (DIVD).

Objectives. The study focused on the value of the platelet-to-lymphocyte ratio (PLR), neutrophil-to-lymphocyte ratio (NLR) and the inflammatory multiple indices (MIs), and aimed to compare its efficiency with the preoperative and postoperative pain scale and scoring algorithms.

Materials and methods. A total of 88 DIVD patients were included in this retrospective clinical cohort study. Visual Analogue Scale Back (VASB) and Visual Analogue Scale Leg (VASL), Oswestry Disability Index (ODI), Roland–Morris Disability Questionnaire (RMDQ), and walking distance (WD) were used to assess pain. The multiple index (MI) was calculated as MI-1 = PLR × C-reactive protein (CRP) and MI-2 = NLR × CRP.

Results. Comparing the MI with ODI, no correlation was found in preoperative values, while a positive correlation (MI-1: r = 0.398, p < 0.001; MI-2: r = 0.285; p = 0.007) was found between the postoperative measurements. A significant correlation was found for VASB and both MI-1 (preoperative: r = 0.373, p = 0.001; postoperative: r = 0.232, p = 0.041) and MI-2 (preoperative: r = 0.388, p < 0.001; postoperative: r = 0.206, p = 0.044). The MI-1 index showed 71.4% sensitivity and 73.3% specificity, while the MI-2 index exhibited 78.6% sensitivity and 68.9% specificity.

Conclusions. MI-1 and MI-2 showed a positive correlation with pre- and post-operative VASB score and had strong potential to predict postoperative pain in DIVD. They are easy-to-use, noninvasive and low-cost indices; therefore, our results are promising for routine application.

Key words: pain scoring, degenerated intervertebral disc, inflammation index

Background

Low back pain is accepted as a derivative of multi-origin somatic pain with its physical, psychogenic and social aspects together, and the degenerated intervertebral disc (DIVD) problem emerges as the most important source of this pain in the lumbar spine.[1] Stretching and degeneration of the facet joints, especially in the posterior location of the vertebral body, is often pointed out as an important factor contributing to pain.[2] The only conventional surgical treatment available to prevent further deterioration is based on the surgical fusion of the 2 vertebral bodies, namely spinal fusion, spondylodesis or arthrodesis, although its clinical results vary.[3] Currently, the biggest surgical difficulty is diagnosing the problematic disc region according to the source and degree of pain.[4] Analyzing the inflammation that occurs in the painful area and evaluating the correlation with pain will be illustrative in the detection and grading of pain, and the choice of surgical approach.[5]

The pathophysiology of the anatomical deterioration of the disc is a set of symptoms that develop as a result of inflammatory developments and remodeling facet joint processes.[6] In addition to prostaglandins, numerous cytokines such as tumor necrosis factor (TNF), interleukin 1 (IL-1) and IL-6 worsen this picture by causing osteoarthritic changes.[4,7] These cytokines and matrix-degrading enzymes disrupt chondrocyte metabolism and thus lead to cartilage transformation. In a vicious circle, changes in cartilage cause intense pathological remodeling in the subchondral bone, stimulating a recurrent inflammatory process.[8,9] It may be easier to follow these processes clinically in order to investigate their relevance to pain using hematological (platelet) indices, indirectly influenced by pain, rather than expensive and difficult-to-measure markers such as TNF and IL.[5] The inflammatory process frequently causes changes in numerous hematological parameters, such as peripheral blood cell counts and levels of C-reactive protein (CRP). In comparison, peripheral blood cell counts are easy to measure, inexpensive and widely available in routine clinical practice.[10,11]

Hematology-related inflammatory indices, including platelet-to-lymphocyte ratio (PLR) and neutrophil-to-lymphocyte ratio (NLR), are used as single hematological parameters in routine laboratory examinations for inflammatory disease and are investigated for potential new roles.[12,13] However, their combination with CRP has not been performed for inflammation-related disease, which had mostly an inflammatory process similar to DIVD.[14]

Objectives

These inflammatory indices can be useful for neurosurgeons to understand and grade pain in DIVD, and consequently, to plan the surgical approaches. The study focused on the value of multiple indices (MIs) combined with PLR, NLR and CRP for DIVD as compared to preoperative and postoperative pain scale and scoring algorithms.

Materials and methods

Study design

This study was conducted in adherence to the Declaration of Helsinki and with an approval of the ethics committee of Siirt Training and Research Hospital, Siirt, Turkey (approval No. 2021/06/15, 12782). Eighty-eight patients diagnosed with DIVD from 2018 to 2021 were enrolled into this retrospective clinical cohort study. Informed consent was obtained from all patients included into the study.

Patient selection criteria

According to our inclusion criteria, the DIVD patients enrolled in the study should have had the following characteristics: having experienced chronic low back/leg pain for at least 3 months, not responding to regular physical therapy, and receiving drugs with anti-inflammatory activity for at least 1 month. Patients with comorbidities other than DIVD were not included in the study. The NLR and PLR are useful markers for assessing inflammatory response and disease activity in autoimmune diseases, including systemic lupus erythematosus (SLE). In recent years, markers of inflammation (e.g., NLR) have also been studied in cardiovascular disease (CVD). They could influence many factors, such as malignancies and viral infections, and thus individuals with ongoing infectious or inflammatory diseases receiving treatment for a different disease or systemic disease, or having a different clinical condition diagnosed before or during surgery were excluded.

We used Carragee classification, which divides disc herniations into 4 types as follows: 1) fragment-fissure herniations (with minimal annular defect disc herniations and the presence of an extruded or sequestered fragment); 2) fragment-effect herniations (presence of extruded or sequestered fragment with extensive annular tear over 6 mm); 3) fragment-contained herniations (intact annulus but with 1 or more fragments below the annulus; such fragments are removed by oblique incision to the annulus); 4) no fragment-contained herniations (characterized by the intact annulus and no free fragments under the annulus). Since there were few cases in the type 1 and we performed a different surgical procedure than to types 2, 3 and 4, Carragee type 1 was not taken into account to ensure standardization of the study.

Surgical intervention

The surgical intervention included a single-level unilateral partial hemilaminectomy and foraminotomy

to remove the herniated disc and to decompress the affected nerve root. A skin incision was made in the middle of the back over the appropriate vertebrae. The length of the incision varied depending on how many laminectomies were performed. The back muscles were split in half and moved to either side, exposing the lamina of each vertebra. After the lamina and ligamentum flavum were removed, the protective covering of the spinal cord (dura mater) was made visible. The protective sac of the spinal cord and nerve root was gently pulled back to remove the bony spurs and thickened ligaments. Facet joints, located directly above the nerve roots, were undercut to make more room for the nerve roots.

Clinical assessment and scaling

The magnetic resonance imaging (MRI) findings were recorded to clarify the diagnosis of DIVD and follow-up results of patients with similar clinical conditions, including the type and location of the herniated disc. To evaluate the clinical changes of DIVD that occurred following surgery, pain, disability and walking distance (WD) were measured and the pre-and postoperative periods were compared by means of demographic data and indices. Visual Analogue Scale Back (VASB) and Visual Analogue Scale Leg (VASL) were used to evaluate the pain conditions at preoperative and postoperative period.[15] Oswestry Disability Index (ODI) was used to measure the back and leg pain in terms of pain reduction and functional improvement following the surgery.[16] The ODI responses were requested from all DIVD participants of the study, taking into account the severity of their complaints in the last 10 days, and the results were expressed using the 0–50-point system. The Roland–Morris Disability Questionnaire (RMDQ) was used to evaluate the self-rated physical disability caused by low back pain.[17] In addition to those, we observed the WD for all the patients at preoperative and postoperative period.[18]

Laboratory data analysis

Study data obtained from the participants included the demographics (such as age, gender, etc.), clinical records, and pre- and postoperative routine blood examination results. Venous samples were taken from all patients at the day before the surgery and the day following the surgery. Blood samples were taken during non-medication hours. The MIs were calculated using the following equations:

$$MI\text{-}1 = PLR \times CRP$$

and

$$MI\text{-}2 = NLR \times CRP$$

and compared with pain scales.

Statistical analyses

All data analyses were performed using the IBM SPSS v. 25 software (IBM Corp., Armonk, USA), and statistical significance was considered if $p < 0.05$ was obtained. The Shapiro–Wilk test was used to evaluate the distribution of the index presented in Table 1 (PLR, NLR, MI-1, and MI-2) and the surgery data presented in Table 2 (ODI, RMDQ, VASL, VASB, WD). All the parameters indicated a normal distribution. Hence, we compared patients' preoperative and postoperative outcomes and index using a paired t-test. In the Spearman's correlation analysis, we evaluated the relationship among all the data. The receiver operating characteristic (ROC) curve was drawn to estimate the diagnostic value between the preoperative and postoperative pain values of the participants and to determine the cutoff value for analysis (Fig. 1). A receiver operating characteristic (ROC) curve analysis was performed to assess the diagnostic value of the inflammatory indices.
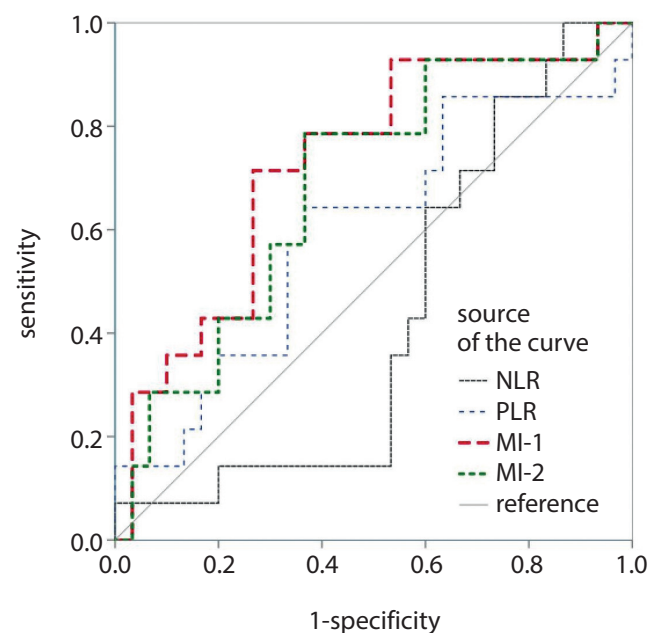
Fig. 1. Receiver operating characteristic (ROC) analysis of postoperative Visual Analogue Scale Back (VASB) in the patients with degenerated intervertebral disc (DIVD)

NLR – neutrophil-to-lymphocyte ratio; PLR – platelet-to-lymphocyte ratio; MI – multiple index.

Results

Preoperative and postoperative comparisons

In the preoperative and postoperative pain assessment, leg pain values according to VASL decreased from

Table 1. ROC data for the diagnosis of VASB including PLR, NLR, MI-1, and MI-2

Variables	Area	SE[a]	Asymptotic Sig.[b]	95% CI	
				lower	upper
NLR	0.429	0.063	0.282	0.305	0.552
PLR	0.593	0.068	0.162	0.460	0.726
MI-1	0.726	0.058	0.001	0.612	0.840
MI-2	0.683	0.060	0.006	0.565	0.801

ROC – receiver operating characteristic; VASB – Visual Analogue Scale Back; NLR – neutrophil-to-lymphocyte ratio; PLR – platelet-to-lymphocyte ratio; CRP – C-reactive protein; MI – multiple index; SE – standard error; 95% CI – 95% confidence interval; [a] under the nonparametric assumption; [b] null hypothesis: true area = 0.5.

Table 2. Paired scale results before and after the surgery

Variables	Mean	SD	SE	95% CI		t	df	p-value
				lower	upper			
ODI	68.9	12.1	1.29	66.3	71.4	53.8	87	<0.001
RMDQ	12.79	3.33	0.35	12.1	13.5	36.1	87	<0.001
VASL	6.59	1.65	0.17	6.24	6.94	37.4	87	<0.001
VASB	2.18	1.87	0.2	1.78	2.57	10.9	87	<0.001
WD	−374.2	114.9	12.2	−398.5	−349.8	−30.5	87	<0.001

ODI – Oswestry Disability Index; RMDQ – Roland–Morris Disability Questionnaire; VASL – leg pain visual analog scale; VASB – back pain visual analog scale; WD – walking distance; SE – standard error; SD – standard deviation; 95% CI – 95% confidence interval; df – degrees of freedom.

8.02 ±1.5 to 1.32 ±0.9 (p < 0.001). Similarly, according to VASB, back pain values decreased significantly following the surgery (from 4.77 ±2.26 to 2.5 ±1.12; p < 0.001). The ODI values regressed from 82.9 ±7.9 preoperatively to 14 ±10.1 postoperatively (p < 0.001). Similar to ODI, RMDQ also showed a strong statistical decrease (from 17.9 ±3.2 to 5.14 ±2.5; p < 0.001). When examined in terms of WD, a strong increase was noted as a result of the surgery. The patients who could walk 57 ±23.1 m on average before surgery reached an average WD of 430 ±114 m postoperatively (p < 0.001). Scale values before and after surgery are given in Table 2.

Correlation with demographics

In the DIVD patients, the number of comorbidities (r = 0.729, p < 0.001) and length of hospital stay (r = 0.318, p < 0.001) showed a significantly positive correlation with age. While body mass index (BMI) was not associated with the length of hospital stay, it showed a significantly correlated increase for hospitalization duration (r = 0.318, p < 0.001), similarly to correlation with age. In the analysis of the correlation of BMI and age with MI-1 and MI-2, it was observed that these 2 parameters increased with increasing age (r = 0.344 and r = 0.317, respectively; p < 0.001) but were not related to BMI and comorbidity count. There was a strong positive correlation between the length of hospitalization and MIs (r = 0.613 and r = 0.741, respectively; p < 0.001). Follow-up time showed a weak correlation with MI-1 (r = 0.232, p = 0.029) and a stronger correlation with MI-2 (r = 0.321, p = 0.002).

Correlation with pain scales

The correlation analysis was performed between the scales and the indices (MI-1 and MI-2) before and after the operation. When comparing indices with ODI, no significant correlation was found in preoperative values, while a strong positive correlation (MI-1: r = 0.398, p < 0.001; MI-2: r = 0.285, p = 0.007) was found with ODI in the postoperative period. In comparison with the RMDQ, a positive relationship was found with the MI-1 index, regarding both preoperative (r = 0.257; p = 0.015) and postoperative (r = 0.501; p < 0.001) values. As regards MI-2, positive correlations were found with both preoperative (r = 0.294; p = 0.005) and postoperative (r = 0.378; p < 0.001) RMDQ values. In terms of VASL, neither preoperative nor postoperative scores were found to be correlated with MI-2; a weak (r = 0.227; p = 0.033) positive relationship was found between MI-1 and postoperative VASL only. However, a significant correlation was found between preoperative and postoperative VASB scores and both MI-1 (preoperative: r = 0.373, p = 0.001; postoperative: r = 0.232, p = 0.041) and MI-2 (preoperative: r = 0.388, p < 0.001; postoperative: r = 0.206, p = 0.044).

ROC analysis

The MI-1 index showed 71.4% sensitivity and 73.3% specificity when the cutoff value was set at 370, while the MI-2 index exhibited 78.6% sensitivity and 68.9% specificity when the cutoff value was set at 7.4. According to the ROC

curve values, while NLR and PLR indices are not effective diagnostic tools for VASB according to ROC curve values, MI-1 and MI-2 seem to be powerful diagnostic parameters (Table 2). The ROC data of VASB including PLR, NLR, MI-1, and MI-2 are presented in Table 1.

Discussion

Nowadays, when diagnostic costs have increased considerably and healthcare systems cause financial problems for governments and private institutions as a result of these costs, the need for cheap diagnostic parameters has increased more than ever. In this sense, since the investigated MIs are a strong indicator of inflammation, are very useful and have a low cost, their results and efficiency in DIVD patients shown in the present study will give them momentum to be used routinely before and after the surgery.

Although inflammation as a type of response mechanism to injury or damage to the skeletal system and related structures, inflammation plays a critical role in the development and worsening of DIVD.[11] In the tissue where chronic inflammation occurs, intense inflammatory secretion formed by cells such as macrophages and platelets is observed.[19] Recent studies have shown that hematological indices change as a result of the systemic inflammatory response and hematological indices are defining factors in the prognosis of various diseases and can be effectively used in follow-up.[4,13,19,20] Under these inflammatory conditions, the increasing neutrophil population can produce large amounts of nitric oxide, the effect of which has been shown regarding pain, resulting in worsening of the clinical condition.

Publications are showing that the measurement of neutrophils in the blood or the values of NLR can predict the outcome of diseases associated with the presence of inflammation.[13] In this manner, lymphocyte and platelet cells, similar to neutrophil cells, can secrete cytokines, which can further reduce the number and function of lymphocytes, and, in consequence, weaken immunological surveillance and defense.[10] In such a case, increased neutrophil-platelet and decreased lymphocyte count can be considered a response to systemic inflammation and accepted as a predictor and damage indicator.[14]

We acknowledged that systemic and local inflammatory conditions occurring around the skeletal system have a critical role in both development and healing of disc herniation. In a recent study, Ethemoğlu and Erkoç analyzed 126 patients with neck pain.[21] They recorded the PLR, NLR, and CRP, and compared them. The cervical disc hernia showed a higher CRP and NLR when compared to discs with a healthy MR image. In their study, comparing patients with cervical disc herniation to patients with neck pain, they found that in those with disc herniation, NLR and CRP were higher. The authors made a recommendation that early preventive approach applied by physicians in patients with high NLR and CRP may play a preventive

role in disc degeneration and hernia. In a study conducted by Bozkurt et al. to investigate the relationship between NLR and pain intensity, a significant positive correlation of VAS scores was found when they was used to assess pain in the preoperative and postoperative period in the patient group with lumbar disc hernia.[22] Although they found negative correlation coefficients between pain levels and preoperative VAS scores, they found a positive correlation between postoperative VAS and pain intensity. Bozkurt et al. assessed the relationship between NLR and pain severity in the preoperative and postoperative period using VAS in patients with lumbar disc herniation and found a significant positive correlation. Negative correlation coefficients were found between the serum urate (SU) levels and preoperative VAS scores; in contrast, positive correlation coefficients were found between the SU levels and the postoperative VAS scores.[22]

In our study, in preoperative and postoperative pain assessment, leg pain values according to VASL decreased following the surgery. Similarly, according to VASB, back pain decreased significantly following the surgery. Likewise, ODI and RMDQ showed a strong decrease after the surgery. When examined in terms of WD, a strong increase was noted as a result of the surgery. When the indices were compared with ODI, no significant correlation was found in preoperative values, while a strong positive correlation was found between the indices and ODI in the postoperative period. When the MIs were compared with the RMDQ, a positive correlation was found with the MI-1 index (with both preoperative and postoperative values). Similarly, regarding MI-2, positive correlations were found with both preoperative and postoperative RMDQ values. In terms of VASL, neither preoperative nor postoperative scores were found to be correlated with MI-2 scores. A significant correlation was found between preoperative and postoperative VASB scores and both MIs.

The MI-1 and MI-2, whose diagnostic value we investigated, are useful guides for us because they are cost-effective and easily accessible. In ROC analysis, the MI-1 showed 71.4% sensitivity and 73.3% specificity, while the MI-2 exhibited 78.6% sensitivity and 68.9% specificity. With the inclusion of CRP into both indices, they have become much stronger diagnostic indices than PLR and NLR. Thus, MI-1 and MI-2 are more objective markers than PLR and NLR, and paved the way for the use of MI in DIVD prognosis.

Limitations

There were also some limitations to the present study. First, as it is a retrospective cohort study, patients' selection bias may exist and the number of participants was limited due to the hospital records. The 2nd limitation is that hemogram results may be affected by some unexpected factors such as undetectable infections, abnormal blood circulation, local inflammation, and nutrition, and we were unable to measure

how it affected the index. We tried to obtain the best cutoff value using the ROC. However, the best approach to solve this problem is to perform a prospective, large, single-center study.

Conclusion

The assessment of the systemic inflammatory condition in DIVD may prove beneficial to predict preoperative and postoperative pain. The 2 MIs, MI-1 and MI-2, had a strong significant correlation with preoperative and postoperative VASB scores. They also allowed for a reliable prediction for the pain in the postoperative period in DIVD. These parameters could give surgeons an idea about the pre- and post-operative pain and inflammation in the patients, and thus they would provide cost-free gains in drug administration in order to alleviate pain before and after the operation, and in predicting the healing processes. In addition, the success of performed surgery measured in terms of pain can be an important issue that can be followed up indirectly. These indices are universally available, noninvasive and low-cost, and hence there is a perspective of their routine application.

ORCID iDs

Mustafa Nevzat Firidin https://orcid.org/0000-0002-0927-8848
Mehmet Emin Akyüz https://orcid.org/0000-0003-0626-3509

References

1. Samancı Y, Celik SE. Low back pain and internet: Infopollution. *Turk Neurosurg*. 2016;27(5):804–808. doi:10.5137/1019-5149.JTN.18521-16.1
2. McCormick ZL, Lehman VT, Plastaras CT, et al. Low-pressure lumbar provocation discography according to Spine Intervention Society/International Association for the Study of Pain Standards does not cause acceleration of disc degeneration in patients with symptomatic low back pain: A 7-year matched cohort study. *Spine*. 2019; 44(19):E1161–E1168. doi:10.1097/BRS.0000000000003085
3. Benzakour A, Benzakour T. Lumbar disc herniation: Long-term outcomes after mini-open discectomy. *Int Orthop*. 2019;43(4):869–874. doi:10.1007/s00264-019-04312-2
4. Goode AP, Schwartz TA, Kraus VB, et al. Inflammatory, structural, and pain biochemical biomarkers may reflect radiographic disc space narrowing: The Johnston County Osteoarthritis Project. *J Orthop Res*. 2020;38(5):1027–1037. doi:10.1002/jor.24534
5. Zhang C, Gullbrand SE, Schaer TP, et al. Inflammatory cytokine and catabolic enzyme expression in a goat model of intervertebral disc degeneration. *J Orthop Res*. 2020;38(11):2521–2531. doi:10.1002/jor.24639
6. Shen J, Xu S, Xu S, Ye S, Hao J. Fusion or not for degenerative lumbar spinal stenosis: A meta-analysis and systematic review. *Pain Physician*. 2018;21(1):1–8. PMID:29357326.
7. Ozaki M, Fujita N, Miyamoto A, et al. Impact of knee osteoarthritis on surgical outcomes of lumbar spinal canal stenosis. *J Neurosurg Spine*. 2020;32(5):710–715. doi:10.3171/2019.10.SPINE19886
8. Piccirilli M, Delfinis CP, Santoro A, Salvati M. Mesenchymal stem cells in lumbar spine surgery: A single institution experience about red bone marrow and fat tissue derived MSCs. *J Neurosurg Sci*. 2016;61(2): 124–133. doi:10.23736/S0390-5616.16.03266-X
9. Xu J, Ding X, Wu J, et al. A randomized controlled study for the treatment of middle-aged and old-aged lumbar disc herniation by Shis spine balance manipulation combined with bone and muscle guidance. *Medicine (Baltimore)*. 2020;99(51):e23812. doi:10.1097/MD.0000 000000023812
10. Sirin D, Ozcelik F, Uzun C, Ersahan S, Yesilbas S. Association between C-reactive protein, neutrophil to lymphocyte ratio and the burden of apical periodontitis: A case-control study. *Acta Odontol Scand*. 2019;77(2):142–149. doi:10.1080/00016357.2018.1522447
11. Gucyetmez B, Atalan HK. C-reactive protein and hemogram parameters for the non-sepsis systemic inflammatory response syndrome and sepsis: What do they mean? *PLoS ONE*. 2016;11(2):e0148699. doi:10.1371/journal.pone.0148699
12. Ozmen S, Timur O, Calik I, et al. Neutrophil-lymphocyte ratio (NLR) and platelet-lymphocyte ratio (PLR) may be superior to C-reactive protein (CRP) for predicting the occurrence of differentiated thyroid cancer. *Endocr Regul*. 2017;51(3):131–136. doi:10.1515/enr-2017-0013
13. Qin B, Ma N, Tang Q, et al. Neutrophil to lymphocyte ratio (NLR) and platelet to lymphocyte ratio (PLR) were useful markers in assessment of inflammatory response and disease activity in SLE patients. *Modern Rheumatol*. 2016;26(3):372–376. doi:10.3109/14397595.2015. 1091136
14. Bora Makal G, Yıldırım O. Are the C-reactive protein/albumin ratio (CAR), neutrophil-to-lymphocyte ratio (NLR), and platelet-to-lymphocyte ratio (NLR) novel inflammatory biomarkers in the early diagnosis of postoperative complications after laparoscopic sleeve gastrectomy? *Obes Res Clin Pract*. 2020;14(5):467–472. doi:10.1016/j.orcp. 2020.07.003
15. Koenders N, Rushton A, Verra ML, Willems PC, Hoogeboom TJ, Staal JB. Pain and disability after first-time spinal fusion for lumbar degenerative disorders: A systematic review and meta-analysis. *Eur Spine J*. 2019;28(4):696–709. doi:10.1007/s00586-018-5680-3
16. Fairbank JCT, Pynsent PB. The Oswestry Disability Index. *Spine*. 2000; 25(22):2940–2953. doi:10.1097/00007632-200011150-00017
17. Chiarotto A, Maxwell LJ, Terwee CB, Wells GA, Tugwell P, Ostelo RW. Roland-Morris Disability Questionnaire and Oswestry Disability Index: Which has better measurement properties for measuring physical functioning in nonspecific low back pain? Systematic review and meta-analysis. *Phys Ther*. 2016;96(10):1620–1637. doi:10.2522/ptj.20150420
18. Lane R, Ellis B, Watson L, Leng GC. Exercise for intermittent claudication. *Cochrane Database Syst Rev*. 2014;2014(4):CD000990. doi:10.1002 /14651858.CD000990.pub3
19. Suner A, Carr B, Akkiz H, et al. Inflammatory markers C-reactive protein and PLR in relation to HCC characteristics. *J Transl Sci*. 2018;5(3). doi:10.15761/JTS.1000260
20. Tekesin A, Tunç A. Inflammatory markers are beneficial in the early stages of cerebral venous thrombosis. *Arq Neuropsiquiatr*. 2019;77(2): 101–105. doi:10.1590/0004-282x20190001
21. Ethemoğlu KB, Erkoç YS. Is there any relationship between cervical disc herniation and blood inflammatory response? *Cureus*. 2020;12(8): e10161. doi:10.7759/cureus.10161
22. Bozkurt H, Arac D, Cigdem B. The effect of the preoperative uric acid level and neutrophil lymphocyte ratio on preoperative and postoperative visual pain scores in patients with lumbar disc hernia: A cross-sectional study. *Turk Neurosurg*. 2019;29(5):705–709. doi:10.5137/1019-5149.JTN.25897-19.2

The effect of breathing an oxygen-enriched mixture on tissue saturation in obese women

Agnieszka Ewa Zawada[1,A–D], Aldona Juchacz[2,A,C,D,F], Radosław Palutka[2,B,C], Karolina Zaleśna[2,C], Artur Drużdż[3,C,D,F], Agnieszka Dobrowolska[1,C,E,F], Katarzyna Domaszewska[4,A,B,D–F]

[1] Department of Gastroenterology, Dietetics and Internal Diseases, Poznan University of Medical Sciences, Poland

[2] Greater Poland Center of Pulmonology and Thoracic Surgery of Eugenia and Janusz Zeyland, Poznań, Poland

[3] 1st Department of Neurology, Józef Struś Multi-Specialist Municipal Hospital, Poznań, Poland

[4] Department of Physiology and Biochemistry, Poznan University of Physical Education, Poland

A – research concept and design; B – collection and/or assembly of data; C – data analysis and interpretation; D – writing the article; E – critical revision of the article; F – final approval of the article

Abstract

Background. Physical activity undertaken in the treatment process additionally increases the oxygen demand of the working muscles. It seems interesting to see whether a delivery of an enriched respiratory mixture can have an impact on lower acidification of working muscles and oxygenation of tissues.

Objectives. To assess tissue saturation and the level of acidification at rest and during exercise while breathing atmospheric air or an oxygen-enriched mixture.

Materials and methods. Tissue saturation and lactate concentration at rest and during exercise were assessed in 18 females with an average body mass index (BMI) of 42 kg/m^2. The study regimen was as follows: day 1 – cardiopulmonary exercise testing (CPET) – determination of the threshold load; day 2 – 20 min of physical effort on a cycloergometer (threshold load, breathing atmospheric air); day 3 – 20 min of physical effort on a cycloergometer (threshold load, breathing mixture enriched with oxygen). Saturation measurements were performed in 3 places on the patient's body by measuring absorbance via near-infrared spectroscopy (NIRS).

Results. A significant decrease in heart rate (HR) at rest was found when using the oxygen-enriched air mixture ($Z = 2.1339$, $p = 0.0328$ (effect size (ES) = 0.478)). During the exercise, a significant decrease in saturation was shown only for the midpoint of the quadriceps muscles ($Z = 2.1572$, $p = 0.309$ (ES = 0.600)). Medium effect sizes were shown by the difference in resting and exercising lactate concentration change between the experimental models studied ($Z = 2.5041$, $p = 0.0122$ (ES = 0.707)). In the experimental models studied, different medium effect sizes were demonstrated in the resting and exercising lactate concentration change.

Conclusions. Oxygen-enriched air mixture contributes to reducing hypoxia in working muscles of obese people. Oxygen supplementation can result in higher physical fitness levels. The implementation of oxygen-enriched air mixture is a promising therapeutic strategy for obese patients who exhibit high lactate concentrations after exercise.

Key words: obesity, tissue saturation, near-infrared spectroscopy (NIRS)

Background

Obesity as a chronic disease

Obesity is currently considered an increasingly severe social and health-related issue. World Health Organization (WHO) qualifies obesity as a chronic disease along with circulatory diseases, diabetes, cancer, and respiratory diseases. Treating excess weight and obesity remains a major challenge, faced by both doctors and patients. The primary treatment of obesity consists of exercise and diet. Pharmacological therapy or surgical interventions are recommended in cases where insufficient weight loss was achieved following primary treatment. It has been shown that obesity has a major impact on respiratory function. In obese people, a reduction in chest compliance due to adipose tissue and a rise of the diaphragm in the resting position caused by fat accumulation in the abdominal cavity results in a significant decrease in respiratory mobility. Additionally, the excess of adipose tissue leads to the collapse of soft tissues of the upper respiratory tract, causing respiratory disturbances during sleep and obstruction in the lower respiratory tract. This may promote the exacerbation of asthma and chronic obstructive pulmonary disease (COPD), which often coexist with obesity.[1] The described functional disorders manifest themselves in the form of decreased forced vital capacity (FVC), decreased functional residual capacity (FRC), decreased expiratory reserve volume (ERV), and decreased forced expiratory volume in 1 s (FEV1).[2] The consequences of impaired respiratory mechanics are ventilation disorders manifested by increased physiological venous leakage. The adequate ventilation/blood perfusion ratio is responsible for gas exchange in the lungs. Under physiological conditions, the ratio is higher in the upper lung fields (more ventilation, less perfusion), optimal in the middle parts and lower in the lower fields (less ventilation, more perfusion).

The lower lung fields represent a higher percentage of the mass involved in ventilation and thus they affect average gas exchange values. In line with the above data, obesity additionally impairs the lower lung ventilation. As a consequence of the increasing imbalance between perfusion and ventilation, gas exchange disturbances may lead to hypoxemia and, over time, hypercapnia. An increased oxygen concentration in respiratory mixtures reduces physiological venous leakage. There are numerous factors influencing the effectiveness of obesity therapy and treatment of excess weight.[3,4]

Oxygen as an important element in the treatment of obesity

The most important factor in the treatment of obesity seems to be the (individually dependent) metabolic rate. One of the most essential components in the metabolic process is oxygen. Moderate and long-lasting physical activity is associated with a higher metabolism rate of adipose tissue.[5] Combustion is carried out in the process of oxidative phosphorylation coupled with the respiratory chain and requires the adequate supply of oxygen to the cells. It has been proven that people with obesity require larger amounts of O_2 in order to carry out life functions at a basic level.[6] The increased demand for oxygen by working muscles is observable during incremental physical activity.[7] Kress and Hall confirmed that the use of oxygen at rest by people suffering from morbid obesity is 16% higher in comparison to people with proper body weight.[8,9] At the same time, their maximal O_2 uptake (VO_{2max}) is considerably lower. This might be due to a lower blood flow and metabolic rate at the muscular level. In patients with obesity, the factors limiting oxygen supply are respiratory dysfunctions, such as restriction and hypoventilation syndrome, leading to both hypoxia and hypoxemia. This condition is exacerbated during physical activity, leading to excessive purine nucleotide degradation, an increase in free radical transformation, and the acid-base disorder that increases fatigue symptoms. A decrease in oxygen content in arterial blood may reduce the exercise capacity in healthy individuals and in people with respiratory and circulatory diseases or anemia.[10–12] A significant mechanism, which is not fully understood, is the effect of oxygen levels on peripheral skeletal muscle fatigue induced by systemic exercise. Hyperoxia during moderate exercise in patients with COPD without hypoxemia affects the dynamics of the growth rate of oxygen consumption and reduces the transient increase in lactate. Furthermore, the lower demand for ventilation caused by O_2 supplementation is not correlated with the improvement of muscle function, but may result from the direct inhibition of chemoreceptors.[13] Studies have shown that the prevention of vigorous exercise-induced arterial hypoxemia significantly reduced quadriceps fatigue as assessed through stimulation of the femoral nerve before and after exercise.[14,15] A study by Amann et al. assessed whether peripheral muscle fatigue is sensitive to changes in arterial oxygen content during exercise. It was shown that hypoxia, normoxia and hyperoxia during strenuous systemic exercise influenced the rate of development of peripheral muscle fatigue.[16]

Bioenergetically, O_2 supplementation leads to an improvement in the phosphocreatine/inorganic phosphate ratio and the total adenosine triphosphate (ATP) content through more efficient oxidative metabolism associated with reduced lactate production and ATP decomposition with the simultaneous formation of harmful free radicals.[17] Andrade et al., based on an extensive analysis of studies on the effectiveness of O_2 supplementation during physical activity, showed less inflammation with a greater intensity of exercise achieved by the respondents.[18] Consequently, the use of oxygen supplementation in training people with respiratory failure was

implemented. Freitag et al. reached similar conclusions in their publication. He emphasized the importance of using air mixture enriched with oxygen in patients with numerous chronic diseases, such as obesity, during physical training.[19]

Hypothesis

The physiology of exercise is different in obese and lean people. In people with obesity, lactate accumulation and acidification occur faster during exercise. The accumulation of lactate reduces the possibility of further physical activity or its increased intensity. We hypothesize that respiration with an oxygen-enriched mixture leads to an alteration in saturation levels and positive metabolic changes in muscles during physical effort. Besides, increasing the amount of oxygen by preventing metabolic acidosis has a generally beneficial effect on the body. A study by Ehrsam et al. assessed the impact of metabolic acidosis on metabolism during exercise in healthy subjects and subjects with rheumatoid arthritis. Measurements were made at rest and during traning (at 30% and 60% of the maximum O_2 uptake (VO_{2max}), after 20 min). The study found that in hypercapnia, the metabolic effects of acidosis are modified by increased levels of circulating catecholamines, blood pressure and ventilation. The increased effect of circulating catecholamines, especially in obese patients, can cause many detrimental effects. Increasing the oxygen supply may counteract this outcome.[20]

Objectives

The aim of the study was to assess tissue saturation (abdominal fat around the navel and muscle tissue around the quadriceps muscle of the thigh and gastrocnemius muscle) at rest and during exercise while breathing atmospheric air or an oxygen-enriched breathing mixture.

Materials and methods

Patients were qualified by a physician (diabetologist) during a visit to the Metabolic Outpatient Clinic of the Heliodor Święcicki Clinical Hospital in Poznań, Poland. During qualifying visits, detailed interviews were conducted and the available medical documentation on concomitant illnesses was analyzed. A body composition analysis was made, as well as basic laboratory tests. In addition, during the visit, the patient signed a consent form to participate in the research. On the basis of these procedures, it was assessed whether the patient met the inclusion criteria outlined in Table 1.

Assessed for eligibility (n = 35)

Date of examination I
Excluded (n = 10)
10 people from the patients registered in the Metabolic Clinic were not able to perform the stress test on the first day of the study

Date of examination II
Excluded (n = 2)
2 people withdrew from the project after the exercise test

Date of examination III
Excluded (n = 5)
After the entire study, 5 men were excluded from further analysis due to the small size of this group

test group (n = 18)

Fig. 1. The course of patient recruitment

Table 1. Patient inclusion and exclusion criteria

Patient inclusion criteria	Patient exclusion criteria (presence of at least 1 of the factors listed below)
age above 18 years	positive electrocardiographic stress test, ischemic heart disease, unstable state after bypass surgery, implanted heart stimulator (cardioverter, defibrillator – ICD, heart pacemaker), endovascular prosthesis, patients after an ischemic or hemorrhagic stroke (<6 months), post-STEMI patients with a drug-eluting stent implantation, nSTEMI (<12 months)
increased content of overall adipose tissue measured with bioelectrical impedance method females: aged 20–39 years >33%, aged 40–59 years >34%, aged 60–70 years >37%. males: aged 20–39 years >20%, aged 40–59 years >22%, aged 60–70 years >25%[21]	antibiotic therapy, steroid therapy, (ongoing) drug/alcohol addiction (daily consumption of more than 1 portion of alcohol)
absence of diseases of the locomotor system preventing independent movement	patients with active or post cancerous disease (ongoing radiation/chemotherapy treatment), patients with liver diseases (ALT > 3 × border line) except for patients with fatty liver disease, CKD, eGFR < 30 mL/1.73 m^2/min, acute inflammation CRP > 5 mg/dL, inherited metabolic disorders: phenylketonuria, galactosemia, autoimmune diseases (acute thyroiditis, celiac disease, systemic connective tissue disease, hemolytic anemia, vitiligo, Addison's disease, hyperbilirubinemia), nonspecific enteritis (Crohn's disease, ulcerative colitis)
consent to take part in the study	pregnancy, psychological disorders, eating disorders such as anorexia or bulimia, a vegetarian or any other alternative diet

ICD – implanted cardiac device; (n)STEMI – (non-)ST-segment-elevation myocardial infarction; ALT – alanine transaminase; CKD – chronic kidney disease; eGFR – estimated glomerular filtration rate; CRP – C-reactive protein.

Table 2. Selected anthropometric factors and CPET results of the study group

Parameter	Average	Standard deviation	Median	IQR
Age [years]	39.9	14.4	33.5	29.0–50.0
Body height [m]	1.7	6.6	1.7	1.6–1.7
Body mass [kg]	113.8	18.9	115.5	97.0–125.0
BMI [kg/m^2]	41.8	7.4	42.0	36.1–45.2
WC [cm]	114.9	12.7	115.5	105.0–127.0
HC [cm]	132.4	9.5	134.0	130.0–138.0
WHR [n]	0.9	0.1	0.9	0.8–0.9
TBF [%]	64.0	82.5	44.6	41.7–49.5
TBF [kg]	52.6	14.7	51.3	40.6–59.5
FFM [kg]	65.9	11.2	64.2	56.8–71.8
MM [kg]	61.2	8.1	60.9	53.9–67.8
CPET results				
VO$_{2max}$ [mL/kg/min]	17.2	3.5	17.5	15.1–19.0
Load$_{max}$ [W]	120.0	21.3	117.5	102.0–144.0
HR$_{max}$ [beat/min]	135.0	23.8	142.5	112.0–156.0
Load$_{VT}$ [W]	68.8	17.7	50.0	60.0–80.0
HR$_{VT}$ [beat/min]	125.1	23.9	131.0	100.0–141.0

Values are presented as average ± standard deviation and median (IQR).
IQR – interquartile range; CPET – cardiopulmonary exercise testing;
BMI – body mass index; VO$_{2max}$ – maximal oxygen uptake;
HR$_{max}$ – maximum heart rate; HR$_{VT}$ – heart rate at VT; WC – waist
circumference; HC – hip circumference; WHR – waist-to-hip ratio;
TBF – total body fat; FFM – free fat mass; MM – muscle mass;
VT – ventilatory threshold.

Initially, 35 patients were qualified for the project. Seventeen patients were excluded from further procedures (Fig. 1). Tests were carried out in a group of patients (n = 18, all female), mean age 33 years (IQR: 29–50), body mass 115.5 kg, (IQR: 97–125), body height 1.7 m (IQR: 1.6–1.7), with an average body mass index (BMI) of 42 kg/m^2 (IQR: 36.1–45.2), who were hospitalized in Greater Poland Center of Pulmonology and Thoracic Surgery of Eugenia and Janusz Zeyland in Poznań, Poland. The characteristics of the study group are presented in Table 2. The study was conducted according to the Declaration of Helsinki and the National Statement and Human Research Ethics Guidelines, and was approved by Institute for Research in Biomedicine (IRB) at the Poznan University of Medical Sciences (ethis approval No. 429/17 from April 6, 2017). The study was conducted in the ergospirometry suite of the Greater Poland Center of Pulmonology and Thoracic Surgery of Eugenia and Janusz Zeyland over a period of 8 months (October 2018–June 2019). The exercise stress test laboratory was adequately equipped to provide advanced life support in the event of a cardiac arrest.

Body mass composition analysis

Component measurement of body mass in women was performed in the first phase of the cycle with bioelectrical impedance analysis (BIA).[21] All measurements were taken at 7 AM, patients were fasting for at least 9 h. The patients were instructed not to consume alcohol for at least 48 h prior to the test, not perform vigorous physical exercise for at least 12 h before, to avoid saunas for at least 12 h before, and to void the bladder 30 min before the test. Patients with implanted cardiac devices (ICDs, i.e., defibrillators), pacemakers or metal implants, epilepsy, hemiparesis, or with wounds or skin lesions on hands or feet were excluded from the study.

The body composition analyzer used for the measurements was a Tanita BC 980 (Tanita Corp., Tokyo, Japan). The body composition analyzer MC-980 MA (Tanita Corp.) is intended for professional use in specialized health centers, hospitals and medical institutions, as well as universities for research. The analyzer has the MDD CLASS IIa and NAVI CLASS III medical certificate required for the use of medical equipment in clinical setting. Eight integrated electrodes allow for performing analysis with segment reading. The current flows at 6 frequencies: 1 kHz, 5 kHz, 50 kHz, 250 kHz, 500 kHz, and 1000 kHz, which maximizes the accuracy of the measurements.

Among the body mass components, the following values were estimated: fat mass (FAT; kg and %) and muscle mass (MM; kg and %). Patient norms have been established based on previously published reports.[22] In order to perform the body composition test, it was necessary to measure 2 basic somatic features (body height in cm and body weight in kg), based on which the BMI was calculated.[23] The waist-to-hip ratio (WHR; ratio of waist circumference to hip circumference) was measured using anthropometric measuring tape. The measurement was taken 3 times and the average value was drawn.

Assessment of aerobic fitness

The exercise tests were conducted on the 1st day of the experiment between 8:00 AM and noon, in an air-conditioned laboratory, 2 h after consuming a light breakfast. The duration of the physical exercise was 20 min. The test was performed on a cycloergometer (Kettler® DX1 Pro; Kettler GmbH, Ense-Parsit, Germany), as follows: after a 3-minute warm-up with a load of 25 W, the load was increased by 10 W (60 RPM) every 90 s. The test lasted until refusal or inability to maintain the given cadence. On this day, the threshold load was determined for each patient with cardiopulmonary exercise testing.

Physiological measurements

Expired gases, minute ventilations (Ve) and heart rate (HR) during graded exercise test (GXT) were monitored continuously with an automated START 2000 M system (MES Sp. z o.o., Kraków, Poland). Oxygen intake (VO$_2$) and carbon dioxide output (VCO$_2$) were measured breath-by-breath and were averaged at 15-second periods. Before each trial, the system was calibrated according

to the manufacturer's instructions. Ambient conditions, including temperature, humidity and barometric pressure, were recorded by the sensors. With a 2-point volume calibration (0.2 L/s and 2 L/s), flow values were measured automatically at the set measuring points. The gas analyzer calibration was done using standard gas mixture containing 5% CO_2 and 16% O_2. To determine the threshold load (VT), the V-slope method was used, applying computerized regression analysis of the slopes of the CO_2 output compared to O_2 uptake plot, which detects the beginning of excess CO_2 output generated from the buffering of [H+]. This method involves the analysis of the behavior of VCO_2 as a function of VO_2 during GXT with a consequent increase in VCO_2. During the direct test, peak oxygen consumption (peakVO_2) was determined for each examined person.

Measurement of tissue saturation

The near-infrared spectroscopy (NIRS) method is based on the transparency of human tissue to light in the near-infrared range (700–1000 nm), which is dependent on the oxidation of oxyhemoglobin (HbO_2) and deoxyhemoglobin (Hb).[24] The depth of NIRS light penetration amounts to approx. 3 mm, which allows a camera to measure the level of skeletal muscle O_2 saturation (StO_2) in subcutaneous tissues.[25] The NIRS was used in our research to assess tissue oxygen saturation in 3 areas of the body. It was performed on days 2 and 3 of the experiment. On day 1, using the ergospirometric method, individual load levels were set for each patient. The exercise protocol included riding a cycloergometer (Kettler® DX1 Pro) with a 3-minute warm-up and a 25 W load, followed by an effort with a threshold load assigned individually for each patient (60 RPM) without oxygen (day 2) and after supplementation with oxygen-enriched air mixture with a flow rate of 6 L/min (day 3).[26–29] A description of the tests performed on the following days of the experiment is presented in Fig. 2. Rest measurements were taken on both day 2 and day 3 during a 5-minute rest before starting the exercise test, breathing the atmospheric air on day 2 and the oxygen-enriched air on day 3. For each person, the effort phase always lasted 20 min. The threshold load was on average 50.0 (IQR: 60.0–80.0) W. The oxygen-enriched air mixture with a flow rate of 6 L/min on day 3 was administered to the patient through a nasal catheter during exercise. Simultaneously, CO_2 retention was measured. In obese people, ventilation disorders such as restrictions are observed, resulting in decreased ventilation and a tendency to accumulate carbon dioxide. The decrease of StO_2 associated with exercise is a mechanism stimulating hyperventilation. If this mechanism is limited by oxygen supplementation in obese patients, hidden respiratory ventilation failure may appear and hypercapnia may be observed.

The saturation assessment was performed on each patient 2 times per day on days 2 and 3, at rest and during

---

DAY 1

- eligibility for the study (inclusion and exclusion criteria)
- BIA body composition analysis
- CPET and determination of threshold loads

DAY 2

- experiment – 20-minute exercise test without oxygen (WO)
- saturation, lactate and heart rate were measured before and after the exercise test

DAY 3

- experiment – 20-minute exercise test with oxygen (O)-enriched respiratory mixture
- before and after the exercise test lactate saturation and heart rate were measured

Fig. 2. Description of the tests on the following days of the experiment

BIA – bioelectrical impedance analysis; CPET – cardiopulmonary exercise testing.

---

exercise after stabilization. Saturation measurements were performed in 3 places on the patient's body by measuring absorbance via NIRS with the INOVOS 5100C device (Somanetics/Covidien, Mansfield, USA). The arrangement of the electrodes is shown in Fig. 3. Fat tissue thickness was assessed using ultrasound with a Siemens Acuson device (Siemens AG, Munich, Germany). This measurement was used to determine the place of saturation measurement. Blood lactate level, saturation and HR were measured at rest before and after the actual exercise test. During each trial, HR and blood lactate levels were also measured. Capillary blood lactate measurement was determined using the EDGE Blood Lactate Test Strip (ApexBio; Hsinchu, Taiwan), while HR was measured with a Nonin 8500 pulse oximeter (Nonin Medical, Inc., Plymouth, USA).

Statistical analyses

We calculated the sample size in the present study based on a study by Maltais et al.[12] They determined the effects of oxygen supplementation on the peak exercise capacity during exercise in COPD. After calculation power analysis of Mann–Whitney test (adopting a power as 1-beta error probability: 80%, effect size (ES): 0.98, and error assumed as alpha: 0.05 (2-sided)), 11 participants were indicated for allocation equally for each test. We decided to accrue more participants in each test due to a possible dropout. Therefore, the present study was initiated with 18 women. The distribution of normality was measured using the Shapiro–Wilk test. Because the hypothesis of normality of distribution was rejected (at $p < 0.05$) for

Fig. 3. Measurement of tissue saturation at the (A) midpoint of the quadriceps muscle, in the abdominal plane, on the right side; (B) 1/3 proximal part of the gastrocnemius muscle on the right calf; (C) 2 cm to the right of the umbilicus

many variables (13 of 52), nonparametric tests were used for analysis of all variables. A significance test for 2 mean values was performed using the Wilcoxon signed rank test, according to the assumption that population data do not follow a normal distribution and tested differences are symmetric with respect to a common median. The Spearman's rank analysis was used to calculate correlation coefficients. The level of statistical significance was set at $p \leq 0.05$. The obtained results were analyzed statistically using the Dell STATISTICA data analysis software system v. 13 (Dell Inc., Round Rock, USA).

Nonparametric ES was calculated according to the formula (where n is the total number of observations, and Z correlation coefficient is the same as the r coefficient between –1.00 to 1.00).[30]

The difference between means divided by the pooled standard deviation (SD) was calculated. Using Cohen's (1988) criteria, an effect size ≥ 0.20 and < 0.50 was considered small, ≥ 0.50 and < 0.80 medium, and ≥ 0.80 large.

Results

Table 2 presents the characteristics of the study group. The subjects displayed a high BMI of 42.0 kg/m^2 (36.1; 45.2). The level of cardiopulmonary fitness (VO$_{2max}$) was 17.5 mL/kg/min (15.1; 19.0) in the subjects, amounting to only approx. 50% of the expected value and being significantly reduced. The mean values of the threshold load for the study group are shown in Table 2.

The administration of additional breathing mixtures in obese patients resulted in a significant decrease in HR only at rest (Z = 2.1339, p = 0.0328, r = 0.3556). In response to an exercise with a threshold load, a lower effort increase was observed in the examined indicator without statistical significance (Z = 1.6805, p = 0.0928) (Table 3).

Measurements of saturation were performed in 3 areas of the body (point 1 – midpoint of the quadriceps muscle, in the abdominal plane, on the right side; point 2 – 1/3 proximal part of the gastrocnemius muscle on the right calf;

Table 3. Saturation at the 3 measurement points, HR and lactic acid level at rest and during exercises with and without supplementation of air mixture containing oxygen with a flow of 6 L/min

Parameter	Rest			Exercises			Δ rest-exercises WO group	Δ rest-exercises O group	p-value
	WO group n = 18	O group n = 18	p-value	WO group n = 18	O group n = 18	p-value			
LA [mmol/L]	1.9 ±1.2 2.1 (1.4–2.5)	1.9 ±1.2 1.4 (1.0–2.9)	0.8276	4.1 ±2.0 3.7 (2.3–6.0)	2.9 ±1.5 2.8 (1.7–4.0)	**0.0032**	2.1 ±1.6 1.7 (0.9–3.1)	1.1 ±1.3 0.8 (0.3–1.7)	**0.0122**
HR [beats/min]	77.7 ±12.2 79.0 (67.0–85.0)	71.4 ±14.2 66.5 (58.0–83.0)	**0.0328**	115.6 ±17.5 110.0 (102.0–133.0)	114.0 ±18.5 116.5 (97.0–126.0)	0.3318	37.8 ±14.8 33.5 (27.0–53.0)	42.7 ±16.8 45.5 (29.0–55.0)	0.0928
StO$_2$ [%] (meas. point 1)	72.8 ±7.9 75.0 (65.0–82.0)	69.8 ±9.8 70.0 (59.0–78.0)	0.9306	81.9 ±7.6 82.5 (78.0–88.0)	80.2 ±10.1 80.0 (71.0–90.0)	**0.0309**	9.0 ±9.6 8.0 (6.0–13.0)	10.4 ±12.4 7.0 (0.0–16.0)	0.1221
StO$_2$ [%] (meas. point 2)	82.9 ±10.6 86.5 (79.0–90.0)	82.3 ±9.2 85.0 (79.0–89.0)	0.1329	88.8 ±8.3 94.0 (84.0–95.0)	85.1 ±8.0 87.0 (77.0–91.0)	0.4379	6.7 ±9.3 5.0 (1.0–10.0)	2.8 ±8.2 2.5 (−2.0–5.0)	0.5694
StO$_2$ [%] (meas. point 3)	82.9 ±7.1 82.0 (80.0–87.0)	84.3 ±7.4 83.0 (79.0–90.0)	0.6495	85.1 ±5.5 83.0 (80.0–93.0)	85.4 ±4.8 87.0 (85.0–90.0)	0.8276	2.1 ±5.8 1.5 (−1.0–5.0)	1.1 ±6.8 1.0 (−5.0–7.0)	0.5521

Wilcoxon signed-rank test. Values are presented as average ± standard deviation (SD) and median (IQR); IQR – interquartile range; WO – without oxygen supplementation; O – oxygen supplementation; LA – lactic acid; HR – heart rate; StO$_2$ – oxygen saturation; meas. point 1 – measurement of tissue saturation at the midpoint of the quadriceps muscle in the abdominal plane, on the right side; meas. point 2 – measurement of tissue saturation at the 1/3 proximal part of the gastrocnemius muscle on the right calf; meas. point 3 – measurement of tissue saturation 2 cm to the right of the umbilicus. Values in bold are statistically significant.
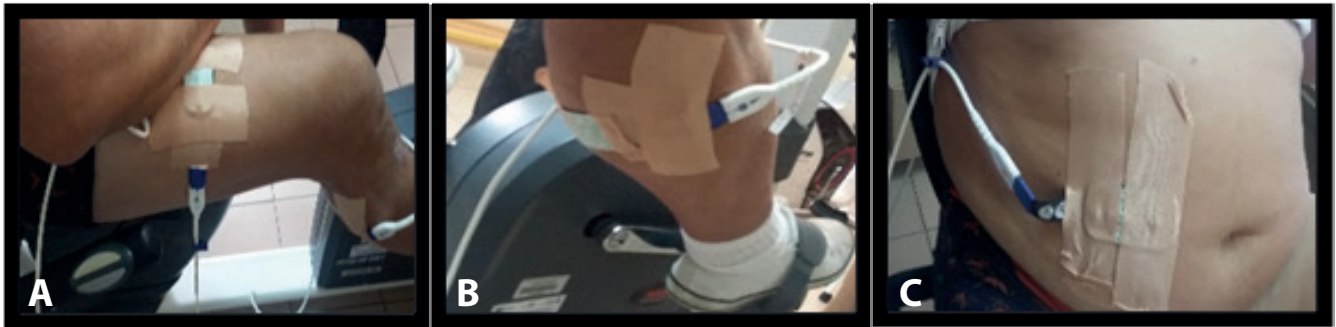
point 3 – 2 cm to the right of the umbilicus).[31,32] They were conducted at rest and during exercise, both without and with supplementation of an oxygen-enriched air mixture. A significant decrease in saturation was shown only for the midpoint of the quadriceps muscle (Z = 2.1572, p = 0.0309, r = 0.3595). No significant difference in oxygenation between the 2 experimental models was found (Table 3).

The experimental model did not demonstrate an effect of the administration of additional O_2 in the respiratory mixture on the resting lactate concentration in blood. However, the difference was statistically significant in the experimental model in which patients performed an effort at the level of individual threshold load, with and without administration of oxygen in the respiratory mixture (Z = 2.9394, p = 0.0032, r = 0.4899). In addition, medium effect sizes were shown in the difference in resting and exercising lactate concentration change between the experimental models studied (Z = 2.5041, p = 0.0122, r = 0.4174) (Table 3).

The Spearman's rank correlation showed a negative relationship between the exercise change in blood lactate concentration and tissue saturation at the midpoint of the quadriceps muscle only in the experiment without supplementation with an oxygen-enriched air mixture (p = 0.0185, r = −0.5631).

Discussion

People with obesity may present an impaired ability to use fat as fuel during moderate-intensity exercise. This may be associated with impaired mobilization of fat reserves, low activity of β-oxidation enzymes and low activity of skeletal muscle lipoprotein lipase.[33,34] Thus, obesity treatment should include interventions that can increase the ability of skeletal muscles to utilize fat. Endurance training in lean individuals causes increased fat oxidation during submaximal exercise at constant load.[35,36] Increased oxidation of resting fat after endurance training has also been shown.[37] Impaired ability to mobilize and utilize fat in obese individuals may suggest that physical training has a different effect on fat oxidation in obese and lean individuals. A study by van Aggel-Leijssen et al. evaluated the effect of physical exercise of different intensities on fat oxidation in obese men.[38] At rest, total fat oxidation did not change in any group. During exercise, after low intensity training, fat oxidation increased by 40% (p < 0.05). This was due to the increased oxidation of fatty acids outside the plasma (p < 0.05). Based on their research, they concluded that the total fat oxidation during exercise did not change during high-intensity training. It seems that in obese patients, only low-intensity training increases fat oxidation during exercise. A long-term exercise of an intensity corresponding to 60–80% of VO_{2max} leads to the depletion of glycogen stores in the muscle,

which is associated with fatigue. Insufficient energy supply results from the limited supply of the substrate (acetyl-CoA) to the Krebs cycle and increases fatigue during prolonged exercise.[39,40] The duration of exercise is also closely related to the pre-exercise glycogen content in the muscles. However, the effort tasks used in our study were not that intense, but tailored to the capabilities of a given patient. An important marker of fatigue in this type of exercises is lactic acid.

The energy of metabolic changes during low-intensity exercise is mainly based on O_2 mitochondrial changes. Unlimited access to oxygen contributes to the effectiveness of lipolytic changes. One of the products of metabolic changes having an inhibitory effect on the rate of lipolytic changes is lactate.

Low-intensity physical exercise does not cause a sharp increase in blood lactate concentration.[41] In healthy people, during exercise with a load of about 50–70% VO_{2max}, rapid accumulation of lactate in the blood is observed. High lactate concentration leads to the development of metabolic acidosis in the working muscle, thus limiting its exercise capacity.[42] This process, which in people who exercise regularly is a desirable phenomenon, in patients with reduced exercise tolerance leads to the development of changes due to fatigue at a low exercise load. As a result of the aforementioned changes in homeostasis, obese people are not able to fully implement training programs. It can be assumed that the supplementation of an oxygen-enriched air mixture proposed by us, administered intranasally during physical exercise, resulted in a decrease in blood lactate levels after an exercise test. A lower accumulation of lactate extends the duration of exercise due to the delayed development of metabolic acidosis in the working muscle. Thus, owing to a decrease in the production of lactate in the working muscle, a person is able to exercise for an extended period of time with an intensity below the individual threshold load. In addition, acidosis may also affect contraction efficiency by disrupting ATP production processes. Hydrogen ions also influence the activity of creatine kinase and other glycolytic enzymes – hence the indirect influence of acidosis on energy metabolism and the contraction process.[39] Decreasing intracellular pH may influence the level of oxidative enzyme activity and ryanodine receptor activity.[43] The best-known markers of muscle fatigue related to ATP metabolism are serum lactate, ammonia and oxypurines (xanthine and hypoxanthine). Elevated serum lactate is associated with insufficient aerobic ATP production, which must be supplemented by its anaerobic production. In non-fit people, the lactate threshold is at 50–60% of the maximum load, whereas in athletes it is as much as 70–90% of that load.

Serum lactate concentration does not increase with age or gender but with exercise intensity in healthy and non-healthy (e.g., with comorbidities) subjects.[44] During prolonged endurance exercise with constant stress, lactate levels usually rise by <5 mmol/L. However, this

parameter especially increases in patients with impaired oxidative phosphorylation (mitochondrial disorders) and lung diseases. It also increases significantly in people with COPD during a gradual exercise test on a cycloergometer.[45] Therefore, lactate level and an increase in calcium with a concomitant decrease in magnesium are very useful markers of fatigue following moderate-intensity exercise.[46]

After analyzing the literature, no studies on the validity and effectiveness of supplementation with an oxygen-enriched mixture in obese patients during physical training were found. On the other hand, the high effectiveness of the use of an oxygen-enriched breathing mixture in the training of patients with impaired respiratory efficiency has been demonstrated.

In the study by Nixon at al., a group of cystic fibrosis patients performed progressive exercise tests until exhaustion on a bicycle ergometer while breathing normoxic air (21% O_2) during one test and hyperoxic air (30% O_2) during another one. It has been shown that O_2 supplementation minimizes O_2 desaturation and allows cystic fibrosis patients to exercise with reduced ventilation and cardiovascular effort.[47] At rest, the body uses about 22% of oxygen, which is supplied to the tissues in arterial blood. During exercise, the O_2 consumption of working muscles increases, i.e., venous blood leaving the working muscles is far less oxygenated than when at rest. This difference can even be as high as 90%. The increase in oxygen extraction is highly beneficial upon analyzing changes at the mitochondrial level. The contracting muscle receives much more O_2 during a single blood passage, and deoxygenated hemoglobin is again saturated with oxygen in the lungs, which does not cause any side effects. The introduction of additional O_2 supplementation in the group of untrained, obese patients resulted in a decrease in saturation within the blood vessels of the muscle due to its increased uptake by mitochondria. This may be indicated by the metabolic response measured with blood lactate concentration in response to providing patients with an oxygen-enriched air mixture.[48] The meta-analysis conducted by Fiogbé et al. showed that physical exercise alone, depending on the patient's condition, improves the oxygenation of various muscle areas.[49] Oxygen supplementation may intensify this effect.

Oxygen supplementation has a major beneficial effect on the effectiveness of exercise in patients with COPD. A study by Rooyackers et al. examined whether training with O_2 supplementation enhances training effects during indoor air breathing in patients with severe COPD. The study showed that O_2 supplementation increases exercise tolerance in the maximum incremental test. Oxygen supplementation has an important ergogenic effect, and muscle damage caused by overload is positively correlated with overall muscle performance.[50]

The degree of muscle tissue deoxygenation during physical exercise was also assessed with NIRS in a study by Koga et al. They found that this method can accurately assess the temporal and spatial diversity of oxygenation.[51] This can be considered particularly consequential since earlier studies conducted with less complicated methods of measurement indicated that, at the onset of exercise, only a few seconds are required for the increase of oxygen uptake in exercising, while O_2 extraction peaks after 50 s of exercise. Bangsbo et al. claimed that insufficient oxygen availability is not the reason for limited O_2 utilization in the initial phase of intense exercise.[52] On a similar note, Segal et al. suggested that several motor units are supplied by individual activated microvascular units.[53] In these, increased blood flow can increase O_2 supply to muscle fibers, resulting in unchanged or increased O_2 saturation, as measured using NIRS. In addition, differences in tissue saturation may also apply to different muscle groups and their regions. This will depend on the blood flow, as well as contractions in blood vessels during exercise.

Over 95% of body fat is accumulated in adipose tissue and stored as triglycerides.[54] The metabolism of adipose tissue is influenced by hormones such as insulin and catecholamines, autocrine and paracrine factors, as well as nutritional status and exercise.[55] Physical effort causes an increase in lipolysis through a marked increase in catecholamine concentration; however, pronounced changes are most often observed only 30 min after the exercise commences.[56] Lipolysis intensification and acceleration is a particularly beneficial process, especially in people with obesity. In the obese patients examined in our research, it was observed that in the fat tissue in the abdomen at rest, there is an increase in saturation depending on O_2 supplementation. However, there is no change in tissue saturation during effort. Conversely, the 20-minute effort may be too short for significant changes in the metabolism of this tissue.

In the examined tissues (muscle and adipose tissue), there was a smaller effort increase in saturation in patients supplemented with an oxygen-enriched mixture. Thus, it can be concluded that there is an increase in the use of O_2 in the metabolism of working muscle and adipose tissues, which results in lower physical acidification of the body while performing the same effort. Such exercise exerts beneficial changes in metabolism and has an impact on reducing cardiovascular risk.[57]

The study also observed the effect of supplementation with an oxygen-enriched mixture on tissue saturation of fat located over working muscle (quadriceps muscle). A decrease in the saturation of this fat over working muscle was observed when supplementing an oxygen-enriched air mixture during exercise, while there was no change in fat oxygenation at rest. This confirms that better oxygenated fat tissue releases triglycerides to a greater extent, enhances lipid metabolism and fat burning. However, physical effort in this situation must last longer because of the increase in the intensity of lipolytic changes during the first 30 min of exercise in people with low aerobic capacity.[58]

The study group consisted of people with obesity or morbid obesity who trained rarely. In such persons, lipolysis in adipose tissue occurs only 20–25 min after the start

of exercise, while the average time of exercise in the study was 20 min. Oxygen supplied additionally to adipose tissue was not used up before the end of exercise, which indicates an increase in saturation in this tissue. On the other hand, the supply of additional oxygen to muscle tissue caused an enhanced O_2 use for metabolic changes, which increased the amount of energy obtained from oxygen processes and caused a decrease in blood lactate levels. The use of O_2 supplementation during exercise may be clinically significant. Oxygen supplementation can be used during physical activity, especially in patients preparing for bariatric surgery, when people who are often extremely obese must reduce their weight within a short period of time. It can be assumed that in these patients, the administration of O_2 during exercise can extend the time before significant acidification of the muscles is reached, and thus, enable them to exercise longer and more willingly, at the same time helping them to faster achieve the weight expected before operation.

According to the study by Andrade et al., the positive effect of O_2 supplementation cannot be attributed only to the improvement of the oxygen content in the blood and the reduction of HR.[18]

In addition, in terms of the analysis of cardiological parameters, a reduction in the resting frequency of heart contractions was found as a result of breathing an oxygen-enriched mixture. Arterial chemoreceptors located in the cervical glomeruli are the main recipients responding to changes in O_2 and CO_2 pressure in a hypoxic situation, increasing myocardial activity and causing tachycardia. Increased saturation of arterial blood leads to the inhibition of chemoreceptor stimulation and a decrease in HR at rest and during exercise. In the present study, people supplemented with an oxygen-enriched air mixture could therefore exercise for a prolonged period of time without a rapid increase in HR. Similarly, in a study by Nonoyama et al.,[59] oxygen supplementation in patients with COPD increased mean exercise time from 6 min to 14 min and caused significant improvement in Borg scale score after the shuttle walk test.

Based on the results of this study, it can be concluded that O_2 supplementation increases the use of oxygen in the mitochondria and intensifies the oxygen metabolic processes in the working muscle.

The use of this type of therapy in combination with optimized exercise can contribute to improve physical activity, reduce changes due to fatigue, and, as a consequence, lead to weight loss. The NIRS measurement method used in the study is a highly effective noninvasive method for monitoring tissue saturation in real time. In contrast to pulse oximetry, which indicates the saturation of hemoglobin in pulsating arterial blood, the onset of hypoxia may be delayed by up to 90 s. Unlike NIRS, arterial blood gas measurement is an invasive assessment that is delayed by the time needed to perform the laboratory analysis of the sample taken.

Limitation of the study

A limitation of this pilot study was the small number of patients qualified for the project and the absence of obese patients with restrictive respiratory disorders.

Conclusions

Lower increase in exercise saturation in muscle and fat tissues in patients supplemented with oxygen-enriched mixture may occur due to an increased use of oxygen during mitochondrial metabolic changes and lower acidification of the muscle under stress. Increased saturation of arterial blood due to supplementation with oxygen-enriched mixture leads to the inhibition of chemoreceptor stimulation and a decrease in HR at rest. Physical effort with peri-threshold intensity in conditions of increased O_2 supply led to less fatigue, and thus it may result in longer exercise routines in obese persons who get tired more easily. The supplementation of this respiratory mixture in addition to optimized exercise can result in improved physical fitness.

ORCID iDs

Agnieszka Ewa Zawada https://orcid.org/0000-0001-6995-090X
Aldona Juchacz https://orcid.org/0000-0003-1866-0536
Agnieszka Dobrowolska https://orcid.org/0000-0002-3647-5070
Katarzyna Domaszewska https://orcid.org/0000-0001-8117-1714

References

1. Redlarski G, Jaworski J. Modeling of respiratory mechanics in obesity. *PAK*. 2013;59(3):266–269. http://yadda.icm.edu.pl/baztech/element/bwmeta1.element.baztech-cffaf406-b7de-495c-870a-4864d96a09f0. Accessed on July 11, 2019.
2. Kushner RF, Witkowska M, Kumar Z, Olszanecka-Glinianowicz M, Lawrence V. *Otyłość: Podręczny podręcznik kliniczny*. Warszawa: Medipage; 2017. ISBN:978-83-64737-37-4.
3. Svendstrup M, Allin KH, Ängquist L, et al. Is abdominal obesity at baseline influencing weight changes in observational studies and during weight loss interventions? *Am J Clin Nutr*. 2018;108(5):913–921. doi:10.1093/ajcn/nqy187
4. Savastano S, Barrea L, Savanelli MC, et al. Low vitamin D status and obesity: Role of nutritionist. *Rev Endocr Metab Disord*. 2017;18(2):215–225. doi:10.1007/s11154-017-9410-7
5. Stanford KI, Goodyear LJ. Exercise regulation of adipose tissue. *Adipocyte*. 2016;5(2):153–162. doi:10.1080/21623945.2016.1191307
6. Rowland TW. Effects of obesity on aerobic fitness in adolescent females. *Am J Dis Child*. 1991;145(7):764–768. PMID:2058607.
7. Misquita NA, Davis DC, Dobrovolny CL, Ryan AS, Dennis KE, Nicklas BJ. Applicability of maximal oxygen consumption criteria in obese, postmenopausal women. *J Wom Health Gend Base Med*. 2001;10(9):879–885. doi:10.1089/152460901753285787
8. Kress JP, Hall JB. ICU-acquired weakness and recovery from critical illness. *N Engl J Med*. 2014;370(17):1626–1635. doi:10.1056/NEJMra1209390
9. Sarsan A, Ardiç F, Özgen M, Topuz O, Sermez Y. The effects of aerobic and resistance exercises in obese women. *Clin Rehabil*. 2006;20(9):773–782. doi:10.1177/0269215506070795
10. Gledhill N, Warburton D, Jamnik V. Haemoglobin, blood volume, cardiac function, and aerobic power. *Can J Appl Physiol*. 1999;24(1):54–65. doi:10.1139/h99-006

11. Gosselin N, Durand F, Poulain M, et al. Effect of acute hyperoxia during exercise on quadriceps electrical activity in active COPD patients. *Acta Physiol Scand*. 2004;181(3):333–343. doi:10.1111/j.1365-201X.2004.01290.x

12. Maltais F, Simon M, Jobin J, et al. Effects of oxygen on lower limb blood flow and O_2 uptake during exercise in COPD. *Med Sci Sports Exerc*. 2001;33(6):916–922. doi:10.1097/00005768-200106000-00010

13. Somfay A, Pórszász J, Lee SM, Casaburi R. Effect of hyperoxia on gas exchange and lactate kinetics following exercise onset in nonhypoxemic COPD patients. *Chest*. 2002;121(2):393–400. doi:10.1378/chest.121.2.393

14. Dempsey JA, Wagner PD. Exercise-induced arterial hypoxemia. *J Appl Physiol*. 1999;87(6):1997–2006. doi:10.1152/jappl.1999.87.6.1997

15. Romer LM, Haverkamp HC, Lovering AT, Pegelow DF, Dempsey JA. Effect of exercise-induced arterial hypoxemia on quadriceps muscle fatigue in healthy humans. *Am J Physiol Regul Integr Comp Physiol*. 2006;290(2):R365–R375. doi:10.1152/ajpregu.00332.2005

16. Amann M, Romer LM, Pegelow DF, Jacques AJ, Hess CJ, Dempsey JA. Effects of arterial oxygen content on peripheral locomotor muscle fatigue. *J Appl Physiol*. 2006;101(1):119–127. doi:10.1152/japplphysiol.01596.2005

17. Payen JF, Wuyam B, Levy P, et al. Muscular metabolism during oxygen supplementation in patients with chronic hypoxemia. *Am Rev Respir Dis*. 1993;147(3):592–598. doi:10.1164/ajrccm/147.3.592

18. Andrade DR, Pinto KC, de Castro JS, et al. Oxygen supplementation increases the total work and muscle damage markers but reduces the inflammatory response in COPD patients. *Respir Physiol Neurobiol*. 2020;280:103475. doi:10.1016/j.resp.2020.103475

19. Freitag N, Doma K, Neunhaeuserer D, Cheng S, Bloch W, Schumann M. Is structured exercise performed with supplemental oxygen a promising method of personalized medicine in the therapy of chronic diseases? *J Pers Med*. 2020;10(3):135. doi:10.3390/jpm10030135

20. Ehrsam RE, Heigenhauser GJ, Jones NL. Effect of respiratory acidosis on metabolism in exercise. *J Appl Physiol*. 1982;53(1):63–69. doi:10.1152/jappl.1982.53.1.63

21. Dehghan M, Merchant AT. Is bioelectrical impedance accurate for use in large epidemiological studies? *Nutr J*. 2008;7(1):7–26. doi:10.1186/1475-2891-7-26

22. Gallagher D, Heymsfield SB, Heo M, Jebb SA, Murgatroyd PR, Sakamoto Y. Healthy percentage body fat ranges: An approach for developing guidelines based on body mass index. *Am J Clin Nutr*. 2000;72(3):694–701. doi:10.1093/ajcn/72.3.694

23. Wyleżoł M, Gaździńska A, Kaniewska E, Mojkowska A. Proposal for an expanded classification of obesity severity according to body mass index (BMI) in patients referred for bariatric treatment. *Lekarz POZ*. 2016;2:123–125. https://www.termedia.pl/Propozycja-poszerzonej-klasyfikacji-stopnia-zaawansowania-otylosci-wedlug-wskaznika-masyciala-BMI-u-chorych-kierowanych-na-leczenie-bariatryczne,98,27541,1,0.html.c Accessed on July 11, 2019.

24. Bakker A, Smith B, Ainslie P, Smith K. Near-infrared spectroscopy. In: Ainslie P, ed. *Applied Aspects of Ultrasonography in Humans*. InTech; 2012. doi:10.5772/32493

25. Välisuo P, Kaartinen I, Tuchin V, Alander J. New closed-form approximation for skin chromophore mapping. *J Biomed Opt*. 2011;16(4):046012. doi:10.1117/1.3562976

26. Skrypnik D, Bogdański P, Mądry E, et al. Effects of endurance and endurance strength training on body composition and physical capacity in women with abdominal obesity. *Obes Facts*. 2015;8(3):175–187. doi:10.1159/000431002

27. Ratajczak M, Skrypnik D, Krutki P, Karolkiewicz J. Effects of an indoor cycling program on cardiometabolic factors in women with obesity vs. normal body weight. *Int J Environ Res Public Health*. 2020;17(23):8718. doi:10.3390/ijerph17238718

28. Domaszewska K, Koper M, Wochna K, et al. The effects of Nordic walking with poles with an integrated resistance shock absorber on cognitive abilities and cardiopulmonary efficiency in postmenopausal women. *Front Aging Neurosci*. 2020;12:586286. doi:10.3389/fnagi.2020.586286

29. Jamka M, Mądry E, Bogdański P, et al. The effect of endurance and endurance-strength training on bone mineral density and content in abdominally obese postmenopausal women: A randomized trial. *Healthcare*. 2021;9(8):1074. doi:10.3390/healthcare9081074

30. Tomczak M, Tomczak E. The need to report effect size estimates revisited: An overview of some recommended measures of effect size. *Trends Sport Sci*. 2014;1(21):19–25. http://tss.awf.poznan.pl/files/3_Trends_Vol21_2014__no1_20.pdf. Accessed on July 11, 2019.

31. Bredella MA. Sex differences in body composition. In: Mauvais-Jarvis F, ed. *Sex and Gender Factors Affecting Metabolic Homeostasis, Diabetes and Obesity*. Vol 1043. Advances in Experimental Medicine and Biology. Cham, Switzerland: Springer International Publishing; 2017:9–27. doi:10.1007/978-3-319-70178-3_2

32. Bentham Science Publisher BSP. Metabolic obesity: The paradox between visceral and subcutaneous fat. *Curr Diabetes Rev*. 2006;2(4):367–373. doi:10.2174/1573399810602040367

33. Blaak EE, Van Baak MA, Kemerink GJ, Pakbiers MT, Heidendal GA, Saris WH. Beta-adrenergic stimulation of energy expenditure and forearm skeletal muscle metabolism in lean and obese men. *Am J Physiol Endocrinol Metab*. 1994;267(2):E306–E315. doi:10.1152/ajpendo.1994.267.2.E306

34. Zurlo F, Nemeth PM, Choksi RM, Sesodia S, Ravussin E. Whole-body energy metabolism and skeletal muscle biochemical characteristics. *Metabolism*. 1994;43(4):481–486. doi:10.1016/0026-0495(94)90081-7

35. Sial S, Coggan AR, Hickner RC, Klein S. Training-induced alterations in fat and carbohydrate metabolism during exercise in elderly subjects. *Am J Physiol Endocrinol Metab*. 1998;274(5):E785–E790. doi:10.1152/ajpendo.1998.274.5.E785

36. Phillips SM, Green HJ, Tarnopolsky MA, Heigenhauser GJF, Hill RE, Grant SM. Effects of training duration on substrate turnover and oxidation during exercise. *J Appl Physiol*. 1996;81(5):2182–2191. doi:10.1152/jappl.1996.81.5.2182

37. Calles-Escandon J, Goran MI, O'Connell M, Nair KS, Danforth E. Exercise increases fat oxidation at rest unrelated to changes in energy balance or lipolysis. *Am J Physiol Endocrinol Metab*. 1996;270(6):E1009–E1014. doi:10.1152/ajpendo.1996.270.6.E1009

38. van Aggel-Leijssen DPC, Wim HM, Saris AJM, Wagenmakers,Senden JM, van Baak MA. Effect of exercise training at different intensities on fat metabolism of obese men. *J Appl Physiol*. 2002;92:1300–1309. doi:10.1152/japplphysiol.00030.2001

39. Sahlin K, Tonkonogi M, Söderlund K. Energy supply and muscle fatigue in humans: Energy supply and muscle fatigue. *Acta Physiol Scand*. 1998;162(3):261–266. doi:10.1046/j.1365-201X.1998.0298f.x

40. Äyrämö S, Vilmi N, Mero AA, et al. Maturation-related differences in neuromuscular fatigue after a short-term maximal run. *Hum Mov*. 2017;18(3):17–25. doi:10.1515/humo-2017-0027

41. De Feo P, Di Loreto C, Lucidi P, et al. Metabolic response to exercise. *J Endocrinol Invest*. 2003;26(9):851–854. doi:10.1007/BF03345235

42. Faude O, Kindermann W, Meyer T. Lactate threshold concepts: How valid are they? *Sports Med*. 2009;39(6):469–490. doi:10.2165/00007256-200939060-00003

43. Bellinger AM, Mongillo M, Marks AR. Stressed out: The skeletal muscle ryanodine receptor as a target of stress. *J Clin Invest*. 2008;118(2):445–453. doi:10.1172/JCI34006

44. Siegel AJ, Januzzi J, Sluss P, et al. Cardiac biomarkers, electrolytes, and other analytes in collapsed marathon runners: Implications for the evaluation of runners following competition. *Am J Clin Pathol*. 2008;129(6):948–951. doi:10.1309/4L0M60MGAQBCHMV7

45. Maltais F, Simard AA, Simard C, Jobin J, Desgagnés P, LeBlanc P. Oxidative capacity of the skeletal muscle and lactic acid kinetics during exercise in normal subjects and in patients with COPD. *Am J Respir Crit Care Med*. 1996;153(1):288–293. doi:10.1164/ajrccm.153.1.8542131

46. Finsterer J. Biomarkers of peripheral muscle fatigue during exercise. *BMC Musculoskelet Disord*. 2012;13(1):218. doi:10.1186/1471-2474-13-218

47. Nixon PA, Orenstein DM, Curtis SE, Ross EA. Oxygen supplementation during exercise in cystic fibrosis. *Am Rev Respir Dis*. 1990;142(4):807–811. doi:10.1164/ajrccm/142.4.807

48. Rall JA. Energetic aspects of skeletal muscle contraction: Implications of fiber types. *Exerc Sport Sci Rev*. 1985;13:33–74. PMID:3159582.

49. Fiogbé E, de Vassimon-Barroso V, de Medeiros Takahashi AC. Exercise training in older adults: What effects on muscle oxygenation? A systematic review. *Arch Gerontol Geriatr*. 2017;71:89–98. doi:10.1016/j.archger.2017.03.001

50. Rooyackers JM, Dekhuijzen PNR, Van Herwaarden CLA, Folgering HTM. Training with supplemental oxygen in patients with COPD and hypoxaemia at peak exercise. *Eur Respir J*. 1997;10(6):1278–1284. doi:10.1183/09031936.97.10061278

51. Koga S, Barstow TJ, Okushima D, et al. Validation of a high-power, time-resolved, near-infrared spectroscopy system for measurement of superficial and deep muscle deoxygenation during exercise. *J Appl Physiol*. 2015;118(11):1435–1442. doi:10.1152/japplphysiol.01003.2014

52. Bangsbo J, Krustrup P, González-Alonso J, Boushel R, Saltin B. Muscle oxygen kinetics at onset of intense dynamic exercise in humans. *Am J Physiol Regul Integr Comp Physiol*. 2000;279(3):R899–R906. doi:10.1152/ajpregu.2000.279.3.R899

53. Segal SS. Dynamics of microvascular complications n sceletal muscle: Exercise and circulation in health and disease. *Human Kinetics*. 2000;1:141–153.

54. Hurley BF, Nemeth PM, Martin WH, Hagberg JM, Dalsky GP, Holloszy JO. Muscle triglyceride utilization during exercise: Effect of training. *J Appl Physiol*. 1986;60(2):562–567. doi:10.1152/jappl.1986.60.2.562

55. Bergman BC, Butterfield GE, Wolfel EE, Casazza GA, Lopaschuk GD, Brooks GA. Evaluation of exercise and training on muscle lipid metabolism. *Am J Physiol Endocrinol Metab*. 1999;276(1):E106–E117. doi:10.1152/ajpendo.1999.276.1.E106

56. Romijn JA, Coyle EF, Sidossis LS, Rosenblatt J, Wolfe RR. Substrate metabolism during different exercise intensities in endurance-trained women. *J Appl Physiol*. 2000;88(5):1707–1714. doi:10.1152/jappl.2000.88.5.1707

57. Grassi B, Quaresima V, Marconi C, Ferrari M, Cerretelli P. Blood lactate accumulation and muscle deoxygenation during incremental exercise. *J Appl Physiol*. 1999;87(1):348–355. doi:10.1152/jappl.1999.87.1.348

58. Coyle EF, Jeukendrup AE, Wagenmakers AJ, Saris WH. Fatty acid oxidation is directly regulated by carbohydrate metabolism during exercise. *Am J Physiol Endocrinol Metab*. 1997;273(2):E268–E275. doi:10.1152/ajpendo.1997.273.2.E268

59. Nonoyama M, Brooks D, Lacasse Y, Guyatt GH, Goldstein R. Oxygen therapy during exercise training in chronic obstructive pulmonary disease. Cochrane Airways Group, ed. *Cochrane Database Syst Rev*. 2007;2010(1):CD005372. doi:10.1002/14651858.CD005372.pub2

Real-world diagnostic value of a nationwide standardized COVID-19 triage chart in Turkey

Reyhan Öztürk[1,A–F], Gokhan Tazegul[2,A–F]

[1] Department of Infectious Diseases and Clinical Microbiology, Ankara Polatlı Duatepe State Hospital, Turkey

[2] Department of Internal Medicine Clinic, Ankara Polatlı Duatepe State Hospital, Turkey

A – research concept and design; B – collection and/or assembly of data; C – data analysis and interpretation;
D – writing the article; E – critical revision of the article; F – final approval of the article

Address for correspondence
Gokhan Tazegul
E-mail: drgtazegul@gmail.com

Conflict of interest
None declared

Abstract

Background. Effective triage is critical during the coronavirus disease 2019 (COVID-19) pandemic. An appropriate triage plan is crucial to direct suspected COVID-19 cases to a designated area, in order to separate such patients from other patients and staff.

Objectives. To report the diagnostic value of the "Possible Coronavirus Disease 2019 (COVID-19) Case Questioning Guide for Outpatients", a nationwide standard triage chart, and of the individual questions within the triage chart for detecting COVID-19 in patients admitted to our hospital.

Materials and methods. A total of 39,681 outpatients admitted to our hospital between April 1 and April 30, 2021, underwent triage questioning. The triage chart consisted of 3 symptom questions and 4 contact and travel questions. Patients who responded "yes" to at least 1 question were referred to the pandemic area; others were considered low-risk and did not undergo routine COVID-19 polymerase chain reaction (PCR) test.

Results. Briefly, 3529 outpatients were referred to the pandemic area; among them, 1055 were PCR-positive. Among 36,152 low-risk patients, 94 were PCR-positive. The sensitivity of the triage chart was 91.82%, specificity was 93.58%, positive likelihood ratio was 14.30, and negative likelihood ratio was 0.09. Triage questions were in moderate agreement with PCR results (Cohen's Kappa: 0.429, p < 0.0001). The diagnostic value of the triage chart was mainly attributed to the questions regarding possible COVID-19 infection symptoms rather than contact history. However, the questions included in the triage chart had none to slight agreement with the PCR test results in the pandemic outpatients.

Conclusions. The triage chart has high sensitivity and specificity for discriminating possible COVID-19 cases in all outpatients, but has unsatisfactory diagnostic value for predicting PCR positivity in pandemic outpatients. Therefore, the current triage chart should be used accordingly, i.e., to define possible COVID-19 cases rather than PCR-positive cases. Further studies regarding COVID-19 triage for possible and PCR-positive cases should also focus on the individual diagnostic value of less prevalent symptoms.

Key words: COVID-19, coronavirus, triage, viral pneumonia

Background

Coronavirus disease 2019 (COVID-19) has become an important emerging health problem worldwide, as it spreads rapidly, causing a pandemic and a staggering number of deaths. To prevent transmission and spread, which is an essential step in fighting the disease, people who are suspected of COVID-19 infection should be tested and those diagnosed with the disease should isolate themselves early.[1,2]

Hospital transmission of COVID-19 is widely recognized, and although the mode of infection remains unclear, ward-based transmission is highly suspected.[3] Nosocomial transmission carries the risk of infecting susceptible patients with preexisting medical conditions, who are at higher risk of severe illness and death due to COVID-19 infection.[4] Since hospitals are among the areas where people with confirmed or suspected COVID-19 infection are likely to encounter other patients and spread the disease, patients should be assessed at the hospital entrance according to an appropriate triage plan, and patients who are suspected of COVID-19 infection should be directed to a designated pandemic outpatient area to separate them from other patients and staff. A fast and effective triage is critical for early treatment, cohorting and effective allocation of hospital resources.[5]

Objectives

Our hospital, a 300-bed secondary care center serving a population of approx. 300,000, underwent reorganization at a procedural level, and a designated triage unit has been established at the entrance to the hospital to screen and refer potential COVID-19 cases to the pandemic outpatient unit. Triage units of all hospitals in Turkey implemented a routine questioning tool for COVID-19 symptoms and contact using a standard triage chart named "Possible COVID-19 Case Questioning Guide for Outpatients", created by the Turkish Ministry of Health at the beginning of the COVID-19 pandemic. Although many studies identify predictors of critical illness,[6–9] the information about available criteria for identifying patients infected with COVID-19 in a triage setting is limited. In this study, we aimed to report the real-world data for the diagnostic value of the "Possible COVID-19 Case Questioning Guide for Outpatients" triage chart, and of the individual questions within this chart for detecting COVID-19 in patients admitted to our hospital.

Materials and methods

This retrospective descriptive study was conducted in adherence to the Declaration of Helsinki by obtaining data usage permission from Ankara Polatlı Duatepe State Hospital Administration (Ankara, Turkey). The researchers were provided with fully anonymized data for the study. The Etlik Zübeyde Hanım Gynecology Training and Research Hospital (Ankara, Turkey) Hospital Ethics committee approved this study (approval date: June 9, 2021, approval No. 62). The necessity of written informed consent was waived in this retrospective study.

Study setting

Since the beginning of the COVID-19 pandemic, all patients admitted to our center have been routinely questioned for COVID-19 contact and symptoms with a standard triage chart. The healthcare personnel routinely carried out this questioning using the "Possible COVID-19 Case Questioning Guide for Outpatients" triage chart while positioned at the hospital entrance, wearing a gown, medical mask, face shield, and goggles. During the triage procedure, healthcare personnel also measured each patient's temperature [°C] and peripheral capillary oxygen saturation (SpO_2). The "Possible COVID-19 Case Questioning Guide for Outpatients" triage chart consists of 7 questions: the first 3 questions concern the patient's complaints, and the subsequent 4 questions cover the contact and travel history. The 7 questions are as follows:

1) Do you have a fever or a history of fever?
2) Do you have a cough?
3) Do you have shortness of breath, sore throat, headache, myalgia, loss of taste and smell, or diarrhea?
4) Have you been abroad in the last 14 days?
5) Have any of your relatives/household members come from abroad in the last 14 days?
6) Have any of your relatives/household members been hospitalized for respiratory disease in the last 14 days?
7) Have any of your relatives/household members been diagnosed with COVID-19 in the last 14 days?

Data acquisition

The COVID-19 triage charts of all outpatients admitted to our hospital between April 1 and April 30, 2021, were evaluated retrospectively. No exclusion criteria were employed; triage questioning was applied to all patients during the study period, including those with severe illness (e.g., intubated, unresponsive patients). As a hospital rule, data regarding the patient's symptoms and travel and contact history were obtained from the patient's relatives if the patient was unresponsive. In rare instances where it was not possible to obtain a clear history, severely ill patients were assumed to have a positive triage questioning and were referred to the pandemic outpatient clinic. Patients who responded "yes" to at least 1 of the questions during the triage were referred to the pandemic outpatient clinic located within an isolated area of the hospital. The age and gender of these patients, temperature and SpO_2 measurements, answers to the questions in the triage chart, and polymerase chain reaction (PCR) test results were collected

retrospectively from the data in the triage charts. Patients with a fever higher than 38.2°C were considered positive for question 1, and patients with a SpO_2 lower than 92% were considered positive for question 3. After triage, cases of all patients with suspected COVID-19 were discussed by a multidisciplinary team consisting of consultants in internal medicine, infectious disease and pulmonology, and were diagnosed and treated according to the recommendations of Turkish Ministry of Health. A COVID-19 PCR test served as a standard for diagnosis. In the case of an initial negative or indeterminate PCR assay, repeat testing was routinely performed at intervals of 1 day or more. Among these patients, those found to be PCR-positive for any reason within 14 days of initial hospital admission were considered positive for COVID-19 infection and positive for the COVID-19 triage, and treated accordingly. Patients who responded "no" to all 7 questions were considered low-risk during triage; such patients were directed to a relevant clinic to be examined further. Low-risk patients did not undergo routine PCR screening; it was ordered only if a patient was in preoperative evaluation, developed a new symptom or if contact screening was necessary. Among such patients, those found to be PCR-positive for any reason within 14 days of initial hospital admission were considered positive for COVID-19 infection and false negative for the COVID-19 triage, and treated accordingly.

Triage results were analyzed using a 2-step approach. First, the sensitivity, specificity, and positive and negative likelihood ratios of the triage chart for COVID-19 infection were assessed as a whole. Second, all individual questions on the triage chart were separately analyzed for sensitivity, specificity, and positive and negative likelihood ratios within the triage-positive patient group and all admitted patients.

Statistical analyses

The SPSS statistical software (IBM SPSS for Windows v. 23.0; IBM Corp., Armonk, USA) and MedCalc Diagnostic Test Evaluation Calculator (MedCalc Software, Ostend, Belgium) were used for data analysis. Continuous variables were expressed as mean and standard deviation (SD), and categorical data were expressed as values and percentages. In the comparative analysis, χ^2 tests were performed for the categorical data. Sensitivity and specificity (presented as percentages) and positive and negative likelihood ratios (with 95% confidence intervals (95% CIs)) were calculated using MedCalc online Diagnostic Test Evaluation Calculator (https://www.medcalc.org/calc/diagnostic_test.php). Confidence intervals for sensitivity and specificity were "exact" Clopper–Pearson CIs, while CIs for the likelihood ratios were calculated using the "log method".[10,11] The receiver operator characteristics (ROC) curve analysis and curve method were used to determine the area under the curve (AUC). An inter-rater reliability analysis using Cohen's kappa statistic was performed to determine the consistency between the triage questions and PCR results. For all statistical tests, $p < 0.05$ was accepted as the limit of statistical significance.

Results

A total of 39,681 outpatients were admitted to our hospital between April 1 and April 30, 2021. All patients have undergone "Possible COVID-19 Case Questioning Guide for Outpatients" triage questioning. Of the 39,681 patients, 22,181 (55.8%) of the patients were male, and 17,500 (44.2%) were female. The mean age of the patients was 38.1 ±15.8 years.

Following the triage, 3529 patients (8.8% of all admissions) were referred to the pandemic outpatient clinic. Of these patients, 1055 (29.9% of the patients referred to the pandemic outpatient clinic and 2.6% of all admissions) were PCR-positive. Among the 36,152 patients who were considered low-risk after triage questioning, 94 patients (0.26% of low-risk patients and 8.1% of all PCR-positive cases) were found to be PCR-positive for COVID-19. The responses to the questions from the "Possible COVID-19 Case Questioning Guide for Outpatients" chart are presented in Table 1. The most common positive responses concerned

Table 1. Responses to the questions for "Possible COVID-19 Case Questioning Guide for Outpatients" triage chart

Question	Yes, n	Positive % within pandemic outpatients	Positive % within all outpatients
Q1: Fever or a history of fever	996	28.2	2.5
Q2: Cough	2164	61.3	5.4
Q3: Shortness of breath, sore throat, headache, myalgia, loss of taste and smell, or diarrhea	2566	72.2	6.4
Q4: Abroad travel in the last 14 days	5	0.14	0.012
Q5: Relative/household member came from abroad in the last 14 days	3	0.085	0.0075
Q6: Relative/household member hospitalized for respiratory disease in the last 14 days	35	1	0.08
Q7: Relative/household member diagnosed with COVID-19 in the last 14 days	467	13.2	1.17

COVID-19 – coronavirus disease 2019.

968

R. Öztürk, G. Tazegul. COVID-19 triage chart

the symptoms of coughing (Q2) and shortness of breath, sore throat, headache, myalgia, loss of taste and smell, or diarrhea (Q3). Positive responses to the COVID-19 contact questions comprised fewer than 1%, apart from the question about relatives/household members diagnosed with COVID-19 in the last 14 days (Q7).

Diagnostic test evaluation for the triage chart

Of the 3529 patients referred to the pandemic outpatient clinic for further examination, 1055 PCR-positive patients were considered true positive cases; the remainder were considered false positive for the diagnostic performance of the triage chart. Among the 36,152 patients considered low-risk after triage questioning, 94 patients who were PCR-positive for COVID-19 were considered false negative cases; the remainder were considered true negative cases. The sensitivity of the triage chart was 91.82% (95% CI: [90.08%; 93.34%]); the specificity was 93.58% (95% CI: [93.33%; 93.82%]); the positive likelihood ratio was 14.30 (95% CI: [13.71; 14.91]); and the negative likelihood ratio was 0.09 (95% CI: [0.07; 0.11]). The ROC analysis determined an AUC of 0.927 (95% CI: [0.918; 0.936]). The Cohen's kappa between the PCR and the triage questions showed a moderate agreement (kappa value: 0.429, $p < 0.0001$).

Diagnostic test evaluation for individual triage questions

Seven questions included in the "Possible COVID-19 Case Questioning Guide for Outpatients" triage chart were individually compared with the COVID-19 PCR positivity. Only the answers to the first 3 questions, which pertain the patients' complaints, were significantly different between the PCR-negative and the PCR-positive patients. The distribution of answers to the other 4 questions about the contact and travel history was similar between the groups.

Sensitivity, specificity, and positive and negative likelihood ratios for the first 3 triage questions were calculated using a 2-step approach. To obtain the sensitivity, specificity, and positive and negative likelihood ratio data for the pandemic outpatient clinic cases, the data presented in Table 2 served as the basis for calculation. To obtain the sensitivity, specificity, and positive and negative likelihood ratio data for all outpatients, true positive and false positive case data were based on the data presented in Table 2. Among the 36,152 patients considered low-risk after triage questioning, 94 patients who were PCR-positive for COVID-19 were considered false negative cases; the remainder were considered true negative cases. Questions 4–7 were not included in the analysis due to a low number of positive responses and similar percentages of positive and negative responses in the PCR-positive and PCR-negative pandemic outpatient cases.

Overall, question 3, which included several symptoms (shortness of breath, sore throat, headache, myalgia, loss of taste and smell, or diarrhea), had the highest sensitivity and negative likelihood ratio. Question 1 (fever and a history of fever) had the highest specificity and positive likelihood ratio. In this instance, Cohen's kappa, which demonstrates inter-rater agreement, showed none to slight agreement between the PCR results and the triage

Table 2. Frequency and percentage distribution of responses to individual triage questions in relation to PCR results of patients referred to the pandemic outpatient clinic, as compared using χ^2 tests

| Question | Answer | PCR result | | χ^2 test | p-value |
		negative (2474) n (%)	positive (1055) n (%)		
Q1: Fever or a history of fever	no	1860 (75.2)	673 (63.8)	47.368	<0.001
	yes	614 (24.8)	382 (36.2)		
Q2: Cough	no	1014 (41)	351 (33.3)	18.566	<0.001
	yes	1460 (59)	704 (66.7)		
Q3: Shortness of breath, sore throat, headache, myalgia, loss of taste and smell, or diarrhea	no	711 (28.7)	252 (23.9)	8.778	0.002
	yes	1763 (71.3)	803 (76.1)		
Q4: Abroad travel in the last 14 days	no	2471 (99.9)	1053 (99.8)	0.244	0.47
	yes	3 (0.1)	2 (0.2)		
Q5: Relative/household member came from abroad in the last 14 days	no	2473 (99.9)	1053 (99.8)	1.937	0.21
	yes	1 (0.1)	2 (0.2)		
Q6: Relative/household member hospitalized for respiratory disease in the last 14 days	no	2446 (98.9)	1048 (99.3)	1.652	0.13
	yes	28 (1.1)	7 (0.7)		
Q7: Relative/household member diagnosed with COVID-19 in the last 14 days	no	2155 (87.1)	907 (86)	0.829	0.19
	yes	319 (12.9)	148 (14)		

PCR – polymerase chain reaction; COVID-19 – coronavirus disease 2019.

Table 3. Diagnostic value of individual triage questions, presented as sensitivity and specificity percentages, and positive and negative likelihood ratios (with 95% confidence intervals (95% CIs) calculated using exact Clopper–Pearson method for sensitivity and specificity and log method for likelihood ratios), receiver operating characteristic (ROC) area under the curve (AUC) measurements; and inter-rater reliability, calculated using the Cohen's kappa statistic, of patients referred to the pandemic outpatient clinic and all outpatients

Question	Patients	Sensitivity [%] (95% CI)	Specificity [%] (95% CI)	Positive likelihood ratio (95% CI)	Negative likelihood ratio (95% CI)	ROC AUC (95% CI)	p-value for ROC AUC	Cohen's kappa (95% CI)	p-value for Cohen's kappa
Q1: Fever or a history of fever	pandemic outpatients	36.2 [33.3; 39.1]	75.1 [73.4; 76.8]	1.46 [1.31; 1.62]	0.85 [0.81; 0.89]	0.577 [0.536; 0.578]	<0.001	0.116 [0.082; 0.149]	<0.001
	all outpatients	33.2 [30.5; 36.0]	98.4 [98.2; 98.5]	20.86 [18.63; 23.37]	0.68 [0.65; 0.71]	0.658 [0.639; 0.677]	<0.001	0.338 [0.312; 0.363]	<0.001
Q2: Cough	pandemic outpatients	66.7 [63.8; 69.5]	40.9 [39.0; 42.9]	1.13 [1.07; 1.19]	0.81 [0.74; 0.90]	0.539 [0.518; 0.559]	<0.001	0.059 [0.031; 0.086]	<0.001
	all outpatients	61.2 [58.3; 64.1]	96.2 [96.0; 96.4]	16.17 [15.11; 17.31]	0.4 [0.37; 0.43]	0.787 [0.770; 0.805]	<0.001	0.402 [0.380; 0.423]	<0.001
Q3: Shortness of breath, sore throat, headache, myalgia, loss of taste and smell, or diarrhea	pandemic outpatients	76.1 [73.4; 78.6]	28.7 [26.9; 30.5]	1.07 [1.02; 1.11]	0.83 [0.73; 0.94]	0.524 [0.504; 0.545]	0.022	0.034 [0.012; 0.055]	0.003
	all outpatients	69.8 [67.1; 72.5]	95.4 [95.2; 95.6]	15.27 [14.39; 16.21]	0.32 [0.29; 0.34]	0.827 [0.811; 0.843]	<0.001	0.409 [0.389; 0.428]	<0.001

questions for the pandemic outpatients. Questions 2 and 3 showed moderate agreement, whereas question 1 showed fair agreement between the PCR results and the triage questions for all outpatients (Table 3).

Discussion

Effective triage is essential for preventing the transmission and ensuring rapid isolation of probable or definite cases in fighting the COVID-19 pandemic. The triage involves not only a ranking based on importance, but also an appropriate allocation of limited medical resources and isolation of highly contagious cases to limit the spread of the disease to other patients and healthcare workers.[12] Moreover, it was previously hypothesized that using a telephonic triage and asking the patients to delay hospital admissions for 14 days if they have symptoms such as fever, cough or shortness of breath, travel or contact history, could reduce in-hospital COVID-19 positivity.[13] Although the Turkish medical system does not discourage admitting patients to the hospital during the pandemic, the "Possible COVID-19 Case Questioning Guide for Outpatients" triage chart is utilized as a tool to triage possible COVID-19 cases to the relevant areas within the hospital. Herein, we aimed to report the real-world data for the diagnostic value of the triage chart and the individual questions in the triage chart for detecting COVID-19 PCR positivity in patients admitted to our hospital.

In a triage setting outside the hospital, patients can be directed to the pandemic outpatient clinic using the questions about symptoms and contact history. The literature suggests that patients are considered low-risk in the absence of COVID-19-related symptoms.[5] Our results show that positive responses to the questions regarding possible COVID-19 symptoms are much more frequent than

positive responses to questions concerning contact history. In the context of selecting possible COVID-19 cases from all outpatients, the triage chart showed high sensitivity and specificity, with an AUC of 0.927 and moderate agreement with PCR positivity. However, the contact history questions are rarely positively responded by patients; therefore, these results are mainly based on patients' symptoms. Moreover, these results reflect real-world data; since no routine PCR screening was conducted in all outpatients, the absolute diagnostic values would be expected to be lower than the current results. In contrast, the individual questions of the triage chart showed unsatisfying AUCs, and none to slight agreement with PCR results within pandemic outpatients. Although the triage chart is used to select possible cases that should be referred to pandemic area, this result limits the practical application of the triage chart.

Patients infected with COVID-19 may present with a broad spectrum of mild to severe symptoms. Flu-like symptoms, fever, headache, dry cough, myalgia, loss of taste and smell, sore throat, fatigue, and diarrhea are the most frequently noted mild symptoms. More severe manifestations, such as dyspnea, bilateral viral pneumonia, acute respiratory distress syndrome, and respiratory failure, may also be observed. In various studies, the most common symptoms of COVID-19 were fever (83–98% of patients) and cough (66–82%).[14–19] However, using fever as a marker for PCR positivity yielded unsatisfactory results. A literature review reported that while 85% of patients with COVID-19 had fever during the infection, only 45% had fever in the early period. Using fever as a marker of PCR positivity among oncological and transplant patients had a sensitivity of 15.09%, and a cutoff point of 37.3°C for fever had low validity for PCR positivity. Of the 5231 individuals screened, 49 tested positive for fever, of which only 5 were PCR-positive. In comparison, 48 patients were PCR-positive

without a fever. The sensitivity of fever for PCR positivity was 9.43% (95% CI: [3.13; 20.66%]), whereas the specificity was 99.15% (95% CI: [98.86%; 99.38%]).[20] Similarly, our results demonstrate that fever or a history of fever was positive in 36.2% of PCR-positive pandemic outpatient cases, whereas it was also positive in 24.8% of PCR-negative pandemic outpatient cases. Therefore, fever or a history of fever has low diagnostic value for choosing patients for the pandemic area or PCR positivity. Cough also yielded unsatisfactory results, with a higher sensitivity and lower specificity than fever.

Other symptoms related to COVID-19, namely shortness of breath, sore throat, headache, myalgia, loss of taste and smell, or diarrhea were considered as a whole in the "Possible COVID-19 Case Questioning Guide for Outpatients" triage chart. Several studies reported that between 5% and 85% of infected patients lose their sense of smell.[21] Other symptoms, such as shortness of breath, are seen in 18–55% of infected patients, and myalgia and fatigue in 11–44%. Confusion, sore throat, nasal discharge or congestion, chest pain, diarrhea, nausea and vomiting, hemoptysis, and headache are observed in less than 10% of infected patients.[14,16,19] Since the question included in the triage chart is an umbrella question and covers symptoms as a whole, we could not perform an analysis of individual symptoms. However, these symptoms had the highest positivity rate among the triage chart questions.

There is a paucity of data in the literature regarding triage charts as a tool to single out possible COVID-19 cases and the association of triage charts with PCR positivity. A Saudi Arabian study that evaluated the prediction of a positive PCR test using a triage chart reported that the sensitivity, specificity, positive predictive value, and negative predictive value were 64%, 55.7%, 31.1%, and 83.2%, respectively.[22] A ROC curve analysis reported AUC value of 0.60 (95% CI: [0.57; 0.64]). Male sex, being a healthcare worker or their family member, and fever were predictive of PCR positivity.[22] Another similar triage study was conducted by Mansella et al., who reported that COVID-19 PCR positivity was significantly associated with symptoms such as fever, cough, myalgia, and headache; however, symptoms such as dyspnea, wheezing and sore throat have been reported as having a significant association with PCR negativity.[23] A risk tool developed by Lundon et al., which includes body mass index (BMI), age, gender, and temperature, had an AUC of 0.77 for COVID-19 positivity.[24] A Qatar-based study presented a scoring system based on a logistic regression model using predictors identified by random forest, which includes emergency department indicators (demographic data, chief complaint and vital signs) for COVID-19 positivity; the model had a 5.9 positive likelihood ratio and a 19.3 negative likelihood ratio at different cutoff points.[25] In contrast to these studies, a similar scoring system from southern Tunisia, which included contact history, fever, cough and/or dyspnea, sore throat, nausea/vomiting/diarrhea, renal/respiratory, or cardiac failure,

had insufficient AUC to discriminate COVID-19 cases.[26] Our results demonstrate that the "Possible COVID-19 Case Questioning Guide for Outpatients" triage chart had high sensitivity and specificity value as a whole, with a considerable AUC for discriminating possible COVID-19 cases, similar to the currently published literature. However, it had an unsatisfactory diagnostic value for predicting PCR positivity in patients referred to the pandemic outpatient area, underlying a poor correlation with PCR positivity within possible cases. Although fever was reported to have low sensitivity and specificity,[20] several triage chart studies and our study included fever as an item for triage.[22–24] The differences regarding the diagnostic performance of triage charts can be explained by the way the triage charts are implemented, as the "Possible COVID-19 Case Questioning Guide for Outpatients" considers any question answered positively as a possible case, whereas others require multiple items and a cutoff for positivity.[22,24] Moreover, triage charts also differ regarding the way of inclusion of symptoms and contact history. Also, positive symptomatology and cultural differences in defining contact history may influence the results.

Limitations

There are certain limitations to our study. First, due to the retrospective nature of our study, only the triage charts and patient COVID-19 PCR outcomes were available without data loss. Second, we were unable to break down and individually analyze symptoms in question 3 within the "Possible COVID-19 Case Questioning Guide for Outpatients" triage chart, which is an umbrella question including shortness of breath, sore throat, headache, myalgia, loss of taste and smell, or diarrhea. Moreover, not all patients considered low-risk during triage were screened with PCR for COVID-19. Among 36,152 patients who were considered low-risk after triage questioning, 94 patients were PCR-positive for COVID-19. However, these patients underwent PCR screening for preoperative evaluation, if they developed a new symptom or for contact screening. Therefore, the results should be evaluated accordingly.

Conclusion

Effective triage is the first step in preventing in-hospital transmission of COVID-19. The "Possible COVID-19 Case Questioning Guide for Outpatients" triage chart created by the Turkish Ministry of Health presents high sensitivity and specificity for discriminating possible COVID-19 cases to refer them to pandemic area, but has unsatisfactory diagnostic value for predicting PCR positivity in pandemic outpatients. The diagnostic value of the triage chart is mainly attributed to questions regarding possible COVID-19 infection symptoms rather than these concerning contact history. Therefore, the current triage

chart should be used accordingly, i.e., to define possible COVID-19 cases rather than PCR-positive cases. Further studies regarding COVID-19 triage for possible and PCR-positive cases should focus also on the individual diagnostic value of less prevalent symptoms.

ORCID iDs

Reyhan Öztürk https://orcid.org/0000-0002-0969-3961
Gokhan Tazegul https://orcid.org/0000-0002-0737-9450

References

1. Anderson RM, Heesterbeek H, Klinkenberg D, Hollingsworth TD. How will country-based mitigation measures influence the course of the COVID-19 epidemic? *Lancet*. 2020;395(10228):931–934. doi:10.1016/S0140-6736(20)30567-5
2. Peros G, Gronki F, Molitor N, et al. Organizing a COVID-19 triage unit: A Swiss perspective. *Emerg Microbes Infect*. 2020;9(1):1506–1513. doi:10.1080/22221751.2020.1787107
3. Rickman HM, Rampling T, Shaw K, et al. Nosocomial transmission of coronavirus disease 2019: A retrospective study of 66 hospital-acquired cases in a London teaching hospital. *Clin Infect Dis*. 2021;72(4):690–693. doi:10.1093/cid/ciaa816
4. Erika P, Andrea V, Cillis MG, Ioannilli E, Iannicelli T, Andrea M. Triage decision-making at the time of COVID-19 infection: The Piacenza strategy. *Intern Emerg Med*. 2020;15(5):879–882. doi:10.1007/s11739-020-02350-y
5. Liang W, Liang H, Ou L, et al. Development and validation of a clinical risk score to predict the occurrence of critical illness in hospitalized patients with COVID-19. *JAMA Intern Med*. 2020;180(8):1081. doi:10.1001/jamainternmed.2020.2033
6. Du Y, Zhou N, Zha W, Lv Y. Hypertension is a clinically important risk factor for critical illness and mortality in COVID-19: A meta-analysis. *Nutr Metab Cardiovasc Dis*. 2021;31(3):745–755. doi:10.1016/j.numecd.2020.12.009
7. Zhou Y, Chi J, Lv W, Wang Y. Obesity and diabetes as high-risk factors for severe coronavirus disease 2019 (Covid-19). *Diabetes Metab Res Rev*. 2021;37(2):e3377. doi:10.1002/dmrr.3377
8. Liang W, Yao J, Chen A, et al. Early triage of critically ill COVID-19 patients using deep learning. *Nat Commun*. 2020;11(1):3543. doi:10.1038/s41467-020-17280-8
9. MedCalc Software Ltd. Diagnostic Test Evaluation Calculator v. 20.009. https://www.medcalc.org/calc/diagnostic_test.php. Accessed August 15, 2021.
10. Altman DG, ed. *Statistics with Confidence: Confidence Intervals and Statistical Guidelines*. 2nd ed. London, UK: BMJ Books; 2011:109. ISBN:978-0-7279-1375-3.
11. Kucewicz-Czech E, Damps M. Triage during the COVID-19 pandemic. *Anaesthesiol Intensive Ther*. 2020;52(4):312–315. doi:10.5114/ait.2020.100564
12. Tolone S, Gambardella C, Brusciano L, del Genio G, Lucido FS, Docimo L. Telephonic triage before surgical ward admission and telemedicine during COVID-19 outbreak in Italy: Effective and easy procedures to reduce in-hospital positivity. *Int J Surg*. 2020;78:123–125. doi:10.1016/j.ijsu.2020.04.060
13. Hui DS, I Azhar E, Madani TA, et al. The continuing 2019-nCoV epidemic threat of novel coronaviruses to global health: The latest 2019 novel coronavirus outbreak in Wuhan, China. *Int J Infect Dis*. 2020;91:264–266. doi:10.1016/j.ijid.2020.01.009
14. Chen N, Zhou M, Dong X, et al. Epidemiological and clinical characteristics of 99 cases of 2019 novel coronavirus pneumonia in Wuhan, China: A descriptive study. *Lancet*. 2020;395(10223):507–513. doi:10.1016/S0140-6736(20)30211-7
15. Yang X, Yu Y, Xu J, et al. Clinical course and outcomes of critically ill patients with SARS-CoV-2 pneumonia in Wuhan, China: A single-centered, retrospective, observational study. *Lancet Respir Med*. 2020;8(5):475–481. doi:10.1016/S2213-2600(20)30079-5
16. Huang C, Wang Y, Li X, et al. Clinical features of patients infected with 2019 novel coronavirus in Wuhan, China. *Lancet*. 2020;395(10223):497–506. doi:10.1016/S0140-6736(20)30183-5
17. Giacomelli A, Pezzati L, Conti F, et al. Self-reported olfactory and taste disorders in patients with severe acute respiratory coronavirus 2 infection: A cross-sectional study. *Clin Infect Dis*. 2020;71(15):889–890. doi:10.1093/cid/ciaa330
18. Docherty AB, Harrison EM, Green CA, et al. Features of 20 133 UK patients in hospital with covid-19 using the ISARIC WHO Clinical Characterization Protocol: Prospective observational cohort study. *BMJ*. 2020;369:m1985. doi:10.1136/bmj.m1985
19. Kakodkar P, Kaka N, Baig M. A comprehensive literature review on the clinical presentation, and management of the pandemic coronavirus disease 2019 (COVID-19). *Cureus*. 2020;2(4):e7560. doi:10.7759/cureus.7560
20. Panǎ BC, Lopes H, Furtunescu F, et al. Real-world evidence: The low validity of temperature screening for COVID-19 triage. *Front Public Health*. 2021;9:672698. doi:10.3389/fpubh.2021.672698
21. Izquierdo-Dominguez A, Rojas-Lechuga M, Mullol J, Alobid I. Olfactory dysfunction in the COVID-19 outbreak. *J Investig Allergol Clin Immunol*. 2020;30(5):317–326. doi:10.18176/jiaci.0567
22. Aldobyany A, Touman A, Ghaleb N, et al. Correlation between the COVID-19 respiratory triage score and SARS-COV-2 PCR test. *Front Med*. 2020;7:605689. doi:10.3389/fmed.2020.605689
23. Mansella G, Rueegg M, Widmer AF, et al. COVID-19 triage and test center: Safety, feasibility, and outcomes of low-threshold testing. *J Clin Med*. 2020;9(10):3217. doi:10.3390/jcm9103217
24. Lundon DJ, Kelly BD, Nair S, et al. A COVID-19 test triage tool, predicting negative results and reducing the testing burden on healthcare systems during a pandemic. *Front Med (Lausanne)*. 2021;8:563465. doi:10.3389/fmed.2021.563465
25. Pathan SA, Thomas CE, Bhutta ZA, et al. Qatar prediction rule using ED indicators of COVID-19 at triage. *Quatar Med J*. 2021;2021(2):18. doi:10.5339/qmj.2021.18
26. Jmaa MB, Ayed HB, Kassis M, et al. Epidemiological profile and performance of triage decision-making process of COVID-19 suspected cases in southern Tunisia. *Afr J Emerg Med*. 2022;12(1):1–6. doi:10.1016/j.afjem.2021.10.001

The influence of cord blood renalase and advanced oxidation protein products (AOPPs) on perinatal and anthropometric parameters of newborns of mothers with gestational hypertension

Justyna Czubilińska-Łada[1,A,C,D], Andrzej Badeński[2,C,D], Elżbieta Świętochowska[3,B,C],
Lucyna Nowak-Borzęcka[4,B,D], Beata Sadownik[4,B,E], Jakub Behrendt[1,E], Maria Szczepańska[2,A,E,F]

[1] Department of Neonatal Intensive Care, Faculty of Medical Sciences in Zabrze, Medical University of Silesia in Katowice, Poland

[2] Department of Pediatrics, Faculty of Medical Sciences in Zabrze, Medical University of Silesia in Katowice, Poland

[3] Department of Medical and Molecular Biology, Faculty of Medical Sciences in Zabrze, Medical University of Silesia in Katowice, Poland

[4] Department of Neonatology, Multi-Specialist Hospital, Gliwice, Poland

A – research concept and design; B – collection and/or assembly of data; C – data analysis and interpretation;
D – writing the article; E – critical revision of the article; F – final approval of the article

Address for correspondence
Justyna Czubilińska-Łada
E-mail: jczubilinska.lada@gmail.com

Abstract

Background. Renalase is an enzyme secreted by the kidneys, which takes part in the regulation of arterial pressure, myocardial contractility and modulation of vascular resistance, but its effect on renalase levels in newborns has not been studied yet. The levels of advanced oxidation protein products (AOPPs) were also evaluated as a marker of oxidative stress.

Objectives. This study examined whether renalase and AOPP levels are different in the cord blood of newborns exposed to gestational hypertension (HT). The association of both factors with perinatal and anthropometric data among the studied patients was assessed.

Materials and methods. The study included 89 newborns: 30 newborns from the study group, whose mothers were diagnosed with gestational HT, and 59 newborns born from normal pregnancies, who formed the control group. Anthropometric measurements and perinatal data in newborns in both groups were recorded.

Results. A significantly lower ($p < 0.001$) concentration of renalase was found in the study group (median (Q1–Q3): 23.96 µg/mL (20.63–26.91 µg/mL)) as compared to the control group (median (Q1–Q3): 37.54 µg/mL (33.78–40.02 µg/mL)). In case of AOPPs, a significantly higher ($p < 0.001$) concentration of AOPPs was observed in the study group (median (Q1–Q3): 131.65 µmol/L (113.80–146.10 µmol/L)) than in the controls (median (Q1–Q3): 93.70 µmol/L (87.10–111.20 µmol/L)).

Conclusions. A significant difference between renalase and AOPP concentrations between the study and control groups has been demonstrated. Both factors may influence anthropometric and perinatal outcomes of newborns.

Key words: cord blood, gestational hypertension, newborns, renalase, oxidative stress

Background

Pregnancy is associated with many physiological hemodynamic changes; however, hypertensive disorders of pregnancy (HDP) affect as much as 6–10% of pregnant women in Europe and the USA. Gestational hypertension is a condition characterized by newly diagnosed hypertension (HT) after 20 weeks of pregnancy, without accompanying proteinuria or other biochemical or hematological disturbances. Gestational HT can lead to the development of more complex HDP, such as preeclampsia or eclampsia, which, in addition to HT, are characterized by proteinuria and/or maternal kidney and liver injury, neurological symptoms, hemolysis or thrombocytopenia, and often serious complications in the newborn.[1,2]

Complications of gestational HT are currently considered to be one of the most common causes of maternal death. The life and health of newborns is also endangered due to the increased risk of intrauterine growth retardation or placental abruption, which may result in premature birth and other serious complications requiring hospitalization in the neonatal intensive care unit (NICU). In addition, the risk of an urgent cesarean section is increased, which threatens both mother and child.[3]

Renalase is a recently described flavoprotein oxidase, which takes part in the regulation of the cardiovascular system.[4,5] Numerous clinical studies have proven a significant impact of renalase on heart rate, myocardial contractility and vascular tone. Regardless of its function as an inducer of catecholamine degradation, renalase also has the properties of cytokine: it causes cytoprotective and anti-inflammatory effects, and inhibits cell hypoxia and apoptosis.[6,7] Genetic investigations have revealed the occurrence of single nucleotide polymorphisms (SNPs) in the renalase gene and the association of some of them with selected cardiovascular diseases, kidney diseases, type 1 diabetes, ischemic stroke, female infertility schizophrenia, as well as gestational HT and preeclampsia.[8–12] Renalase is secreted into the blood mainly by the kidneys, but its expression has also been shown in many other organs and tissues such as heart, skeletal muscles, endothelium, small intestine, adipose tissue, brain, liver, as well as in the reproductive/steroidogenic system, which is an interesting finding in the context of this study.[13,14]

Oxidative stress takes part in the development of numerous pathologic conditions and by affecting the prenatal life it may have a deleterious effect by causing perinatal disorders and subsequent neonatal diseases. The oxidative stress is defined as an imbalance between oxidants and antioxidants, which results in the formation of reactive oxygen species (ROS) that react mainly with proteins but also with DNA, nucleotides, lipids, carbohydrates, and cell membrane structure elements. The result of these reactions is a destruction of tissue in the mechanism of hypoxia, hyperoxia, ischemia, and local inflammation.[15,16] Pregnancy-induced HT is a condition of increased risk of exposure to oxidative stress, which can affect both the mother and the child.[17,18]

Advanced oxidation protein products (AOPPs) are albumins whose structure has been modified under oxidative stress generated by ROS, and as a result of these changes in their structure, their antioxidant properties are significantly reduced. Due to their characteristics, AOPPs are well-known and easily quantifiable oxidative stress markers, whose high levels have been determined in patients with diabetes mellitus, cardiovascular diseases, HT, and atherosclerosis.[19–21]

Objectives

In the present study, the umbilical cord blood has been used as a study material due to its good reflection of the neonate condition in the perinatal period and convenient sampling. The study examined how AOPPs and renalase in the umbilical cord blood of newborns of mothers suffering from gestational HT differ from those parameters in neonates who were born from normotensive pregnancies. Both factors were examined because of their possible association with gestational HT the study group. Furthermore, the investigation was extended by analyzing the association between renalase and AOPP level and neonatal anthropometric measurements and demographic data. The aim was to determine whether changes in cord blood renalase and AOPP concentrations induced by HT affect neonatal outcome data.

Materials and methods

Study design and participant criteria

The study included 89 newborns divided into 2 groups: the study group (HT group) including 30 newborns from pregnancies complicated by gestational HT, and the control group consisting of 59 newborns from normotensive pregnancies. All newborns were born in the Multi-Specialist Hospital in Gliwice, Poland, between 2018 and 2020. Mothers of patients from the HT group did not suffer from other diseases besides the gestational HT and did not have arterial HT before pregnancy. Gestational HT was diagnosed according to the guidelines of the Polish Society of Gynaecologists and Obstetricians as HT occurring after 20 weeks of pregnancy, when blood pressure values in office measurements are above 140 mm Hg for systolic blood pressure (SBP) and/or higher than 90 mm Hg for diastolic blood pressure (DBP), without accompanying proteinuria or other biochemical and hematological disorders. Patients qualified to the control group came from physiological pregnancies, their mothers did not have any accompanying diseases before and during pregnancy, and their arterial blood pressure values were normal.

Ethical issues

This study was conducted in full accordance with the Declaration of Helsinki and was approved by the Bioethics

Committee of the Silesian Medical University in Katowice, Poland (resolution No. KNW/022/KB1/109/18). All participating women were familiarized with the method and purpose of research and signed the informed consent to participate.

Data and sample collection

Medical data concerning both the mother (age, history of pregnancies and deliveries, accompanying diseases), delivery (course of delivery, gestational age, a group B Streptococcus test result, color of waters) and the newborn (Apgar score, sex, birth weight, body length, head circumference, chest circumference) were recorded. Cord blood was collected from the umbilical vein in the 3rd stage of labor, just after the umbilical cord was tightened. Blood was collected into the ethylenediaminetetraacetic acid (EDTA) tubes, samples were centrifuged and then the serum samples were frozen and stored at −80°C.

Measurements

Renalase and AOPP concentration determinations were performed at the Department of Medical and Molecular Biology (Faculty of Medical Sciences in Zabrze, Medical University of Silesia in Katowice, Poland). The determination of renalase concentrations was performed with the commercially available enzyme-linked immunosorbent assay (ELISA) kit (Cloud-Clone, Katy, USA). The sensitivity of the set was 1.37 ng/mL, intra-serial error was <10% and extra-serial error was <12%. The AOPP concentrations were determined with spectrophotometric method, using commercial test (Immundiagnostik AG, Bensheim, Germany). The sensitivity of the kit was 11 µmol/L, intra-serial error was <5.6% and extra-serial error was <14.3%.

Statistical analyses

Because the study variables did not meet the assumptions of normal distribution in each group, the data were presented as median with interquartile range (IQR). The distributions were evaluated using the Shapiro–Wilk test, and in all the variables $p < 0.05$ was considered significant.

The Mann–Whitney U test was used to compare variables between groups. The Spearman's rank correlation coefficient was used to analyze the relationship between the variables. Rstudio package and Seaborn library for Python language in Jupyter notebook environment were used to perform the analysis (https://seaborn.pydata.org/).

Results

Perinatal data on neonates obtained in both groups are presented in Table 1. In both groups, males (58.4%) predominated over the females (41.6%). Most of the newborns included in the study were born by vaginal delivery (89.9%), and a smaller part by cesarean section (10.1%). In case of neonates qualified for the study who were born by cesarean section, the operative delivery took place for elective indications (ophthalmological, orthopedic indications). In the whole group of mothers of children included in the study, a similar percentage of nulliparous (49.4%) and multiparous women (50.6%) was observed.

Mothers of children were 20–41 years old, all the infants were eutrophic, rated on the Apgar scale above 8 points due to good condition and born from clear amniotic fluid at the time of delivery (between 37 and 42 weeks of pregnancy). Among the anthropometric factors (Table 2), a statistically significant difference in gestational age,

Table 1. Perinatal data of the patients

Variable	HT group (n = 30)	Control group (n = 59)	Both groups (n = 89)
Gender			
Female	13 (43.3%)	24 (40.7%)	37 (41.6%)
Male	17 (56.7%)	35 (59.3%)	52 (58.4%)
Delivery			
Normal vaginal	25 (83.3%)	55 (93.2%)	80 (89.9%)
Cesarean section	5 (16.7%)	4 (6.8%)	9 (10.1%)
Parity			
Nulliparous	14 (46.7%)	30 (50.8%)	44 (49.4%)
Multiparous	16 (53.3%)	29 (49.2%)	45 (50.6%)

HT – hypertension.

Table 2. Anthropometric characteristics of the 2 studied groups

Parameter	HT group (n = 30)			Control group (n = 59)			p-value*
	median	Q1	Q3	median	Q1	Q3	
Age of the mother [years]	30.0	27.0	32.0	30.0	27.0	32.0	0.213
Gestational age [weeks]	39.0	38.5	40.0	40.0	39.0	40.0	**0.029**
Birth weight [g]	3265.0	3290.0	3745.0	3300.0	3090.0	3650.0	0.284
Body length [cm]	53.8	53.5	56.0	55.0	54.0	56.0	**0.006**
Head circumference [cm]	33.0	33.0	34.5	34.0	32.0	35.0	0.098
Chest circumference [cm]	32.0	32.0	35.0	33.0	32.0	34.0	**0.048**

*p-values for Mann–Whitney U test. HT – hypertension; Q1 – 1st quartile; Q3 – 3rd quartile. Values in bold are statistically significant.
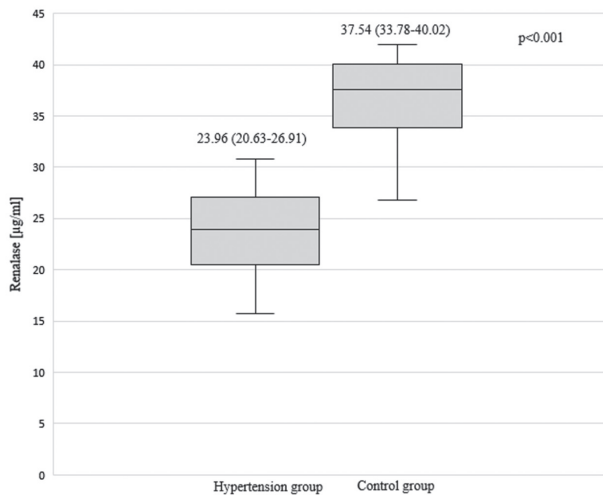
Fig. 1. Renalase concentrations in studied groups. Data are presented as median and interquartile range (IQR). *p-values for Mann–Whitney U test. Z-score value is at 6.787. The graph was prepared without taking outliers into account

Fig. 2. Advanced oxidation protein product (AOPP) concentrations in studied groups. Data are presented as median and interquartile range (IQR). *p-values for Mann–Whitney U test. Z-score value is at –6.427. The graph was prepared without taking outliers into account

body length and chest circumference was observed: infants in the HT group had a statistically significant lower gestational age, as well as lower body length and chest circumference compared to the control group.

The comparison of renalase and AOPP values in the HT and control groups is presented on a graph and as a median with IQR (Fig. 1,2). A significantly lower (p < 0.001) renalase concentration was found in the HT group (23.96 (20.63–26.91) µg/mL) as compared to the control group (37.54 (33.78–40.02) µg/mL). In case of AOPPs, a significantly higher (p < 0.001) AOPP concentration was measured in the HT group (131.65 (113.80–146.10) µmol/L) than in the control group (93.70 (87.10–111.20) µmol/L).

In order to establish the association between studied factors and the fetal development, the correlation between the concentrations of the given substances and the demographic, perinatal and anthropometric data of the newborns were analyzed (Table 3). No correlation was found between gestational age and AOPP concentration, as well as between renalase and AOPP concentrations and other studied parameters such as body weight, body length, head circumference, and chest circumference. Renalase and

AOPP concentrations were compared in relation to selected perinatal parameters such as gender, type of delivery and parity. A statistically significant difference was found for renalase concentration and parity in the control group, and a significant correlation between AOPP concentration and the type of delivery in the whole population of children included in the study (Table 4,5).

Discussion

Renalase

Numerous clinical studies indicate that renalase has a significant effect on the cardiovascular system through its active participation in catecholamine degradation. Probably affecting the reduction of catecholamines in the blood, it directs hemodynamic changes such as a decrease in arterial pressure, myocardial contractility or vascular resistance.[3,5] The pathogenesis of HDP is multifactorial, and one of the most probable theories concerns microcirculation disorders in uterine arteries resulting in impaired

Table 3. Correlation coefficients between anthropometric parameters and renalase and AOPP levels

Parameter	Renalase				AOPP			
	HT group (n = 30)	p-value	control group (n = 59)	p-value	HT group (n = 30)	p-value	control group (n = 59)	p-value
Gestational age	0.07	0.696	0.13	0.326	–0.15	0.425	0.04	0.771
Birth weight	–0.16	0.392	0.06	0.657	0.04	0.846	0.13	0.329
Birth length	0.14	0.445	–0.03	0.809	0.19	0.31	0.06	0.681
Head circumference	–0.06	0.773	–0.01	0.913	–0.07	0.717	0.10	0.457
Chest circumference	–0.13	0.509	–0.01	0.919	–0.09	0.652	0.09	0.492

Selected values of Spearman's rank correlation. Statistically significant values (p < 0.05) were not observed. HT – hypertension; AOPP – advanced oxidation protein product.

Table 4. Renalase concentrations [μg/mL] among neonates exposed to gestational HT in the control group and all neonates included in the study, according to selected perinatal data

Variable	HT group	Z	p-value*	Control group	Z	p-value*	All neonates	Z	p-value*
Gender									
Female	23.0 (21.4–27.9)	−0.02	0.982	36.4 (33.0–40.0)	−0.71	0.477	33.3 (27.6–39.4)	−0.4	0.690
Male	24.2 (20.1–26.9)			37.6 (34.5–40.0)			35.5 (26.9–38.3)		
Delivery									
Normal vaginal	24.5 (21.0–27.2)	71.0	0.210	37.0 (33.8–38.9)	123.5	0.174	35.1 (29.0–38.3)	1.69	0.091
Cesarean section	23.0 (17.6–25.6)			40.1 (32.9–41.8)			26.8 (22.9–40.0)		
Parity									
Nulliparous	24.0 (20.1–29.7)	0.19	0.852	37.7 (36.5–40.2)	1.97	**0.049**	36.6 (29.0–40.1)	1.51	0.132
Multiparous	24.0 (20.7–26.6)			35.5 (33.4–38.1)			33.4 (26.2–37.7)		

Data are presented as median and interquartile range (IQR). *p-values and Z-score for Mann–Whitney U test; p-values statistically significant (<0.05) are bolded. In subgroups, all the parameters were significantly different between HT group and control group. HT – hypertension.

Table 5. Advanced oxidation protein product (AOPP) concentrations [μmol/L] among neonates exposed to gestational HT in the control group and all neonates included in the study, according to selected perinatal data

Variable	HT group	Z	p-value*	Control group	Z	p-value*	All neonates	Z	p-value*
Gender									
Female	131.0 (109.7–142.2)	−0.82	0.413	94.5 (76.8–112.0)	−0.57	0.568	105.1 (88.3–121.6)	−0.55	0.581
Male	129.7 (118.5–153.2)			93.7 (88.9–103.2)			102.8 (90.6–122.0)		
Delivery									
Normal vaginal	131.1 (111.8–153.3)	−0.33	0.741	94.1 (86.7–112.0)	−0.32	0.752	102.7 (88.9–118.9)	−2.05	**0.041**
Cesarean section	132.5 (121.5–143.8)			93.5 (91.2–104.3)			120.7 (102.3–135.2)		
Parity									
Nulliparous	134.4 (118.5–146.1)	0.17	0.868	93.5 (88.4–112.8)	0.16	0.874	103.7 (89.3–121.7)	−0.07	0.944
Multiparous	128.8 (113.3–147.3)			96.5 (86.2–105.8)			105.8 (87.7–122.5)		

Data are presented as median and interquartile range (IQR). *p-values and Z-score for Mann–Whitney U test; p-values statistically significant (<0.05) are bolded. In subgroups, all the parameters were significantly different between HT group and control group. HT – hypertension.

placental blood flow.[22] The evaluation of the effect of renalase on the development of microcirculation in the placenta may give an interesting diagnostic and therapeutic effect. Relationships between renalase and the female reproductive system as well as pregnancy were demonstrated in many fields. Zhou et al. presented results showing high expression of renalase in both male and female gonads, as well as in the renal cortex. Further investigation has shown that the treatment of mice with gonadotropin-releasing hormone (GnRH) antagonist, which reduces the production of steroids, is also associated with reduced expression of renalase in gonads.[15] Clinical trials

have also been carried out to link renalase with the occurrence of HDP. The strongest evidence of such connection is proven for rs2576178 and rs10887800 polymorphisms of the renalase genes or their combination. It was also noticed that values of SBP and DBP depend on the genotype dominance.[7–9]

To the best of our knowledge, no studies have been carried out so far to present the evaluation of cord blood renalase concentration among newborns. Publications demonstrating the determinations of serum renalase in pregnant women by Yılmaz et al. and El Niadany et al. reported that the renalase was significantly lower in groups

of pregnant women with HDP compared to the control subjects.[23,24] We observed a similar trend in our study, when lower renalase levels were dectected in the cord blood of neonates exposed to gestational HT than in those from healthy pregnancies.

The observations from the above study provide a clear indication that cord blood renalase concentration is altered as a result of exposure to gestational HT. Considering the knowledge on the various effects of renalase, it seems important to know the exact influence of its concentration fluctuations on neonatal development. To extend the evaluation of the effect of reduced renalase levels on child growth, we correlated renalase concentrations with perinatal and anthropometric parameters of newborns. This analysis has not answered whether anthropometric and perinatal variables are in any way associated with fluctuations in renalase levels.

Advanced oxidation protein products

Literature data indicate a significant influence of oxidative stress on the development of HDP. Free radicals generate destructive effects on the endothelium of placental blood vessels, and cause increased immunological response, which may lead to the development of HT.[25] The AOPP levels in peripheral blood of pregnant women in various groups of HDP were described as higher than in healthy pregnant women.[18,19] The assessment of the influence of oxidative stress in newborns, especially premature infants, is presented in many studies covering children affected by such conditions as retinopathy of prematurity (ROP), bronchopulmonary dysplasia (BPD), necrotizing enterocolitis (NEC), patent ductus arteriosus (PDA), periventricular leukomalacia (PVL), and intraventricular hemorrhage (IVH), together forming a group of free radical-related diseases (FRD). A greater exposure to FRD among premature infants than among children born on their due dates was explained by the fact that the lower the gestational age, the worse the antioxidant response of the fetus. In addition, elevated levels of oxidative stress markers have been proven in newborns exposed to pain.[26–28] Elevated levels of AOPPs and other oxidative stress markers such as ischemia-modified albumin (IMA), thiobarbituric acid reactive substance (TBARS) or serum malondialdehyde (MDA) were detected in peripheral blood of pregnant women with HDP. In addition, it has been observed that in preeclampsia patients, elevated levels of lipid peroxides, which are formed under the influence of ROS, are associated with reduced levels of vitamin E and C, known as first-line antioxidants.[26–28]

Considering the literature data suggesting that oxidative stress occurring in the perinatal period has a significant influence on the development of complications in newborns, we decided to determine the concentration of AOPPs as a well-known marker of oxidative stress in the studied groups. The obtained results clearly show that in the group

of neonates born from mothers with gestational HT, the level of AOPPs in cord blood was significantly higher than in the control group. The increased concentration of AOPPs in cord blood in the HT group may provide evidence that exposure to gestational HT induces oxidative stress, which has a direct effect on the child. This conclusion is consistent with observations from other studies stating that the pathogenesis of gestational HT involves the destruction of the endothelium of the placental blood vessels under oxidative stress. Extending the scope of the study to compare anthropometric and perinatal data did not provide a clear answer on the effect of oxidative stress on child development.

Limitations of the study

Notwithstanding the fact that the results clearly show an association between changes in renalase and AOPP concentrations under the influence of gestational HT, the limitations of our work must be considered. In this study, only neonates born at term and eutrophic were included. The development of gestational HT predisposes to preterm birth and intrauterine hypotrophy, and thus we consider that studies among children with such perinatal complications should be continued. Furthermore, the determination of peripheral blood renalase concentrations in neonates in correlation with blood pressure measurements could explain the process of renalase homeostasis. The relatively small size of the groups was also a limitation of this study, but in the pediatric groups in a single-center research, it is difficult to collect a more numerous study groups.

Conclusions

A significant difference for both renalase and AOPP concentrations between the study group and the control group has been demonstrated, as well as a correlation of renalase concentration with gestational age. Both factors may influence anthropometric and perinatal outcomes of newborns. Taking into account other literature data on the relaxing effect of renalase on blood vessels, it is likely that renalase disturbances and elevated levels of oxidative stress markers contribute to disorders of placental microcirculation. Further studies aimed at determining renalase and AOPPs in both umbilical and peripheral blood of newborn infants may provide a more complex answer on the causes of HDP and their impact on the development of newborns.

ORCID iDs

Justyna Czubilińska-Łada   https://orcid.org/0000-0003-2842-3307
Andrzej Badeński   https://orcid.org/0000-0001-6947-005X
Elżbieta Świętochowska   https://orcid.org/0000-0001-5787-7880
Jakub Behrendt   https://orcid.org/0000-0002-2387-3133
Maria Szczepańska   https://orcid.org/0000-0002-6772-1983

References

1. Prejbisz A, Dobrowolski P, Kosiński P, et al. Management of hypertension in pregnancy: Prevention, diagnosis, treatment and long-term prognosis. *Kardiol Pol*. 2019;77(7–8):757–806. doi:10.33963/KP.14904

2. Agrawal A, Wenger NK. Hypertension during pregnancy. *Curr Hypertens Rep*. 2020;22(9):64. doi:10.1007/s11906-020-01070-0

3. American College of Obstetricians and Gynecologists (ACOG). ACOG Practice Bulletin No. 202: Gestational hypertension and preeclampsia. *Obstet Gynecol*. 2019;133(1):1. doi:10.1097/AOG.0000000000003018

4. Desir GV, Tang L, Wang P, et al. Renalase lowers ambulatory blood pressure by metabolizing circulating adrenaline. *J Am Heart Assoc*. 2012;1(4):e002634. doi:10.1161/JAHA.112.002634

5. Xu J, Li G, Wang P, et al. Renalase is a novel, soluble monoamine oxidase that regulates cardiac function and blood pressure. *J Clin Invest*. 2005;115(5):1275–1280. doi:10.1172/JCI24066

6. Fatima SS, Rehman R, Martins RS, Alam F, Ashraf M. Single nucleotide polymorphisms in *Renalase* and *KCNQ1* genes and female infertility: A cross-sectional study in Pakistan. *Andrologia*. 2019;51(10):e13434. doi:10.1111/and.13434

7. Bagci B, Karakus S, Bagci G, Sancakdar E. Renalase gene polymorphism is associated with increased blood pressure in preeclampsia. *Pregnancy Hypertens*. 2016;6(2):115–120. doi:10.1016/j.preghy.2016.04.002

8. Elsetohy KA, Al-Ghussein MA, Sabry D, Nada M, Eldaly AA, Wahba AH. Are renalase rs2576178 and rs10887800 polymorphisms associated with pregnancy induced hypertension? *World J Pharm Pharm Sci*. 2014;3(8):177–192. https://scholar.cu.edu.eg/?q=kelsetohy/files/renalase_and_pih.pdf

9. Teimoori B, Moradi-Shahrebabak M, Rezaei M, Mohammadpour-Gharehbagh A, Salimi S. Renalase rs10887800 polymorphism is associated with severe pre-eclampsia in southeast Iranian women. *J Cell Biochem*. 2019;120(3):3277–3285. doi:10.1002/jcb.27595

10. Guo X, Wang L, Velazquez H, Safirstein R, Desir GV. Renalase: Its role as a cytokine, and an update on its association with type 1 diabetes and ischemic stroke. *Curr Opin Nephrol Hypertens*. 2014;23(5):513–518. doi:10.1097/MNH.0000000000000044

11. Wiśniewska M, Serwin N, Dziedziejko V, et al. Chronic kidney disease is associated with increased levels of renalase in serum and decreased in erythrocytes. *Pol Arch Intern Med*. 2019;129(11):790–797. doi:10.20452/pamw.15049

12. Serwin NM, Wiśniewska M, Cecerska-Heryć E, Safranow K, Skwirczyńska E, Dołęgowska B. Serum-to-urine renalase ratio and renalase fractional excretion in healthy adults and chronic kidney disease patients. *BMC Nephrol*. 2020;21(1):77. doi:10.1186/s12882-020-01737-5

13. Hennebry SC, Eikelis N, Socratous F, Desir G, Lambert G, Schlaich M. Renalase, a novel soluble FAD-dependent protein, is synthesized in the brain and peripheral nerves. *Mol Psychiatry*. 2010;15(3):234–236. doi:10.1038/mp.2009.74

14. Xu J, Desir GV. Renalase, a new renal hormone: Its role in health and disease. *Curr Opin Nephrol Hypertens*. 2007;16(4):373–378. doi:10.1097/MNH.0b013e3281bd8877

15. Zhou M, Liang T, Wang Y, et al. Expression and tissue localization of renalase, a novel soluble FAD-dependent protein, in reproductive/steroidogenic systems. *Mol Biol Rep*. 2013;40(6):3987–3994. doi:10.1007/s11033-012-2476-0

16. Piwowar A, Żurawska-Płaksiej E, Knapik-Kordecka M, Warwas M. Relationship between advanced oxidation protein product plasma level and cathepsin B activity in plasma and polymorphonuclear cells in patients with type 2 diabetes mellitus. *Adv Clin Exp Med*. 2009;18(4):345–351. https://advances.umw.edu.pl/en/article/2009/18/4/345/. Accessed November 5, 2021.

17. Draganovic D, Lucic N, Jojic D. Oxidative stress marker and pregnancy-induced hypertension. *Med Arch*. 2016;70(6):437. doi:10.5455/medarh.2016.70.437-440

18. D'Souza JMP, Harish S, Pai VR, Shriyan C. Increased oxidatively modified forms of albumin in association with decreased total antioxidant activity in different types of hypertensive disorders of pregnancy. *Indian J Clin Biochem*. 2017;32(2):200–206. doi:10.1007/s12291-016-0584-7

19. Mohanty S, Sahu PK, Mandal MK, Mohapatra PC, Panda A. Evaluation of oxidative stress in pregnancy induced hypertension. *Indian J Clin Biochem*. 2006;21(1):101–105. doi:10.1007/BF02913074

20. Piwowar A, Knapik-Kordecka M, Warwas M. AOPP and its relations with selected markers of oxidative/antioxidative system in type 2 diabetes mellitus. *Diabetes Res Clin Pract*. 2007;77(2):188–192. doi:10.1016/j.diabres.2006.12.007

21. Colombo G, Reggiani F, Astori E, et al. Advanced oxidation protein products in nondiabetic end stage renal disease patients on maintenance haemodialysis. *Free Radic Res*. 2019;53(11–12):1114–1124. doi:10.1080/10715762.2019.1690651

22. Malik R, Kumar V. Hypertension in pregnancy. In: Islam S, ed. *Hypertension: From Basic Research to Clinical Practice*. Vol. 956. Advances in Experimental Medicine and Biology. Cham, Switzerland: Springer International Publishing; 2016:375–393. doi:10.1007/5584_2016_150

23. Yılmaz ZV, Akkaş E, Yıldırım T, Yılmaz R, Erdem Y. A novel marker in pregnant with preeclampsia: Renalase. *J Matern Fetal Neonatal Med*. 2017;30(7):808–813. doi:10.1080/14767058.2016.1186637

24. El Niadany SS, El Gayed AMA, El Gayed EMA. Renalase rs10887800 gene polymorphism and its serum level in preeclampsia. *Meta Gene*. 2020;24:100649. doi:10.1016/j.mgene.2020.100649

25. Watanabe K, Mori T, Iwasaki A, et al. Increased oxygen free radical production during pregnancy may impair vascular reactivity in preeclamptic women. *Hypertens Res*. 2013;36(4):356–360. doi:10.1038/hr.2012.208

26. Longini M, Belvisi E, Proietti F, Bazzini F, Buonocore G, Perrone S. Oxidative stress biomarkers: Establishment of reference values for isoprostanes, AOPP, and NPBI in cord blood. *Mediators Inflamm*. 2017;2017:1–6. doi:10.1155/2017/1758432

27. Perrone S, Tataranno ML, Negro S, et al. Early identification of the risk for free radical-related diseases in preterm newborns. *Early Hum Dev*. 2010;86(4):241–244. doi:10.1016/j.earlhumdev.2010.03.008

28. Perrone S, Bellieni CV, Negro S, et al. Oxidative stress as a physiological pain response in full-term newborns. *Oxid Med Cell Longev*. 2017;2017:1–7. doi:10.1155/2017/3759287

The assessment of the risk of COVID-19 infection and its course in the medical staff of a COVID-only and a non-COVID hospital

*Marta Madej[1,A–F], *Agata Sebastian[1,A–F], Ewa Morgiel[1,A–F], Lucyna Korman[1,A–F], Magdalena Szmyrka[1,A–F], Renata Sokolik[1,A–F], Maria Chodyra[2,B,F], Małgorzata Walas-Antoszek[2,B,F], Iga Andrasiak[3,C,F], Jerzy Świerkot[1,A–F]

[1] Department of Rheumatology and Internal Medicine, Wroclaw Medical University, Poland

[2] Department of Internal Medicine, Healthcare Complex in Boleslawiec, Poland

[3] WroMedica Research Center, Wrocław, Poland

A – research concept and design; B – collection and/or assembly of data; C – data analysis and interpretation;
D – writing the article; E – critical revision of the article; F – final approval of the article

Address for correspondence
Agata Sebastian
E-mail: agatasebastian@vp.pl

Abstract

Background. Medical workers are a group that is particularly vulnerable to infection during the coronavirus disease 2019 (COVID-19) pandemic.

Objectives. The study aimed to assess the risk of COVID-19 infection and its course in the medical staff of a COVID-only and a non-COVID hospital.

Materials and methods. The observational study included 732 participants who were medical workers. The study was conducted between June 2020 and December 2020, before widespread COVID-19 immunization was introduced.

Results. Of the 732 employees of the hospitals, 377 had a history of COVID-19. The risk of disease was twice as high in the medical staff of the COVID-only hospital compared to the medical staff of the non-COVID hospital (odds ratio (OR) = 2.0; $p < 0.001$). Among medical personnel, 20.6% of the participants were asymptomatic and 6.4% required hospitalization. For the non-COVID hospital, the employees who were most frequently infected with COVID-19 were nurses/paramedics/medical caretakers. The factor influencing the risk of infection was body mass index (BMI; OR = 1.05; $p = 0.004$). The risk of COVID-19 infection was lower in the influenza vaccine group (OR = 2.23, $p < 0.001$).

Conclusions. The study results indicate that employees of the hospital treating only COVID patients have a higher risk of infection. Previous observations on factors predisposing to COVID-19 infection like gender and BMI were confirmed. However, the observations carried out on the studied population did not confirm the influence of other factors, such as the coexistence of chronic diseases (apart from diabetes) on the risk of developing COVID-19. In addition, we noticed that seasonal influenza vaccination has a beneficial effect in patients with COVID-19 infection.

Key words: epidemiology, medical staff, COVID-19, risk of infection

Background

Since the turn of 2019 and 2020, we are struggling with the coronavirus disease 2019 (COVID-19) pandemic. Due to the high transmission rate of the virus, millions of people worldwide contracted COVID-19 within a short period. The severe acute respiratory syndrome coronavirus 2 (SARS-CoV-2) infection shows a broad spectrum of clinical presentation. In approx. 20% of patients, the disease leads to respiratory failure or damage to other organs. In symptomatic cases, the course of the disease depends on many factors, including age, gender and comorbidities.[1,2] By identifying and assessing risk factors and implementing appropriate strategies, the risk of complications can be reduced. Age-related changes in innate and acquired immunity against COVID-19 infection have not yet been studied in detail, and the impairment and dysregulation of both kinds of immunity in older age can be inferred from examples of other viral infections, including flu. Kim et al. have noted an impaired interferon (IFN) type 1 response in the elderly, which is responsible for the increased replication of flu virus in cell culture.[3] In addition, several common nonstructural proteins of SARS-CoV-2 suppress IFN type 1 responses, and such suppression leads to a poor response of CD8^{+} cell and T cell to viral infection.[4,5]

Obesity is another risk factor for severe SARS-CoV-2 course, and this correlation is mainly attributed to impaired innate and acquired immunity among the overweight.[6] In adipose tissue, the expression of ACE2 receptors is higher than in the lung. Adipose tissue performs immune functions by maintaining chronic low-grade inflammation. Macrophages in the tissue can, under favorable conditions, activate a systemic acute inflammatory response, with the synthesis of pro-inflammatory cytokines: interleukin 6 (IL-6), tumor necrosis factor alpha (TNF-α) and others. In the case of COVID-19 infection, it is thought that this process may contribute to the development of the so-called cytokine storm. Adipocytes in adipose tissue release adiponectin and leptin, which are among the risk markers for cardiovascular disease (CVD) and are also associated with inflammation.[6]

Diabetes in COVID-19 patients has been found to increase the risk of hospitalization, severe complications and death in the course of the disease.[7] It is known that diabetes is associated with impaired innate as well as acquired immunity, which is due to impaired phagocytosis and function of macrophages and neutrophils, T cell function and clearance of viral particles. In addition, diabetic patients suffer from chronic inflammation with increased levels of pro-inflammatory cytokines such as IL-1, IL-6 and TNF-α.

Previous data on the association of smoking with the risk of COVID-19 infection and severity of COVID-19 are inconclusive. Virus entry into host cells occurs via ACE2 receptors. The study by Leung et al. showed an increased ACE2 receptor expression on airway cells of active tobacco smokers, which could explain the increased risk

and more severe course of SARS-CoV-2 in this subgroup.[8] In a cross-sectional study, Jackson et al. demonstrated a nearly 2 times higher incidence of COVID-19 among active smokers compared to non-smokers, regardless of gender, age and comorbidities.[9] Another meta-analysis showed not only an increased risk of severe COVID-19 in active smokers, but also a higher risk of severity and death during hospitalization and the need for mechanical ventilation in former smokers.[10,11] On the other hand, the attention is paid to the so-called smoker's paradox and the anti-inflammatory effect of nicotine.[12] Some observational studies have shown a lower number of active smokers among COVID-19 patients; moreover, no adverse effect of smoking on the disease course was observed.[13] A meta-analysis of 32 studies found that active smokers have a lower risk of COVID-19 infection compared to non-smokers.[14]

The literature also highlights the increased risk of COVID-19 infection among healthcare professionals. A meta-analysis of 49 studies showed that seroconversion to anti-SARS-CoV-2 IgG[+] in the study group affects 8.7% of the population. Risk factors for seropositivity were: male sex, black race, Asian and Hispanic origin, working in a unit dedicated to COVID-19 patients, working in direct contact with patients, and using inappropriate personal protective equipment.[15]

The medical staff has been the group working on the front line in the fight against the virus. When the COVID-19 pandemic began, 2 types of hospitals were established in our country. Some admitted only patients with COVID-19 infection (dedicated COVID hospitals), while other treated only patients with negative results for COVID-19 infection (non-COVID hospitals).

Objectives

The purpose of this study was to assess the risk of COVID-19 infection among medical staff from 2 hospitals: a dedicated COVID-19 hospital and a non-COVID facility.

Materials and methods

Study design

The study group consisted of medical staff from 2 hospitals: a dedicated COVID-19 hospital and a non-COVID-19 hospital. After obtaining individuals' informed consent to participate in the study, the following data were obtained from all participants: age, height, body weight, type of work performed in the case of medical staff (doctor, nurse, paramedic, medical attendant, orderly, hospital cleaner, physiotherapist, laboratory worker, technician, pharmacist), housing conditions (number of people living in a shared household), physical activity (defined as regular physical activity of moderate intensity at least 2 times a week for at least

30 min), history of flu vaccination during the year preceding the survey, comorbidities, and smoking. In addition, the following information regarding the course of SARS-CoV-2 infection was obtained: COVID-19 infection confirmation method (positive polymerase chain reaction (PCR) test based on nasopharyngeal swab, positive antigen test of the nasopharyngeal swab, or positive results of antibodies against SARS-CoV-2), symptoms of SARS-CoV-2 infection, and the severity of the course of the disease.

The participant with past COVID-19 infection was defined as a person who: 1) had a history of positive PCR and/or antigen test results based on a nasopharyngeal swab, and/or 2) was tested positive for immunoglobulin G (IgG) and/or IgM anti-SARS-CoV-2 antibodies (semi-quantitative or quantitative research) at the time of the current study (tested before COVID-19 vaccination).

Other participants who did not meet the above conditions were considered as those with no past COVID-19 infection.

Laboratory tests

Anti-SARS-CoV-2 antibodies were detected using enzyme-linked immunosorbent assay (ELISA). This assay uses semi-quantitative or quantitative method of detecting antibodies present in human serum following COVID-19 infection and arising from the vaccines based on the S1/RBD subunit of coronavirus.

The samples for the study were collected from medical staff after they provided their written consent to participate in the study. The ELISAs were performed in the laboratory of Euroimmun Polska sp. z o.o. (Wrocław, Poland) on ANALYSER I machines. The method was standard for determining antibodies: anti-SARS-CoV-2 in IgG, IgA and IgM classes and Quantivac IgG tests. Appropriately diluted test serum was placed on a 96-well microplate coated with a specific antigen. The antibodies present in the serum bind to solid-phase antigens. They are detected during the second step, which involves the addition of an immunoglobulin antibody conjugate and an enzyme. The addition of substrate for the enzyme catalyzes a color reaction whose measured intensity is proportional to the number of antibodies.

All reagents were supplied by Euroimmun Polska sp. z o.o. Anti-SARS-CoV-2 antibodies were measured in the IgG, IgA and IgM classes using a semi-quantitative method based on the determination of the ratio coefficient. In addition, anti-IgG-positive sera were further assayed to obtain a quantitative antibody titer result, recorded as BAU/mL international units. For the semi-quantitative method, results above 1.1 were considered positive, while for the quantitative method, the cutoff point was a value of ≥35.2 BAU/mL.

This study received approval from the institutional ethics committee of Wroclaw Medical University, Wrocław, Poland (approval No. KB 634/2020), and adhered to the ethical guidelines of the Declaration of Helsinki.

Statistical analyses

Analyses were performed using R software package v. 4.0.5 (R Foundation for Statistical Computing, Vienna, Austria) and STATISTICA v. 13.1 (TIBCO Software Inc., Palo Alto, USA). Categorical variables were presented as frequencies with percentages, whereas median and interquartile range (IQR) were used to describe continuous variables. Categorical variables were compared using the χ^2 test or Fisher's exact test. The evaluation of data normality was performed using the Shapiro–Wilk test, and non-normally distributed continuous variables were compared using the Mann–Whitney test. For multiple comparisons, the Kruskal–Wallis test and a post hoc Dunn's test with Benjamini–Hochberg correction were applied. The effect of risk factors on the probability of critical course of SARS-CoV-2 infection was estimated with univariate logistic regression. Outliers were checked with standardized residuals analysis. A p-value of 0.05 was considered statistically significant.

Results

Analysis of COVID-19 incidence and SARS-CoV-2 course in a COVID-19 hospital and a non-COVID hospital

Risk of disease by workplace – COVID hospital compared to non-COVID hospital

The study group consisted of 732 medical staff, of whom 460 were employees of a non-COVID hospital and 272 were employees of a COVID hospital. The staff included 568 females (78%) and 164 males (22%); the average age of the staff was 47 years. The characteristics of the study group are described in Table 1.

Of 732 hospital workers, 377 had COVID-19 infection in the past. There was a statistically significant relationship ($\chi^2 = 20.58$; $p < 0.001$), indicating that the number of cases depended on the place of work. The risk of disease was twice higher for COVID hospital medical staff than for non-COVID hospital medical staff – 62% and 45%, respectively (odds ratio (OR) = 2.0, $p < 0.001$).

Hospitalized patients were older than those with mild or asymptomatic COVID-19. In the analyzed population, hospitalized patients had a significantly higher median age than those who did not require hospitalization – 57 (54–60) years and 48 (39–56) years, respectively ($p < 0.001$) (Fig. 1). In the univariate model, the chance of being hospitalized was 10% higher with age increasing by 1 year (OR = 1.1, $p < 0.001$). Data on regression, 95% confidence intervals (95% CIs) for ORs, statistical significance for the entire model, and a measure of goodness-of-fit (Nagelkerke pseudo R^2) are presented in Table 2.

984

M. Madej et al. COVID-19 and its course in the medical staff

Table 1. Characteristics of medical staff in a COVID hospital and a non-COVID hospital

Variable	n (%)			p-value
	total (n = 732)	COVID hospital (n = 272)	non-COVID hospital (n = 460)	
Age, mean (SD) [years]	47 (12)	47 (11)	46 (12)	0.92*
Gender male female	164 (22) 568 (78)	51 (19) 221 (81)	113 (25) 347 (75)	0.07**
BMI, mean (SD) [kg/m²]	26 (5)	27 (5)	26 (4)	0.83*
Smoking non-smoker former smoker passive smoker active smoker	478 (65) 125 (17) 20 (3) 109 (15)	171 (63) 47 (17) 7 (3) 47 (17)	306 (66) 78 (17) 13 (3) 63 (14)	0.65***
Number of persons in a household 1 2 >2	94 (13) 266 (36) 372 (51)	32 (12) 92 (34) 148 (54)	62 (13) 174 (38) 224 (49)	0.30***
Number of households with children <5 years of age	63 (9)	24 (9)	39 (9)	1**
Number of households with persons >65 years of age	61 (8)	23 (9)	38 (8)	1**
Chronic diseases	240 (33)	96 (35)	144 (31)	0.17**
Renal diseases	6 (1)	2 (1)	4 (1)	1****
Cardiovascular diseases	69 (9)	19 (7)	50 (11)	0.15**
Pulmonary diseases	17 (2)	3 (1)	14 (3)	0.18****
Systemic connective tissue diseases	3 (0.4)	0 (0)	3 (1)	<0.001****
Neurological diseases	12 (2)	6 (2)	6 (1)	0.48**
Hashimoto's thyroiditis	67 (9)	23 (9)	44 (9)	0.83**
Diabetes	15 (2)	4 (1)	11 (2.5)	0.006****

COVID – coronavirus disease; SD – standard deviation; BMI – body mass index; * Mann–Whitney U test; ** χ^2 test; *** Kruskal–Wallis test; **** Fisher's exact test.
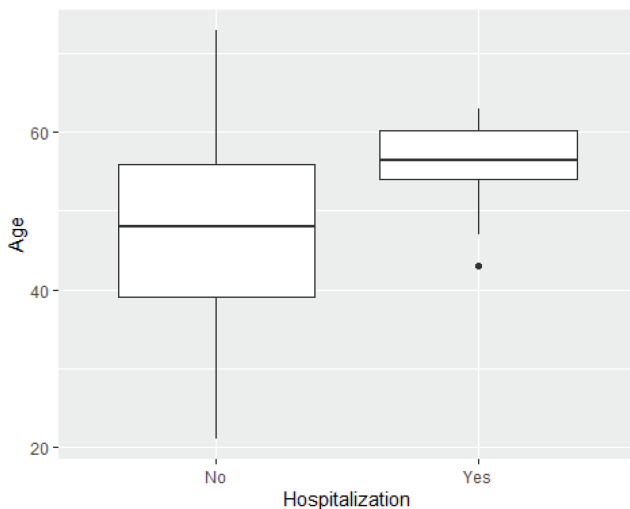
Fig. 1. Relationship between age and the hospitalization due to coronavirus disease 2019 (COVID-19) infection

Among the studied medical staff, 48% of women and 62% of men have been infected with COVID-19 in the past. In 20.6% the course of the disease was asymptomatic, in 73% required only home treatment and in 6.4% required hospitalization. In terms of severity, there were no statistically significant differences between COVID and non-COVID hospitals.

Risk of disease according to occupational groups

Risk for all hospital staff

A statistically significant relationship between occupational group and risk of infection ($\chi^2 = 20.05$; p = 0.0012) was demonstrated for all medical staff. The group of medical staff who were most likely to be infected with COVID-19 were the nurses/paramedics/medical caretakers (60%), orderlies/hospital cleaners (55%) and physiotherapists (53%). Lab workers/technicians/pharmacists were the least likely to be infected (38%).

Risk of disease by workplace (COVID compared to non-COVID hospital)

For the medical staff as a whole, the group of employees who were most frequently infected with COVID-19 were nurses/paramedics/medical caretakers (56%) and the group of employees who were least frequently infected were administrative workers (23%). The above relationship was not observed for a COVID-19 hospital. There were no statistically significant correlations in incidence rates between occupational groups (p = 0.37) (Table 3).

Table 2. Data on regression, confidence intervals for odds ratios, statistical significance for the entire model, and a measure of goodness-of-fit (Nagelkerke pseudo R^2)

Variable	Model	Estimate	SE	p-value	OR	95% CI	Nagelkerke pseudo R^2
Age	univariate	0.095	0.03	<0.001	1.10	[1.05; 1.16]	0.12
	multivariate	0.09	0.03	0.001	1.09	[1.04; 1.16]	0.14
Male sex	univariate	−1.26	0.75	0.092	0.28	[0.04; 0.99]	0.03
	multivariate	−0.98	0.77	0.200	0.37	[0.06; 1.37]	0.14

SE – standard error; OR – odds ratio; 95% CI – 95% confidence interval.

Table 3. Risk of disease by workplace (COVID-19 hospital compared to non-COVID hospital)

Variable		Workplace						p-value
		administrative workers n (%)	nurses/paramedics/ medical caretakers n (%)	orderlies/ hospital cleaners n (%)	physio-therapists n (%)	lab workers/ technicians/ pharmacists n (%)	treating physicians n (%)	
Non-COVID hospital	COVID-19-positive	7 (23)	86 (56)	6 (46)	7 (44)	31 (38)	73 (43)	0.009*
	COVID-19-negative	24 (77)	68 (44)	7 (54)	9 (56)	50 (62)	98 (57)	
COVID hospital	COVID-19-positive	25 (69)	104 (64)	10 (67)	3 (100)	4 (36)	21 (55)	0.370*
	COVID-19-negative	11 (31)	59 (36)	5 (33)	0 (0)	7 (64)	17 (45)	

COVID-19 – coronavirus disease 2019; * χ² test.

Effect of analyzed factors on risk of infection and on COVID-19 infection and the severity of the course of the disease

BMI and physical activity and the risk of infection and the severity of the course of the disease

For medical staff, the risk of COVID-19 infection was 5% greater with an increase in body mass index (BMI) by 1 unit (OR = 1.05, p = 0.004), whereas the risk of COVID-19 infection was 85% greater for those who were overweight or obese compared to those who were underweight or of normal weight (OR = 1.85, p < 0.001). In addition, there was a statistically significant correlation between the severity of infection (no symptoms, home treatment, hospitalization) and BMI (χ^2 = 17.028, p < 0.001). Among hospitalized patients, a significantly higher median BMI was noted compared to non-hospitalized patients – 26.8 (IQR 25.3–30.3) kg/m² and 26.2 (IQR 23.5–29.4) kg/m², respectively (p = 0.043) (Fig. 2).

There was no correlation between the physical activity declared by the persons and the risk of infection and the severity of the course of the disease.

Impact of comorbidities and smoking on COVID-19 incidence and the course of the disease

Among the medical staff surveyed, diabetes was present in a small group of 15 people (2%). The study results did not show that diabetic patients developed COVID-19 more frequently than those in the general population (Table 1). The influence of diabetes on the risk of hospitalization was observed in the group of COVID-19-positive patients. The history of diabetes was more than 5 times more frequent (OR = 5.5; p = 0.049) among hospitalized patients compared to non-hospitalized patients (8.3% and 1.6%, respectively).

We took into account the coexistence of chronic diseases in general and we divided these conditions into cardiovascular, pulmonary and renal disease, systemic connective tissue disease, neurological disease, and Hashimoto's thyroiditis. Participants with chronic diseases were not shown
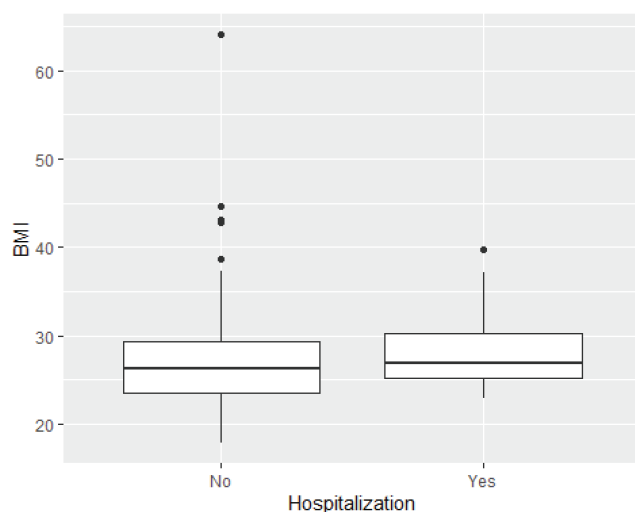

Fig. 2. Box plot of the correlation of body mass index (BMI) and coronavirus disease 2019 (COVID-19) infection. The horizontal line marks the median, the box marks the interquartile range (IQR; Q1–Q3), and the whiskers mark the range of outliers. Empty bubbles are outliers

to be more likely to have COVID-19 than those without these diseases. Among the medical staff in the study group, only 3 persons had systemic connective tissue disease, and all of them had COVID-19, but because of the very small group size, we were unable to draw firm conclusions.

Smoking did not have a significant impact on the incidence of COVID-19 (p = 0.58).

Association of flu vaccination with COVID-19 infection rates and SARS-CoV-2 course severity

Data on past flu vaccination was available for only a subset of the non-COVID hospital staff. The percentage of those who were vaccinated against flu and became infected was significantly lower than of those who were not vaccinated and became infected (χ^2 = 17.401;

p < 0.001). The chance of COVID-19 infection was more than twice as high among those not vaccinated against flu (OR = 2.23, p < 0.001). The analysis of the severity of infection is difficult because only 5 participants out of 460 analyzed with data concerning flu vaccination were hospitalized (among them 3 were not vaccinated against flu).

The correlation of COVID-19 incidence and number of people living in a shared household

There was no statistical relationship between the number of people living in the same household and the frequency of COVID-19 infection and severity. The number of infections and their severity was similar regardless of living with children under 5 and with persons over 65 in the same household (Table 1,4).

Table 4. COVID-19 infections among medical staff at a COVID hospital and a non-COVID hospital

Variable	n (%)			p-value
	total (n = 732)	COVID-19-positive (n = 377)	COVID-19-negative (n = 355)	
Age, mean (SD) [years]	47 (12)	47 (12)	47 (12)	0.73*
Sex male female	164 (22) 568 (78)	103 (62.8) 272 (48)	61 (37.2) 296 (52)	0.001**
BMI, mean (SD)	26 (5)	26.7	25.5	<0.001*
BMI underweight normal weight overweight obesity	11 (2) 333 (45) 260 (35) 128 (18)	3 (1) 147 (39) 155 (41) 72 (19)	8 (2) 186 (52) 105 (30) 56 (16)	0.001***
Smoking non-smoker former smoker passive smoker active smoker	478 (65) 126 (17) 19 (3) 109 (15)	240 (64) 77 (20) 12 (3) 48 (13)	238 (67) 49 (14) 7 (2) 61 (17)	0.05***
Number of persons in a household 1 2 >2	96 (13) 267 (36) 369 (51)	44 (12) 142 (38) 191 (51)	52 (15) 125 (35) 178 (50)	0.47***
Number of households with children <5 years of age	63 (9)	29 (8)	34 (10)	0.52**
Number of households with persons >65 years of age	61 (8)	33 (9)	28 (8)	0.79**
Chronic diseases	240 (33)	124 (33)	116 (33)	1**
Renal diseases	6 (1)	3 (1)	3 (1)	1****
Cardiovascular diseases	69 (9)	35 (9)	34 (10)	0.87**
Pulmonary diseases	17 (2)	6 (1)	11 (3)	0.16**
Systemic connective tissue diseases	3 (1)	3 (1)	0 (0)	<0.001****
Neurological diseases	12 (2)	6 (2)	6 (2)	1**
Hashimoto's thyroiditis	67 (9)	39 (10)	28 (8)	0.3**
Diabetes	15 (2)	8 (2)	7 (2)	1**
Flu vaccination (460)	235 (51)	83 (40)	152 (59)	<0.001**
Physical activity	323 (44)	159 (42)	164 (46)	0.34**

COVID-19 – coronavirus disease 2019; SD – standard deviation; BMI – body mass index; *Mann–Whitney U test; ** χ^2 test; *** Kruskal–Wallis test; **** Fisher's exact test.

Discussion

In the presented study, we showed the relationship between BMI, age and coexistence of diabetes mellitus with the risk of hospitalization due to COVID-19 in the population of medical professionals. We have shown that previous influenza vaccination is a factor that may influence the risk of COVID-19 infection. Other analyzed risk factors, including comorbidities other than diabetes, smoking and socioeconomic factors, did not affect the risk of COVID-19 infection and the course of the disease.

By analyzing the risk of COVID-19 infection among medical staff, it was shown that the risk of COVID-19 infection is 2 times higher among employees of a COVID hospital. The greatest risk of infection was for staff in direct contact with patients, namely nurses/paramedics/medical caretakers, orderlies, hospital cleaners, and physiotherapists. The staff who was not in direct contact with the patient (laboratory technicians, pharmacists) got infected least frequently. In the analysis of incidence patterns in a COVID hospital compared to a non-COVID hospital, this incidence profile was only retained for the non-COVID hospital. The COVID hospital workers showed no significant differences between occupational groups, which can be explained by the high risk of exposure to COVID-19, despite the personal protection methods used. This indicates that the employees of COVID hospitals have a higher risk of contracting the disease without even having direct contact with the patients. It may be related to the exposure to infection from other hospital employees. The presented analysis concerned data obtained before the introduction of universal vaccination against COVID-19, which is also important for the frequency and severity of cases among medical personnel. Because of this, medical staff members require prophylactic methods (vaccination), appropriate personal protective equipment and early diagnosis of possible infection.

Similar to other publications, among out study group, men were more likely to contract COVID-19, which confirms that it is one of the most important non-modifiable risk factors.[16–18] The reason for this tendency has not yet been fully examined. It is suspected that this may be related to the distribution of sex-specific hormones and their effects on specific receptors. As demonstrated by anothers authors, estradiol, which is present at high levels in women, causes an increase in expression and activity of ADAM17.[19,20] The ADAM17 protein is more highly expressed in the lung and liver, which is associated with the excretion of surface proteins such as ACE2. The ADAM17 activity increased by estradiol results in increased ACE2 solubility in women, which ultimately may be one of the reasons for the reduced incidence of COVID-19 in women compared with men.[20,21] Men were more likely to require intensified treatment, including hospitalization, which is consistent with the literature.[22]

No relationship between COVID-19 incidence and severity of the infection and the number of people living in the same household was found. We also did not observe such an association when considering children under 5 and elderly people in the household, although infections were more likely if people over 65 lived in the household, which may be due to the small number of such households in our analysis. A meta-analysis conducted by Madewell et al. demonstrated a higher prevalence of COVID-19 infection in households with the elderly than with children.[23]

Another risk factor for more severe SARS-CoV-2 infection is age. Hospitalized patients were on average 9 years older than those with mild or asymptomatic SARS-CoV-2 course. Age-related decline and dysregulation of immune function, i.e., immunosenescence and inflammaging, play a major role in contributing to the increased susceptibility to severe sequelae of SARS-CoV-2 in older age.[24,25]

The epidemiology of COVID-19 incidence based on analyses of large populations shows a clear association with body weight, especially with obesity.[26,27]

In a study conducted in a group of medical staff employed at both COVID and non-COVID hospitals, BMI values were higher for those who had an infection compared to those who were not infected. Consistent with our studies, Popkin et al. found an increased number of COVID-19-positive individuals among obese ones; in addition, individuals with obesity were more likely to be hospitalized.[28] Overweight and obesity were risk factors for hospitalization, mechanical ventilation and death.[29]

Based on a prospective study, Gao et al. confirmed the relationship of BMI with hospitalization and death due to SARS-CoV-2; the relationship was J-shaped and meant a worse prognosis for people with malnutrition.[30] In our study group, only 11 persons had below-normal BMI, and 3 of them had an infection. Determining the cutoff line for BMI at which the risk of COVID-19 infection and/or severity increases is an interesting and important challenge for further research on the epidemiology of COVID-19.

Physical activity is related to weight reduction and redistribution of body fat. It also reduces the risk of metabolic and CVD and depression, and stimulates the immune system. Nevertheless, the studies on the effect of physical activity on the risk of COVID-19 infection and the severity of the course of infection are limited and remain inconclusive, which may be related to the methodology used.[31–33] In the study group, no correlation between the declared level of physical activity and the risk of COVID-19 infection or severity of SARS-CoV-2 was found.

Although diabetic patients are exposed to a higher incidence of various infections, we have not shown that they have an increased frequency of COVID-19 infection and the results of our study confirm the previous observations. However, people with diabetes have a more severe course of SARS-CoV-2 infection. Pro-inflammatory activation of vascular endothelial cells and pro-thrombotic state, co-occurring with diabetes, may be responsible for this. These processes may influence both an increased inflammatory response in the form of a "cytokine storm" in COVID-19

as well as more frequent thromboembolic complications. Hypertension, CVD[7] and chronic obstructive pulmonary disease (COPD) increased the risk of severe COVID-19[34]; however, we did not confirm this observations in our study. In the present study, COVID-19 patients with coexisting diabetes were more likely to require hospitalization, which is consistent with the literature data.[7,35]

The foregoing findings do not allow firm conclusions to be drawn regarding the association between smoking and COVID-19 infection. The results of our study did not show a link between smoking and the risk of developing a disease. The study population was dominated by non-smokers.

The idea of a possible effect of seasonal flu virus vaccination on reducing the risk of COVID-19 infection or a milder course of SARS-CoV-2 was based on the potential role of the nonspecific immune response. We have shown that the risk of contracting COVID-19 is more than twice as high in persons not vaccinated against flu. Our observations confirm the results of the studies published so far. A retrospective analysis of a medical record database showed a beneficial effect of past flu vaccination on the risk of COVID-19 infection in a population older than 65.[36] Also, Candelli et al. indicated the benefits of flu vaccination in the population over 65. In a retrospective analysis of COVID-19 patients, these authors showed a lower risk of death over a 60-day period among those vaccinated.[37] On the other hand, a study conducted on a group of 3500 medical staff showed neither positive nor negative association between COVID-19 infection and flu vaccination during the preceding 5 flu seasons.[38] A broader aspect of the impact of flu vaccination on the course of COVID-19 infection includes mainly, in addition to the nonspecific immune response, a reduction in the risk of co-infection. Flu virus causes increased expression of ACE2 receptors on airway cells, which could potentially worsen SARS-CoV-2 course.[39]

Limitations of the study

Our observations did not confirm previous data on the association of certain chronic diseases and smoking with the risk of developing COVID-19. However, the presented results should be interpreted with caution, because only 24 people of those who experienced COVID-19 required hospitalization.

Conclusions

The results of our study showed that the incidence of COVID-19 infection was 2 times higher among COVID hospital medical staff. The highest risk of infection for a non-COVID hospital was for staff who had direct contact with patients, whereas for a COVID hospital, the risk of infection was the same among all hospital staff. Based on the literature and our study, it appears that gender may influence the pathogenetic mechanisms of COVID-19, the risk of infection and severity of disease, and thus the sequelae. Our study confirmed that BMI value is important for infection risk and severity of COVID-19. In addition, we have shown that while diabetes does not increase the risk of developing SARS-CoV-2, it significantly affects the risk of hospitalization among people infected with COVID-19. We have also confirmed the importance of flu vaccination, i.e., the chance of the infection was more than twice as high among non-vaccinated individuals. The COVID-19 pandemic remains a global problem, despite the tremendous progress that has been made in a short period of time in the diagnosis and prevention of the disease.

ORCID iDs

Marta Madej ⓘ https://orcid.org/0000-0002-4523-9272
Agata Sebastian ⓘ https://orcid.org/0000-0001-6332-8714

References

1. Huang C, Wang Y, Li X, et al. Clinical features of patients infected with 2019 novel coronavirus in Wuhan, China. *Lancet*. 2020;395(10223): 497–506. doi:10.1016/S0140-6736(20)30183-5
2. Rashedi J, Mahdavi Poor B, Asgharzadeh V, et al. Risk factors for COVID-19. *Infez Med*. 2020;28(4):469–474. PMID:33257620.
3. Kim JA, Seong RK, Shin OS. Enhanced viral replication by cellular replicative senescence. *Immune Netw*. 2016;16(5):286. doi:10.4110/in.2016.16.5.286
4. Fung SY, Yuen KS, Ye ZW, Chan CP, Jin DY. A tug-of-war between severe acute respiratory syndrome coronavirus 2 and host antiviral defence: Lessons from other pathogenic viruses. *Emerg Microbes Infect*. 2020; 9(1):558–570. doi:10.1080/22221751.2020.1736644
5. Manners C, Larios Bautista E, Sidoti H, Lopez OJ. Protective adaptive immunity against severe acute respiratory syndrome coronaviruses 2 (SARS-CoV-2) and implications for vaccines. *Cureus*. 2020;12(6):e8399. doi:10.7759/cureus.8399
6. Landecho M, Marin-Oto M, Recalde-Zamacona B, Bilbao I, Frühbeck G. Obesity as an adipose tissue dysfunction disease and a risk factor for infections: Covid-19 as a case study. *Eur J Intern Med*. 2021;91:3–9. doi:10.1016/j.ejim.2021.03.031
7. Azar WS, Njeim R, Fares AH, et al. COVID-19 and diabetes mellitus: How one pandemic worsens the other. *Rev Endocr Metab Disord*. 2020; 21(4):451–463. doi:10.1007/s11154-020-09573-6
8. Leung JM, Yang CX, Tam A, et al. ACE-2 expression in the small airway epithelia of smokers and COPD patients: Implications for COVID-19. *Eur Respir J*. 2020;55(5):2000688. doi:10.1183/13993003.00688-2020
9. Jackson SE, Brown J, Shahab L, Steptoe A, Fancourt D. COVID-19, smoking and inequalities: A study of 53 002 adults in the UK. *Tob Control*. 2021;30(e2):e111–e121. doi:10.1136/tobaccocontrol-2020-055933
10. Reddy RK, Charles WN, Sklavounos A, Dutt A, Seed PT, Khajuria A. The effect of smoking on COVID-19 severity: A systematic review and meta-analysis. *J Med Virol*. 2021;93(2):1045–1056. doi:10.1002/jmv.26389
11. Grundy E, Suddek T, Filippidis F, Majeed A, Coronini-Cronberg S. Smoking, SARS-CoV-2 and COVID-19: A review of reviews considering implications for public health policy and practice. *Tob Induc Dis*. 2020;18:58. doi:10.18332/tid/124788
12. Xie J, Zhong R, Wang W, Chen O, Zou Y. COVID-19 and smoking: What evidence needs our attention? *Front Physiol*. 2021;12:603850. doi:10.3389/fphys.2021.603850
13. Tsigaris P, Teixeira da Silva JA. Smoking prevalence and COVID-19 in Europe. *Nicotine Tob Res*. 2020;22(9):1646–1649. doi:10.1093/ntr/ntaa121
14. Simons D, Shahab L, Brown J, Perski O. The association of smoking status with SARS-CoV-2 infection, hospitalization and mortality from COVID-19: A living rapid evidence review with Bayesian meta-analyses (version 7). *Addiction*. 2021;116(6):1319–1368. doi:10.1111/add.15276

15. Galanis P, Vraka I, Fragkou D, Bilali A, Kaitelidou D. Seroprevalence of SARS-CoV-2 antibodies and associated factors in healthcare workers: A systematic review and meta-analysis. *J Hosp Infect*. 2021;108: 120–134. doi:10.1016/j.jhin.2020.11.008

16. Chen N, Zhou M, Dong X, et al. Epidemiological and clinical characteristics of 99 cases of 2019 novel coronavirus pneumonia in Wuhan, China: A descriptive study. *Lancet*. 2020;395(10223):507–513. doi:10.1016/S0140-6736(20)30211-7

17. Lu R, Zhao X, Li J, et al. Genomic characterisation and epidemiology of 2019 novel coronavirus: Implications for virus origins and receptor binding. *Lancet*. 2020;395(10224):565–574. doi:10.1016/S0140-6736 (20)30251-8

18. Zhou F, Yu T, Du R, et al. Clinical course and risk factors for mortality of adult inpatients with COVID-19 in Wuhan, China: A retrospective cohort study. *Lancet*. 2020;395(10229):1054–1062. doi:10.1016/S0140-6736(20)30566-3

19. Rizzo P, Vieceli Dalla Sega F, Fortini F, Marracino L, Rapezzi C, Ferrari R. COVID-19 in the heart and the lungs: Could we "Notch" the inflammatory storm? *Basic Res Cardiol*. 2020;115(3):31. doi:10.1007/s00395-020-0791-5

20. Black RA, Rauch CT, Kozlosky CJ, et al. A metalloproteinase disintegrin that releases tumour-necrosis factor-α from cells. *Nature*. 1997; 385(6618):729–733. doi:10.1038/385729a0

21. Zipeto D, Palmeira J da F, Argañaraz GA, Argañaraz ER. ACE2/ ADAM17/TMPRSS2 interplay may be the main risk factor for COVID-19. *Front Immunol*. 2020;11:576745. doi:10.3389/fimmu.2020.576745

22. Dutkiewicz J, Mackiewicz B, Lemieszek M. COVID 19: Possible interrelations with respiratory comorbidities caused by occupational exposure to various hazardous bioaerosols. Part I. Occurrence, epidemiology and presumed origin of the pandemic. *Ann Agric Environ Med*. 2020;27(4):491–504. doi:10.26444/aaem/130871

23. Madewell ZJ, Yang Y, Longini IM, Halloran ME, Dean NE. Household transmission of SARS-CoV-2: A systematic review and meta-analysis. *JAMA Netw Open*. 2020;3(12):e2031756. doi:10.1001/jamanetworkopen. 2020.31756

24. Chen Y, Klein SL, Garibaldi BT, et al. Aging in COVID-19: Vulnerability, immunity and intervention. *Ageing Res Rev*. 2021;65:101205. doi:10. 1016/j.arr.2020.101205

25. O'Driscoll M, Ribeiro Dos Santos G, Wang L, et al. Age-specific mortality and immunity patterns of SARS-CoV-2. *Nature*. 2021;590(7844): 140–145. doi:10.1038/s41586-020-2918-0

26. Bil J, Możeńska O. The vicious cycle: A history of obesity and COVID-19. *BMC Cardiovasc Disord*. 2021;21(1):332. doi:10.1186/s12872-021-02134-y

27. Booth A, Reed AB, Ponzo S, et al. Population risk factors for severe disease and mortality in COVID-19: A global systematic review and meta-analysis. *PLoS ONE*. 2021;16(3):e0247461. doi:10.1371/journal. pone.0247461

28. Popkin BM, Du S, Green WD, et al. Individuals with obesity and COVID-19: A global perspective on the epidemiology and biological relationships. *Obes Rev*. 2020;21(11):e13128. doi:10.1111/obr.13128

29. Kompaniyets L, Goodman AB, Belay B, et al. Body mass index and risk for COVID-19-related hospitalization, intensive care unit admission, invasive mechanical ventilation, and death: United States, March– December 2020. *MMWR Morb Mortal Wkly Rep*. 2021;70(10):355–361. doi:10.15585/mmwr.mm7010e4

30. Gao M, Piernas C, Astbury NM, et al. Associations between body mass index and COVID-19 severity in 6.9 million people in England: A prospective, community-based, cohort study. *Lancet Diabetes Endocrinol*. 2021;9(6):350–359. doi:10.1016/S2213-8587(21)00089-9

31. Lee SW, Lee J, Moon SY, et al. Physical activity and the risk of SARS-CoV-2 infection, severe COVID-19 illness and COVID-19 related mortality in South Korea: A nationwide cohort study [published online ahead of print on July 22, 2021]. *Br J Sports Med*. 2021. doi:10.1136/ bjsports-2021-104203

32. Pinto AJ, Goessler KF, Fernandes AL, et al. No independent associations between physical activity and clinical outcomes among hospitalized patients with moderate to severe COVID-19. *J Sport Health Sci*. 2021;10(6):690–696. doi:10.1016/j.jshs.2021.08.001

33. Sallis R, Young DR, Tartof SY, et al. Physical inactivity is associated with a higher risk for severe COVID-19 outcomes: A study in 48 440 adult patients. *Br J Sports Med*. 2021;55(19):1099–1105. doi:10.1136/ bjsports-2021-104080

34. Wang B, Li R, Lu Z, Huang Y. Does comorbidity increase the risk of patients with COVID-19: Evidence from meta-analysis. *Aging (Albany NY)*. 2020; 12(7):6049–6057. doi:10.18632/aging.103000

35. Magdy Beshbishy A, Oti VB, Hussein DE, et al. Factors behind the higher COVID-19 risk in diabetes: A critical review. *Front Public Health*. 2021;9:591982. doi:10.3389/fpubh.2021.591982

36. Huang K, Lin SW, Sheng WH, Wang CC. Influenza vaccination and the risk of COVID-19 infection and severe illness in older adults in the United States. *Sci Rep*. 2021;11(1):11025. doi:10.1038/s41598-021-90068-y

37. Candelli M, Pignataro G, Torelli E, et al. Effect of influenza vaccine on COVID-19 mortality: A retrospective study. *Intern Emerg Med*. 2021; 16(7):1849–1855. doi:10.1007/s11739-021-02702-2

38. Belingheri M, Paladino ME, Latocca R, De Vito G, Riva MA. Association between seasonal flu vaccination and COVID-19 among healthcare workers. *Occup Med (Lond)*. 2020;70(9):665–671. doi:10.1093/occmed/kqaa197

epidemiology, medical staff, COVID-19, risk of infection

Platelet sTWEAK and plasma IL-6 are associated with 18F-fluorodeoxyglucose uptake in right ventricles of patients with pulmonary arterial hypertension: A pilot study

Remigiusz Kazimierczyk[1,A–E], Piotr Szumowski[2,C], Stephan Nekolla[3,A,C,E], Łukasz Małek[4,A,C,E], Piotr Błaszczak[5,B], Marcin Hładuński[2,B,C], Ewa Tarasiuk[1,C], Janusz Myśliwiec[2,E], Bożena Sobkowicz[1,E], Karol Kamiński[1,6,A–D,F]

[1] Department of Cardiology, Medical University of Bialystok, Poland

[2] Department of Nuclear Medicine, Medical University of Bialystok, Poland

[3] Department of Nuclear Medicine, Technical University of Munich, Germany

[4] Department of Epidemiology, Cardiovascular Disease Prevention and Health Promotion, National Institute of Cardiology, Warszawa, Poland

[5] Department of Cardiology, Cardinal Wyszynski Hospital, Lublin, Poland

[6] Department of Population Medicine and Lifestyle Diseases Prevention, Medical University of Bialystok, Poland

A – research concept and design; B – collection and/or assembly of data; C – data analysis and interpretation;
D – writing the article; E – critical revision of the article; F – final approval of the article

Address for correspondence
Karol Kamiński
E-mail: fizklin@wp.pl

Abstract

Background. Cytokines soluble tumor necrosis factor-like weak inducer of apoptosis (sTWEAK) and interleukin 6 (IL-6) are involved in immune response, proliferation, apoptosis, and cardiovascular pathologies. We have previously confirmed that changes of their platelet or plasma contents are associated with pulmonary arterial hypertension (PAH). The positron emission tomography/magnetic resonance imaging (PET/MRI) hybrid imaging provides detailed insight into right ventricle (RV) hemodynamic and metabolic function.

Objectives. To evaluate the relationship between RV parameters obtained using PET/MRI and concentrations of plasma and platelet sTWEAK and IL-6 in stable PAH patients.

Materials and methods. Eighteen stable PAH patients (48.44 ±16.7 years) had simultaneous PET/MRI scans with 18F-fluorodeoxyglucose (^{18}F-FDG) performed. Its uptake was presented as a standardized uptake value (SUV) for RV and left ventricle (LV). Cytokines concentrations were measured in platelet-poor plasma and platelet lysate. Follow-up time of this study was 58 months; the combined endpoint (CEP) was defined as death or clinical deterioration.

Results. We observed significant correlations between platelet sTWEAK levels, plasma IL-6 and PET parameter $SUV_{RV/LV}$ (r = −0.57, p = 0.011; r = 0.50, p = 0.032, respectively). In logistic regression, platelet sTWEAK and IL-6 were both prognostic factors for unfavorable ratio of $SUV_{RV/LV}$ higher than 1 (hazard ratio (HR) = 0.44, 95% confidence interval (95% CI): [0.23; 0.84], p = 0.017; and HR = 3.62, 95% CI: [1.21; 10.17], p = 0.011, respectively). Furthermore, their concentrations were related with prognostically important higher late gadolinium enhancement mass index (LGEMI) and RV global longitudinal strain/systolic pulmonary artery pressure (RV GLS/sPAP) values. Patients who had CEP in follow-up (n = 13) had significantly lower platelet sTWEAK content and higher plasma IL-6 at baseline than stable patients. Lower platelet sTWEAK was related to a worse prognosis in log-rank test (p = 0.006). Platelet sTWEAK and plasma IL-6 together with RV GLS/sPAP, RV ejection fraction (RVEF), mean pulmonary arterial pressure (mPAP), and $SUV_{RV/LV}$ were significantly associated with time to CEP in univariate Cox analysis.

Conclusions. The sTWEAK and IL-6 concentrations in PAH patients are linked with metabolic and functional changes of RV visualized in PET/MRI, and both sTWEAK and IL-6 predict clinical deterioration.

Key words: pulmonary arterial hypertension, IL-6, imaging, PET, sTWEAK

Background

Pulmonary arterial hypertension (PAH) is a multifactorial disease characterized by proliferation and vasoconstriction in pulmonary vasculature. These lead to subsequent increase of pulmonary vascular resistance (PVR), right-sided heart failure (HF) and premature death.[1] The development of PAH involves inflammatory processes together with in situ thrombosis, where circulating cytokines (also those released by platelets at the site of endothelium injury) play an important role.[2–5] Some studies revealed that not only the excess of platelet-derived cytokines, but also their deficiency may be associated to PAH and its progression, and thus platelet blockade may not be a correct action to treat PAH.[6–8] Platelets are one of the main sources of circulating tumor necrosis factor-like weak inducer of apoptosis (TWEAK) and we have shown that it is platelet TWEAK concentration that provides prognostic information in PAH.[6] Our previous studies have proven that PAH patients present lower serum and platelet lysate soluble TWEAK (sTWEAK) concentrations than the control group, which is also associated with a worse prognosis. However, possible mechanism resulting in lower sTWEAK in these patients as well as its involvement in the pathogenesis of the disease are still unclear.

Interleukin 6 (IL-6) is a pleiotropic cytokine involved in acute phase of inflammation, which acts via many receptors, e.g., CD126, gp130 (also called CD130) or the soluble form of IL-6 receptor (sIL-6R).[9] In our previous project, we have demonstrated that patients with PAH have higher concentrations of serum and plasma IL-6 together with sIL-6R than healthy volunteers, with no significant differences in soluble gp130 (sgp130) levels, which strongly indicates enhanced IL-6 trans-signaling in patients with PAH.[5] Unlike sTWEAK, IL-6 plasma concentration is more important in PAH than its platelet content.[10] There is evidence for an important role of IL-6 in lipid cardiac metabolism.[11,12]

Physiologically, most (even 95%) of energy in cardiomyocytes is derived from phosphorylation processes occurring in mitochondria (predominantly from fatty acids and, to a lesser extent, carbohydrate metabolism), with the remainder coming from process of glycolysis.[13–15] Interleukin 6 is involved in maintaining the balance between fatty acid oxidation and cardiac lipotoxicity, where its deficiency results in intracellular toxic lipid accumulation, thereby precipitating mitochondrial oxidative phosphorylation and thus overall cardiac dysfunction.[12,16]

However, no previous studies focused on the possible link between the levels of IL-6 or sTWEAK and quantitative measure of altered cardiac metabolism in case of HF. In PAH, increased PVR and following right ventricle (RV) pressure overload is associated with higher ^{18}F-fluorodeoxyglucose (^{18}F-FDG) uptake in positron emission tomography (PET) imaging.[17,18] The newly introduced quantitative measurement of RV ^{18}F-FDG uptake, presented as standardized uptake value $(SUV)_{RV/LV}$, correlates with PAH progression and unfavorable outcomes.[19]

Objectives

The main aim of this study was to assess whether the concentrations of inflammatory cytokines are linked with metabolic and functional changes of RV, as assessed with PET/magnetic resonance imaging (MRI) in PAH patients. We also hypothesized that the alterations presented above may precede clinical deterioration in almost 5-year follow-up.

Materials and methods

Setting and participants

We enrolled 18 clinically stable adult patients diagnosed with PAH into our pilot study. The diagnosis of PAH was made using right heart catheterization (RHC) according to the European guidelines.[1] The control group consisted of 10 healthy controls who were matched based on sex and age (44.75 ±13.5 years). The exclusion criteria as well as the examination protocol were described previously.[18,19]

The clinical follow-up lasted 58 months. Death, World Health Organization (WHO) class worsening, hospitalization due to PAH, or right-sided HF were used as combined endpoint (CEP) for Kaplan–Meier analysis.

The study was approved by the Bioethics Commitee of Medical University of Bialystok, Poland (approval No. R-I-002/140/2015) and is compliant with the declaration of Helsinki.

Blood sampling

Fasting peripheral venous blood samples were obtained from patients with PAH as well as controls. Ethylenediaminetetraacetic acid (EDTA) plasma aliquots of 1.5 mL were stored at −80°C. Concentrations of plasma sTWEAK, IL-6 and sIL-6R were determined using commercially available enzyme-linked immunosorbent assay (ELISA) kits (R&D Systems, Minneapolis, USA) according to the manufacturer's instructions. The mean minimum detectable value was 9.7 pg/mL for sTWEAK, 0.039 pg/mL for IL-6 and 6.5 pg/mL for sIL-6R. All analyses were performed according to the baseline values of the measured cytokines. Platelets were processed as described previously.[6,10] To better present platelet storage of TWEAK, IL-6 and sIL-6R, independently of the platelet count, the amounts of these cytokines were normalized to the concentration of protein in the platelet lysates and presented as a ratio in the manuscript.

Myocardial PET/MRI hybrid imaging

The PET/MRI hybrid imaging was performed with a 3T Biograph mMR hybrid system (Siemens Healthcare, Erlangen, Germany) at baseline visit within a median of 4 (2–6) days of RHC during the same patients'

hemodynamic status, according to the previously described protocol.[18–20]

For semi-quantitative analysis of ^{18}F-FDG metabolism in the myocardium, the ratio of standardized uptake value of glucose of RV and left ventricle (LV) was used ($SUV_{RV/LV}$). The late gadolinium enhancement mass index (LGEMI = LGE mass/body surface area) parameter and RV-arterial coupling estimation parameter (RV global longitudinal strain/systolic pulmonary artery pressure (RV GLS/sPAP) ratio) were assessed as described in previous studies.[18,21]

Statistical analyses

The distribution of all variables was verified using the Shapiro–Wilk test. The data are expressed as a mean standard deviation (SD) or median (interquartile range (IQR)). Statistical analysis was performed using Student's t or Mann–Whitney tests for continuous data. The Spearman's correlation coefficient was used to examine the relationship between 2 continuous variables. The Benjamini–Hochberg correction was used to account for multiple comparisons in correlation analysis. Logistic regression was used to predict a dependent categorical target variable. Univariable Cox proportional hazards regression analyses were performed to identify independent variables associated with endpoint. Receiver operator characteristic (ROC) curves were plotted to determine the area under the curve (AUC) and sensitivity and specificity of the optimal cutoffs (binomial method). To investigate the occurrence of clinical endpoints Kaplan–Meier method with log-rank test was implemented. A value of p < 0.05 was deemed statistically significant. A statistical software package Stata v. 13 (StataCorp LLC, College Station, USA) was used for the analysis.

Results

General results

Most PAH patients were in WHO class III (77%, n = 14). Mean pulmonary artery pressure (mPAP) derived from RHC was 50.33 ±18.96 mm Hg and PVR was 9.23 ±5.74 Wood units. Idiopathic PAH etiology was diagnosed in 64% (n = 12) of patients, PAH associated with connective tissue diseases (systemic scleroderma and mixed connective tissue disease) in 18% (n = 3) and congenital heart diseases with small left–right defects in 18% (n = 3). At the time of enrolment, 5 patients (27%) were incident cases. The clinical, functional and hemodynamic characteristics as well as laboratory data and echo results of subjects are presented in Table 1.

The PAH patients had statistically significantly lower platelet content of sTWEAK/total protein ratio than the healthy controls (6.19 ±2.72 × 10^{-8} compared to 9.77 ±2.21 × 10^{-8}, p = 0.006, Fig. 1A), with no significant differences in plasma levels (537.4 ±153.3 pg/mL compared to 577.5 ±59.3 pg/mL, p = 0.383). Interleukin 6 and sIL-6R plasma concentrations were significantly higher in PAH group (2.25 ±1.50 pg/mL compared to 0.82 ±0.38 pg/mL, p = 0.023 (Fig. 1B) and 45.45 ±12.11 ng/mL compared to 31.97 ±74.23 ng/mL, p = 0.004, respectively). In platelets lysate, levels of sIL-6R (normalized to total protein concentration) were significantly higher in PAH patients than in the control group (Table 1).

As reported previously,[19] mean standard uptake value of right ventricle to left ventricle ($SUV_{RV/LV}$) was higher in the PAH group (Table 1) and strongly correlated with RHC/MRI parameters of RV (Table 2).
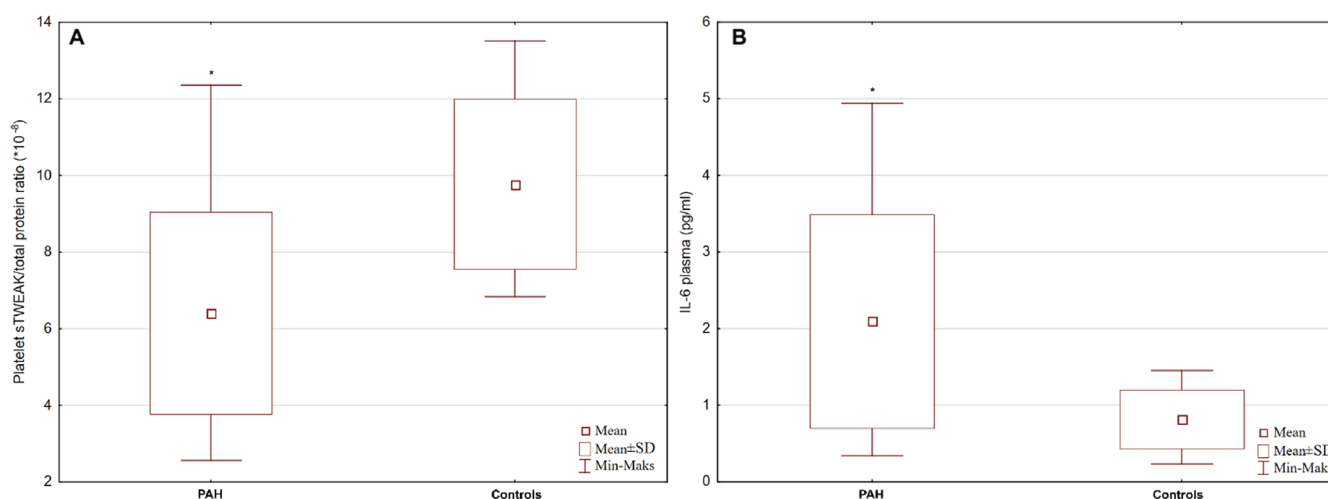
Fig. 1. sTWEAK/total protein concentrations ratio (×10^{-8}) in platelet lysate was significantly lower in PAH patients than in the control group (p = 0.006). A. IL-6 plasma concentration was significantly higher in PAH patients than in controls (p = 0.023); B. Student's t-test was used to compare 2 variables

PAH – pulmonary arterial hypertension; sTWEAK – soluble tumor necrosis factor-like weak inducer of apoptosis; SD – standard deviation; IL-6 – interleukin 6; * p-value < 0.05.

994

R. Kazimierczyk et al. PET/MRI and cytokines in PAH

Table 1. Basic characteristics of pulmonary arterial hypertension (PAH) group and healthy controls

Variables	PAH	Controls	p-value
Subjects, n	18	10	N/A
Age [years]	48.44 ±16.71	44.75 ±13.51	0.262
Females, % (n)	72 (13)	60 (6)	N/A
6MWT distance [m]	380 ±114	N/A	N/A
BNP [pg/mL]	212 (IQR 46–335)	N/A	N/A
Idiopathic/heritable pulmonary arterial hypertension, % (n)	64 (12)	N/A	N/A
Connective tissue disease related to pulmonary arterial hypertension, % (n)	18 (3)	N/A	N/A
Congenital heart disease related to pulmonary arterial hypertension, % (n)	18 (3)	N/A	N/A
Phosphodiesterase type 5 inhibitors, % (n)	50 (9)	N/A	N/A
Endothelin receptor antagonists, % (n)	18 (3)	N/A	N/A
Phosphodiesterase type 5 inhibitors + endothelin receptor antagonists, % (n)	18 (3)	N/A	N/A
Hemodynamics			
Systemic pulmonary artery pressure [mm Hg]	79.6 ±30.7	N/A	N/A
Diastolic pulmonary artery pressure [mm Hg]	33.6 ±14.8	N/A	N/A
Mean pulmonary artery pressure [mm Hg]	50.33 ±18.95	N/A	N/A
Pulmonary capillary wedge pressure [mm Hg]	10.72 ±2.57	N/A	N/A
Diastolic pulmonary gradient [mm Hg]	23.41 ±14.01	N/A	N/A
Pulmonary vascular resistance [Wood units]	9.22 ±5.74	N/A	N/A
Cardiac index [L/min/m^2]	2.51 ±0.59	N/A	N/A
Right atrium pressure [mm Hg]	8.66 ±3.21	N/A	N/A
RV parameters (MRI)			
RV ejection fraction, %	43.99 ±9.2	63.81 ±5.81	<0.001
RV EDV/BSA [mL/m^2]	121.4 ±32.7	73.65 ±12.21	0.001
RV ESV/BSA [mL/m^2]	69.3 ±27.7	28.25 ±9.06	<0.001
RV mass/BSA [g/m^2]	42.75 ±18.82	23.8 ±4.9	<0.001
RV GLS/sPAP [%/mm Hg]	−0.26 ±0.19	N/A	N/A
LGEMI [g/m^2]	3.06 ±2.33	N/A	N/A
Myocardial metabolism (PET)			
SUV$_{RV/LV}$ ratio	1.23 ±0.86	0.19 ±0.08	<0.001
Cytokines			
sTWEAK, plasma [pg/mL]	537.4 ±153.7	577.8 ±59.7	0.383
sTWEAK/total protein, platelets (×10^{-8})	6.19 ±2.72	9.77 ±2.21	0.006
IL-6, plasma [pg/mL]	2.25 ±1.50	0.82 ±0.38	0.023
IL-6/total protein, platelets (×10^{-10})	0.62 ±0.51	0.50 ±0.25	0.912
sIL-6R, plasma [ng/mL]	45.45 ±12	31.97 ±7.43	0.004
sIL-6R/total protein, platelets (×10^{-7})	1.79 ±0.61	1.31 ±0.23	0.053

Data are presented as mean ± standard deviation (SD) (normal distribution; Student's t-test was used to compare 2 variables) or median (interquartile range (IQR)) (non-normal distribution; Mann–Whitney test was used to compare 2 variables). 6MWT – 6-minute walk test; BSA – body surface area; BNP – brain natriuretic peptide; EDV – end-diastolic volume; ESV – end-systolic volume; GLS – global longitudinal strain; IL-6 – interleukin 6; LGEMI – late gadolinium enhancement mass index; LV – left ventricle; MRI – magnetic resonance imaging; PAH – pulmonary arterial hypertension; PET – positron emission tomography; RV – right ventricle; sIL-6R – soluble interleukin 6 receptor; sPAP – systolic pulmonary artery pressure; sTWEAK – soluble tumor necrosis factor-like weak inducer of apoptosis; SUV – standardized uptake value; N/A – not applicable.

Cytokines and hemodynamics interactions

We observed statistically significant correlations between platelet sTWEAK levels and PET SUV$_{RV/LV}$ (r = −0.57, p = 0.011, Fig. 2A), and between plasma IL-6 levels and SUV$_{RV/LV}$ (r = 0.50, p = 0.032, Fig. 2B). Importantly, plasma IL-6 concentration did not correlate with established hemodynamic parameters of RV dysfunction – RV ejection

Table 2. Spearman's correlations between cytokines and PET/MRI/RHC-derived parameters

Correlation coefficient (r); p-value (p)	sTWEAK, platelets	IL-6, plasma	SUV$_{RV/LV}$
6MWT distance	r = 0.08; p = 0.723	r = −0.51; p = 0.046	r = −0.38; p = 0.113
BNP	r = −0.09; p = 0.714	r = 0.18; p = 0.552	r = 0.44; p = 0.062
RVEF	r = 0.56; p = 0.019^	r = −0.10; p = 0.672	r = −0.52; p = 0.024^
mPAP	r = −0.43; p = 0.048^	r = 0.45; p = 0.051	r = 0.78; p < 0.001^
PVR	r = −0.24; p = 0.312	r = 0.22; p = 0.362	r = 0.62; p = 0.007^
SUV$_{RV/LV}$	r = −0.57; p = 0.011^	r = 0.50; p = 0.032^	–

^ p-value significant (lower than 0.05) after Benjamini–Hochberg correction; 6MWT – 6-minute walk test; BNP – serum brain natriuretic peptide; IL-6 – interleukin 6; LV – left ventricle; mPAP – mean pulmonary arterial hypertension; MRI – magnetic resonance imaging; PET – positron emission tomography; PVR – pulmonary vascular resistance; RHC – right heart catheterization; RV – right ventricle; RVEF – right ventricle ejection fraction; sTWEAK – soluble tumor necrosis factor-like weak inducer of apoptosis; SUV – standardized uptake value.
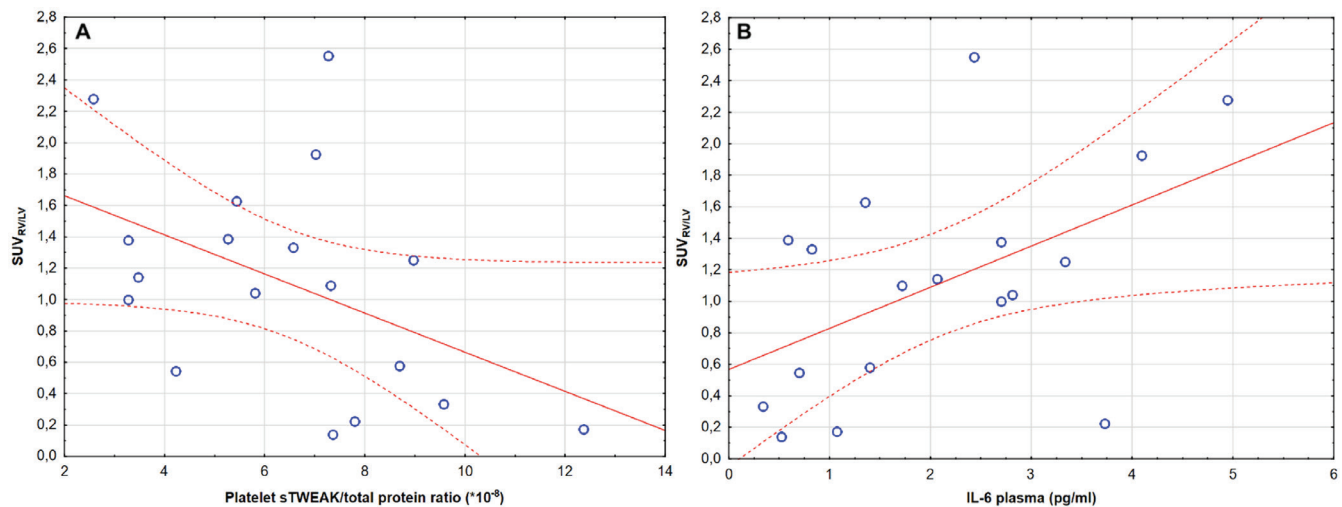
Fig. 2. Spearman's correlations between mean SUV$_{RV/LV}$ ratio and (A) sTWEAK platelet content (r = −0.57, p = 0.011) and (B) IL-6 plasma concentration (r = 0.50, p = 0.032)

SUV – standardized uptake value; RV – right ventricle; LV – left ventricle; PAH – pulmonary arterial hypertension; sTWEAK – soluble tumor necrosis factor-like weak inducer of apoptosis; IL-6 – interleukin 6.

fraction (RVEF), PVR, mPAP, or cardiac index, but it was a predictor of clinically significant SUV$_{RV/LV}$ threshold >1 in the univariate logistic regression analysis (hazard ratio (HR) = 3.62, 95% confidence interval (95% CI): [1.21; 10.17], p = 0.011). Also, platelet sTWEAK was a predictor of SUV$_{RV/LV}$ > 1 (HR = 0.44, 95% CI: [0.23; 0.84, p = 0.017).

In logistic regression, platelet sTWEAK was a predictor of RVEF < 40% (related with worse prognosis[19]; HR = 0.58, 95% CI: [0.33; 1.12], p = 0.048) and of newly established RV dysfunction and PAH prognostic parameter – RV GLS/sPAP > (−)0.29 (HR = 0.46, 95% CI: [0.2; 1.08], p = 0.043). Furthermore, we observed that platelet sTWEAK correlated with MRI and RHC RV parameters – RVEF (r = 0.56, p = 0.019) and mPAP (r = −0.43, p = 0.048), which proves a possible strong relationship between its altered availability and PAH hemodynamics.

Interestingly, plasma IL-6 predicted LGEMI parameter (LGE mass in RV insertion points normalized to body surface area) higher than 2.75 (cutoff value of worse PAH prognosis[21]; HR = 2.32, 95% CI: [0.93; 5.81], p = 0.046).

Survival analysis

We analyzed the concentrations of cytokines in PAH subjects who had met CEP (72%, n = 13). In this study, we extended the follow-up to 58 months. During this period, 4 patients died and 9 patients experienced a WHO class worsening with hospitalization (including 5 patients who required initiation of parenteral prostacyclin analogue). Mean time to clinical worsening was 25.38 ±18.58 months.

Patients with CEP had lower baseline platelet sTWEAK (5.39 ±2.38 × 10^{-8} compared to 8.30 ±2.60 × 10^{-8}, p = 0.032) and higher plasma IL-6 (2.55 ±1.51 pg/mL compared to 1.46 ±0.99 pg/mL, p = 0.041) than stable patients. Furthermore, CEP group presented higher SUV$_{RV/LV}$ ratio together with MRI parameter – RVEF and RHC parameters – mPAP and RAP, which is consistent with our previous results (Table 3).[18,19]

Using ROC curve analysis, we determined cutoff value of sTWEAK/total protein concentration ratio in platelets in prediction of CEP. Patients with a value lower than

Table 3. Comparison of patients with combined endpoint (CEP) and without CEP

Variables	CEP (+) patients	CEP (–) patients	p-value
Patients, n	13	5	N/A
BNP [pg/mL]	252 (IQR 143–507)	146 (IQR 46–252)	0.092
6MWT distance [m]	344 ±108	477 ±70	0.032
$SUV_{RV/LV}$ ratio	1.50 ±0.82	0.64 ±0.49	0.023
RVEF [%]	41.68 ±8.54	48.87 ±8.57	0.094
mPAP [mm Hg]	57.69 ±16.29	31.83 ±9.38	0.002
PVR [Wood units]	11.22 ±5.37	4.38 ±2.08	0.006
RAP [mm Hg]	9.69 ±3.13	6.12 ±1.26	0.013
RV GLS/sPAP [%/mm Hg]	−0.19 ±0.14	−0.47 ±0.19	0.024
LGEMI [g/m^2]	3.81 ±2.12	0.67 ±0.19	0.016
sTWEAK, plasma [pg/mL]	538.7 ±169.7	535.8 ±145.4	0.605
sTWEAK/total protein, platelets ($\times10^{-8}$)	5.39 ±2.38	8.30 ±2.60	0.032
IL-6, plasma [pg/mL]	2.55 ±1.51	1.46 ±0.99	0.041
IL-6/total protein, platelets ($\times10^{-10}$)	0.64 ±0.38	0.58 ±0.65	0.794
sIL-6R, plasma [ng/mL]	44.41 ±9.36	46.95 ±15.7	0.885
sIL-6R/total protein, platelets ($\times10^{-7}$)	1.49 ±0.46	2.19 ±0.57	0.086

Data are presented as mean ± standard deviation (SD) (normal distribution; Student's t-test was used to compare 2 variables) or median (interquartile range (IQR)) (non-normal distribution; Mann–Whitney test was used to compare 2 variables). BNP – brain natriuretic peptide; CO – cardiac output; GLS – global longitudinal strain; IL-6 – interleukin 6; LGEMI – late gadolinium enhancement mass index; LV – left ventricle; mPAP – mean pulmonary artery pressure; PAC – pulmonary arterial compliance; PVR – pulmonary vascular resistance; RAP – right atrial pressure; RV – right ventricle; RVEF – right ventricle ejection fraction; sIL-6R – soluble interleukin 6 receptor; sPAP – systolic pulmonary artery pressure; sTWEAK – soluble tumor necrosis factor-like weak inducer of apoptosis; SUV – standardized uptake value; 6MWD – 6-minute walk test; N/A – not applicable.
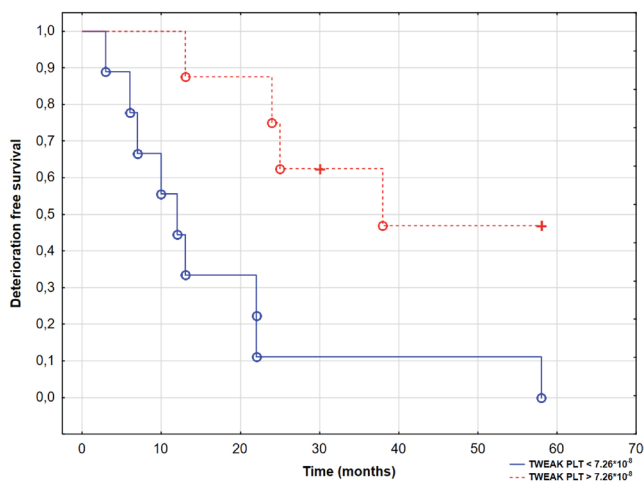
Fig. 3. Kaplan–Meier curves presenting deterioration-free survival in patients with pulmonary arterial hypertension (PAH) based on soluble tumor necrosis factor-like weak inducer of apoptosis (sTWEAK) platelet lysate content, log-rank test, p = 0.006

° – complete events; + – censored events.

7.26×10^{-8} (AUC = 0.78 (95% CI: [0.66; 0.96]), p = 0.021) had worse prognosis; the Kaplan–Meier survival curve and the log-rank test (p = 0.006) are presented in Fig. 3.

Interestingly, the same cutoff value of platelet sT-WEAK/total protein concentration ratio was obtained in prediction of $SUV_{RV/LV}$ ratio higher than 1 in PAH patients (AUC = 0.89 (95% CI: [0.76; 1]), p < 0.001). This suggests that advanced metabolic changes in PAH patients are in strong relation with cytokine levels affecting prognosis.

Finally, univariate Cox proportional hazard analysis revealed that among various parameters, platelet sTWEAK and plasma IL-6 together with RV GLS/sPAP, RVEF, mPAP, and $SUV_{RV/LV}$ were significantly associated with time to CEP (Table 4).

Discussion

In physiological conditions, cardiomyocytes use mainly fatty acid oxidation to produce energy. It changes in case of HF (e.g., PAH) or during ischemia.[17,20] Our previous results suggest that in PAH, possible "metabolic shift" occurs and process of glycolysis is highly increased, especially in RV, which can be assessed with PET imaging.[19] With further PAH progression and RV uncoupling, RV ^{18}F-FDG uptake increases and finally surpasses LV uptake ($SUV_{RV/LV}$ > 1). Importantly, $SUV_{RV/LV}$ ratio may independently predict PAH patients' prognosis preceding significant clinical deterioration requiring hospitalization.[14,19] On the other hand, RV ^{18}F-FDG accumulation may decrease after specific treatment with epoprostenol, proportionally to the degree of reduction in the PVR and RV peak-systolic wall stress.[22]

Next, we were able to confirm that patients with PAH have altered plasma IL-6 concentration together with sIL-6R and diminished platelet sTWEAK content.[6,10] These

Table 4. Univariate Cox proportional hazard analysis for the time to clinical worsening

Value	p-value	HR (95% CI)
Age	0.592	0.99 [0.93; 1.06]
WHO class	0.092	4.52 [0.7; 29.1]
BNP	0.121	1.00 [0.99; 1.02]
6MWT distance	0.062	0.99 [0.98; 1]
Creatinine	0.634	1.12 [0.71; 1.71]
LVEF	0.232	1.05 [0.96; 1.15]
RV EDV/BSA	0.476	1.01 [0.98; 1.03]
RV ESV/BSA	0.113	1.03 [0.99; 1.06]
RV mass/BSA	0.082	1.05 [0.99; 1.11]
RVEF	0.019	0.86 [0.71; 0.95]
mPAP	0.018	1.15 [1.01; 1.31]
PCWP	0.102	1.38 [0.93; 2.02]
DPG	0.068	1.07 [0.99; 1.14]
RAP	0.013	1.61 [1.08; 2.41]
Cardiac index	0.302	0.47 [0.11; 1.95]
PVR	0.048	1.44 [1.07; 1.94]
$SUV_{RV/LV}$	0.017	7.01 [2.24; 19.23]
RV GLS/sPAP	0.019	18.94 [2.23; 28.32]
IL-6, plasma	0.192	1.77 [0.69; 4.54]
sTWEAK, platelet	0.048	0.61 [0.34; 0.92]

HR – hazard ratio; 95% CI – 95% confidence interval; BSA – body surface area; BNP – brain natriuretic peptide; EDV – end-diastolic volume; ESV – end-systolic volume; DPG – diastolic pulmonary gradient; GLS – global longitudinal strain; LGEMI – late gadolinium enhancement mass index; LV – left ventricle; LVEF – left ventricle ejection fraction; mPAP – mean pulmonary artery pressure; sPAP – systolic pulmonary artery pressure; PCWP – pulmonary capillary wedge pressure; PAH – pulmonary arterial hypertension; PVR – pulmonary vascular resistance; RAP – right atrial pressure; RV – right ventricle; RVEF – right ventricle ejection fraction; sTWEAK – soluble tumor necrosis factor-like weak inducer of apoptosis; SUV – standardized uptake value; WHO – World Health Organization; IL-6 – interleukin 6; 6MWT – 6-minute walk test

results are in line with earlier observations. In this study, we have reported for the first time that the levels of these cytokines are also strongly correlated with altered glucose metabolism of cardiomyocytes. Furthermore, we were able to obtain prognostic cutoff value of sTWEAK platelet level, which may help in risk assessment of PAH patients.

Endothelial dysfunction and in situ thrombosis are considered important pathological mechanisms in PAH.[23] Activated platelets release various growth factors and cytokines enhance vasoconstriction and thrombus formation.[24] Platelet-derived mediators can not only initiate or aggravate local vascular remodelling but also attenuate it; therefore, simple platelet inhibition may not be appropriate in PAH. The sTWEAK is described as "healing cytokine" which promotes tissue regeneration or regional healing of pulmonary vasculature.[7] Platelet lysate concentration of this cytokine was linked in our study with worse prognosis in PAH patients, so it seems that local availability of sTWEAK at the site of endothelium injury

is very important and may differ from the amount released during platelet activation.

Interleukin 6 is an important cytokine in PAH pathogenesis.[2,25] Plasma or serum IL-6 levels are elevated both in patients with PAH and in animal models of PAH, and have prognostic value.[10,26] New evidence suggests that IL-6 and sIL-6R play an important role in lipid metabolism.[12] They not only play an anti-obesity role in rodent metabolic homeostasis, but also increase fatty acids oxidation, e.g., in human cardiomyocytes.[16] The IL-6 provides precise balance between fatty acid oxidation and lipotoxicity (excess of fatty acids) in cardiomyocytes, preventing cellular injury (e.g., mitochondria dysfunction, endoplasmic reticulum (ER) stress) and cardiac energy deficit.[27]

As we described before, cardiac metabolism is altered in PAH.[19] The strong relationship between pressure and/or volume overload of RV and enhanced glycolysis in cardiomyocytes is confirmed; however, there are still many questions about the sequence of pathophysiological events underlying this phenomenon. It is still not clear whether "metabolic shift" in RV is secondary to hemodynamic impairment or it results from strongly altered inflammatory processes occurring in PAH (probably the inflammatory processes in PAH are not only limited to pulmonary vasculature). In our results, both platelet sTWEAK and plasma IL-6 content were statistically significantly correlated with glucose uptake measured in PET imaging. The exact mechanism of these interactions is still not clear, but this study provides insight into difficult and multifactorial PAH pathogenesis. We believe that research on the significance of cardiac metabolism and its alterations may be an important step in developing potential therapies based on metabolic modulations.

Furthermore, our previous results considering sTWEAK platelet content and $SUV_{RV/LV}$ have a significant prognostic value which can help in risk assessment and therapy plans of already seriously ill PAH patients. In this study, we presented prolonged observation (up to 5 years) and partially validated prognostic significance of previously discussed parameters.[6,10]

Limitations

We are aware of several limitations of our research. The study group was relatively small (but homogeneous) and consisted of mostly advanced PAH patients. The PET/MRI is still an expensive imaging method and thus the promising results presented above may encourage to undertake a similar research on a larger group of patients. Next, patients were on various approved treatments for PAH, often in combination, and we were not able to assess the impact of disease-modifying therapy on the concentrations of cytokines. Due to small cohort, we also did not perform a multivariate analysis of factors independently affecting clinical deterioration. Additional studies in larger patient cohorts, aimed at establishing the reliability and overall usefulness of presented analysis in predicting survival, are now required.

Conclusions

The sTWEAK and IL-6 concentrations in PAH patients are linked with metabolic and functional changes of RV visualized in PET/MRI imaging and occurring before clinical deterioration. This may suggest that RV dysfunction in PAH is caused not only by simple pressure and/or volume overload due to pulmonary vasoconstriction, but also results from complex pathogenesis. The interplay between platelets, circulating cytokines and cardiac metabolism may help understand PAH pathogenesis, but further significance of these phenomena should be investigated in prospective studies.

ORCID iDs

Remigiusz Kazimierczyk https://orcid.org/0000-0003-4517-1498
Karol Kamiński https://orcid.org/0000-0002-9465-2581

References

1. Galiè N, Humbert M, Vachiery JL, et al. 2015 ESC/ERS Guidelines for the diagnosis and treatment of pulmonary hypertension: The Joint Task Force for the Diagnosis and Treatment of Pulmonary Hypertension of the European Society of Cardiology (ESC) and the European Respiratory Society (ERS). Endorsed by: Association for European Paediatric and Congenital Cardiology (AEPC), International Society for Heart and Lung Transplantation (ISHLT). *Eur Heart J*. 2016;37(1):67–119. doi:10.1093/eurheartj/ehv317
2. Pullamsetti SS, Seeger W, Savai R. Classical IL-6 signaling: A promising therapeutic target for pulmonary arterial hypertension. *J Clin Invest*. 2018;128(5):1720–1723. doi:10.1172/JCI120415
3. Rabinovitch M, Guignabert C, Humbert M, Nicolls MR. Inflammation and immunity in the pathogenesis of pulmonary arterial hypertension. *Circ Res*. 2014;115(1):165–175. doi:10.1161/CIRCRESAHA.113.301141
4. Jasiewicz M, Moniuszko M, Pawlak D, et al. Activity of the kynurenine pathway and its interplay with immunity in patients with pulmonary arterial hypertension. *Heart*. 2016;102(3):230–237. doi:10.1136/heartjnl-2015-308581
5. Jasiewicz M, Kowal K, Kowal-Bielecka O, et al. Serum levels of CD163 and TWEAK in patients with pulmonary arterial hypertension. *Cytokine*. 2014;66(1):40–45. doi:10.1016/j.cyto.2013.12.013
6. Kazimierczyk R, Błaszczak P, Kowal K, et al. The significance of diminished sTWEAK and P-selectin content in platelets of patients with pulmonary arterial hypertension. *Cytokine*. 2018;107:52–58. doi:10.1016/j.cyto.2017.11.014
7. Meyer T, Amaya M, Desai H, et al. Human platelets contain and release TWEAK. *Platelets*. 2010;21(7):571–574. doi:10.3109/09537104.2010.512403
8. Burkly LC, Michaelson JS, Hahm K, Jakubowski A, Zheng TS. TWEAK-ing tissue remodeling by a multifunctional cytokine: Role of TWEAK/Fn14 pathway in health and disease. *Cytokine*. 2007;40(1):1–16. doi:10.1016/j.cyto.2007.09.007
9. Rose-John S. Therapeutic targeting of IL-6 trans-signaling. *Cytokine*. 2021;144:155577. doi:10.1016/j.cyto.2021.155577
10. Kazimierczyk R, Blaszczak P, Jasiewicz M, et al. Increased platelet content of SDF-1alpha is associated with worse prognosis in patients with pulmonary prterial hypertension. *Platelets*. 2019;30(4):445–451. doi:10.1080/09537104.2018.1457780

11. Zhao J, Turpin-Nolan S, Febbraio MA. IL-6 family cytokines as potential therapeutic strategies to treat metabolic diseases. *Cytokine*. 2021;144:155549. doi:10.1016/j.cyto.2021.155549
12. Chabowski A, Zmijewska M, Górski J, Bonen A, Kamiński K, Winnicka MM. Effect of IL-6 deficiency on myocardial expression of fatty acid transporters and intracellular lipid deposits. *J Physiol Pharmacol*. 2007;58(1):73–82. PMID:17440227.
13. Ohira H, deKemp R, Pena E, et al. Shifts in myocardial fatty acid and glucose metabolism in pulmonary arterial hypertension: A potential mechanism for a maladaptive right ventricular response. *Eur Heart J Cardiovasc Imaging*. 2016;17(12):1424–1431. doi:10.1093/ehjci/jev136
14. Li W, Wang L, Xiong CM, et al. The prognostic value of 18F-FDG uptake ratio between the right and left ventricles in idiopathic pulmonary arterial hypertension. *Clin Nucl Med*. 2015;40(11):859–863. doi:10.1097/RLU.0000000000000956
15. Barger PM, Kelly DP. Fatty acid utilization in the hypertrophied and failing heart: Molecular regulatory mechanisms. *Am J Med Sci*. 1999;318(1):36–42. doi:10.1097/00000441-199907000-00006
16. Xu Y, Zhang Y, Ye J. IL-6: A potential role in cardiac metabolic homeostasis. *Int J Mol Sci*. 2018;19(9):2474. doi:10.3390/ijms19092474
17. Ohira H, deKemp R, Pena E, et al. Shifts in myocardial fatty acid and glucose metabolism in pulmonary arterial hypertension: A potential mechanism for a maladaptive right ventricular response. *Eur Heart J Cardiovasc Imaging*. 2016;17(12):1424–1431. doi:10.1093/ehjci/jev136
18. Kazimierczyk R, Malek LA, Szumowski P, et al. Multimodal assessment of right ventricle overload-metabolic and clinical consequences in pulmonary arterial hypertension. *J Cardiovasc Magn Reson*. 2021;23(1):49. doi:10.1186/s12968-021-00743-2
19. Kazimierczyk R, Szumowski P, Nekolla SG, et al. Prognostic role of PET/MRI hybrid imaging in patients with pulmonary arterial hypertension. *Heart*. 2021;107(1):54–60. doi:10.1136/heartjnl-2020-316741
20. Rischpler C, Nekolla SG, Kunze KP, Schwaiger M. PET/MRI of the heart. *Semin Nucl Med*. 2015;45(3):234–247. doi:10.1053/j.semnuclmed.2014.12.004
21. Kazimierczyk R, Małek ŁA, Szumowski P, et al. Prognostic value of late gadolinium enhancement mass index in patients with pulmonary arterial hypertension. *Adv Med Sci*. 2021;66(1):28–34. doi:10.1016/j.advms.2020.11.002
22. Oikawa M, Kagaya Y, Otani H, et al. Increased [18F]fluorodeoxyglucose accumulation in right ventricular free wall in patients with pulmonary hypertension and the effect of epoprostenol. *J Am Coll Cardiol*. 2005;45(11):1849–1855. doi:10.1016/j.jacc.2005.02.065
23. Kazimierczyk R, Kamiński K. The role of platelets in the development and progression of pulmonary arterial hypertension. *Adv Med Sci*. 2018;63(2):312–316. doi:10.1016/j.advms.2018.04.013
24. Zanjani KS. Platelets in pulmonary hypertension: A causative role or a simple association? *Iran J Pediatr*. 2012;22(2):145–157. PMID:23056879. PMCID:PMC3446075.
25. Kanda T, Takahashi T. Interleukin-6 and cardiovascular diseases. *Jpn Heart J*. 2004;45(2):183–193. doi:10.1536/jhj.45.183
26. Humbert M, Monti G, Brenot F, et al. Increased interleukin-1 and interleukin-6 serum concentrations in severe primary pulmonary hypertension. *Am J Respir Crit Care Med*. 1995;151(5):1628–1631. doi:10.1164/ajrccm.151.5.7735624
27. Myśliwiec P, Choromańska B, Winnicka MM, et al. Interleukin-6 deficiency modifies the effect of high fat diet on myocardial expression of fatty acid transporters and myocardial lipids. *J Physiol Pharmacol*. 2018;69(4). doi:10.26402/jpp.2018.4.11

Efficacy of different intensity of aquatic exercise in enhancing remyelination and neuronal plasticity using cuprizone model in male Wistar rats

Zareena Begum[1,A–E], Vijayalakshmi Subramanian[1,A,F], Gunapriya Raghunath[1,A,B], Karthikeyan Gurusamy[1,C,E], Rajagopalan Vijayaraghavan[2,C–E], Senthilkumar Sivanesan[2,A,D,E]

[1] Department of Anatomy, Saveetha Medical College, Chennai, India

[2] Department of Research and Development, Saveetha Insititute of Medical & Technical Sciences, Chennai, India

A – research concept and design; B – collection and/or assembly of data; C – data analysis and interpretation;
D – writing the article; E – critical revision of the article; F – final approval of the article

Address for correspondence
Zareena Begum
E-mail: zareenabegumm@gmail.com

Abstract

Background. Multiple sclerosis (MS) is a chronic demyelinating disease of the central nervous system (CNS). Most exercise studies concentrate on the impact of exercise on cardiovascular system; this study aims to present the effects of exercise of varying intensity on the nervous system. Most recently in MS, positive outcomes were obtained with resistance and high-intensity exercises. This study also analyzes the effects of a prior conditioning program before the induction of demyelination and subsequent neuroprotective effects of such program.

Objectives. To study and determine the neuroprotective and remyelinating effects of different intensity of aquatic exercise and a preconditioning exercise program on demyelination induced by oral administration of cuprizone (Cup).

Materials and methods. Six groups of animals, each containing 6 rats, were used in the study. The groups were as follows: group I – control group; group II – Cup group; group III – treated with methylprednisolone (MP); group IV – treated with low-intensity exercise (LIE), free swimming for 40 min and high-intensity exercise (HIE); group V – treated with a resistance of 9% body weight and free swimming for 40 min; group VI – treated with preconditioning exercise (free swimming for 40 min for 3 weeks) before Cup administration followed by the same exercise protocol as for group V. All data were analyzed using one-way analysis of variance (ANOVA) with Tukey's test, by means of SigmaPlot v. 14.5 software.

Results. Similarly to the MP group, group VI showed a positive outcome. A value of p < 0.001 was considered statistically significant. Also, group VI showed improved areas of remyelination in histopathology, an increased expression of myelin basic protein (MBP), reduced expression of glial fibrillary acidic protein (GFAP) in corpus callosum, and improved gene expression of brain-derived neurotrophic factor (BDNF) in the hippocampus region.

Conclusions. General fitness achieved through a preconditioning program combined with HIE showed neuroprotective effects, as evidenced by increased areas of remyelination and improved neuronal plasticity, observed mostly in group VI (conditioning+HIE).

Key words: demyelination, exercise, neuronal plasticity, cuprizone, conditioning

Background

The number of patients diagnosed with multiple sclerosis (MS) is increasing because of an increased access to magnetic resonance imaging (MRI) and early diagnosis. Multiple sclerosis is essentially an inflammatory disease of the central nervous system (CNS). The precise cause of the disease is still debatable and ascribed to autoimmune pathology. Genetic factors have also been taken into account in the literature.[1,2] Moreover, a disturbance in the reduction–oxidation metabolism has been pointed out as a causative factor for MS.[3] The treatment of MS involves the use of steroids and interferon therapy, and has greatly evolved over the past years. A combination of agents that modify the course of the disease and have various effects on immunity is used for treatment at different phases of the disease.[4,5] Vitamin plus interferon therapy and the use of medical cannabis have also been studied as methods of treatment in MS.[6,7] This disease leads to a widespread demyelination caused by selective involvement of oligodendrocytes and axonal loss. Additional psychobehavioral symptoms such as anxiety, dementia and depression are also observed.[8] At times, neurodegenerative disorders following substance abuse can mimic features of MS, which needs careful evaluation.[9] Potential biomarkers, such as myelin basic protein (MBP), glial fibrillary acidic protein (GFAP) and CNPase, can play a role in the diagnosis and assessment of therapeutic agents in MS.[10,11]

Cuprizone (bis-cyclohexanone oxaldihydrazone; Cup) has been successfully used for inducing demyelination.[12] It is a primary copper chelator which causes selective apoptosis of oligodendrocytes and induces CNS demyelination in rats. A 3-week exposure to Cup causes cerebral cortical demyelination and white matter damage in mice.[13] Cuprizone was the chosen method in the present study, as cessation of administration of Cup leads to spontaneous remyelination, which mimics the relapsing-remitting stage of MS (RRMS).[14]

Other methods for induction of demyelination include 1) experimental autoimmune encephalomyelitis (EAE) induced by myelin oligodendrocyte glycoprotein (MOG) antibodies, 2) viral model using Theiler's virus, and 3) toxic model of demyelination involving the use of lysolecithin, which leads to demyelination within 2 days of administration.[15–17]

Methylprednisolone (MP) is the standard drug of choice for MS.[18] It is a chemical modification of naturally occurring glucocorticosteroid – hydroxycortisone. This drug alleviates the inflammatory cycle by reducing the cytokine response and T cell inhibition and facilitating apoptosis of activated immune cells.

Exercise as a disease-modifying agent and a rehabilitation tool (which can slow down the effects of the disease) also plays a very important role. Exercise regimens that are commonly used in animal studies include free voluntary running in a wheel, forced running in the treadmill and resistance swimming models.[19] Also, it has been observed that in animal models of cerebral ischemia in MS, growth factors of neurons and factors inhibiting apoptosis of neurons were increased by treadmill exercise.[20] Exercise was also found to have a positive impact in dementia with cognitive disorder features and improved recovery from post-acute injuries of CNS.[21] In particular, exercises have positive correlations with improved neuronal plasticity and neuronal regeneration.[22] According to Rossi et al., exercise was found to confer neuronal protection in experimental autoimmune encephalomyelitis.[23] Exercise forms one of basis for treatment models of MS, reversing changes such as axonal demyelination and degradation of MBP.[24] This study employed a Wistar rat animal model using Cup to induce demyelination, which mimics the RRMS.

Objectives

The aim of this study was to determine the effects of aquatic exercise of varying intensity as a neuroprotective factor and a method of promoting neuronal plasticity using animal study. The authors aimed to determine the efficacy of varying intensity of exercise against demyelination induced by Cup, and to analyze the effects of exercise on oligodendrocyte regeneration in the corpus callosum using Luxol fast blue (LFB) staining and MBP immunohistochemistry, subsequent astrogliotic proliferation using glial fibrillary acidic protein (GFAP) immunofluorescence, and neuronal plasticity changes in the hippocampus region of the rat brain caused by brain-derived neurotrophic factor (BDNF) expression using quantitative real-time polymerase chain reaction (qRT-PCR), and finally to compare all the above results with the neuroprotective effects of MP administration.

Materials and methods

Animals and chemicals

Male Wistar rats weighing 150–200 g were used in the study. Animals were procured from Biogen Laboratory Animal Facility (Bangalore, India). The animals were maintained in an air-conditioned room with a 12-h light/12-h dark cycle; standard chow diet and water were provided ad libitum throughout the experimental period. The study was conducted between September and October 2020, after receiving proper Institutional Animal Ethical Clearance from the Saveetha University, Chennai, India (approval No. SU/CLAR/RD/010/12/2020).

The 0.2% Cup was purchased from Sigma-Aldrich (St. Louis, USA), and hydroxypropyl cellulose was obtained from Sisco Research Laboratories (Mumbai, India).

Experimental procedure and design

The animals were divided into 6 groups, with 6 rats in each group. After a week of acclimatization, the experiment was carried out for 8 weeks for groups I–V and 11 weeks for group VI. The animals in group I (control group) were administered 1.5 mL of 1% hydroxypropyl cellulose (HPC)/kg body weight (b.w.), per oral (p.o.) for 35 days. Group II (Cup group) was administered 450 mg of Cup/kg b.w. dissolved in 1.5 mL of 1% HPC p.o. for 5 weeks.[25] Group III (Cup+MP group) rats were administered 450 mg of Cup/kg b.w. p.o. for 5 weeks, and from the 3rd week, in addition to Cup administration, 20 mg of MP/kg b.w. were administered intraperitoneally for 3 weeks. Group IV (Cup+low-intensity exercise (LIE) group) rats were administered 450 mg of Cup/kg b.w. p.o. for 5 weeks, and from the 3rd week of Cup administration, free swimming with no resistance for 40 min for 5 weeks was included. Group V (Cup+high-intensity exercise (HIE) group) rats were administered 450 mg of Cup/kg b.w. p.o. for 5 weeks, and from the 3rd week of Cup administration, swimming with an added resistance of 9% b.w. for 5 weeks was included. Rats in group VI (conditioning (Cn)+Cup+HIE group) were made to swim 40 min a day without additional resistance for 3 weeks; after 3 weeks, the administration of 450 mg of Cup/kg b.w. p.o. commenced and was continued for 5 weeks; finally, from the 3rd week of Cup administration, an exercise program, the same as in group V, was initiated.

The Cup solution was prepared according the dosage precribed for a given day and administered through oral gavage.

Exercise regimen

The rats in group VI were preconditioned with free swimming in a circular tank with a depth of more than 50 cm, with a water temperature of 30 ±5°C for 40 min, 5 times a week, before Cup administration. After 3 weeks of Cup administration, rats in the Cup+LIE group were made to swim with no additional resistance for 40 min, 5 days a week, for 5 weeks.[26] For Cup+HIE and Cn+Cup+HIE groups, a resistance of 9% of b.w. in the form of a metal ring was tied around the tails of the rats, and they were made to swim for 40 min, 5 days a week for 5 weeks.[27] In case of slippage of the ring from the tail, the timer was paused, the ring was put back and timer continued for the remaining duration of the exercise. The intensity grading based on the load was adapted from a study performed by Gobatto et al.[28]

Induction of demyelination and methylprednisolone administration

Cuprizone, a primary copper chelator, induces selective oligodendrocyte apoptosis after 3 weeks of administration, which is followed by activation of innate neuroglial and immune cells in the brain by astrocytes and microglial proliferation. Finally, Cup administration leads to demyelination of distinct white and grey matter areas.[29] There is only a minimal involvement of the blood–brain barrier and cells of the immune system are believed to play a role in demyelination induced by Cup.[30]

Demyelination induction was achieved by administration of 450 mg of Cup/kg b.w. dissolved in 1.5 mL of 1% HPC.[31] The control group received 1.5 mL of 1% HPC. After 3 weeks of Cup administration, 20 mg of MP/kg b.w. were administered intraperitoneally for 3 weeks.[32]

Tissue preparation

After the assigned experimental period, the rats were euthanized by an overdose of 1% isoflurane. After the rats were perfused intracardially with 50 mM phosphate-buffered saline (PBS), the brain tissue was carefully dissected, washed in PBS and transferred to formalin containers for histopathology. The brain specimens intended for immunohistochemistry, immunofluorescence and qRT-PCR were wrapped in aluminum foil and kept in refrigeration at –80°C.

Luxol fast blue staining

This procedure was carried out as described in the literature.[33] The coronal sections of brain tissue were stained with LFB. Brain tissue slides were incubated in LFB solution (0.1%; Polysciences Inc., Warrington, USA) for 24 h at room temperature. The sections were rinsed thoroughly in distilled water and then dipped in lithium carbonate solution (0.05%; Polysciences Inc.) several times. The differentiation of the sections was then continued by repeatedly dipping the sections in alcohol reagent (70%) until the gray matter became colorless and the white matter remained blue. Then, the sections were rinsed in distilled water and incubated with cresyl echt violet (0.1%; Polysciences Inc.) for 2–5 min. Next, the sections were rinsed quickly in distilled water, dehydrated quickly in 3 changes of absolute alcohol, cleared in 3 changes of xylene, and mounted using a mounting medium. The slides were viewed under the Olympus binocular bright-field microscope (model DM 1000 LED; Olympus Corp., Tokyo, Japan) at ×60 magnification.

MBP immunohistochemistry

This procedure was carried out according to the method designed by Khodanovich et al.[34] The tissues were immersed in ice-cold PBS followed by immersion in freshly prepared filtered 4% paraformaldehyde (PFA) in PBS. After embedding, the tissues were cut using the Leica cryostat CM1850 (Leica Biosystems, Deer Park, USA) and stored in cryoprotective solution (25% glycerol, 25% ethylene glycol in PBS) at –20°C. The sections were incubated with polyclonal rabbit anti-MBP (1:1000; Abcam, Cambridge, UK)

overnight at 25°C, and then treated with streptavidin-per-oxidase complex (1:200; Abcam). Sections were visualized using the reaction with 3,3-diaminobenzidine tetrachloride (Sigma-Aldrich) in 0.1 M Tris-HCl buffer (pH 7.2), and then dehydrated, mounted on a slide and visualized under a bright field microscope (Labomed Lx-500 HL Binocular Miscroscope; Labomed, Mumbai, India).

GFAP immunofluorescence

Chronic demyelination usually leads to astrocyte proliferation. This procedure was carried out with the method outlined by Madadi et al.[35] The frozen sections of corpus callosum (10 μm) were dried for 2 h at room temperature and then fixed with 4% PFA in PBS for 20 min. After blocking nonspecific antibody binding with 5% non-fat dried milk for 20 min, the sections were incubated overnight with rabbit anti-GFAP (1:4000; Enzo Life Sciences, Farmingdale, USA) diluted in blocking buffer at 4°C. Subsequently, the sections were washed in Tris-buffered saline (TBS) and incubated in a dark, humid chamber with the appropriate fluorescently labeled IgGs-Alexa Fluor 594 (1:400; Enzo Life Sciences) combined with donkey anti-rabbit IgG Alexa Fluor 488 (1:400; Enzo Life Sciences) diluted in TBS with Tween 20 (TBS-T) for 2 h at room temperature. After several washes in TBS, the sections were mounted using polyvinyl alcohol mounting medium. Immunofluorescence was examined using a Leica confocal laser scanning microscope (Leica Microsystems, Wetzlar, Germany).

Gene expression level of BDNF in the hippocampus detected with qRT-PCR

This procedure was carried out using the method previously described by Altieri et al.[36] The total RNA was prepared from the brain tissue using a TRIzol reagent (RNeasy® Mini kits; Qiagen, Hilden, Germany). The qPCR Master Mix Kit was purchased from Invitrogen (Waltham, USA). Complementary DNA was first synthesized from total RNA using reverse transcriptase. The qRT-PCR was performed using Applied Biosystems instrument QuantStudio 7 Pro (Waltham, USA). The operating conditions were as follows: for glyceraldehyde-3-phosphate dehydrogenase (GAPDH) – 30 cycles of denaturation at 95°C for 30 s, annealing at 58°C for 30 s and extension at 72°C for 30 s; for BDNF – 27 cycles of denaturation at 95°C for 30 s, annealing at 57°C for 30 s and extension at 72°C for 30 s. The PCR products were separated on 1.2% agarose gels and stained with ethidium bromide. The density of each band was quantified using an image analyzing system (optical detection module in QuantStudio 7 Pro). The expression levels were compared with each other by calculating the relative density of the target band, such as BDNF, to that of GAPDH. The primer sequence is presented in Table 1.

Statistical analyses

All data are expressed as mean ± standard deviation (SD). Normality and equal variance of the data were analyzed using the Shapiro–Wilk test and the Brown–Forsythe test, respectively. Comparisons between groups were made using one-way analysis of variance (ANOVA) with Tukey's post hoc multiple comparison test. All statistical analyses were performed using SigmaPlot v. 14.5 (Systat Software Inc., Chicago, USA). A value of $p < 0.001$ was considered statistically significant. Immunostained slides were quantified using ImageJ software (National Institutes of Health (NIH), Bethesda, USA). The expression of the *BDNF* gene was measured using GAPDH as an internal control.

Results

Exercise improved remyelination as seen in LFB staining of the corpus callosum

The LFB staining was conducted to assess the myelin content in the corpus callosum. Widespread demyelination with increased degradation and vacuolation was evident in the Cup group (group II) compared to normal myelination observed in the control group. The Cn+Cup+HIE group showed better remyelination, as detected with blue staining of the myelinated areas visible in Fig. 1, similarly to the control and Cup+MP group images, with minimal areas of remyelination seen in Cup+LIE and Cup+HIE groups. Figure 1 presents the effect of exercise in Cup-induced changes on LFB staining in the corpus callosum region.

Distribution of data

The assumptions of ANOVA were based on normality and equal variance test. The data were found to be normally distributed in all groups. In the analysis of the percentage of cells that show MBP expression (MBP+ve cells %) and the percentage of the cells that show GFAP expression (GFAP+ve cells %), and the analysis of BDNF expression in the hippocampus, normal distribution was found, with $p = 0.893$, $p = 0.395$ and $p = 0.979$, respectively. Similarly, equal variance, determined using Brown–Forsythe test,

Table 1. Primer sequence for quantitative real-time polymerase chain reaction (qRT-PCR) brain-derived neurotrophic factor (BDNF) in the hippocampus region

Genes	Primer right	Primer left
BDNF (153bp)	5′-CAG GGG CAT AGA CAA AAG-3′	5′-CTT CCC CTT TTA ATG GTC-3′
GAPDH (409bp)	5′-ATC CCATCA CCA TCT TCC AG-3′	5′-CCT GCTTCA CCA CCT TCT TG-3′

control group
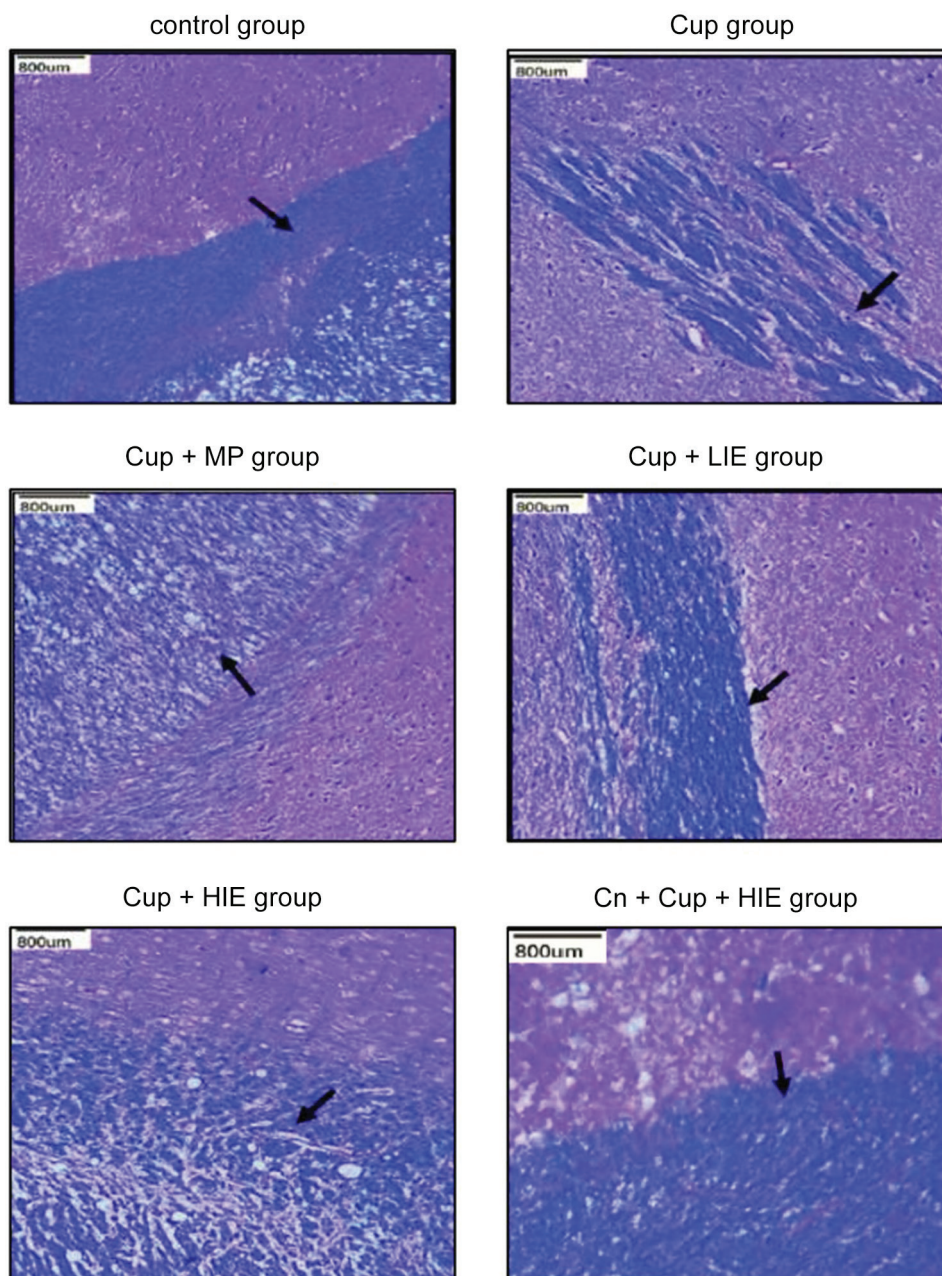
Cup group

Fig. 1. Effect of exercise in Cup-induced changes on LFB staining. The control group showed normal myelination of the corpus callosum, while the Cup group showed more demyelination. The Cup+MP group showed improved myelin formation. The Cup+LIE and Cup+HIE groups showed remyelination in a minimum area. The Cn+Cup+HIE group showed an increased area of remyelination, which was almost as same as control

Cup – cuprizone; LIE – low-intensity exercise; HIE – high-intensity exercise; MP – methylprednisolone; LFB – Luxol fast blue; Cn – conditioning.

Cup + MP group

Cup + LIE group

Cup + HIE group

Cn + Cup + HIE group

was also found, with p = 0.489, p = 0.883 and p = 0.270, respectively, for all 3 above parameters.

Exercise improves MBP expression in the corpus callosum

The MBP is the initial and reliable marker for remyelination. Therefore, MBP expression can act as a reliable guide to establish remylination criteria. MBP immunopositivity in the corpus callosum of the rat brain was drastically reduced in the Cup group and substantially improved in the Cup+MP group and Cn+Cup+HIE group. The Cup+LIE and Cup+HIE groups showed similar minimal expression. The quantitative analysis of cells expressing MBP showed a considerable decrease in MBP expression in the Cup group (8.267 ±0.351)

compared to the control group (30.033 ±0.569%), with p < 0.001. It was found that MBP expression was increased in the Cup+MP group (22.967±0.473) and in Cn+Cup+HIE group (21.733 ±0.777); when these 2 groups were compared, p-value was found to be 0.128, with no statistical difference between Cup+MP (standard drug group) and Cn+Cup+HIE group, thereby showing that they produced similar results. The Cup+LIE group (13.333 ±0.306) and Cup+HIE group (17.467±0.153) presented moderate improvement, showing statistical significance when compared with control, Cup and Cup+MP groups.

Figure 2 presents the effect of exercise on Cup-induced changes, measured with MBP immunohistochemistry and quantitative analysis of MBP expression in corpus callosum.

control group

Cup group

Cup + MP group

Cup + LIE group

Cup + HIE group

Cn + Cup + HIE group

Fig. 2. Effect of exercise in Cup-induced changes measured with MBP immunohistochemistry and quantitative analysis of expression of cells expressing MBP in corpus callosum, analyzed with ImageJ software (National Institutes of Health (NIH),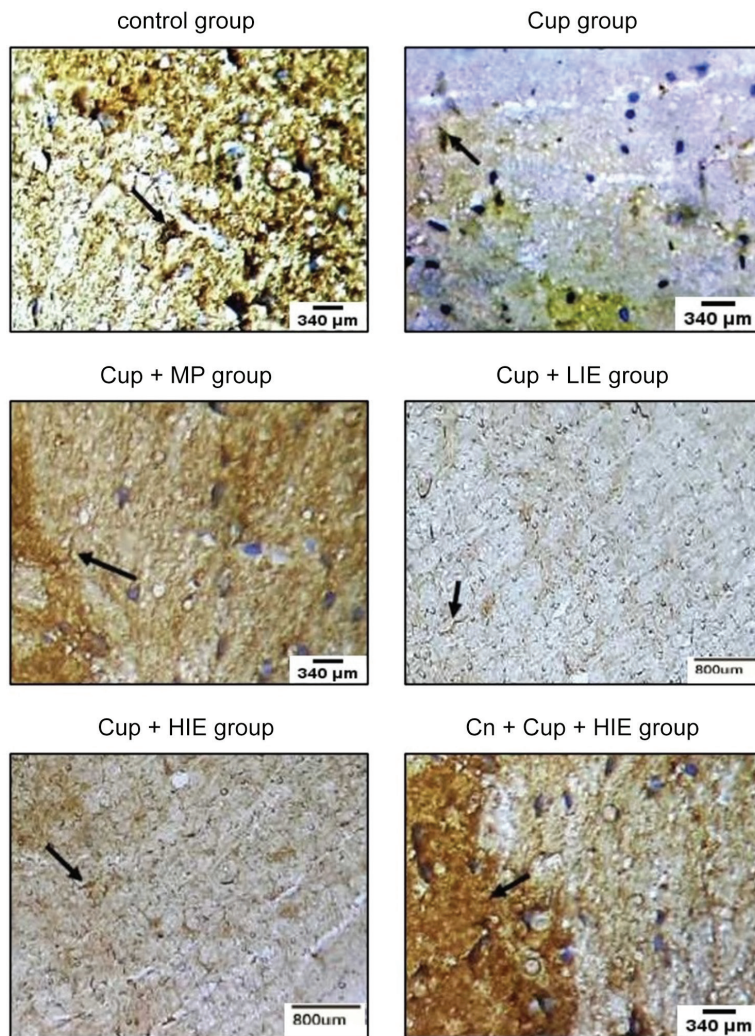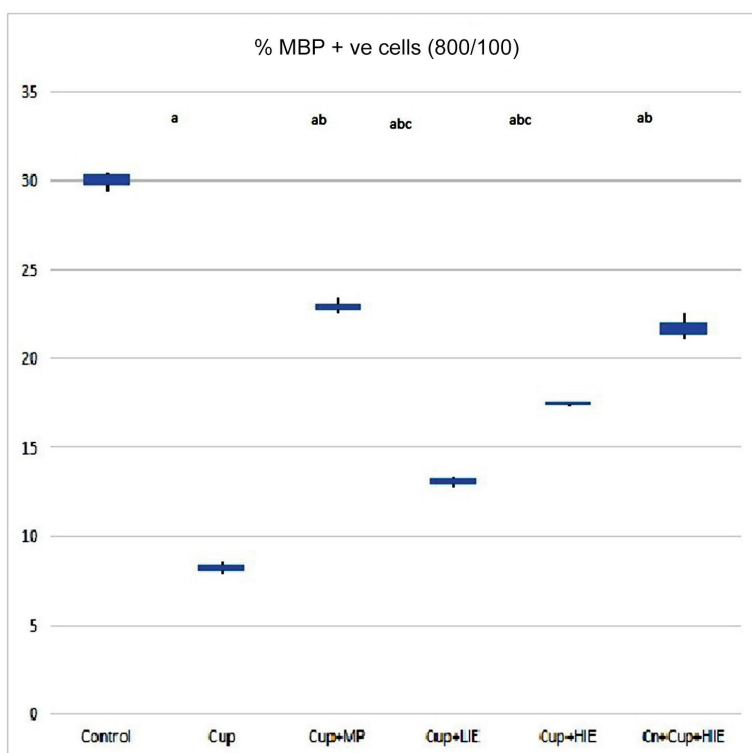 Bethesda, USA) and presented with a 800-μm scale bar and ×100 magnification. The MBP expression in the corpus callosum of the rat brain is shown with the arrow mark. The MBP immunopositive cells were less expressed in the Cup group compared to the control group. The highest expression was seen in the Cup+MP group, and only slightly lower the Cn+Cup+HIE group, even lower in the Cup+HIE group, and the lowest in Cup+LIE group. Values are presented as mean ± standard deviation (SD; n = 6 in each group). The F-values and p-values were determined using one-way ANOVA with Tukey's test

MBP – myelin basic protein; Cup – cuprizone; LIE – low-intensity exercise; HIE – high-intensity exercise; Cn – conditioning; MP – methylprednisolone; ANOVA – analysis of variance; a – significantly different from the control group; b – significantly different from the Cup group; c – significantly different from the MP group.

Exercise caused reduced GFAP expression measured with immunofluorescence

Active astrocytic proliferation is observed in chronic stages of demyelination. As presented in Fig. 3, high expression of GFAP was seen in the Cup group, while Cn+Cup+HIE group and Cup+MP group showed a reduced expression of GFAP in the corpus callosum. The Cup+HIE and Cup+LIE groups showed moderate GFAP expression. The quantitative analysis of cells expressing GFAP showed a definite increase in the Cup group (112.867 ±0.551) compared to the control group (30.550 ±1.054). This result was statistically significant ($p < 0.001$). The Cup+MP group showed a decline in GFAP expression (61.233 ±0.643), while the Cn+Cup+HIE group showed a better response than the Cup+MP group (50.367 ±0.513) ($p < 0.001$). The Cn+Cup+HIE group showed a 17.74% decrease of GFAP expression in comparison to Cup+MP (standard drug) group, which shows that there was less astrogliosis in Cn+Cup+HIE group compared to Cup+MP group. The Cup+LIE (80.900 ±1.127) and Cup+HIE (77.000 ±0.557) groups showed moderate response in comparison to the control, Cup and Cup+MP groups. This result was statistically significant ($p < 0.001$).

Figure 3 presents the effect of exercise on Cup-induced changes, measured with GFAP immunofluorescence and quantitative analysis of expression of cells expressing GFAP in the corpus callosum.

% MBP + ve cells (800/100)

control group / Cup group / Cup + MP group / Cup + LIE group / Cup + HIE group / Cn + Cup + HIE group

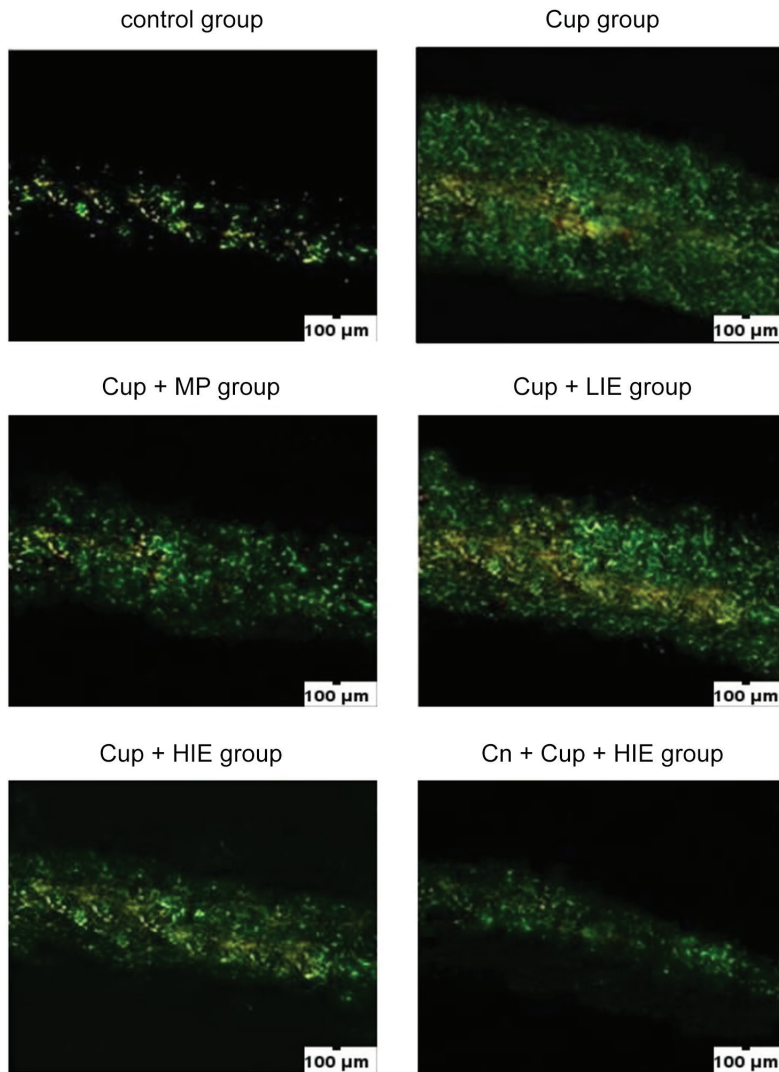**Fig. 3.** Effect of exercise on Cup-induced changes measured with GFAP immunofluorescence and quantitative analysis of expression of cells expressing GFAP in the corpus callosum, analyzed using ImageJ software (National Institutes of Health (NIH), Bethesda, USA) and presented with a 100-µm scale bar and ×100 magnification. Immunopositivity to GFAP was higher in the Cup group compared to the control group. Lower expression was observed in the Cup+MP group, and the Cn+Cup+HIE group showed markedly declined expression, while Cup+HIE and Cup+LIE groups showed moderate expression. Values are presented as mean ± standard deviation (SD; n = 6 in each group). The F-values and p-values were determined using one-way ANOVA with Tukey's test

Cup – cuprizone; LIE – low-intensity exercise; HIE – high-intensity exercise; Cn – conditioning; MP – methylprednisolone; GFAP – glial fibrillary acidic protein; ANOVA – analysis of variance; a – significantly different from the control group; b – significantly different from the Cup group; c – significantly different from the MP group.

Gene expression levels of BDNF in hippocampus region measured with qRT-PCR

The BDNF is an important marker for neuroplasticity. Its expression was the lowest in the Cup group and the highest BDNF expression in the Cn+Cup+HIE group compared to Cup+MP and control groups. The second lowest BDNF expression was found in the Cup+LIE group, and it was comparably low in the Cup+HIE group, as seen in Fig. 4. The quantitative analysis revealed reduced BDNF expression in the Cup group (0.653 ±0.0651%) compared to the control group (2.693 ±0.179%) ($p < 0.001$). The highest expression was seen in the Cn+Cup+HIE group (3.470 ±0.0436%) followed by the Cup+MP group (3.123 ±0.0961%) ($p < 0.001$). The Cn+Cup+HIE group showed a 28.85% higher BDNF expression compared to the control group, whereas Cup+MP group showed a 15.96% higher expression compared to the control group. In comparison to the Cup+MP group, the Cn+Cup+HIE group showed an 11.11% increase in BDNF expression, whereas BDNF expression in the hippocampal region in the Cn+Cup+HIE group exceeded such expression in the standard drug Cup+MP group. The BDNF expression in the Cup+LIE (0.973 ±0.121) and Cup+HIE (1.823 ±0.0929) groups did not show much improvement. Cup+LIE group showed no statistical significance when compared to Cup group and showed decreased BDNF expression in comparison to the control and Cup+MP groups, which was statistically significant

1006

Z. Begum et al. Effects of exercise in remyelination
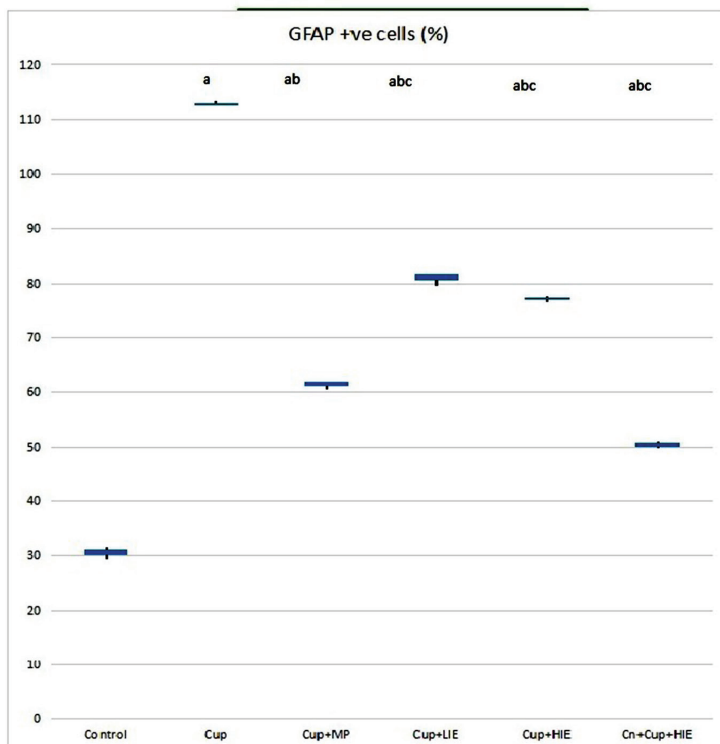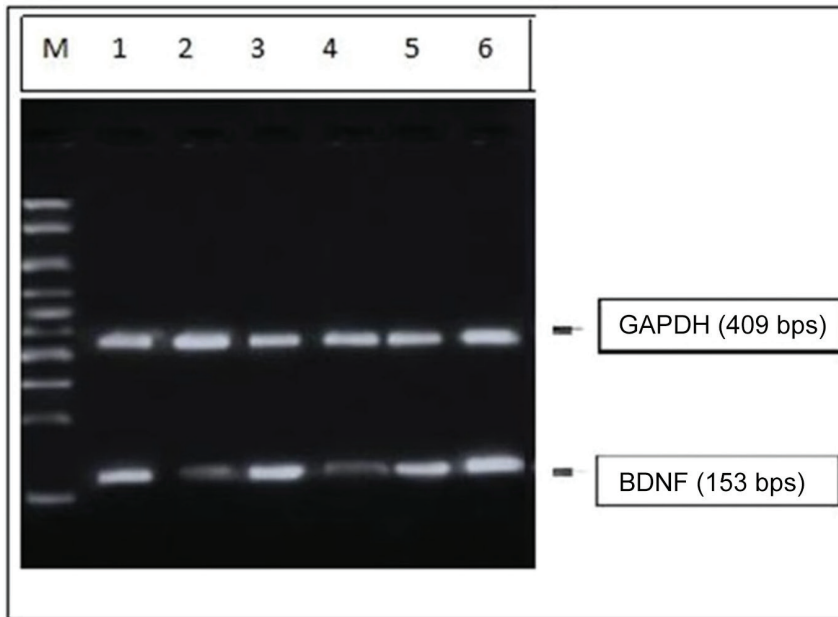
Fig. 4. Effect of exercise on Cup-induced changes of the gene expression, measured with BDNF and quantitative analysis of BDNF expression in the hippocampus region. Lane 1 – control; lane 2 – Cup group; lane 3 – Cup+MP group; lane 4 – Cup+LIE group; lane 5 – Cup+HIE group; lane 6 – Cn+Cup+HIE group. The BDNF expression was found to be the lowest in the Cup group and the second lowest in the Cup+LIE group. The highest expression of BDNF was found in the Cn+Cup+HIE group, followed by the Cup+MP group and Cup+HIE group. The BDNF expression in the Cn+Cup+HIE group was found to be higher than in the control group. Values are presented as mean ± standard deviation (SD; n = 6 in each group). The F-values and p-values were determined using one-way ANOVA with Tukey's test

Cup – cuprizone; LIE – low-intensity exercise; HIE – high-intensity exercise; Cn – conditioning; MP – methylprednisolone; BDNF – brain-derived neurotrophic factor; ANOVA – analysis of variance; GAPDH – glyceraldehyde-3-phosphate dehydrogenase; a – significantly different from the control group; b – significantly different from the Cup group; c – significantly different from the MP group.
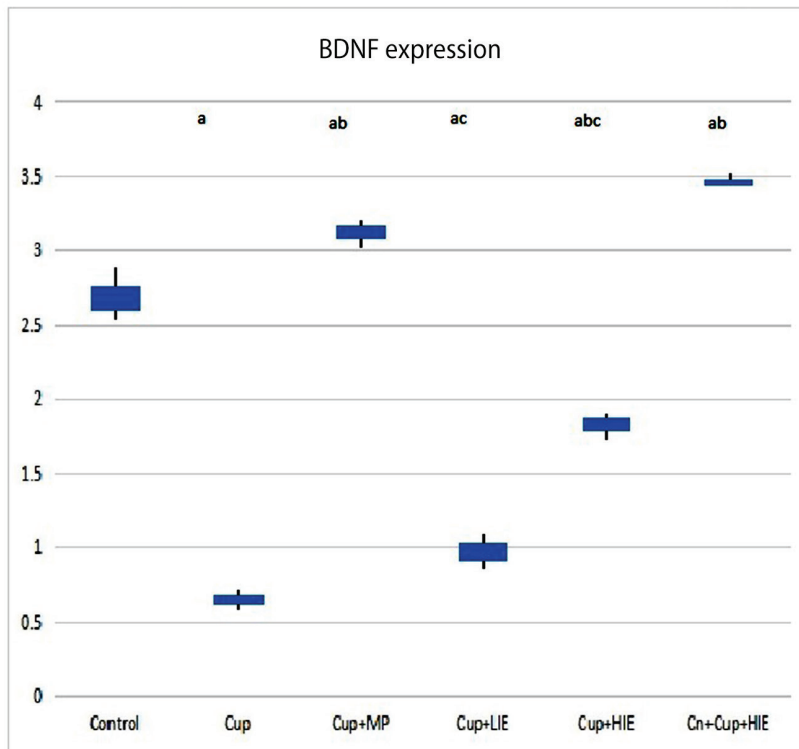
(p < 0.001). The expression of the Cup+LIE group showed no statistical difference when compared to the Cup group (p = 0.053). The expression of the Cup+HIE group (1.823 ±0.0929%) was found to be statistically significant in comparison with control, Cup and Cup+MP groups.

Figure 4 presents the effect of exercise on Cup-induced changes, measured with the gene expression of BDNF and quantitative analysis of BDNF expression, in the hippocampus region.

The summary of mean and SD levels of all groups with degrees of freedom (df), sum of squares (SS), mean of sum of squares (MS), and with F-values and p-values for all parameters mentioned is presented in Table 2.

Discussion

For the experimental study of MS pathology, a toxic model using Cup can work as an appropriate model to study the remyelination process.[37] In this model, the corpus callosum is the primary area showing white matter degeneration; other brain regions such as basal ganglia and

Table 2. Comparative effectiveness of MP, LIE, HIE, and Cn+HIE in Cup-induced demyelination, measured using quantitative analysis of 1) MBP+ve cells %, 2) GFAP+ve cells % in the corpus callosum region and 3) BDNF expression in hippocampal region

Sample	Parameters	Groups	Mean	SD	df	SS	MS	F-value	p-value
1	MBP+ve cells % in corpus callosum region, measured with ImageJ software and presented with a 800-μm scale bar and ×100 magnification	control Cup Cup+MP Cup+LIE Cup+HIE Cn+Cup+HIE	30.033 8.267 22.967 13.133 17.467 21.733	0.569 0.351 0.473 0.306 0.153 0.777	5	890.660	178.132	768.915	<0.001
2	GFAP+ve cells % in the corpus callosum region, measured with Image J software and presented with a 100-μm scale bar	control Cup Cup+MP Cup+LIE Cup+HIE Cn+Cup+HIE	30.500 112.867 61.233 80.900 77.000 50.367	1.054 0.551 0.643 1.127 0.557 0.513	5	12058.358	2411.672	3942.787	<0.001
3	quantitative analysis of BDNF expression in the hippocampus region	control Cup Cup+MP Cup+LIE Cup+HIE Cn+Cup+HIE	2.693 0.653 3.123 0.973 1.823 3.470	0.179 0.065 0.096 0.121 0.092 0.043	5	20.135	4.027	342.407	<0.001

SD – standard deviation; df – degrees of freedom; SS – sum of squares; MS – mean of sum of squares; BDNF – brain-derived neurotrophic factor; Cup – cuprizone; LIE – low-intensity exercise; HIE – high-intensity exercise; MP – methylprednisolone; MBP – myelin basic protein; GFAP – glial fibrillary acidic protein; MBP+ve cells % – percentage of cells that show MBP expression; GFAP+ve % cells – percentage of cells that show GFAP expression.

hippocampus are also affected.[38] In the present study, it was found that conditioned animals subjected to HIE encompassing swimming regimen showed improved areas of remyelination as seen in LFB staining, improved expression of MBP measured using immunohistochemistry, improved expression of GFAP measured using immunofluorescence, and improved genetic expression of BDNF in the hippocampal region analyzed using qRT-PCR. These results were concurrent with findings of Kim and Sung regarding MBP expression.[39] Selective ablation of astrocytes leads to a better remyelination response, as documented in a study by Madadi et al., with GFAP expression measured using immunofluorescence and improved areas of remyelination visualized with LFB staining.[35] In a study conducted by Gentile et al. and employing swimming protocol, BDNF levels were found to be significantly increased in mice with induced EAE.[40]

Aquatic exercise is particularly beneficial for MS patients due to its 3 vital effects: 1) buoyancy, whereby the load and stress on the joints are reduced; 2) viscosity, which leads to decreased drag and multiplanar movements; and, most importantly, 3) thermodynamics. As per the Uhthoff's phenomenon, symptoms of MS worsen in case of a setting that increases the body temperature.[41] Swimming exercise does not increase the temperature levels and maintains an optimum body temperature.[42] The LFB staining, one of the standard methods of visualizing white matter, showed improved effects of physical activity in the experimental groups (Cn+Cup+HIE and Cup+HIE groups), as was evidenced by the increased myelination in the exercise groups, which was in accordance with a study by Kim and Sung, where the demyelination in the spinal cord was studied.[39]

Myelin basic protein is important for maintaining the structural stability of myelin and is an essential component for efficient nerve conduction.[43] Prior regular exercise has been shown to have a positive impact on reducing demyelination and axonal damage in the spinal cord of EAE animals, as well as on dendritic damage in striatal neurons.[44] A decrease in MBP expression reflects the demyelinating status of MS.[45] The present study showed a decrease in MBP levels in the Cup group, and, conversely, improved MBP expression in Cup+MP and Cn+Cup+HIE gropus. The Cup+HIE and Cup+LIE groups showed only negligible improvement. Similar results regarding MBP expression were observed in the spinal cord, where the effects of free swimming were analyzed.[39] This study was the first to throw light on the neuroprotective effects of the preconditioning exercise program introduced together with the HIE regimen. Astrocytes are found to be promoters of demyelinating lesions, which are carried out by secretion of chemokines that recruit microglial inflammatory cells, which in turn restrict the process of remyelination.[46] Astrogliosis is a feature observed in chronic stages of MS.[47] The GFAP, a marker for astrogliosis, is found to be elevated in chronic stages of demyelination.[48] Better results with reduced astrocyte proliferation were observed in the Cn+Cup+HIE group. An improved remyelination was also reported in a study by Madadi et al., who performed selective astrocyte ablation with long-term Cup administration.[35]

Immunomodulatory effects of exercise (in the form of treadmill training) against neural damage and demyelination were analyzed and found to cause improvement in patients' condition.[49] One of the strongest and most reliable effects of exercise on the brain of treated rats was the upregulation of BDNF, an important marker for neuronal plasticity, which increases the number and synaptic uptake of α-amino-3-hydroxy-5-methyl-4-isoxazole

propionic acid (AMPA) receptors in experimental hippocampal slices and hippocampal neuronal cultures.[50]

According to Pencea et al., BDNF stimulates the recruitment of supraventricular zone cells and their migration, and facilitates the differentiation of neurons.[51] The present study showed an increase in expression of BDNF in the hippocampus of conditioned rats subjected to a HIE swimming protocol, which was in accordance with a study by Kim et al.[52] Motor activity in the form of aquatic exercise is found to have more neuroprotective and long-term effects regarding gene expression in the hippocampus of Cup-treated brains of Wistar rats.[53,54]

The fragmentation of DNA was seen in the dentate gyrus of the hippocampus in rats with induced MS. When treated with swimming exercise, reduced fragmentation of DNA and thereby, an improvement in short term memory was noticed.[55] Similar results were found in the present study, where the Cn+Cup+HIE group showed increased effects of neuroprotection with improved areas of remyelination in the corpus callosum and improved neuronal plasticity, as shown by BDNF expression in the hippocampal region. The expression of BDNF was found to be the highest in Cn+Cup+HIE group, even higher than in the standard drug Cup+MP group. It can be corelated with delaying or preventing secondary memory and functioning impairment in MS.

The current study shows the importance of a general exercise routine and thereby an improved fitness level, which, as shown by conditioning program in the current study, induced consistent protective effects on demyelination and also improved expression of BDNF in the hippocampal region. Providing and maintaining a standard and consistent environment for the exercise protocol were found to be challenging in this study. The scope of the study can be expanded by analyzing and comparing other modalities of exercise with aquatic therapy, also in other neurodegenerative disorders.

Limitations

This study examined the acute demyelination and remyelination changes caused by the administration of Cup. If the duration of Cup administration was prolonged, the chronic changes and subsequent effects could have been studied further.

Conclusions

Prior exercise conditioning program confers neuroprotective and remyelinating effects in rats subjected to induction of demyelination with Cup, in addition to leading to better fitness level. High-intensity exercise showed comparable significance, while the least significant effects were observed in LIE. Therefore, in MS, the HIE protocol can be applied, and in the long run, improved

general fitness results in neuroprotection, in addition to the traditional cardioprotective effects documented so far, can be observed. The RRMS is observed in the initial stage. For the initial stage, the treatment involves the use of steroids and maintenance LIE only during relapses. Instead, a challenging HIE program can be the norm, keeping the basal body temperature constant throughout the disease course, irrespective of relapse or remission. Also, this study stresses the importance of an exercise program in general, even in an otherwise healthy population, to bring out better results when a neural pathology may be detected.

ORCID iDs

Vijayalakshmi Subramanian https://orcid.org/0000-0003-1412-6440
Gunapriya Raghunath https://orcid.org/0000-0002-9712-6472
Karthikeyan Gurusamy https://orcid.org/0000-0002-6052-6640
Rajagopalan Vijayaraghavan https://orcid.org/0000-0002-2805-5404
Senthilkumar Sivanesan https://orcid.org/0000-0001-5133-7090

References

1. Hawkes C, Macgregor A. Twin studies and the heritability of MS: A conclusion. *Mult Scler*. 2009;15(6):661–667. doi:10.1177/1352458509104592
2. Willer CJ, Dyment DA, Risch NJ, Sadovnick AD, Ebers GC; The Canadian Collaborative Study Group. Twin concordance and sibling recurrence rates in multiple sclerosis. *Proc Natl Acad Sci U S A*. 2003;100(22): 12877–12882. doi:10.1073/pnas.1932604100
3. Tanaka M, Vécsei L. Monitoring the redox status in multiple sclerosis. *Biomedicines*. 2020;8(10):406. doi:10.3390/biomedicines8100406
4. Arslan B, Arslan GA, Tuncer A, Karabudak R, Dinçel AS. Evaluation of thiol homeostasis in multiple sclerosis and neuromyelitis optica spectrum disorders. *Front Neurol*. 2021;12:716195. doi:10.3389/fneur.2021.716195
5. Zarzuelo-Romero MJ, Pérez-Ramírez C, Cura Y, et al. Influence of genetic polymorphisms on clinical outcomes of glatiramer acetate in multiple sclerosis patients. *J Pers Med*. 2021;11(10):1032. doi:10.3390/jpm11101032
6. Quirant-Sánchez B, Mansilla MJ, Navarro-Barriuso J, et al. Combined therapy of vitamin D3-tolerogenic dendritic cells and interferon-β in a preclinical model of multiple sclerosis. *Biomedicines*. 2021;9(12):1758. doi:10.3390/biomedicines9121758
7. Longoria V, Parcel H, Toma B, Minhas A, Zeine R. Neurological benefits, clinical challenges, and neuropathologic promise of medical marijuana: A systematic review of cannabinoid effects in multiple sclerosis and experimental models of demyelination. *Biomedicines*. 2022;10(3):539. doi:10.3390/biomedicines10030539
8. Tanaka M, Vécsei L. Editorial of Special Issue "Crosstalk between depression, anxiety, and dementia: Comorbidity in behavioral neurology and neuropsychiatry." *Biomedicines*. 2021;9(5):517. doi:10.3390/biomedicines9050517
9. Luca M, Chisari CG, Zanghì A, Patti F. Early-onset alcohol dependence and multiple sclerosis: Diagnostic challenges. *Int J Environ Res Public Health*. 2021;18(11):5588. doi:10.3390/ijerph18115588
10. Bivona G, Gambino CM, Lo Sasso B, et al. Serum vitamin D as a biomarker in autoimmune, psychiatric and neurodegenerative diseases. *Diagnostics*. 2022;12(1):130. doi:10.3390/diagnostics12010130
11. Török N, Tanaka M, Vécsei L. Searching for peripheral biomarkers in neurodegenerative diseases: The tryptophan–kynurenine metabolic pathway. *Int J Mol Sci*. 2020;21(24):9338. doi:10.3390/ijms21249338
12. Carlton WW. Studies on the induction of hydrocephalus and spongy degeneration by cuprizone feeding and attempts to antidote the toxicity. *Life Sci*. 1967;6(1):11–19. doi:10.1016/0024-3205(67)90356-6
13. Skripuletz T, Bussmann JH, Gudi V, et al. Cerebellar cortical demyelination in the murine cuprizone model. *Brain Pathol*. 2010;20(2): 301–312. doi:10.1111/j.1750-3639.2009.00271.x
14. Morell P, Barrett CV, Mason JL, et al. Gene expression in brain during cuprizone-induced demyelination and remyelination. *Mol Cell Neurosci*. 1998;12(4–5):220–227. doi:10.1006/mcne.1998.0715

15. Shindler KS, Ventura E, Dutt M, Rostami A. Inflammatory demyelination induces axonal injury and retinal ganglion cell apoptosis in experimental optic neuritis. *Exp Eye Res*. 2008;87(3):208–213. doi:10.1016/j.exer.2008.05.017

16. Ulrich R, Baumgärtner W, Gerhauser I, et al. MMP-12, MMP-3, and TIMP-1 are markedly upregulated in chronic demyelinating theiler murine encephalomyelitis. *J Neuropathol Exp Neurol*. 2006;65(8):783–793. doi:10.1097/01.jnen.0000229990.32795.0d

17. Jeffery ND, Blakemore WF. Remyelination of mouse spinal cord axons demyelinated by local injection of lysolecithin. *J Neurocytol*. 1995;24(10):775–781. doi:10.1007/BF01191213

18. Brusaferri F, Candelise L. Steroids for multiple sclerosis and optic neuritis: A meta-analysis of randomized controlled clinical trials. *J Neurol*. 2000;247(6):435–442. doi:10.1007/s004150070172

19. Seo DY, Lee SR, Kim N, Ko KS, Rhee BD, Han J. Humanized animal exercise model for clinical implication. *Pflugers Arch*. 2014;466(9):1673–1687. doi:10.1007/s00424-014-1496-0

20. Sim YJ, Kim H, Kim JY, et al. Long-term treadmill exercise overcomes ischemia-induced apoptotic neuronal cell death in gerbils. *Physiol Behav*. 2005;84(5):733–738. doi:10.1016/j.physbeh.2005.02.019

21. Laurin D, Verreault R, Lindsay J, MacPherson K, Rockwood K. Physical activity and risk of cognitive impairment and dementia in elderly persons. *Arch Neurol*. 2001;58(3):498–504. doi:10.1001/archneur.58.3.498

22. Tong L, Shen H, Perreau VM, Balazs R, Cotman CW. Effects of exercise on gene-expression profile in the rat hippocampus. *Neurobiol Dis*. 2001;8(6):1046–1056. doi:10.1006/nbdi.2001.0427

23. Rossi S, Furlan R, De Chiara V, et al. Exercise attenuates the clinical, synaptic and dendritic abnormalities of experimental autoimmune encephalomyelitis. *Neurobiol Dis*. 2009;36(1):51–59. doi:10.1016/j.nbd.2009.06.013

24. Afzalpour ME, Chadorneshin HT, Foadoddini M, Eivari HA. Comparing interval and continuous exercise training regimens on neurotrophic factors in rat brain. *Physiol Behav*. 2015;147:78–83. doi:10.1016/j.physbeh.2015.04.012

25. Basoglu H, Boylu NT, Kose H. Cuprizone-induced demyelination in Wistar rats: Electrophysiological and histological assessment. *Eur Rev Med Pharmacol Sci*. 2013;17(20):2711–2717. PMID:24174351.

26. Klaren RE, Motl RW, Woods JA, Miller SD. Effects of exercise in experimental autoimmune encephalomyelitis (an animal model of multiple sclerosis). *J Neuroimmunol*. 2014;274(1–2):14–19. doi:10.1016/j.jneuroim.2014.06.014

27. Almeida PWM, Gomes-Filho A, Ferreira AJ, et al. Swim training suppresses tumor growth in mice. *J Appl Physiol*. 2009;107(1):261–265. doi:10.1152/japplphysiol.00249.2009

28. Gobatto CA, de Mello MAR, Sibuya CY, de Azevedo JRM, dos Santos LA, Kokubun E. Maximal lactate steady state in rats submitted to swimming exercise. *Comp Biochem Physiol A Mol Integr Physiol*. 2001;130(1):21–27. doi:10.1016/S1095-6433(01)00362-2

29. Kipp M, Clarner T, Dang J, Copray S, Beyer C. The cuprizone animal model: New insights into an old story. *Acta Neuropathol*. 2009;118(6):723–736. doi:10.1007/s00401-009-0591-3

30. Wolf Y, Shemer A, Levy-Efrati L, et al. Microglial MHC class II is dispensable for experimental autoimmune encephalomyelitis and cuprizone-induced demyelination. *Eur J Immunol*. 2018;48(8):1308–1318. doi:10.1002/eji.201847540

31. Abe H, Tanaka T, Kimura M, et al. Cuprizone decreases intermediate and late-stage progenitor cells in hippocampal neurogenesis of rats in a framework of 28-day oral dose toxicity study. *Toxicol Appl Pharmacol*. 2015;287(3):210–221. doi:10.1016/j.taap.2015.06.005

32. Cammer W. The neurotoxicant, cuprizone, retards the differentiation of oligodendrocytes in vitro. *J Neurol Sci*. 1999;168(2):116–120. doi:10.1016/S0022-510X(99)00181-1

33. Yu Q, Hui R, Park J, et al. Strain differences in cuprizone induced demyelination. *Cell Biosci*. 2017;7(1):59. doi:10.1186/s13578-017-0181-3

34. Khodanovich M, Pishchelko A, Glazacheva V, et al. Quantitative imaging of white and gray matter remyelination in the cuprizone demyelination model using the macromolecular proton fraction. *Cells*. 2019;8(10):1204. doi:10.3390/cells8101204

35. Madadi S, Pasbakhsh P, Tahmasebi F, et al. Astrocyte ablation induced by La-aminoadipate (L-AAA) potentiates remyelination in a cuprizone demyelinating mouse model. *Metab Brain Dis*. 2019;34(2):593–603. doi:10.1007/s11011-019-0385-9

36. Altieri M, Marini F, Arban R, Vitulli G, Jansson BO. Expression analysis of brain-derived neurotrophic factor (BDNF) mRNA isoforms after chronic and acute antidepressant treatment. *Brain Res*. 2004;1000(1–2):148–155. doi:10.1016/j.brainres.2003.12.028

37. Kalman B, Laitinen K, Komoly S. The involvement of mitochondria in the pathogenesis of multiple sclerosis. *J Neuroimmunol*. 2007;188(1–2):1–12. doi:10.1016/j.jneuroim.2007.03.020

38. Silvestroff L, Bartucci S, Soto E, Gallo V, Pasquini J, Franco P. Cuprizone-induced demyelination in CNP::GFP transgenic mice. *J Comp Neurol*. 2010;518(12):2261–2283. doi:10.1002/cne.22330

39. Kim TW, Sung YH. Regular exercise promotes memory function and enhances hippocampal neuroplasticity in experimental autoimmune encephalomyelitis mice. *Neuroscience*. 2017;346:173–181. doi:10.1016/j.neuroscience.2017.01.016

40. Gentile A, Musella A, De Vito F, et al. Immunomodulatory effects of exercise in experimental multiple sclerosis. *Front Immunol*. 2019;10:2197. doi:10.3389/fimmu.2019.02197

41. Frohman TC, Davis SL, Beh S, Greenberg BM, Remington G, Frohman EM. Uhthoff's phenomena in MS: Clinical features and pathophysiology. *Nat Rev Neurol*. 2013;9(9):535–540. doi:10.1038/nrneurol.2013.98

42. Davis SL, Wilson TE, White AT, Frohman EM. Thermoregulation in multiple sclerosis. *J Appl Physiol*. 2010;109(5):1531–1537. doi:10.1152/japplphysiol.00460.2010

43. Shanshiashvili LV, Kalandadze IV, Ramsden JJ, Mikeladze DG. Adhesive properties and inflammatory potential of citrullinated myelin basic protein peptide 45–89. *Neurochem Res*. 2012;37(9):1959–1966. doi:10.1007/s11064-012-0816-z

44. Sandroff BM, Motl RW, Scudder MR, DeLuca J. Systematic, evidence-based review of exercise, physical activity, and physical fitness effects on cognition in persons with multiple sclerosis. *Neuropsychol Rev*. 2016;26(3):271–294. doi:10.1007/s11065-016-9324-2

45. Mastronardi FG, Moscarello MA. Molecules affecting myelin stability: A novel hypothesis regarding the pathogenesis of multiple sclerosis. *J Neurosci Res*. 2005;80(3):301–308. doi:10.1002/jnr.20420

46. Frohman EM, Racke MK, Raine CS. Multiple sclerosis: The plaque and its pathogenesis. *N Engl J Med*. 2006;354(9):942–955. doi:10.1056/NEJMra052130

47. Correale J, Farez MF. The role of astrocytes in multiple sclerosis progression. *Front Neurol*. 2015;6:180. doi:10.3389/fneur.2015.00180

48. Yamamoto S, Gotoh M, Kawamura Y, et al. Cyclic phosphatidic acid treatment suppress cuprizone-induced demyelination and motor dysfunction in mice. *Eur J Pharmacol*. 2014;741:17–24. doi:10.1016/j.ejphar.2014.07.040

49. Vaynman S, Gomez-Pinilla F. License to run: Exercise impacts functional plasticity in the intact and injured central nervous system by using neurotrophins. *Neurorehabil Neural Repair*. 2005;19(4):283–295. doi:10.1177/1545968305280753

50. Caldeira MV, Melo CV, Pereira DB, et al. Brain-derived neurotrophic factor regulates the expression and synaptic delivery of alpha-amino-3-hydroxy-5-methyl-4-isoxazole propionic acid receptor subunits in hippocampal neurons. *J Biol Chem*. 2007;282(17):12619–12628. doi:10.1074/jbc.M700607200

51. Pencea V, Bingaman KD, Wiegand SJ, Luskin MB. Infusion of brain-derived neurotrophic factor into the lateral ventricle of the adult rat leads to new neurons in the parenchyma of the striatum, septum, thalamus, and hypothalamus. *J Neurosci*. 2001;21(17):6706–6717. doi:10.1523/JNEUROSCI.21-17-06706.2001

52. Kim JY, Yi ES, Lee H, et al. Swimming exercise ameliorates symptoms of MOG-induced experimental autoimmune encephalomyelitis by inhibiting inflammation and demyelination in rats. *Int Neurourol J*. 2020;24(Suppl 1):S39–S47. doi:10.5213/inj.2040156.078

53. Li L, Tang BL. Environmental enrichment and neurodegenerative diseases. *Biochem Biophys Res Commun*. 2005;334(2):293–297. doi:10.1016/j.bbrc.2005.05.162

54. Magalon K, Cantarella C, Monti G, Cayre M, Durbec P. Enriched environment promotes adult neural progenitor cell mobilization in mouse demyelination models: Environment enrichment in demyelination models. *Eur J Neurosci*. 2007;25(3):761–771. doi:10.1111/j.1460-9568.2007.05335.x

55. Jin JJ, Ko IG, Kim SE, Shin MS, Kim SH, Jee YS. Swimming exercise ameliorates multiple sclerosis-induced impairment of short-term memory by suppressing apoptosis in the hippocampus of rats. *J Exerc Rehabil*. 2014;10(2):69–74. doi:10.12965/jer.140103

MiR-218 promotes oxidative stress and inflammatory response by inhibiting SPRED2-mediated autophagy in HG-induced HK-2 cells

Lanfang Fu[1,A,D,F], Xinxin Huang[1,B,C], Juyun Zhang[1,C,E], Zhu Lin[1,C,E], Guijun Qin[2,A,E,F]

[1] Department of Endocrinology, Haikou Affiliated Hospital of Central South University, Xiangya School of Medicine, China

[2] Department of Endocrinology, The First Affiliated Hospital of Zhengzhou University, China

A – research concept and design; B – collection and/or assembly of data; C – data analysis and interpretation;
D – writing the article; E – critical revision of the article; F – final approval of the article

Address for correspondence
Guijun Qin
E-mail: guijun5544@163.com

Abstract

Background. Diabetic nephropathy (DN) is one of the most common complications of diabetes mellitus (DM). MicroRNA (miR)-218 is associated with the development of diabetes. Besides, sprouty-related EVH1 domain containing 2 (SPRED2), the downstream target of miR-218, is involved in insulin resistance and inflammation.

Objectives. Since inflammation plays a key role in DN, and SPRED2 is known to facilitate cell autophagy, the present study aimed to investigate the role and molecular mechanism of miR-218 and SPRED2-mediated autophagy in high glucose (HG)-induced renal tubular epithelial cells using an in vitro model.

Materials and methods. The HK-2 cells were cultured in 5.5 mM or 30 mM D-glucose medium. Quantitative real-time polymerase chain reaction (qRT-PCR) was used to detect the expression of miR-218 and SPRED2. Western blotting was performed to calculate the levels of SPRED2, inflammatory cytokines, autophagy-related and apoptosis-related proteins. Reactive oxygen species (ROS) level was evaluated using cellular ROS assay kit, superoxide dismutase (SOD) activity was detected using SOD activity assay kit, and malondialdehyde (MDA) content was measured using lipid peroxidation. The levels of interleukin (IL)-1β, IL-6, IL-4, and tumor necrosis factor alpha (TNF-α) were detected with enzyme-linked immunosorbent assay (ELISA). Cell apoptosis was evaluated using flow cytometry analysis. The targeting relationship between miR-218 and SPRED2 was identified with a luciferase reporter. The LC3-II expression was detected with immunofluorescence.

Results. The miR-218 expression was upregulated and SPRED2 expression was downregulated in HG-induced HK-2 cells. The miR-218 was proven to target SPRED2 and negatively regulate SPRED2 expression. Besides, downregulated miR-218 alleviated inflammatory response, oxidative stress and cell apoptosis, but aggravated autophagy. We also showed that downregulated SPRED2 reversed the effect of miR-218 on inflammation, cell apoptosis and autophagy in HG-induced HK-2 cells.

Conclusions. The miR-218 can promote oxidative stress and inflammatory response in HG-induced renal tubular epithelial cells by inhibiting SPRED2-mediated autophagy. This study might bring novel understanding for molecular mechanism of DN.

Key words: miR-218, renal tubular epithelial cell, autophagy, SPRED2, high glucose

1012

L. Fu et al. MiR-218/SPRED2/autophagy in HG renal cells

Background

Diabetic nephropathy (DN) is one of the most common complications of diabetes mellitus (DM) that might eventually develop into chronic nephropathy.[1–3] During the development of diabetes, high glucose (HG) condition can induce cell apoptosis, inflammation and oxidative stress in renal cells, e.g., renal tubular epithelial cells, leading to renal injuries, and finally resulting in DN and chronic nephropathy.[4–6] Therefore, it is of great importance to find new and potential biomarkers involved in renal tubular cells for better DN therapy.

Currently, various kinds of miRNAs have been illustrated to play important roles in diabetes and its complications by regulating biological pathways related to DN.[7–9] As reported, kidney hypoxia triggered the upregulation of miR-218 expression in endothelial progenitor cells that might promote endocapillary repair.[10,11] The miR-218 was also found to be a biomarker for type 1 DM in children.[12] Moreover, as stated in the study by Zhang et al., miR-218 was upregulated in the plasma samples of patients with type 2 DM-induced atherosclerosis.[13] Circulating evidence indicated that miR-218 plays a mediatory role in the pathogenesis of DN. However, deeper insight is still needed to illustrate the role of miR-218 in the development of DN.

As a member of sprouty-related EVH1 domain containing proteins family, sprouty-related EVH1 domain containing 2 (SPRED2) is usually expressed in various tissues.[14–16] It has been reported that SPRED2 negatively regulated high-fat diet-induced obesity, adipose tissue inflammation, metabolic abnormalities, and insulin resistance.[17] The SPRED2 was identified as a novel regulator of cardiac autophagy, and its deficiency could arouse cardiac dysfunction and life-threatening arrhythmias through impaired autophagy.[18–20] In addition, SPRED2 affected the development of lipopolysaccharide-induced lung inflammation by negatively regulating the ERK-MAPK pathway.[21] Since SPRED2 influences diabetes-related diseases including insulin resistance, obesity, as well as inflammation, which plays a key role in DN, it may also participate in DN process. However, limited research revealed the role of SPRED2 in autophagy, inflammation and oxidative stress during DN development.

Objectives

In the present study, we investigated the molecular mechanism of miR-218 and SPRED2 and their actions in DN in a well-accepted in vitro model using HG-induced HK-2 cells. Many studies used similar in vitro models to investigate DN.[22–24] These findings might provide new promising therapeutic strategies for DN.

Materials and methods

Cell culture and treatment

Renal tubular epithelial cells (HK-2) were purchased from American Type Culture Collection (ATCC; Rockville, USA). The cells were cultured in Dulbecco's modified Eagle's medium (DMEM; Life Technologies BRL, Gaithersburg, USA) supplemented with fetal bovine serum (FBS), 100 μg/mL streptomycin and 100 U/mL penicillin (Gibco BRL, Carlsbad, USA) at 37°C with 5% CO_2 in appropriate humidity.

The HK-2 cells were divided into a HG group and a normal glucose (NG) group. The HK-2 cells in the HG group were treated with a HG concentration of 30 mM, while the NG cells were treated with 5.5 mM glucose. Both groups were incubated with 5% CO_2 at 37°C for 48 h. For inhibition of cell autophagy, 3-MA (Sigma-Aldrich, St. Louis, USA) was used to treat the cells with a dose of 3 mmol/L.

Cell transfection

The cells were transfected with 5 nM miR-218 mimics/inhibitor, as well as si-SPRED2, and the corresponding negative controls (NCs). The miRNA mimics, inhibitor and NCs were purchased from Shanghai GenePharma Co., Ltd. (Shanghai, China) without sequence information. The si-SPRED2 was purchased from Sigma-Aldrich (cat. No. EHU029561) with sequence of TCCATGGTGAACGA-CAGAAAGACAAACTGGTGGTATTGGAATGCTATGTA-AGAAAGGACTTGGTCTACACCAAAGCCAATCCAAC-GTTTCATCACTGGAAGGTCGATAATAGGAAGTTTG-GACTTACTTTCCAAAGCCCTGCTGATGCCC-GAGCCTTTGACAGGGGAGTAAGGAAAGCAATC-GAAGACCTTATAGAAGGTTCAACAACGTCATCTTC-CACCATCCATAATGAAGCTGAGCTTGGCGATGAT-GACGTTTTTACAACAGCTACAGACAGTTCTTC-TAATTCCTCTCAGAAGAGAGAGCAACCTACTCG-GACAATCTCCTCTCCCACATCCTGTGAGCACCG-GAGGATTTATACCCTGGGCCACCTCCACGACT-CATACCCCACAGACCACTATCACCTCGATCAGCCG. The siRNA negative control was also obtained from Sigma-Aldrich (cat. No. SIC001) with meaningless sequence. Cell transfection was performed using Lipofectamine 3000 (Thermo Fisher Scientific, Waltham, USA) and detection of transfection efficiency was conducted at 48 h.

Flow cytometry analysis

The treated HK-2 cells were collected into 1.5 mL tubes containing annexin-FITC and propidium iodide (PI) reagents, and cultured in the dark at room temperature for 20 min. Afterwards, 200 μL of PI reagents, with 1 mL phosphate-buffered saline (PBS) were added into the flow tube. Cell apoptosis was quantified using FACSCalibur (Becton Dickinson, Mountain View, USA).

ELISA

The cell supernatant expression of tumor necrosis factor alpha (TNF-α), interleukin (IL)-1β, IL-4, and IL-6 was determined with enzyme-linked immunosorbent assay (ELISA) using commercially available kits (Human TNF alpha ELISA Kit (ab181421), Human IL-1 beta ELISA Kit (ab214025) and Human IL-4 ELISA Kit (ab215089), all purchased from Abcam, Cambridge, USA) according to the manufacturer's instructions.

Measurement of superoxide dismutase, malondialdehyde and reactive oxygen species generation

Reactive oxygen species (ROS) level was evaluated using cellular ROS assay kit (Deep Red; ab186029), superoxide dismutase (SOD) activity was detected by means of superoxide dismutase activity assay kit (Colorimetric; ab65354), and malondialdehyde (MDA) content was measured using Lipid Peroxidation (MDA) Assay Kit (Colorimetric/Fluorometric; ab118970), all purchased from Abcam.

qRT-PCR

Total RNA was extracted from HK-2 cells using Trizol reagent (Invitrogen, Carlsbad, USA). For the detection of miR-218 expression, a miRcute miRNA First-strand cDNA synthesis kit (Tiangen Biotech Co., Beijing, China)was used to convert RNA into cDNA. A miRcute miRNA qPCR detection kit (Tiangen Biotech Co.), performing on a 7900 HT Sequence Detection System (Applied Biosystems, Foster City, USA) was used in quantitative real-time polymerase chain reaction (qRT-PCR). For the detection of SPRED2 expression, a PrimeScript RT reagent Kit (TaKaRa, Tokyo, Japan) was used to convert RNA into cDNA. A Power SYBR Green kit (Thermo Fisher Scientific) with the Stratagene Mx3000P real-time PCR system (Stratagene, La Jolla, USA) was conducted for quantification. The following primers were used in PCRs: F 5'-TGTGAGCACCGGAAGATT-TATACC-3' and R 5'-CGCGGCGGCTTTGTGCTT-3' for SPRED2; F 5'-TAATGGTCGAACGCCTAACGTC-3' and R 5'-CGAGTGCATTTGTGCTTGATCTA-3' for miR-218; 5'-GACACGCAAATTCGTG-3' and 5'-GTGCAGGGTC-CGAGGT-3' for *U6*, and F 5'-GGGTGTGAACCAC-GAGAAAT and R 5'-ACTGTGGTCATGAGCCCTTC-3' for *GAPDH*. The *U6* and *GAPDH* were used as internal controls for miRNA and mRNA, respectively. The relative expression level was calculated using the $2^{-\Delta\Delta Cq}$ method.[25]

Western blotting

The protein extracted from HK-2 cells were loaded on sodium dodecyl sulfate-polyacrylamide gel electrophoresis (SDS-PAGE) and transferred to polyvinylidene difluoride (PVDF) membranes blocked with 5% non-fat milk at a room temperature for 3 h. Afterwards, the membranes were incubated with primary antibody at 4°C overnight, followed by horseradish peroxidase (HRP)-conjugated secondary antibodies at 37°C for 1 h. The primary antibodies were as follows: Anti-SPRED2 (ab153700, 1/500), Anti-caspase-3 (ab13847, 1/500), Anti-BAX (ab182733, 1/2000), Anti-BCL-2 (ab194583, 1/500), Anti-LC3-II/I (ab62721, 1 µg/mL), and Anti-Beclin 1 (ab207612, 1/2000) (all purchased from Abcam). The GAPDH was used as a control. Protein bands were detected using Super Signal West Pico Chemiluminescent Substrate kit (NCM Biotech, Suzhou, China).

Immunofluorescence

Briefly, cells were fixed in 4% paraformaldehyde for 5 min. For fluorescent labeling, cells were washed twice with PBS and permeabilized with 0.2% Triton X-100 for 5 min. Subsequently, cells were incubated with primary antibodies at 4°C overnight, followed with secondary antibodies at room temperature for 1 h. Fluorescence intensities were detected on an Olympus FluoView FV1000 confocal microscope (Olympus Corp., Tokyo, Japan).

Luciferase reporter assay

The binding mode between miR-218 and SPRED2 was predicted using TargetScan 7.2 (http://www.targetscan.org/vert_72/). The wild-type (WT) and mutation (MUT) of 3'-untranslated region (UTR) of SPRED2 sequences containing the binding sequence of miR-218 were amplified and inserted into the p-MIR-report plasmid (Ambion, Austin, USA). Afterwards, HK-2 cells were co-transfected with the miR-19b vector (inhibitor or mimics) or NCs in SPRED2-WT/SPRED2-MUTm, using Lipofectamine 3000 (Invitrogen). Cells were collected for detection using luciferase assay kits (Promega, Madison, USA) 48 h after the transfection. Luciferase activity of cells was normalized to Renilla luciferase activity.

Statistical analyses

The continuous data were presented as mean ± standard deviation (SD). The data normality in each compared group was evaluated with Shapiro–Wilk test. The comparison between 2 groups was made using the Student's t-test, and the comparison among 3 or more groups was conducted using one-way analysis of variance (ANOVA) followed by Tukey's post hoc test. The Levene's test was used for assumption of homogeneity of variances of ANOVA or t-test. The differences were considered statistically significant when $p < 0.05$. All calculations were performed using SPSS v. 18.0 (SPSS Inc., Chicago, USA).

Results

MiR-218 directly targets SPRED2 and negatively regulates SPRED2 expression

The expression levels of miR-218 and SPRED2 were detected under HG and NG conditions. As shown in Fig. 1A,B, SPRED2 expression significantly decreased in HG-induced HK-2 cells compared to the NG group. Nevertheless, qRT-PCR result showed that miR-218 expression visibly increased in the HG group (Fig. 1A). These findings suggested that miR-218 expression was upregulated and SPRED2 expression was downregulated in HK-2 cells under HG conditions.

To further investigate the molecular mechanism of miR-218 in HG-induced HK-2 cells, dual luciferase reporter assay was performed. Firstly, HK-2 cells were transfected with miR-218 mimics or miR-218 inhibitor,

respectively, and the transfection efficiency was confirmed with qRT-PCR. Based on bioinformatics analysis, miR-218 was predicted to bind to the SPRED2 (Fig. 1C). Luciferase reporter assay showed that the fluorescence intensity of SPRED2-WT was significantly decreased by the transfection of miR-218 mimics, but increased by the transfection of miR-218 inhibitor. However, miR-218 mimics/inhibitor had no effect on the fluorescence intensity of SPRED2-MUT (Fig. 1D). As shown in Fig. 1E, miR-218 expression was highly upregulated by the transfection of miR-218 mimics and knockdown by miR-218 inhibitor. Besides, both PCR and western blotting results proved that mRNA and protein levels of SPRED2 could be inhibited by overexpressed miR-218 but elevated by downregulated miR-218 (Fig. 1E,F). The results of ANOVA test are listed in Table 1. The above results indicated that miR-218 directly targeted SPRED2 and negatively regulated SPRED2 expression.
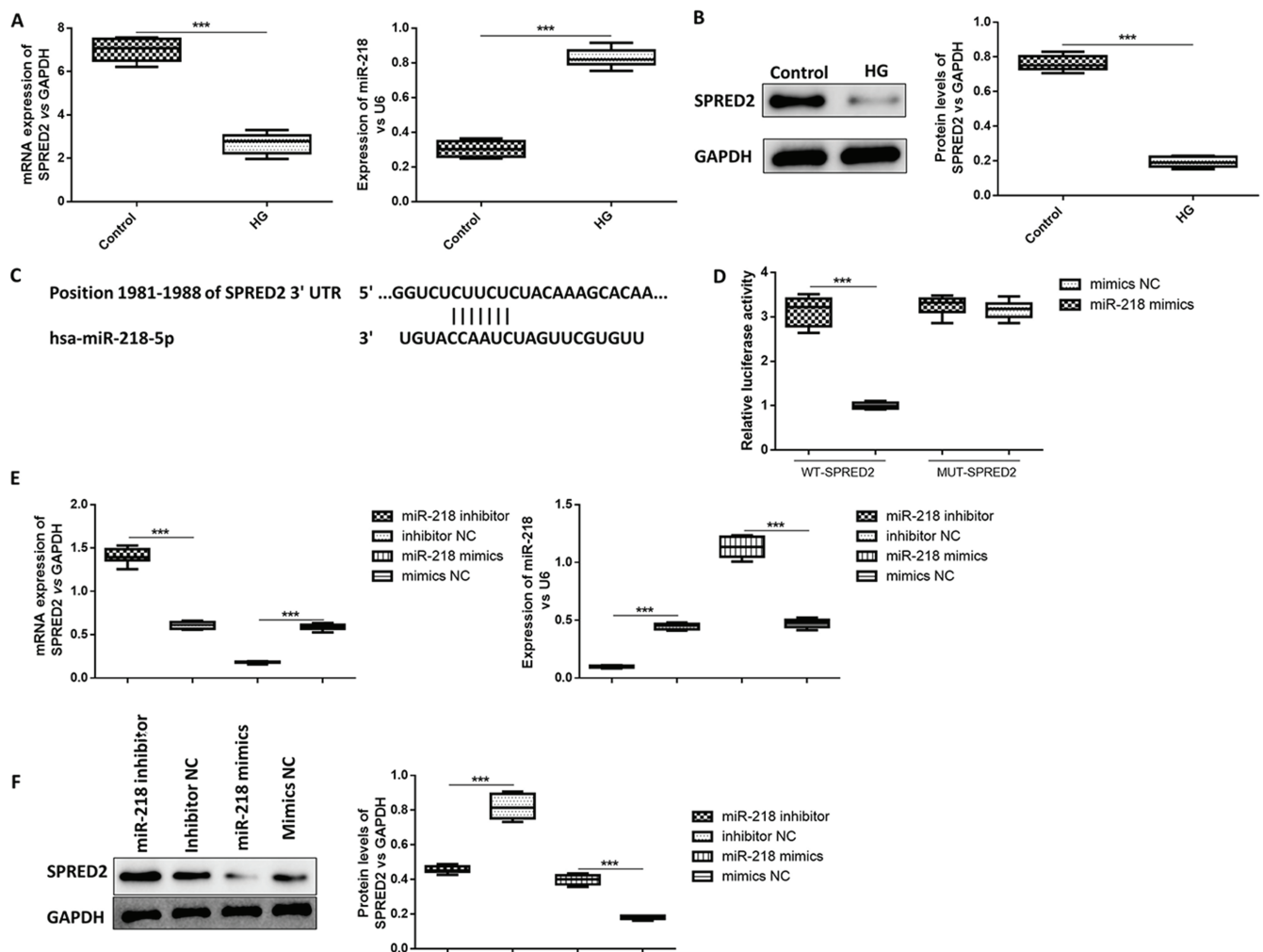
Fig. 1. MiR-218 negatively regulates sprouty-related EVH1 domain containing 2 (SPRED2) expression. A. Expression of miR-218 and SPRED2 was determined using quantitative real-time polymerase chain reaction (qRT-PCR); B. Protein level of SPRED2 was detected using western blotting in the high glucose (HG) group and normal glucose (NG) group; C. The binding sites between miR-218 and SPRED2 were predicted using TargetScan (http://www.targetscan.org/); D. Targeting relationship between miR-218 and SPRED2 was confirmed with dual luciferase reporter assay; E. HK-2 cells were transfected with miR-218 mimics, miR-218 inhibitor or the corresponding NC. The transfection efficiency of miR-218 mimics and miR-218 inhibitor, as well as the expression of SPRED2 in HK-2 were validated using qRT-PCR; F. Protein level of SPRED2 was detected with western blotting

***p < 0.001 (t-test or Tukey's post hoc test following analysis of variance (ANOVA); MUT – mutation; WT – wild-type.

Fig. 2. Inhibition of sprouty-related EVH1 domain containing 2 (SPRED2) or autophagy reverses the effect of miR-218 inhibitor on inflammatory factor secretion and oxidative stress in high glucose (HG)-induced HK-2 cells. A. HK-2 cells were transfected with si-SPRED2 or si-NC. The transfection efficiency of si-SPRED2 in HK-2 was validated with western blotting and quantitative real-time polymerase chain reaction (qRT-PCR); B. HG-induced cells were transfected with miR-218 inhibitor, NC inhibitor, miR-218 inhibitor and si-NC, miR-218 inhibitor and si-SPRED2, or miR-218 inhibitor and treated with 3-MA. Protein level of SPRED2 was calculated with western blotting; C. SPRED2 expression was calculated using qRT-PCR; D. Reactive oxygen species (ROS) level was evaluated using cellular ROS assay kit, superoxide dismutase (SOD) activity was detected using superoxide dismutase activity assay kit, and malondialdehyde (MDA) content was measured with lipid peroxidation (MDA) assay kit; E. The levels of interleukin (IL)-1β, IL-4, IL-6, and tumor necrosis factor alpha (TNF-α) were measured using enzyme-linked immunosorbent assay (ELISA)

***p < 0.001 (t-test or Tukey's post hoc test following analysis of variance (ANOVA)).

Table 1. Results of ANOVA as presented in Fig. 1E,F

Variables		Sum of squares	df	Mean square	F	p-value
mRNA of SPRED2	between groups	7.153	3	2.384	948.571	<0.001
	within group	0.080	32	0.003		
	total	7.234	35	N/A		
miR-218	between groups	5.038	3	1.679	677.637	<0.001
	within group	0.079	32	0.002		
	total	5.117	35	N/A		
Protein of SPRED2	between groups	1.900	3	0.633	385.558	<0.001
	within group	0.053	32	0.002		
	total	1.953	35	N/A		

df – degrees of freedom; ANOVA – analysis of variance; N/A – not applicable; SPRED2 – sprouty-related EVH1 domain containing 2.

Inhibition of SPRED2 or autophagy reverses the effect of miR-218 inhibitor on inflammation and oxidative stress in HG-induced HK-2 cells

The study investigated further the effect of miR-218 and SPRED2 on inflammatory factor secretion and oxidative stress in HG-induced HK-2 cells. First, cells were transfected with si-SPRED2#1, si-SPRED2#2 or si-NC, respectively. The SPRED2 expression was remarkably downregulated by the transfection of si-SPRED2#1 or si-SPRED2#2, but si-SPRED2#2 showed better efficacy for knockdown of SPRED2 expression (Fig. 2A). Hence, si-SPRED2#2 (abbreviated as si- SPRED2) was selected for the following experiments. Reduced SPRED2 expression induced by HG was elevated by miR-218 inhibitor; however, the co-transfection of si-SPRED2 reversed the effect of miR-218 inhibitor on SPRED2 expression (Fig. 2B). Compared to the control, the levels of MDA and ROS were significantly increased and SOD expression was dramatically decreased in HG-induced HK-2 cells, but miR-218 inhibitor suppressed the effect of HG induction on HK-2 cells. At the same time, the transfection of si-SPRED2 or the treatment of 3-MA attenuated the effect of miR-218 inhibitor on oxidative stress factors (Fig. 2C). Moreover, the increased levels of IL-1β, IL-6 and TNF-α and decreased IL-4 expression were found in HG-induced HK-2 cells, and this effect could be suppressed by the transfection of miR-218 inhibitor. However, the transfection of si-SPRED2 or the treatment of 3-MA reversed the effect of miR-218 inhibitor on inflammatory factor secretion in HG-induced HK-2 cells (Fig. 2D,E). The results of ANOVA test are listed in Table 2. All the above results suggested that the inhibition of SPRED2 or autophagy reversed the effect of miR-218 inhibitor on inflammatory factor secretion and oxidative stress in HG-induced HK-2 cells.

Inhibition of SPRED2 or autophagy reverses the suppressive effect induced by miR-218 knockdown on cell apoptosis in HG-induced HK-2 cells

The effect of miR-218 and SPRED2 on apoptosis in HG-induced HK-2 cells was also studied. We observed that miR-218 knockdown attenuated HG-induced cell apoptosis, which could be reversed by SPRED2 silencing or 3-MA treatment (Fig. 3A). The expression of apoptosis-related protein was detected to confirm this result. The level of cleaved caspase-3 and Bax was significantly elevated, and Bcl-2 expression was greatly decreased in HG-induced HK-2 cells. The miR-218 knockdown obviously suppressed the level of cleaved caspase-3 and Bax, but increased Bcl-2 expression in HG-induced HK-2 cells; however, this effect was alleviated by silencing SPRED2 or 3-MA treatment (Fig. 3B). The results of ANOVA test are listed in Table 3. These findings proved that the inhibition of SPRED2 or autophagy reversed the inhibitory effect of miR-218 silencing on cell apoptosis in HG-induced HK-2 cells.

Inhibition of SPRED2 or autophagy reverses the effect induced by miR-218 knockdown on autophagy in HG-induced HK-2 cells

Finally, the role of miR-218 and SPRED2 on autophagy in HG-induced HK-2 cells was studied. The effect of si-SPRED2#1 and si-SPRED2#2 on cell autophagy was analyzed and the result suggested that the transfection of both siRNAs inhibited cell autophagy and si-SPRED2#2 showed more significant effects (Supplementary Figure 1). Autophagy-related protein level of Beclin 1 and the conversion rate of LC3-II/I were detected with western blotting (Fig. 4A). The HG induction obviously suppressed Beclin 1 expression and conversion ratio of LC3-II/I, which was increased by miR-218 inhibitor. However, si-SPRED2 or 3-MA alleviated the effect of miR-218 inhibitor on autophagy-related protein expression. Immunofluorescence result showed
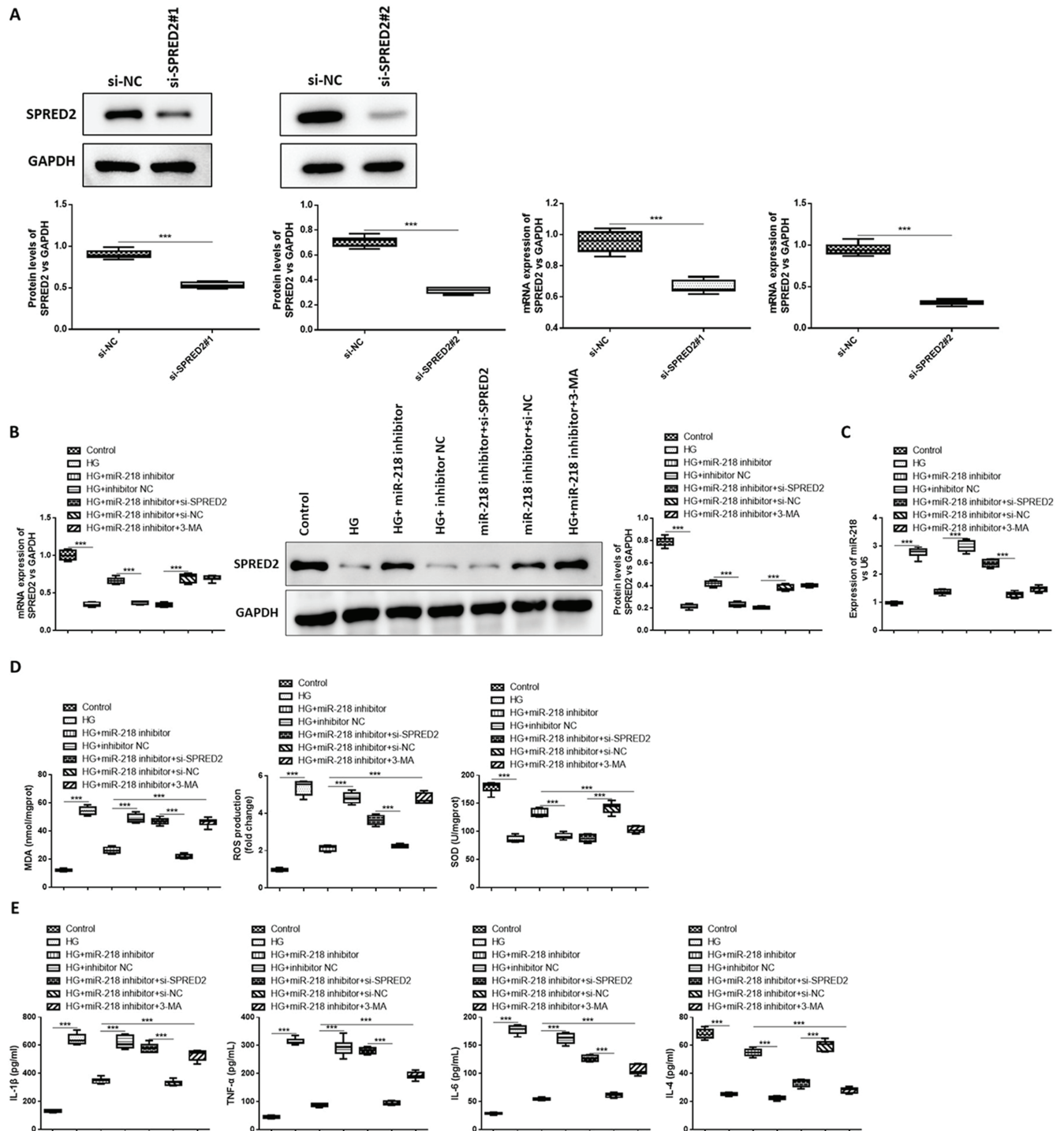
Fig. 3. Inhibition of sprouty-related EVH1 domain containing 2 (SPRED2) or autophagy reverses the inhibition effect of miR-218 inhibitor on apoptosis in HG-high glucose (HG)-induced HK-2 cells. A. Cell apoptosis was detected with flow cytometry; B. Protein levels of caspase-3, Bax and Bcl-2 were determined with western blotting

***$p < 0.001$ (Tukey's post hoc test following analysis of variance (ANOVA)).

that the LC3-II expression was downregulated by HG induction, but it was upregulated by miR-218 knockdown. Moreover, downregulated SPRED2 or 3-MA reversed the regulation of miR-218 on LC3-II expression (Fig. 4B). The results of ANOVA test are listed in Table 4. All these findings indicated that autophagy activated by silencing miR-218 was suppressed by SPRED2 knockdown or autophagy inhibitor.

Discussion

Around 20–40% of DM patients develop DN, and the 5-year survival rate of patients with end-stage renal disease (ESRD) is as low as 20%.[26–29] Recently, autophagy and oxidative stress have gradually become recognized as a new pathogenesis of DN and draw more and more attention.[30–32] In this study, we investigate the effects of miR-218/SPRED2

Table 2. Results of ANOVA as presented in Fig. 2B–E

Variables		Sum of squares	df	Mean square	F	p-value
mRNA of SPRED2	between groups	3.300	6	0.550	340.949	<0.001
	within group	0.090	56	0.002		
	total	3.391	62	N/A		
Protein of SPRED2	between groups	2.248	6	0.375	727.855	<0.001
	within group	0.029	56	0.001		
	total	2.276	62	N/A		
MiR-218	between groups	34.945	6	5.824	378.229	<0.001
	within group	0.862	56	0.015		
	total	35.807	62	N/A		
MDA	between groups	14307.360	6	2384.560	488.574	<0.001
	within group	273.316	56	4.881		
	total	14580.677	62	N/A		
ROS	between groups	149.305	6	24.884	447.134	<0.001
	within group	3.117	56	0.056		
	total	152.421	62	N/A		
SOD	between groups	65545.631	6	10924.272	235.401	<0.001
	within group	2598.797	56	46.407		
	total	68144.427	62	N/A		
IL-1β	between groups	1933782.414	6	322297.069	380.147	<0.001
	within group	47478.055	56	847.822		
	total	1981260.469	62	N/A		
TNF-α	between groups	675694.688	6	112615.781	671.846	<0.001
	within group	9386.803	56	167.621		
	total	685081.491	62	N/A		
IL-6	between groups	174871.250	6	29145.208	808.077	<0.001
	within group	2019.772	56	36.067		
	total	176891.022	62	N/A		
IL-4	between groups	18771.253	6	3128.542	506.702	<0.001
	within group	345.762	56	6.174		
	total	19117.015	62	N/A		

df – degrees of freedom; ANOVA – analysis of variance; N/A – not applicable; MDA – malondialdehyde; ROS – reactive oxygen species; SOD – superoxide dismutase; IL – interleukin; TNF-α – tumor necrosis factor alpha; SPRED2 – sprouty-related EVH1 domain containing 2.

Table 3. Results of ANOVA as presented in Fig. 3A,B

Variables		Sum of squares	df	Mean square	F	p-value
Apoptosis rate	between groups	9012.880	6	1502.147	784.320	<0.001
	within group	107.252	56	1.915		
	total	9120.133	62	N/A		
Caspase-3	between groups	4.286	6	0.714	458.273	<0.001
	within group	0.087	56	0.002		
	total	4.374	62	N/A		
Bax	between groups	4.622	6	0.770	410.626	<0.001
	within group	0.105	56	0.002		
	total	4.727	62	N/A		
Bcl-2	between groups	2.463	6	0.410	585.088	<0.001
	within group	0.039	56	0.001		
	total	2.502	62	N/A		

df – degrees of freedom; ANOVA – analysis of variance; N/A – not applicable.

A

B

I Control; II HG; III HG+ miR-218 inhibitor;
IV HG+ inhibitor NC; V miR-218 inhibitor+si-SPRED2; VI
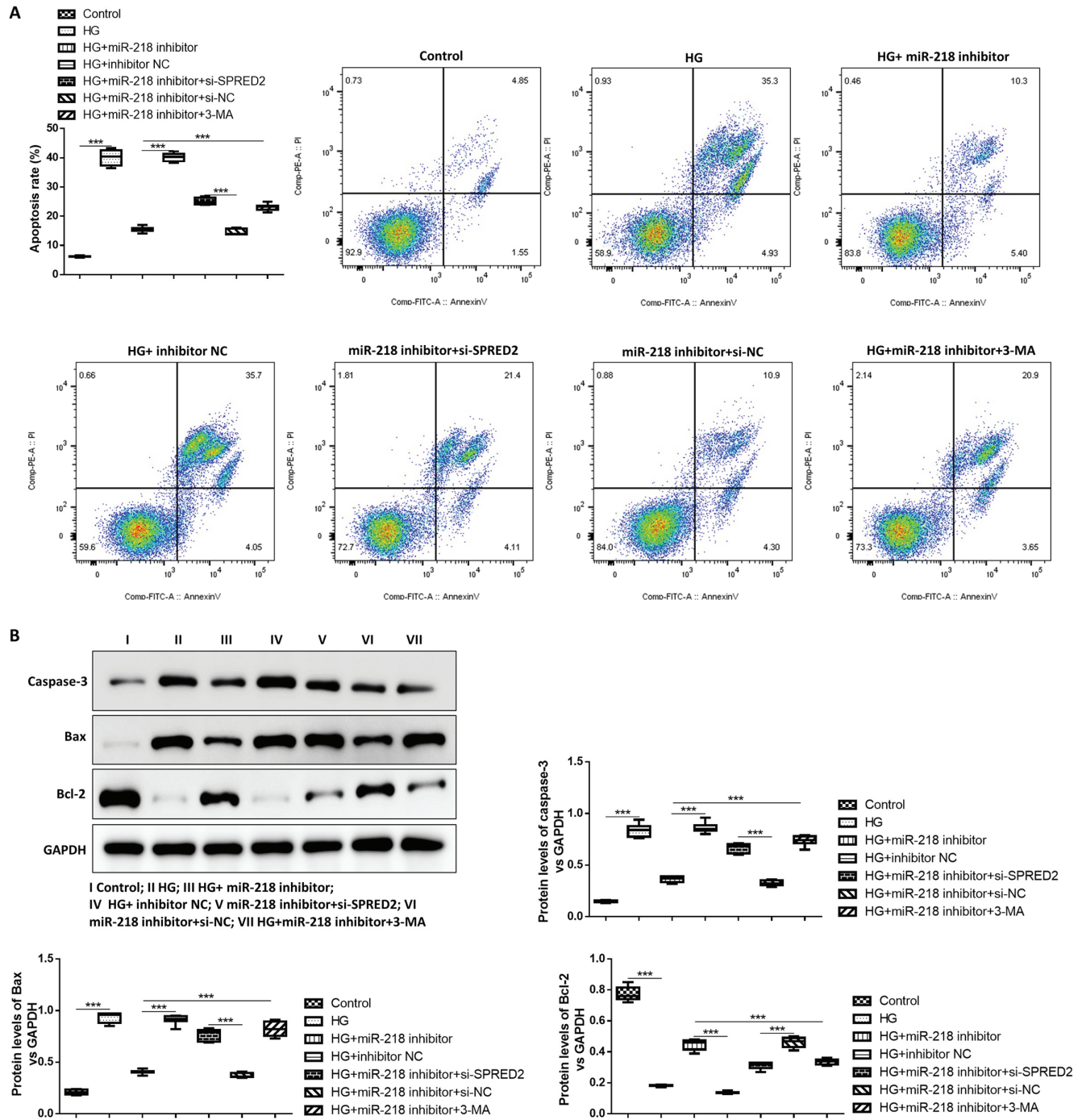miR-218 inhibitor+si-NC; VII HG+miR-218 inhibitor+3-MA
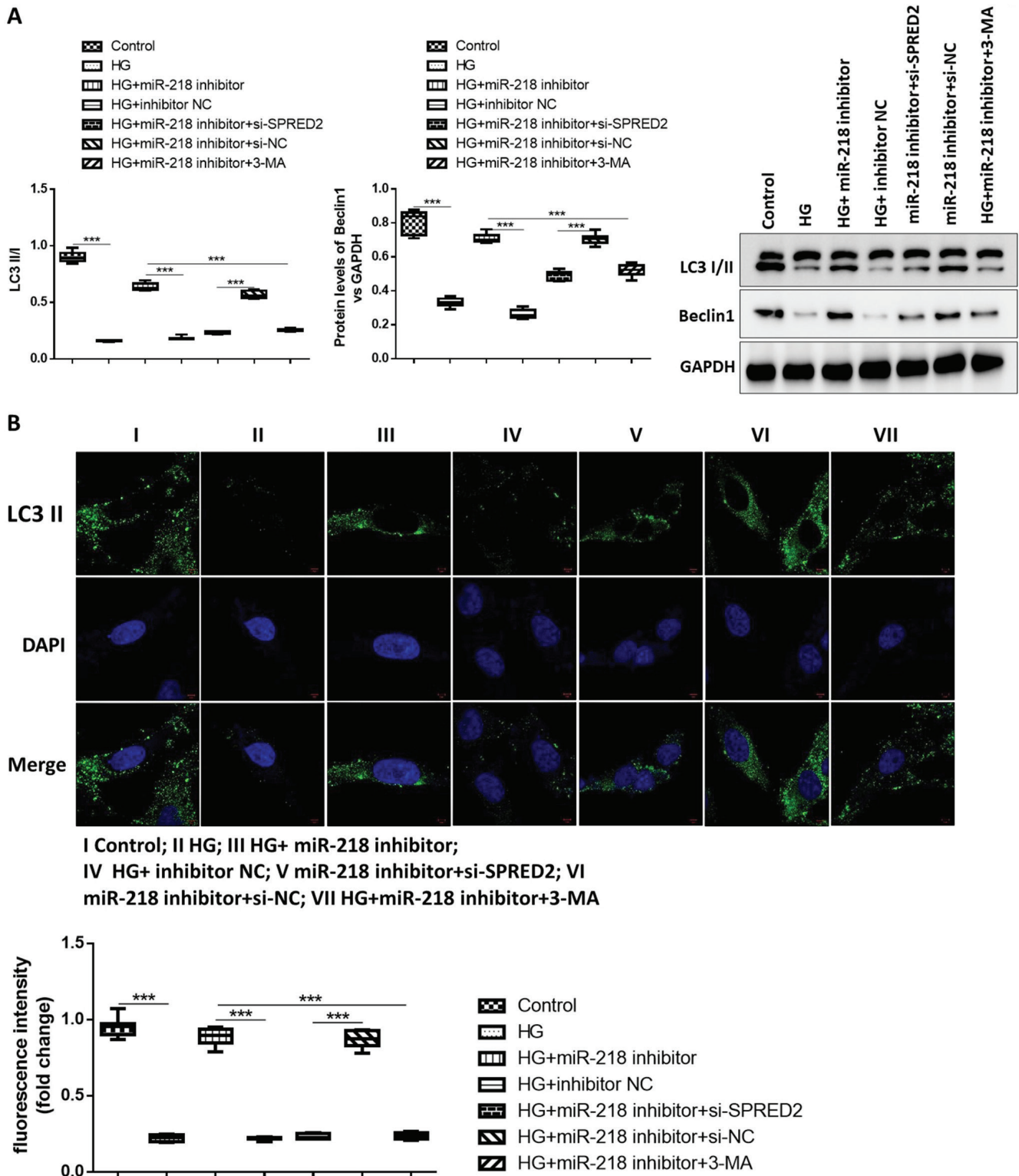
Fig. 4. Inhibition of sprouty-related EVH1 domain containing 2 (SPRED2) or autophagy reverses the promotional effect of miR-218 inhibitor on autophagy in high glucose (HG)-induced HK-2 cells. A. Protein level of LC3-II/I and Beclin 1 was detected with western blotting; B. Immunofluorescence was used to measured LC3-II expression

***$p < 0.001$ (t-test or Tukey's post hoc test following analysis of variance (ANOVA)).

axis on oxidative stress and inflammatory response in HG-induced renal tubular epithelial cells.

In the last decade, numerous evidence surfaced for variety of miRNAs involvement in DN development. A clinical study found that miR-29c regulated the expression of inflammatory cytokines in DN by targeting tristetraprolin.[33] The role of miR-218 in DN was also illustrated in several in vivo and in vitro studies.[34] An in vitro study showed

Table 4. Results of ANOVA as presented in Fig. 4A,B

Variables		Sum of squares	df	Mean square	F	p-value
LC3-II/I	between groups	4.391	6	0.732	1174.293	<0.001
	within group	0.035	56	0.001		
	total	4.426	62	N/A		
Beclin 1	between groups	2.227	6	0.371	280.742	<0.001
	within group	0.074	56	0.001		
	total	2.301	62	N/A		
Fluorescence intensity	between groups	7.078	6	1.180	762.565	<0.001
	within group	0.087	56	0.002		
	total	7.165	62	N/A		

df – degrees of freedom; ANOVA – analysis of variance; N/A – not applicable.

that downregulated miR-218 suppressed the level of inflammatory factors and attenuated the HG-induced injury in renal proximal tubule cell.[35] Moreover, miR-218 expression was upregulated in HG-treated podocytes and miR-218 silencing inhibited apoptosis in HG-treated podocytes.[36] Upregulated miR-218 increased the expression of pro-inflammatory cytokines, decreased the expression of anti-inflammatory cytokines and accelerated the process of epithelial–mesenchymal transition in HG models.[37] All of these studies indicate that miR-218 facilitates inflammation response and oxidative stress in DN, and thus promotes DN development. The present study also found that miR-218 expression was upregulated in HG-induced HK-2 cells, and that downregulated miR-218 alleviated cell apoptosis, inflammation and oxidative stress, and enhanced autophagy in HG-induced HK-2 cells. However, a DN rat model revealed that overexpressing miR-218 was sufficient to alleviate renal injury.[38] This issue needs deep insight in further study.

Autophagy is considered a stress-responsive intracellular system that plays an essential role in promoting cell against hypoxia, endoplasmic reticulum stress or oxidative stress, associated with the pathogenesis of diabetes-related diseases.[39–42] In DN development, cell autophagy also plays important roles, affecting cell apoptosis and inflammation of renal tubular epithelial cells.[43,44] Generally, the dysfunction of autophagy is considered a contributor to DN and renal injury.[45,46] Kitada et al. demonstrated that autophagy activation might be a potential therapeutic option for DN.[47] Meanwhile, a previous study discovered that impaired autophagy in podocyte cells could accelerate renal damage.[48] The SPRED2 was identified as an activator of autophagy and SPRED2 deficiency might affect autophagy, resulting in cardiac dysfunction and life-threatening arrhythmias.[49] Interacting with LC3, SPRED2 promoted autophagosome maturation, thereby leading to cell death in tumor.[50] Based on bioinformatics analysis, SPRED2 was predicted to be one of the target genes of miR-218 in our study. However, no studies illustrate the regulation of expression between miR-218 and SPRED2 in renal tubular epithelial cells;

besides, the molecular mechanism action of SPRED2 in DN was not reported. In a recent study, miR-218 was found to regulate SPRED2 expression in PC12 cells.[51] Therefore, we hypothesized that miR-218 might promote the development of DN by inhibiting SPRED2-mediated autophagy. Our results showed that miR-218 negatively regulated SPRED2 expression in HK-2 cells. We demonstrated for the first time that SPRED2 suppression reversed the effect of downregulated miR-218 on inflammatory factor secretion and oxidative stress, apoptosis and autophagy.

Limitations

The main limitation of this study is that it lacks in vivo evidence. The signaling path ways regulating miR-218 in DN are also unclear.

Conclusions

In summary, miR-218 was upregulated and SPRED2 was downregulated in HG-induced renal tubular epithelial cells. The miR-218 negatively regulates SPRED2 expression, but SPRED2 knockdown reverses the effect of downregulated miR-218 on inflammatory factor secretion and oxidative stress, apoptosis and autophagy. We demonstrated for the first time that miR-218 promoted oxidative stress and inflammatory response in HG-induced renal tubular epithelial cells by inhibiting SPRED2.

Data availability

The Supplementary data are available at https://doi.org/10.5281/zenodo.6383061. They consist of 3 files:

1. Statistical Data is the original file from the SPSS software;

2. Tables of Statistical Data contain the statistical results for calculation of all data in the figures;

3. Supplementary Figure shows the effects of transfection of si-SPRED2#1 and si-SPRED2#2 on cell autophagy.

References

1. Papadopoulou-Marketou N, Chrousos GP, Kanaka-Gantenbein C. Diabetic nephropathy in type 1 diabetes: A review of early natural history, pathogenesis, and diagnosis. *Diabetes Metab Res Rev*. 2017; 33(2):e2841. doi:10.1002/dmrr.2841

2. Selby NM, Taal MW. An updated overview of diabetic nephropathy: Diagnosis, prognosis, treatment goals and latest guidelines. *Diabetes Obes Metab*. 2020;22(S1):3–15. doi:10.1111/dom.14007

3. Donate-Correa J, Luis-Rodríguez D, Martín-Núñez E, et al. Inflammatory targets in diabetic nephropathy. *J Clin Med*. 2020;9(2):458. doi:10.3390/jcm9020458

4. Imasawa T, Obre E, Bellance N, et al. High glucose repatterns human podocyte energy metabolism during differentiation and diabetic nephropathy. *FASEB J*. 2017;31(1):294–307. doi:10.1096/fj.201600293r

5. Warren AM, Knudsen ST, Cooper ME. Diabetic nephropathy: An insight into molecular mechanisms and emerging therapies. *Expert Opin Ther Targets*. 2019;23(7):579–591. doi:10.1080/14728222.2019.1624721

6. Sifuentes-Franco S, Padilla-Tejeda DE, Carrillo-Ibarra S, Miranda-Díaz AG. Oxidative stress, apoptosis, and mitochondrial function in diabetic nephropathy. *Int J Endocrinol*. 2018;2018:1–13. doi:10.1155/2018/1875870

7. Simpson K, Wonnacott A, Fraser DJ, Bowen T. MicroRNAs in diabetic nephropathy: From biomarkers to therapy. *Curr Diab Rep*. 2016; 16(3):35. doi:10.1007/s11892-016-0724-8

8. Wang LP, Gao YZ, Song B, et al. MicroRNAs in the progress of diabetic nephropathy: A systematic review and meta-analysis. *Evid Based Complement Alternat Med*. 2019;2019:1–9. doi:10.1155/2019/3513179

9. Kim H, Bae YU, Jeon JS, et al. The circulating exosomal microRNAs related to albuminuria in patients with diabetic nephropathy. *J Transl Med*. 2019;17(1):236. doi:10.1186/s12967-019-1983-3

10. Wang X, Liu J, Yin W, et al. miR-218 expressed in endothelial progenitor cells contributes to the development and repair of the kidney microvasculature. *Am J Pathol*. 2020;190(3):642–659. doi:10.1016/j.ajpath.2019.11.014

11. Mao P, Liu X, Wen Y, Tang L, Tang Y. LncRNA SNHG12 regulates ox-LDL-induced endothelial cell injury by the miR-218-5p/IGF2 axis in atherosclerosis. *Cell Cycle*. 2021;20(16):1561–1577. doi:10.1080/15384101.2021.1953755

12. Kong Q, Guo X, Guo Z, Su T. Urinary exosome miR-424 and miR-218 as biomarkers for type 1 diabetes in children. *Clin Lab*. 2019;65(6). doi:10.7754/Clin.Lab.2018.180921

13. Zhang JY, Gong YL, Li CJ, Qi Q, Zhang QM, Yu DM. Circulating MiRNA biomarkers serve as a fingerprint for diabetic atherosclerosis. *Am J Transl Res*. 2016;8(6):2650–2658. PMID:27398148. PMCID:PMC4931159.

14. Wang H, Liu S, Kong F, et al. Spred2 inhibits epithelial–mesenchymal transition of colorectal cancer cells by impairing ERK signaling. *Oncol Rep*. 2020;44(1):174–185. doi:10.3892/or.2020.7586

15. Peng W, Li J, Chen R, et al. Upregulated METTL3 promotes metastasis of colorectal cancer via miR-1246/SPRED2/MAPK signaling pathway. *J Exp Clin Cancer Res*. 2019;38(1):393. doi:10.1186/s13046-019-1408-4

16. Motta M, Fasano G, Gredy S, et al. SPRED2 loss-of-function causes a recessive Noonan syndrome-like phenotype. *Am J Hum Genet*. 2021; 108(11):2112–2129. doi:10.1016/j.ajhg.2021.09.007

17. Ohkura T, Yoshimura T, Fujisawa M, et al. Spred2 regulates high fat diet-induced adipose tissue inflammation, and metabolic abnormalities in mice. *Front Immunol*. 2019;10:17. doi:10.3389/fimmu.2019.00017

18. Ullrich M, Aßmus B, Augustin AM, et al. SPRED2 deficiency elicits cardiac arrhythmias and premature death via impaired autophagy. *J Mol Cell Cardiol*. 2019;129:13–26. doi:10.1016/j.yjmcc.2019.01.023

19. Kawara A, Mizuta R, Fujisawa M, et al. Spred2-deficiency enhances the proliferation of lung epithelial cells and alleviates pulmonary fibrosis induced by bleomycin. *Sci Rep*. 2020;10(1):16490. doi:10.1038/s41598-020-73752-3

20. Okada M, Yamane M, Yamamoto S, et al. SPRED2 deficiency may lead to lung ischemia–reperfusion injury via ERK1/2 signaling pathway activation. *Surg Today*. 2018;48(12):1089–1095. doi:10.1007/s00595-018-1696-x

21. Xu Y, Ito T, Fushimi S, et al. Spred-2 deficiency exacerbates lipopolysaccharide-induced acute lung inflammation in mice. *PLoS ONE*. 2014;9(10):e108914. doi:10.1371/journal.pone.0108914

22. Hong GL, Kim KH, Lee CH, Kim TW, Jung JY. NQO1 deficiency aggravates renal injury by dysregulating Vps34/ATG14L complex during autophagy initiation in diabetic nephropathy. *Antioxidants*. 2021; 10(2):333. doi:10.3390/antiox10020333

23. An X, Liao G, Chen Y, et al. Intervention for early diabetic nephropathy by mesenchymal stem cells in a preclinical nonhuman primate model. *Stem Cell Res Ther*. 2019;10(1):363. doi:10.1186/s13287-019-1401-z

24. Liu L, Chen H, Yun J, et al. miRNA-483–5p targets HDCA4 to regulate renal tubular damage in diabetic nephropathy. *Horm Metab Res*. 2021;53(8):562–569. doi:10.1055/a-1480-7519

25. Livak KJ, Schmittgen TD. Analysis of relative gene expression data using real-time quantitative PCR and the 2(−delta delta C(T)) method. *Methods*. 2001;25(4):402–408. doi:10.1006/meth.2001.1262

26. Gnudi L, Coward RJM, Long DA. Diabetic nephropathy: Perspective on novel molecular mechanisms. *Trends Endocrinol Metab*. 2016; 27(11):820–830. doi:10.1016/j.tem.2016.07.002

27. Moreno JA, Gomez-Guerrero C, Mas S, et al. Targeting inflammation in diabetic nephropathy: A tale of hope. *Expert Opin Investig Drugs*. 2018;27(11):917–930. doi:10.1080/13543784.2018.1538352

28. Umanath K, Lewis JB. Update on diabetic nephropathy: Core curriculum 2018. *Am J Kidney Dis*. 2018;71(6):884–895. doi:10.1053/j.ajkd.2017.10.026

29. Sagoo MK, Gnudi L. Diabetic nephropathy: Is there a role for oxidative stress? *Free Radic Biol Med*. 2018;116:50–63. doi:10.1016/j.freeradbiomed.2017.12.040

30. Sifuentes-Franco S, Padilla-Tejeda DE, Carrillo-Ibarra S, Miranda-Díaz AG. Oxidative stress, apoptosis, and mitochondrial function in diabetic nephropathy. *Int J Endocrinol*. 2018;2018:1–13. doi:10.1155/2018/1875870

31. Koch EAT, Nakhoul R, Nakhoul F, Nakhoul N. Autophagy in diabetic nephropathy: A review. *Int Urol Nephrol*. 2020;52(9):1705–1712. doi:10.1007/s11255-020-02545-4

32. Vodošek Hojs N, Bevc S, Ekart R, Hojs R. Oxidative stress markers in chronic kidney disease with emphasis on diabetic nephropathy. *Antioxidants*. 2020;9(10):925. doi:10.3390/antiox9100925

33. Guo J, Li J, Zhao J, et al. MiRNA-29c regulates the expression of inflammatory cytokines in diabetic nephropathy by targeting tristetraprolin. *Sci Rep*. 2017;7(1):2314. doi:10.1038/s41598-017-01027-5

34. Li M, Guo Q, Cai H, Wang H, Ma Z, Zhang X. miR-218 regulates diabetic nephropathy via targeting IKK-β and modulating NK-κB-mediated inflammation. *J Cell Physiol*. 2020;235(4):3362–3371. doi:10.1002/jcp.29224

35. Su SS, Li BP, Li CL, Xiu FR, Wang DY, Zhang FR. Downregulation of MiR-218 can alleviate high-glucose-induced renal proximal tubule injury by targeting GPRC5A. *Biosci Biotechnol Biochem*. 2020;84(6):1123–1130. doi:10.1080/09168451.2020.1717330

36. Yang H, Wang Q, Li S. MicroRNA-218 promotes high glucose-induced apoptosis in podocytes by targeting heme oxygenase-1. *Biochem Biophys Res Commun*. 2016;471(4):582–588. doi:10.1016/j.bbrc.2016.02.028

37. Zhang YL, Wang JM, Yin H, Wang SB, He CL, Liu J. DACH1, a novel target of miR-218, participates in the regulation of cell viability, apoptosis, inflammatory response, and epithelial–mesenchymal transition process in renal tubule cells treated by high-glucose. *Ren Fail*. 2020;42(1):463–473. doi:10.1080/0886022X.2020.1762647

38. Li M, Guo Q, Cai H, Wang H, Ma Z, Zhang X. miR-218 regulates diabetic nephropathy via targeting IKK-β and modulating NK-κB-mediated inflammation. *J Cell Physiol*. 2020;235(4):3362–3371. doi:10.1002/jcp.29224

39. Ebrahim N, Ahmed I, Hussien N, et al. Mesenchymal stem cell-derived exosomes ameliorated diabetic nephropathy by autophagy induction through the mTOR signaling pathway. *Cells*. 2018;7(12):226. doi:10.3390/cells7120226

40. Galluzzi L, Green DR. Autophagy-independent functions of the autophagy machinery. *Cell*. 2019;177(7):1682–1699. doi:10.1016/j.cell.2019.05.026

41. Harris J, Lang T, Thomas JPW, Sukkar MB, Nabar NR, Kehrl JH. Autophagy and inflammasomes. *Mol Immunol*. 2017;86:10–15. doi:10.1016/j.molimm.2017.02.013

42. Doherty J, Baehrecke EH. Life, death and autophagy. *Nat Cell Biol*. 2018;20(10):1110–1117. doi:10.1038/s41556-018-0201-5

43. Liu WJ, Huang WF, Ye L, et al. The activity and role of autophagy in the pathogenesis of diabetic nephropathy. *Eur Rev Med Pharmacol Sci*. 2018;22(10):3182–3189. doi:10.26355/eurrev_201805_15079

44. Chen DD, Xu R, Zhou JY, et al. *Cordyceps militaris* polysaccharides exerted protective effects on diabetic nephropathy in mice *via* regulation of autophagy. *Food Funct*. 2019;10(8):5102–5114. doi:10.1039/C9FO00957D

45. Wei W, An XR, Jin SJ, Li XX, Xu M. Inhibition of insulin resistance by PGE1 via autophagy-dependent FGF21 pathway in diabetic nephropathy. *Sci Rep*. 2018;8(1):9. doi:10.1038/s41598-017-18427-2

46. Zhao Y, Zhang W, Jia Q, et al. High dose vitamin E attenuates diabetic nephropathy via alleviation of autophagic stress. *Front Physiol*. 2019;9:1939. doi:10.3389/fphys.2018.01939

47. Kitada M, Ogura Y, Monno I, Koya D. Regulating autophagy as a therapeutic target for diabetic nephropathy. *Curr Diab Rep*. 2017;17(7):53. doi:10.1007/s11892-017-0879-y

48. Tagawa A, Yasuda M, Kume S, et al. Impaired podocyte autophagy exacerbates proteinuria in diabetic nephropathy. *Diabetes*. 2016; 65(3):755–767. doi:10.2337/db15-0473

49. Cui C, Han S, Tang S, et al. The autophagy regulatory molecule CSRP3 interacts with LC3 and protects against muscular dystrophy. *Int J Mol Sci*. 2020;21(3):749. doi:10.3390/ijms21030749

50. Jiang K, Liu M, Lin G, et al. Tumor suppressor Spred2 interaction with LC3 promotes autophagosome maturation and induces autophagy-dependent cell death. *Oncotarget*. 2016;7(18):25652–25667. doi:10.18632/oncotarget.8357

51. Chen D, Li C, Lv R. MicroRNA-218 aggravates H_2O_2-induced damage in PC12 cells via spred2-mediated autophagy. *Exp Ther Med*. 2021; 22(6):1352. doi:10.3892/etm.2021.10787

Original papers

The influence of venetoclax, used alone or in combination with cladribine (2-CdA), on CLL cells apoptosis in vitro: Preliminary results

Aleksandra Beata Kubiak[1,B–D,F], Ewelina Izabela Ziółkowska[1,B,C,F],
Anna Barbara Korycka-Wołowiec[1,A,C,E,F], Tadeusz Robak[1,E,F], Dariusz Wołowiec[2,C,E,F]

[1] Department of Hematology, Medical University of Lodz, Poland

[2] Department of Hematology, Blood Neoplasms and Bone Marrow Transplantation, Medical University of Wroclaw, Poland

A – research concept and design; B – collection and/or assembly of data; C – data analysis and interpretation;
D – writing the article; E – critical revision of the article; F – final approval of the article

Address for correspondence
Anna Barbara Korycka-Wołowiec
E-mail: anna.korycka-wolowiec@umed.lodz.pl

Abstract

Background. Venetoclax (VEN), a highly selective BCL-2 inhibitor, is successfully used in the treatment of chronic lymphocytic leukemia (CLL). The purine analogue – cladribine (2-CdA) – is also administered to CLL patients, especially as a part of chemoimmunotherapy.

Objectives. To compare the effects of the VEN+2-CdA regimen with that of the 2 drugs used alone on the apoptosis of CLL lymphocytes in vitro.

Materials and methods. Mononuclear cells were collected from 103 previously untreated CLL patients. They were incubated with VEN (40 nM) or/and 2-CdA (16 µM) for 48 h. Cytotoxicity, overall apoptosis, mitochondrial transmembrane potential changes (ΔΨm), and expression of selected apoptosis-involved proteins were measured.

Results. The cytotoxicity, overall apoptosis, caspase-3 or caspase-9 expression, and ΔΨm were significantly higher after VEN+2-CdA addition compared to both drugs used alone, with a very strong synergistic effect observed. The percentage of BCL-2-positive cells decreased after VEN and VEN+2-CdA addition compared to controls. The TP53-expressing cells increased under the influence of all tested regimens. The VEN+2-CdA increased the expression of BIM, BAX and NOXA compared to either controls or VEN or 2-CdA alone. Similar increases in PUMA expression were observed after VEN, 2-CdA and VEN+2-CdA addition. The FAS-associated death-domain protein (FADD) expression was significantly higher after 2-CdA and 2-CdA+VEN addition as compared to control.

Conclusions. Our results confirm the involvement of both VEN and 2-CdA in the intrinsic apoptotic pathway. They also demonstrate that these agents have a synergistic effect on CLL cells in vitro. Further studies are needed to assess the influence of VEN+2-CdA on the expression of apoptosis-involved genes.

Key words: apoptosis, CLL, apoptosis-involved proteins, cladribine, venetoclax

Background

Despite the growing understanding of the molecular pathogenesis of hematological malignancies and the considerable progress in their treatment, many diseases, including chronic lymphocytic leukemia (CLL), still remain incurable. Chronic lymphocytic leukemia is characterized by an uncontrolled clonal accumulation of morphologically mature B cells, which in turn is believed to be caused by the inhibition of intrinsic apoptosis. In this pathway, the most important role is played by overexpression of the intracellular signaling pathway, which allows malignant cells to evade apoptosis by sequestering pro-apoptotic proteins. The key regulators of this pathway are the antiapoptotic BCL-2 family proteins.[1,2]

Recently published preclinical and clinical studies have shown that the small molecule agent venetoclax (VEN) is suitable for clinical use in CLL patients. It is a highly selective inhibitor of the BCL-2 protein that belongs to a novel class of BCL-2-antagonists able to mimic the function of pro-apoptotic BH3-only proteins (BH3s).[3–5] The intrinsic apoptotic pathway plays a crucial role in the mechanism of VEN action.[6–8] An important property of VEN is to directly induce the apoptosis, independently of *TP53*[9–13]; as such, VEN shows activity in CLL patients, including those with deletion (del) 17p and/or mutation of *TP53*, as well as in those without del17p/*TP53* mutation which failed both chemoimmunotherapy and B-cell receptor (BCR) pathway, such as ibrutinib.[9] A number of studies have confirmed the efficacy of VEN in terms of the depth of response, including eradication of minimal residual disease (MRD), which is predictive for various survival parameters such as long progression-free survival.[14]

Although VEN shows efficacy in monotherapy in CLL patients, its activity is enhanced when it is associated with drugs that have different mechanisms of action. The combination of VEN with anti-CD20 antibodies, especially rituximab and obinutuzumab, is currently widely used in the treatment of both treatment-naïve and relapsed/refractory CLL patients. The combination of VEN with ibrutinib allows for high rates of hematological responses and MRD eradication to be achieved.[10–12,15]

Little is known about the usefulness of the combination of VEN with standard CLL chemotherapy containing purine nucleoside analogues (PNAs), which still holds an important place in the management of CLL, especially in first-line treatment of physically fit patients. Although fludarabine is the most commonly used purine analogue for the treatment of CLL patients, some studies have found 2-chlorodeoxyadenosine (cladribine – 2-CdA) to have similar efficacy.[16,17] It is believed to act primarily by triggering the intrinsic mitochondrial *TP53*-dependent apoptotic pathway through inducing BAX protein expression, and the *TP53*-independent pathway by directly binding to proteins located in mitochondrial membrane, leading to caspase cascade activation.[18,19] Although it is possible that the extrinsic apoptotic pathway may also play a role in 2-CdA activity, this idea

remains controversial.[20,21] It is not known whether the agent may demonstrate synergic action in association with VEN towards CLL lymphocytes; however, VEN has demonstrated greater efficacy when combined with bendamustine, a drug which has also purine analogue properties.

Objectives

The aim of the present study was to evaluate the influence of VEN and 2-CdA, used either alone or in combination, on the apoptosis as well as the expression of several intracellular factors involved in apoptosis of CLL lymphocytes after short-term culture in vitro, and to determine whether such combinations are promising for the treatment of CLL patients.

Materials and methods

Patients

Peripheral blood mononuclear cells (PBMNCs) were collected from 103 CLL patients (47 females and 56 males, mean age 68 years (range: 43–88 years)) at the time of diagnosis and before any anticancer therapy, during routine diagnostic procedures in the Department of Hematology, Medical University of Lodz, Poland, and Regional Multispecialist Center of Oncology and Traumatology in Lodz, Poland, in 2019 and 2020. The diagnoses were based on the International Workshop on Chronic Lymphocytic Leukemia (iwCLL) 2018 criteria.[22] The material obtained from 39 patients was used to evaluate the expression of selected proteins involved in the process of apoptosis (Table 1). All patients signed a written informed consent to participate in this study. The study has been approved by the Ethics Committee of the Medical University of Lodz (approval No. RNN/44/17/WE).

Table 1. General characteristics of patients

Characteristics of patients	
Total number of patients	103 (47 F, 56 M)
Age	68 years (range: 43–88 years)
Total number of patients to evaluate the expression of selected proteins	40 (15 F, 25 M)
Clinical state	
RAI 0–2	26
RAI 3–4	14
Cytogenetic aberrations	
del13q	11
del17p	2
del11q	3
tri12+	2
Normal karyotype	7
No information available	17

Drugs

Venetoclax was supplied by Abbvie (Mettawa, USA). In order to determine its cytotoxicity, VEN was used at 11 different concentrations (from 0.5 nM to 320 nM). The concentration of 40 nM was chosen for further studies. Cladribine (2-CdA; Biodribin) was purchased from Institute of Biotechnology and Antibiotics (Warsaw, Poland). In order to determine its cytotoxicity, 2-CdA was used at 21 different concentrations (from 0.1 μM to 120 μM). A concentration of 16 μM was chosen for further studies.

Isolation of peripheral blood mononuclear cells and cell cultures conditions

The PBMNCs were isolated as previously described.[23,24] Briefly, peripheral blood was layered on Histopaque-1077 cell separation medium (Sigma-Aldrich, St. Louis, USA) and centrifuged in a density gradient in 3600 rpm for 20 min. The mean B-cell (CD19$^+$) purity was found to be >95%, as measured with flow cytometry. The PBMNCs were resuspended at a concentration of 1.0×10^6 cells/mL in RPMI-1640 supplemented with 20% (v/v) heat-inactivated fetal calf serum (Gibco, Life Technologies, Waltham, USA) and antibiotics (50 mg/mL of streptomycin and 50 IU/mL of penicillin; Life Technologies, Inchinnan, UK). All cultures were incubated with the abovementioned drugs for 24 h or 48 h at 37°C, in an atmosphere of 5% CO_2 and full humidity. Cultures without drugs were used as controls.

Assessment of cytotoxicity, mitochondrial transmembrane potential changes (ΔΨm) and overall apoptosis of CLL cells

The cytotoxicity and overall level of apoptosis associated with the studied drugs were assessed at baseline and then after 24 h and 48 h of culture using flow cytometry (BD FACS Canto II; Becton Dickinson Pharmingen, San Diego, USA); cytotoxicity was tested with fluorescein isothiocyanate (FITC; Becton Dickinson Pharmingen) and conjugated propidium iodide (PI; Sigma-Aldrich), while ongoing apoptosis was examined with annexin-V (AnnV; Becton Dickinson Pharmingen), as described previously.[23,24] The term 'overall apoptosis' refers to cells which bind AnnV, since phosphatydyloserine externalization occurs in both the intrinsic and extrinsic apoptosis pathways, and is generally used to determine the percentage of apoptotic cells.

Apoptosis was also assessed after 48 h of culture by changes in mitochondrial transmembrane potential (ΔΨm) for the initial step of intrinsic apoptosis. The ΔΨm were evaluated using MitoTracker Red CMX Ros kit (Invitrogen, Waltham, USA), as previously described.[23,24] Briefly, PBMNCs were centrifuged and the cell pellet was gently resuspended in the staining solution containing the MitoTracker probe, prepared according to the manufacturer's protocol, and incubated for 30 min at 37°C. The cells were re-pelleted by centrifugation and resuspended in fresh warmed-up medium. The assays were performed in duplicate and analyzed with flow cytometry (BD FACS Canto II) at 490"20 nm using FL1 standard fluorescent filter, and at 530"20 nm using FL3 standard fluorescent filter.

Assessment of the active forms of caspase-3, caspase-9 and caspase-8

The expression of the active forms of caspase-3, caspase-8 and caspase-9 was evaluated in the PBMNCs before culture and after 48 h of incubation with the tested drugs, used alone or in combination. The analysis of the expression of active forms of caspase-3, caspase-8 and caspase-9 was performed on a flow cytometer. The percentage of cells expressing the active form of caspase-3 was assessed using PE Active Caspase-3 Apoptosis Kit (Becton Dickinson Pharmingen), according to the manufacturer's protocol. Similar analyses of the active forms of caspase-8 and caspase-9 were also performed according to the manufacturer's protocol using FAM-FLICA in vitro Caspase 8 Kit or FAM-FLICA in vitro Caspase 9 Kit (ImmunoChemistry Technologies, Bloomington, USA), respectively. All assays were performed in duplicate.

Detection of apoptosis-regulatory proteins

The following proteins expression was evaluated in fixed, permeabilized cells after 48 h of incubation using direct staining of specific labeled antibodies:

1. P53 (FITC Mouse Anti-Human P53 Set; Becton Dickinson Pharmingen);
2. BCL-2 (FITC Mouse Anti-Human BCL-2; Becton Dickinson Pharmingen);
3. BIM (Rabbit mAb to BIM [Y36] Alexa Fluor 488; Abcam, Cambridge, UK);
4. BAX (Rabbit Anti-BAX antibody [T22-A]; Abcam);
5. PUMA (Rabbit Anti-PUMA Antibody; Abcam);
6. NOXA (Mouse Anti-NOXA [114C307]; Abcam);
7. FADD (Rabbit Anti-FADD Antibody; Abcam).

All investigated proteins apart from P53 (FITC-conjugated) were used with an appropriate secondary antibody (Goat polyclonal Antibody to Rabbit IgG (Abcam); FITC appropriate isotype controls). The fluorescence was measured using BD FACS Canto II flow cytometer at 490"20 nm using FL1 standard fluorescent filter, and at 530"20 nm using FL3 standard fluorescent filter.

Statistical analyses

The normality of data distribution was checked and the distribution of the variables was not normal. All the measurements (control cultures, cultures with 40 nM VEN, 16 μM 2-CdA and their combination) were performed on the blood sample drawn from the same patient. The data regarding cytotoxicity, apoptosis, caspase

expression, mitochondrial transmembrane potential changes, and differences in protein expression profiles were analyzed using the Wilcoxon signed-rank test with Bonferroni's correction for multiple comparisons, where $p < 0.008$ was considered statistically significant. STATISTICA v. 13.1 (StatSoft Inc., Tulsa, USA) software was used for analyses (the p-value was calculated according to the following formula: $p < α/k$; $α = 0.05$ – significance level; $k = 6$ – number of comparisons).

GraphPad Prism v. 5.0 (GraphPad Software, San Diego, USA) and CompuSyn v. 1.0 (https://www.combosyn.com/) software was respectively used to present the cytotoxic effect of drugs as isobolograms, and to calculate IC_{50} (values defined as the concentration of drug that achieved 50% cytotoxicity).

CompuSyn v. 1.0 was also used to calculate combination index (CI), where CI < 0.1 indicates very strong synergy, CI = 0.1–0.3 strong synergy, CI = 0.3–0.7 synergy, CI = 0.7–0.85 moderate synergy, CI = 0.85–0.9 slight synergy, CI = 0.9–1.1 nearly additive effect, and CI > 1.1 antagonistic effect.[25]

Drug-induced cytotoxicity (DICy) was expressed by the difference between the mean percentage of dead cells obtained after incubation with drug(s) studied and the mean percentage of cells in the control culture, calculated for each sample. Drug-induced apoptosis (DIA) was assessed as the difference between the percentage of cells which underwent apoptosis (AnnV+ cells) after incubation with studied drug(s) and the percentage of cells undergoing spontaneous apoptosis in the control cultures, calculated for each sample. Drug-induced $Δψm$ (DI$Δψ$m) was expressed as the difference between the mean percentage of cells with $Δψm$ after incubation with the drug(s) studied and the percentage of cells with $Δψm$ in the control culture, calculated for each sample. Drug-induced caspase expression (DICE) was assessed by the difference between the mean value of the percentage of cells expressing the active forms of caspases after incubation with drug(s) studied and the percentage of cells with expression of the active form of caspases in the control culture, calculated for each sample. Drug-induced protein expression (DIPE) of protein-expressing CLL cells was expressed by the mean value of the differences between the percentage of cells expressing protein after 48 h incubation with drug(s) and the percentage of cells expressing protein in the control culture, calculated for each sample.

Results

Cytotoxic effect of VEN and 2-CdA used alone or in combination on CLL cells in culture in vitro, and the type of interaction

Eleven concentrations of VEN (from 0.5 nM to 320 nM) and 21 concentrations of 2-CdA (from 0.1 μM to 120 μM)

were used to determine the cytotoxicity. At all concentrations, VEN and 2-CdA, used alone, demonstrated significantly stronger cytotoxic effects after 48 h compared to the 24-h period (Fig. 1A,B). After 48 h of incubation, VEN demonstrated higher cytotoxic effects than 2-CdA (Fig. 1C), with the highest cytotoxic effect (48.8%) observed at the concentration of 40 nM (Table 2). In contrast, the highest cytotoxic effect of 2-CdA was 44%, achieved at a concentration of 16 μM (Table 2).

Venetoclax demonstrated significantly higher DICy than 2-CdA (31.7% and 26.9%, respectively, $p < 0.001$) (Table 3). The IC_{50} observed for VEN was 143 nM. The cytotoxicity of 2-CdA was below 50% at all concentrations used, and IC_{50} estimated by extrapolation was 2290 μM (Fig. 1C).

The highest cytotoxic effect for VEN (40 nM) used in combination with 2-CdA (16 μM) was 61.2% and DICy was 44.1%. These values were significantly higher than these found for each drug used separately (Table 3). The combination demonstrated strong synergistic effects at the above concentrations (CI = 0.035; Table 2). In further
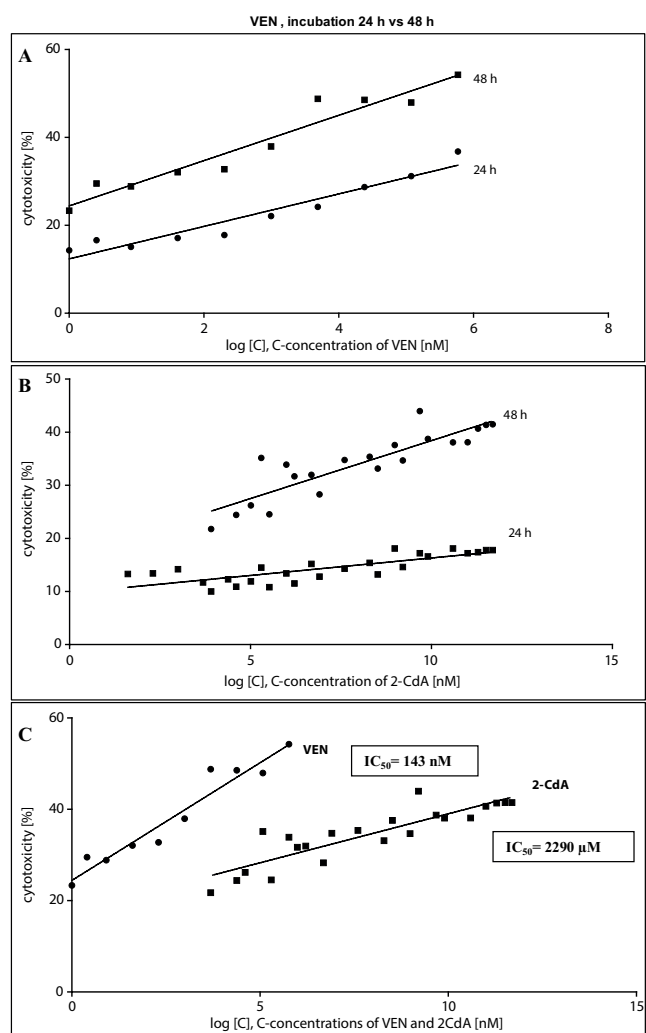

Fig. 1. Isobolograms presenting the relationship between drug concentration and its cytotoxic effect on chronic lymphocytic leukemia (CLL) cells after 24 h and 48 h of incubation. A. Venetoclax (VEN); B. Cladribine (2-CdA); C. VEN and 2-CdA, after 48-h incubation only

Table 2. Cytotoxicity of VEN and 2-CdA used alone, or in combination, and the combination index for both drugs used in 3 selected concentrations after 48 h of incubation

Drug	VEN	VEN 40 nM	VEN 80 nM	VEN 160 nM
2-CdA	cytotoxicity cytotoxicity	48.8% n = 78	48.5% n = 36	47.9% n = 41
2-CdA 4 µM	35.4% n = 47	44.8% n = 33	48.0% n = 16	52.7% n = 11
		CI = 0.75088	CI = 0.81526	CI = 0.69612
2-CdA 8 µM	37.6% n = 44	47.0% n = 33	51.1% n = 11	53.2% n = 11
		CI = 0.50452	CI = 0.46875	CI = 0.62496
2-CdA 16 µM	**44.0%** n = 58	**61.2%** n = 52	50.2% n = 11	52.9% n = 23
		CI = 0.03539	CI = 0.55668	CI = 0.66280

VEN – venetoclax; 2-CdA – cladribine; n – number of samples; CI – combination index: CI < 0.1 very strong synergy, CI 0.1–0.3 strong synergy, CI 0.3–0.7 synergy, CI 0.7–0.85 moderate synergy, CI 0.85–0.9 slight synergy, CI 0.9–1.1 nearly additive, CI > 1.1 antagonistic. Values in bold are the most important.

Table 3. The influence of VEN and 2-CdA used alone or in combination on cytotoxicity or apoptosis of CLL cells in vitro after 48 h of incubation

Drug	Control		VEN 40 nM		2-CdA 16 M		VEN 40 nM + 2-CdA 16 µM		Statistical analysis	
	PI(+)	AnnV(+)	PI(+)	AnnV(+)	PI(+)	AnnV(+)	PI(+)	AnnV(+)	PI(+)	AnnV(+)
	1	2	3	4	5	6	7	8		
n	93	36	78	36	58	33	52	33	**1 vs 3 < 0.001** **1 vs 5 < 0.001** **1 vs 7 < 0.001** 3 vs 5 = 0.033 **3 vs 7 < 0.001** **5 vs 7 < 0.001**	**2 vs 4 < 0.001** **2 vs 6 < 0.001** **2 vs 8 < 0.001** 4 vs 6 = 0.071 **4 < 8 = 0.001** **4 vs 8 < 0.001**
Median	15.3	4.0	49.0	7.1	42.4	8.7	62.0	11.7		
IQR	9.1–22.0	4.9–12.7	36.3–60.1	5.9–14.8	30.9–54.1	6.9–18.8	47.1–75.1	1.3–7.1		
DICy [%]	N/A	N/A	**31.7**	N/A	**26.9**	N/A	**44.1**	N/A	**3 vs 5 < 0.001** **3 vs 7 < 0.001** **5 vs 7 < 0.001**	N/A
DIA [%]	N/A	N/A	N/A	**4.8**	N/A	**5.3**	N/A	**8.9**	N/A	**4 vs 6 < 0.001** **4 vs 8 < 0.001** **6 vs 8 < 0.001**

n – number of samples; PI – propidium iodide; AnnV – annexin-V; IQR – interquartile range (Q1–Q3); VEN – venetoclax; 2-CdA – cladribine; DICy – drug-induced cytotoxicity; DIA – drug-induced apoptosis; N/A – not applicable. Wilcoxon signed-rank test with Bonferroni's correction for multiple comparisons; p < 0.008. Values in bold are statistically significant.

experiments, we used VEN at a concentration of 40 nM and 2-CdA at a concentration of 16 µM.

The influence of VEN and 2-CdA, used alone or in combination, on ΔΨm, overall apoptosis, and the expression of active forms of caspase-3, caspase-8 and caspase-9 in CLL cells in vitro

Mean Δψm was 29.3% for VEN, 34.0% for 2-CdA and 42.9% for VEN+2-CdA. Significantly higher DIΔψm was observed for drugs used in combination than separately (p < 0.0001) (Fig. 2A).

Venetoclax (40 nM) induced apoptosis with DIA = 4.8% and 2-CdA with DIA = 5.3% (Table 3). This difference was not statistically significant. Apoptosis induced by VEN+2-CdA was 11.7%; this was significantly higher

than the apoptosis induced by either drug used separately (p < 0.001) (Table 2).

No significant differences were found between the effects of VEN and 2-CdA used alone and the percentage of cells expressing caspase-3, caspase-9 and caspase-8. In contrast, VEN+2-CdA elicited significantly higher percentages of cells expressing caspase-3 and caspase-9 (p < 0.001) (Fig. 2B); however, for caspase-8, a significant difference was observed only between VEN+2-CdA and 2-CdA alone (p < 0.001).

The influence of VEN and 2-CdA used alone and in combination on selected protein expression in CLL cells in vitro

For all studied proteins, except BCL-2, the percentage of positive cells increased under the influence of VEN compared to controls (Fig. 3A–G). Additionally, VEN application resulted in a significantly greater increase
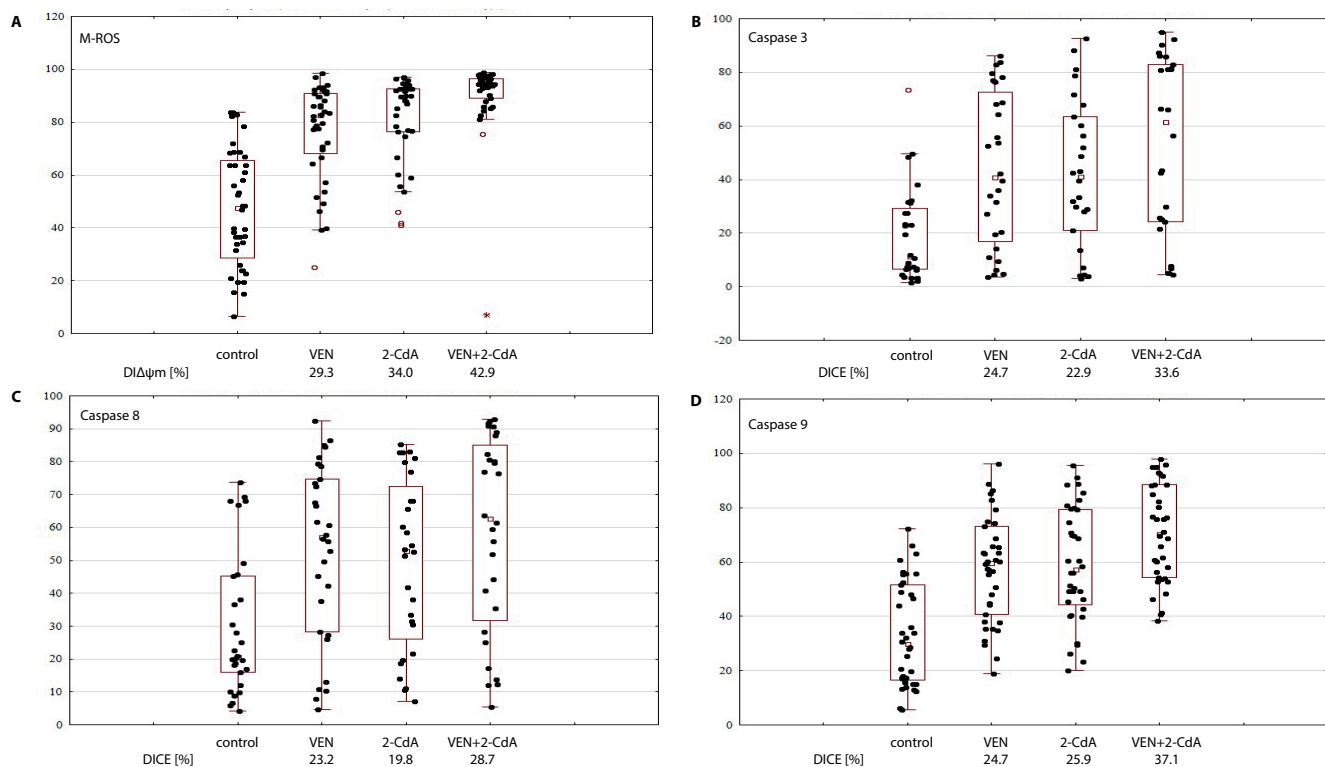
1028

A.B. Korycka-Wołowiec et al. Venetoclax and 2-CdA in CLL cells culture

Fig. 2. The influence of 40 nM venetoclax (VEN) and 16 µM cladribine (2-CdA) used alone or in combination on the chronic lymphocytic leukemia (CLL) cells after 48 h of incubation in vitro. A. Percentage of cells expressing mitochondrial potential changes (Δψm); B. Percentage of cells expressing caspase-3 activity; C. Percentage of cells expressing caspase-8 activity; D. Percentage of cells expressing caspase-9 activity

VEN – venetoclax; 2-CdA – cladribine; DICE – drug-induced caspase expression; DIΔψm – drug-induced mitochondrial potential changes.

in the percentage of cells expressing BIM, BAX and NOXA proteins than 2-CdA (Table 4). However, VEN and VEN+2-CdA significantly decreased BCL-2 expression (Table 4): the median percentage of cells expressing BCL-2 was 77.3% for culture with VEN, 74.3% for 2-CdA and 74.4% for VEN+2-CdA (Fig. 3A). The DIPE values for BCL-2 were −10.7%, −11.2% and −13.9% for VEN, 2-CdA and VEN+2-CdA, respectively, and were significantly different only between 2-CdA and VEN+2-CdA (Fig. 3A).

The expression of P53 and PUMA increased under the influence of VEN, 2-CdA and VEN+2-CdA; however, no significant differences were observed between VEN and 2-CdA used alone (Table 4), and only a borderline difference was found between 2-CdA and VEN+2-CdA. The FAS-associated death-domain protein (FADD) expression increased after VEN, 2-CdA and VEN+2-CdA compared to controls, but the increase observed after VEN was not significant. The VEN+2-CdA treatment resulted in a significantly higher expression of FADD than of VEN alone (Table 4, Fig. 3G).

Discussion

Venetoclax is a new promising small molecule targeted against the antiapoptotic BCL-2 protein, the over-expression of which is one of the molecular hallmarks of CLL. Venetoclax, as a BH3-only mimetic, binds directly to BCL-2 and displaces the BH3 activator BIM from BCL-2, leading to BAX/BAK homooligomerization. The BAX/BAK complex permeabilizes the mitochondrial outer membrane (MOM), promotes the release of cytochrome c from the mitochondria to the cytosol, and induces caspase-mediated apoptosis.[26]

An important clinical advantage of VEN is its independence from functional P53. Although the treatment gives a high percentage of responses when used in monotherapy, it is not curative because of the complexity of the pathogenesis of CLL.[15,27] It is hence reasonable to assume that its efficacy will be enhanced by combination with other drugs which demonstrated the activity in CLL via different mechanisms of action.

The efficacy and safety of VEN have been already extensively studied in combination with anti-CD20 antibodies and BCR inhibitors.[11,15,28,29] Venetoclax has also demonstrated clinical efficacy in combination with bendamustine, a drug combining both alkylating and purine analogue properties.[30–32] The present study examines the influence of VEN and 2-CdA, used alone or in combination, on the viability, apoptosis and expression of selected apoptosis-related factors in vitro, i.e., in lymphocytes obtained from the peripheral blood of CLL patients.

The 2-CdA is a purine analogue, which may be used as an alternative for CLL treatment to fludarabine.

Table 4. The influence of VEN and 2-CdA used alone or in combination on selected proteins expression in CLL cells after 48 h of incubation

Protein		Control	VEN 40 nM	2-CdA 16 μM	VEN 40 nM +2-CdA 16 μM	Statistical analysis (p-value)
		1	2	3	4	
BCL-2	n	36	36	36	36	**1 vs 2 < 0.001** 2 vs 3 = 0.1573 **1 vs 3 < 0.001 2 vs 4 < 0.0001** **1 vs 4 < 0.001** 3 vs 4 = 0.1270
	median	87.0	77.3	74.3	74.4	
	IQR	80.5–90.1	69.0–82.8	65.3–81.8	59.9–80.1	
	DIPE	N/A	10.7↓	11.2↓	13.9↓	
P53	n	36	36	35	35	**1 vs 2 < 0.001** 2 vs 3 = 0.1819 **1 vs 3 = 0.001** 2 vs 4 = 0.3547 **1 vs 4 < 0.001** 3 vs 4 = 0.0116
	median	3.0	3.85	4.4	5.6	
	IQR	1.6–4.6	2.6–10.8	2.6–5.8	3.2–9.8	
	DIPE	N/A	1.8↑	2.6↑	3.4↑	
BIM	n	36	36	36	36	**1 vs 2 < 0.001 2 vs 3 < 0.001** **1 vs 3 < 0.001 2 vs 4 < 0.001** **1 vs 4 < 0.001 3 vs 4 < 0.001**
	median	1.7	20.45	11.0	23.25	
	IQR	1.1–2.4	18.2–23.4	10.3–13.8	21.2–25.5	
	DIPE	N/A	18.5↑	10.2↑	21.3↑	
BAX	n	35	35	35	35	**1 vs 2 < 0.001 2 vs 3 < 0.001** **1 vs 3 < 0.001 2 vs 4 < 0.001** **1 vs 4 < 0.001 3 vs 4 < 0.001**
	median	15.0	22.5	29.9	24.7	
	IQR	10.1–17.3	17.9–26.6	15.5–23.8	21.1–28.1	
	DIPE	N/A	8.3↑	5.6↑	10.3↑	
PUMA	n	34	34	34	34	**1 vs 2 < 0.001** 2 vs 3 = 0.6505 **1 vs 3 < 0.001** 2 vs 4 = 0.9182 **1 vs 4 < 0.001** 3 vs 4 = 0.6505
	median	19.8	28.3	27.95	26.95	
	IQR	17.3–23.2	22.5–32.8	19.8–32.4	23.4–30.4	
	DIPE	N/A	6.5↑	6.3↑	6.5↑	
NOXA	n	36	36	36	36	**1 vs 2 < 0.001 2 vs 3 < 0.001** **1 vs 3 < 0.001 2 vs 4 < 0.001** **1 vs 4 < 0.001 3 vs 4 < 0.001**
	median	11.25	21.5	18.5	23.85	
	IQR	9.1–14.2	17.5–26.6	14.3–21.5	19.4–28.3	
	DIPE	N/A	10.3↑	6.5↑	18.1↑	
FADD	n	33	33	34	34	1 vs 2 = 0.047 2 vs 3 = 0.148 **1 vs 3 = 0.007 2 vs 4 = 0.003** **1 vs 4 < 0.001** 3 vs 4 = 0.015
	median	2.2	2.5	3.4	4.5	
	IQR	1.6–3.0	2.0–3.8	1.9–4.9	2.0–8.7	
	DIPE	N/A	0.9↑	1.2↑	2.9↑	

VEN – venetoclax; 2-CdA – cladribine; CLL – chronic lymphocytic leukemia; n – number of samples; DIPE – drug-induced protein expression; ↑ – increase of expression; ↓ – decrease of expression; IQR – interquartile range (Q1–Q3). Wilcoxon signed-rank test with Bonferroni's correction for multiple comparisons; p < 0.008. Values in bold are statistically significant.

The 2-CdA remains a backbone of chemotherapy regimens for physically fit patients. Its mechanism of action is based on the ability to incorporate into a newly synthesized DNA chain and inhibit DNA repair.[18,33,34] In the intrinsic *TP53*-dependent apoptotic pathway, P53 induces BAX protein expression, leading to the release of cytochrome c from mitochondria to the cytoplasm, apoptosome formation and caspase cascade activation. Moreover, 2-CdA can also act independently of *TP53* by directly binding to proteins located in the mitochondrial membrane, resulting in cytochrome c release and apoptosome formation, or formation of apoptosis-inducing factor (AIF); this in turn can directly lead to chromatin condensation and DNA fragmentation, but without caspase cascade activation.[18,33,34] Despite this, the role of the extrinsic pathway in 2-CdA-induced apoptosis remains controversial.[20,21] The mechanism of action of 2-CdA is therefore different than the mechanism of VEN; however, the common feature is that both drugs trigger the intrinsic pathway of apoptosis.

The present study tested the influence of VEN and 2-CDA on the viability of CLL lymphocytes (drug cytotoxicity), as determined by the percentage of cells incorporating PI and overall apoptosis, measured by AnnV binding capacity. Both phenomena were more visible in cells incubated with the drugs than in control cultures, and higher results were obtained in cells subjected to VEN+2-CdA compared to cells incubated with 1 drug only.

Additionally, both drugs used at the tested concentrations showed a synergistic effect with very low CI value (CI = 0.035), which proves a strong synergy. Similar conclusions can be drawn from the analysis of ΔΨm made at the very early stage of intrinsic pathway of apoptosis.
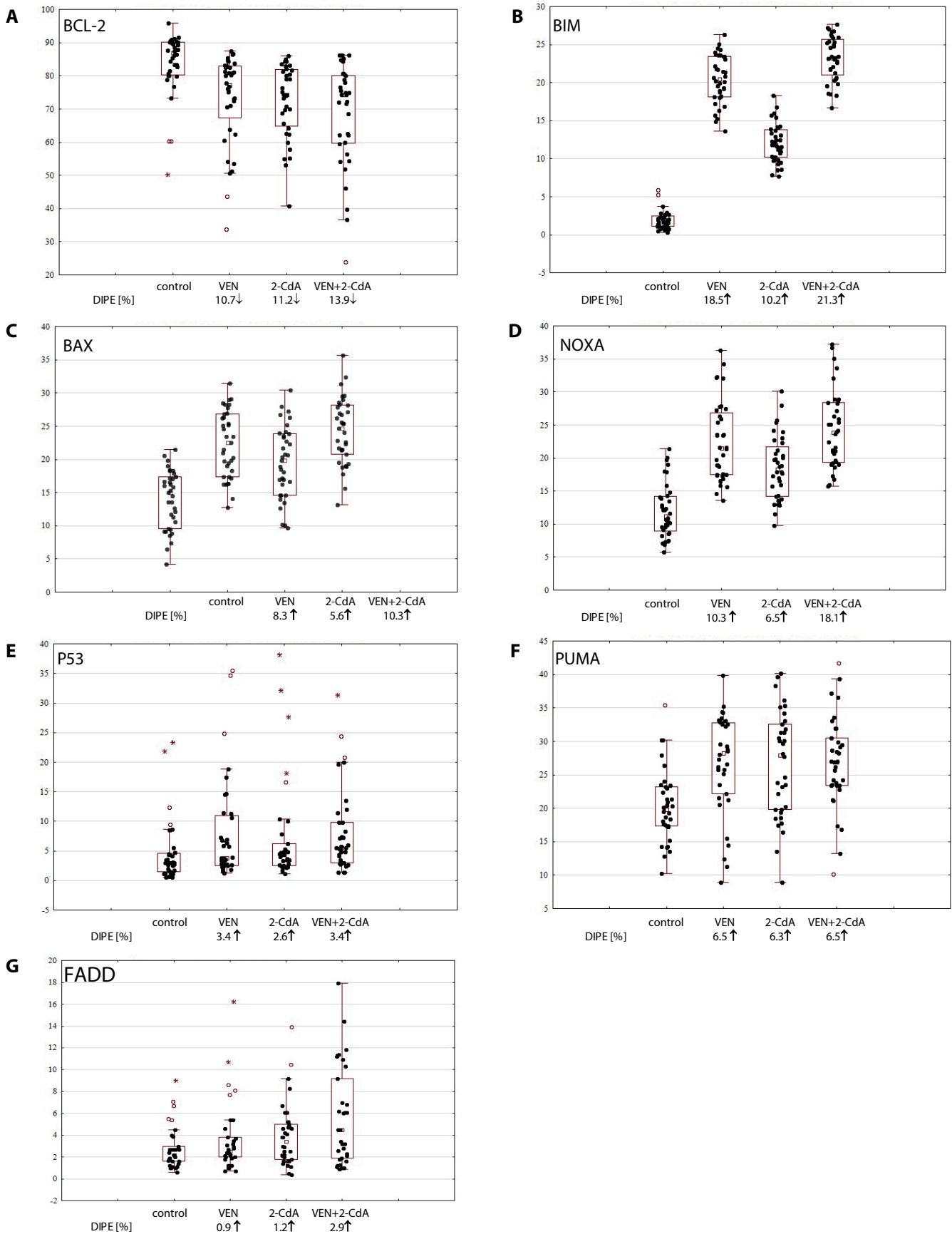
Fig. 3. The influence of 40 nM venetoclax (VEN) and 16 µM cladribine (2-CdA) used alone or in combination on the percentage of chronic lymphocytic leukemia (CLL) cells expressing proteins after 48 h of incubation in vitro. A. BCL-2; B. BIM; C. BAX; D. NOXA; E. P53; F. PUMA; G. FADD

↑ – increase of expression; ↓ – decrease of expression; DIPE – drug-induced protein expression.

Significantly higher ΔΨm values were observed after the action of VEN and 2-CdA used separately when compared to controls, and even higher values were noted after VEN+2-CdA. Accordingly, the cultures exposed to the drugs demonstrated higher percentages of cells expressing caspase-3, caspase-9 and caspase-8 than controls. Interestingly, the percentage of cells expressing caspase-8 was not significantly different for VEN and 2-CdA used alone; however, the use of VEN+2-CdA resulted in a significant increase of the percentage of these cells compared to 2-CdA.

The 2nd part of our study examined the influence of both drugs alone and in combination on the expression of some relevant proteins involved in apoptosis. It was found that the percentage of cells with detectable P53 increased under all 3 treatments. This is somewhat surprising, since it is believed that the mechanism of action of VEN is independent of *TP53*. It is possible that VEN may influence P53 protein expression by an unknown mechanism, e.g., by increasing its stability.

Another finding which needs further explanation is the observed decrease of the percentage of BCL-2-positive cells following VEN addition as compared to the control culture, as well as their even more profound decrease under the influence of 2-CdA and the greatest decrease after VEN+2-CdA. As mentioned above, VEN is believed to form a complex with BCL-2, without apparently affecting the expression of the latter. However, it is possible that BCL-2 expression may be inhibited by the aforementioned increase of P53 expression found in cells subjected to both drugs separately and in combination. Indeed, P53 has been found to have an inhibitory effect on the expression of *BCL-2* gene in both human and murine malignant cells.[35,36] On the other hand, it is also possible that the decrease of the percentage of BCL-2-expressing cells may result from the presence of normal lymphocytes among the mononuclear cells (MNCs) used for culture. The mean purity of CD19+ B cells was found to be approx. 95%, as measured using flow cytometry.

The study then assessed the expression of 4 proapoptotic proteins involved in the intrinsic pathway: BIM, BAX, PUMA, and NOXA. Their expression increased under the influence of VEN and/or 2-CdA above the values found in control cells. The highest increase in cells expressing BIM, BAX and NOXA was found in the cells incubated with VEN+2-CdA, a lower rise was observed after VEN only and the lowest after 2-CdA only. All these proteins appear important for the intracellular activity of anticancer drugs, including VEN.

As mentioned above, VEN binds to the BH3-binding groove of BCL-2 and displaces BIM from its binding site, thus allowing activation of the apoptotic effectors BAX and BAK.[37] The BAX activation leads to its oligomerization and then permeabilization of the MOM, manifested in an increase of the mitochondrial transmembrane potential, release of cytochrome c from mitochondria, apoptosome formation, and caspase cascade activation.[26,27]

As previously shown in M1 murine leukemia cells, BAX is a target of transcriptional activity of P53.[36] This may account, at least partially, for the increase of BAX protein observed together with the increase of P53.

The NOXA protein is less effective than PUMA in induction of *TP53*-mediated apoptosis. The PUMA can bind to all antiapoptotic BCL-2 family members, whereas NOXA antagonizes MCL-1 and A1 proteins only. However, in some cases of apoptosis caused by DNA damage, PUMA and NOXA can cooperate. It is likely that if the functionality of one of the proteins weakens, it can be enhanced by the action of the other.[38] Additionally, autoactivation of BAX and BAK can occur independently of activator BH3s through downregulation of BCL-2, BCL-XL and MCL-1.[15,39] It is also important to note that various P53 family members such as P63 and P73, also have the potential to induce apoptotic outcomes through the induction of the pro-apoptotic BCL-2 family members, such as PUMA and NOXA.[40] Unlike BIM, BAX and NOXA, the percentage of cells expressing PUMA in our experiments increased to a similar degree after VEN, 2-CdA and VEN+2-CdA addition. Therefore, this factor probably does not play an essential role in the interaction of those drugs in inducing CLL cell apoptosis.

Finally, the study examined whether the drugs induced the extrinsic apoptotic pathway. To our knowledge, no experimental data support such activity of VEN, and the involvement of 2-CdA in the extrinsic apoptotic way is controversial. One element of this pathway is FADD. Together with the adaptor FAS and the initiator procaspase-8 (or procaspase-10), FADD forms the death-inducing signaling complex (DISC), which in turn cleaves and activates the executioner caspase-3 and caspase-7, eventually bringing about apoptosis.[27] Nomura et al. suggested that 2-CdA may stimulate both the intrinsic and extrinsic apoptotic pathways.[20] Our findings indicate that the percentage of cells expressing FADD was significantly higher after 2-CdA and 2-CdA+VEN administration as compared to control cells, which would be in line with the possibility that 2-CdA is involved in the extrinsic pathway. The fact that VEN alone had no significant effect on FADD expression is consistent with the current concept of the mechanism of action of VEN. However, the observed higher expression of FADD after VEN+2-CdA administration compared to VEN or 2-CdA administration alone might suggest that VEN, despite being incapable of triggering the extrinsic pathway, may enhance this potential in 2-CdA. This hypothesis remains to be proven by further studies.

Limitations of the study

The only limitation of our study is the quantitative method of assessment of proteins studied, i.e., as a percentage of cells in which protein expression was detectable. It would be interesting to measure the protein expression

semi-qualitatively as the mean fluorescence intensity. However, we felt that intensity of fluorescence in cells after the culture would not have been correlated strongly enough with the actual intracellular concentration of proteins. In particular, we feared that the cell membrane would have been altered by the culture, so that its sensibility to permeabilization during the staining would have been somewhat different as compared to fresh lymphocytes. As a results, the penetration of antibodies into the cytoplasm would have been not strictly comparable to cells before and after culture. Therefore, we preferred to restrict our measures to qualitative assessment of the presence of the protein studied.

It might be objected that the status of *TP53* gene in patients enrolled into the study was not indicated. As a matter of fact, the del17p/mut*TP53* might have influenced the in vitro response of CLL lymphocytes to cladribine. However, the cytogenetic analysis is not included in the initial diagnostic workup of CLL patients unless the initiation of the treatment is planned immediately. Nevertheless, the incidence of del17p/mut*TP53* in treatment-naïve patients is above 10%, so it would probably have been less than 10 patients in our series. Such small group of cases with *TP53* aberrations would not have allowed for any reliable statistical analysis. The possible presence of such patients in our population would not distort the results we have obtained.

Conclusions

To conclude, it is important to note that the regulation of apoptosis of CLL cells in vitro is different than in vivo. The CLL lymphocytes cultured without the support provided by circulating cytokines and factors provided by microenvironmental cells die much quicker than circulating ones. However, the abovementioned findings provide a rationale to extend the investigations on the mechanism of action of VEN in order to clarify the role of P53 and related antiproliferative agents in the mechanism of its action. It must also be noted that although VEN is efficacious in patients with mutated *TP53* and/or deletion of 17p, it cannot fully abolish the negative prognostic significance of those cytogenetic/molecular abnormalities. Moreover, our results confirm the involvement of both VEN and 2-CdA in the intrinsic apoptotic pathway, and demonstrate the synergistic effect of both drugs on CLL cells in vitro. Our findings justify further molecular studies aimed at assessing the feasibility of VEN+2-CdA application in clinical practice.

ORCID iDs

Aleksandra Beata Kubiak ⬤ https://orcid.org/0000-0001-5650-1312
Ewelina Izabela Ziółkowska ⬤ https://orcid.org/0000-0002-4427-9811
Anna Barbara Korycka-Wołowiec
   ⬤ https://orcid.org/0000-0001-9256-0328
Tadeusz Robak ⬤ https://orcid.org/0000-0002-3411-6357
Dariusz Wołowiec ⬤ https://orcid.org/0000-0003-4081-5397

References

1. Plati J, Bucur O, Khosravi-Far R. Apoptotic cell signaling in cancer progression and therapy. *Integr Biol (Camb)*. 2011;3(4):279–296. doi:10.1039/c0ib00144a
2. Roberts A, Huang D. Targeting BCL2 with BH3 mimetics: Basic science and clinical application of venetoclax in chronic lymphocytic leukemia and related B cell malignancies. *Clin Pharmacol Ther*. 2017;101(1):89–98. doi:10.1002/cpt.553
3. Stilgenbauer S, Eichhorst B, Schetelig J, et al. Venetoclax in relapsed or refractory chronic lymphocytic leukaemia with 17p deletion: A multicentre, open-label, phase 2 study. *Lancet Oncol*. 2016;17(6):768–778. doi:10.1016/S1470-2045(16)30019-5
4. Vogler M, Dinsdale D, Dyer MJS, Cohen GM. ABT-199 selectively inhibits BCL2 but not BCL2L1 and efficiently induces apoptosis of chronic lymphocytic leukaemic cells but not platelets. *Br J Haematol*. 2013;163(1):139–142. doi:10.1111/bjh.12457
5. Roberts AW, Davids MS, Pagel JM, et al. Targeting BCL2 with venetoclax in relapsed chronic lymphocytic leukemia. *N Engl J Med*. 2016;374(4):311–322. doi:10.1056/NEJMoa1513257
6. Adams JM, Cory S. The BCL-2 arbiters of apoptosis and their growing role as cancer targets. *Cell Death Differ*. 2018;25(1):27–36. doi:10.1038/cdd.2017.161
7. Dai H, Meng XW, Kaufmann SH. Mitochondrial apoptosis and BH3 mimetics. *F1000Res*. 2016;5:2804. doi:10.12688/f1000research.9629.1
8. Letai A, Bassik MC, Walensky LD, Sorcinelli MD, Weiler S, Korsmeyer SJ. Distinct BH3 domains either sensitize or activate mitochondrial apoptosis, serving as prototype cancer therapeutics. *Cancer Cell*. 2002;2(3):183–192. doi:10.1016/S1535-6108(02)00127-7
9. Gentile M, Petrungaro A, Uccello G, et al. Venetoclax for the treatment of chronic lymphocytic leukemia. *Expert Opin Investig Drugs*. 2017;26(11):1307–1316. doi:10.1080/13543784.2017.1386173
10. Lew TE, Anderson MA, Lin VS, et al. Undetectable peripheral blood MRD should be the goal of venetoclax in CLL, but attainment plateaus after 24 months. *Blood Adv*. 2020;4(1):165–173. doi:10.1182/bloodadvances.2019000864
11. Schieber M, Ma S. The expanding role of venetoclax in chronic lymphocytic leukemia and small lymphocytic lymphoma. *Blood Lymphat Cancer*. 2019;9:9–17. doi:10.2147/BLCTT.S177009
12. Juárez-Salcedo LM, Desai V, Dalia S. Venetoclax: Evidence to date and clinical potential. *Drugs Context*. 2019;8:1–13. doi:10.7573/dic.212574
13. Herling CD, Abedpour N, Weiss J, et al. Clonal dynamics towards the development of venetoclax resistance in chronic lymphocytic leukemia. *Nat Commun*. 2018;9(1):727. doi:10.1038/s41467-018-03170-7
14. Dreger P, Ghia P, Schetelig J, et al. High-risk chronic lymphocytic leukemia in the era of pathway inhibitors: Integrating molecular and cellular therapies. *Blood*. 2018;132(9):892–902. doi:10.1182/blood-2018-01-826008
15. Korycka-Wolowiec A, Wolowiec D, Kubiak-Mlonka A, Robak T. Venetoclax in the treatment of chronic lymphocytic leukemia. *Expert Opin Drug Metab Toxicol*. 2019;15(5):353–366. doi:10.1080/17425255.2019.1606211
16. Robak T, Błoński J, Skotnicki AB, et al. Rituximab, cladribine, and cyclophosphamide (RCC) induction with rituximab maintenance in chronic lymphocytic leukemia: PALG – CLL4 (ML21283) trial. *Eur J Haematol*. 2018;100(5):465–474. doi:10.1111/ejh.13042
17. Robak T, Jamroziak K, Gora-Tybor J, et al. Comparison of cladribine plus cyclophosphamide with fludarabine plus cyclophosphamide as first-line therapy for chronic lymphocytic leukemia: A phase III randomized study by the Polish Adult Leukemia Group (PALG-CLL3 Study). *J Clin Oncol*. 2010;28(11):1863–1869. doi:10.1200/JCO.2009.25.9630
18. Robak T, Korycka A, Lech-Maranda E, Robak P. Current status of older and new purine nucleoside analogues in the treatment of lymphoproliferative diseases. *Molecules*. 2009;14(3):1183–1226. doi:10.3390/molecules14031183
19. Marzo I, Pérez-Galán P, Giraldo P, Rubio-Félix D, Anel A, Naval J. Cladribine induces apoptosis in human leukaemia cells by caspase-dependent and -independent pathways acting on mitochondria. *Biochem J*. 2001;359(3):537–546. doi:10.1042/bj3590537
20. Nomura Y, Inanami O, Takahashi K, Matsuda A, Kuwabara M. 2-Chloro-2′-deoxyadenosine induces apoptosis through the Fas/Fas ligand pathway in human leukemia cell line MOLT-4. *Leukemia*. 2000;14(2):299–306. doi:10.1038/sj.leu.2401649

21. Klöpfer A, Hasenjäger A, Belka C, Schulze-Osthoff K, Dörken B, Daniel PT. Adenine deoxynucleotides fludarabine and cladribine induce apoptosis in a CD95/Fas receptor, FADD and caspase-8-independent manner by activation of the mitochondrial cell death pathway. *Oncogene*. 2004;23(58):9408–9418. doi:10.1038/sj.onc.1207975

22. Hallek M, Cheson BD, Catovsky D, et al. iwCLL guidelines for diagnosis, indications for treatment, response assessment, and supportive management of CLL. *Blood*. 2018;131(25):2745–2760. doi:10.1182/blood-2017-09-806398

23. Smolewski P, Szmigielska-Kaplon A, Cebula B, et al. Proapoptotic activity of alemtuzumab alone and in combination with rituximab or purine nucleoside analogues in chronic lymphocytic leukemia cells. *Leuk Lymphoma*. 2005;46(1):87–100. doi:10.1080/13693780400007151

24. Zaborowska A, Cebula-Obrzut B, Franiak-Pietryga I, et al. Wpływ bendamustyny zastosowanej pojedynczo lub w skojarzeniu z analogami nukleozydów purynowych na przeżywalność oraz apoptozę komórek przewlekłej białaczki limfocytowej w hodowli in vitro. *Acta Heamatol Pol*. 2009;40(4):887–898.

25. Chou TC. The mass-action law based algorithm for cost-effective approach for cancer drug discovery and development. *Am J Cancer Res*. 2011;1(7):925-954. PMID:22016837, PMCID:PMC3196289.

26. Kalkavan H, Green DR. MOMP, cell suicide as a BCL-2 family business. *Cell Death Differ*. 2018;25(1):46–55. doi:10.1038/cdd.2017.179

27. Bose P, Gandhi V, Konopleva M. Pathways and mechanisms of venetoclax resistance. *Leuk Lymphoma*. 2017;58(9):2026–2039. doi:10.1080/10428194.2017.1283032

28. Seymour JF, Kipps TJ, Eichhorst B, et al. Venetoclax-rituximab in relapsed or refractory chronic lymphocytic leukemia. *N Engl J Med*. 2018;378(12):1107–1120. doi:10.1056/NEJMoa1713976

29. Seymour JF, Ma S, Brander DM, et al. Venetoclax plus rituximab in relapsed or refractory chronic lymphocytic leukaemia: A phase 1b study. *Lancet Oncol*. 2017;18(2):230–240. doi:10.1016/S1470-2045(17)30012-8

30. Cramer P, von Tresckow J, Bahlo J, et al. Bendamustine followed by obinutuzumab and venetoclax in chronic lymphocytic leukaemia (CLL2-BAG): Primary endpoint analysis of a multicentre, open-label, phase 2 trial. *Lancet Oncol*. 2018;19(9):1215–1228. doi:10.1016/S1470-2045(18)30414-5

31. Stilgenbauer S, Morschhauser F, Wendtner CM, et al. Phase Ib study (GO28440) of venetoclax with bendamustine/rituximab or bendamustine/obinutuzumab in patients with relapsed/refractory or previously untreated chronic lymphocytic leukemia. *Blood*. 2016;128(22):4393–4393. doi:10.1182/blood.V128.22.4393.4393

32. Stilgenbauer S, Morschhauser F, Wendtner CM, et al. Venetoclax plus bendamustine-rituximab or bendamustine-obinutuzumab in chronic lymphocytic leukemia: Final results of a phase 1b study (GO28440). *Haematologica*. 2021;106(11):2834–2844. doi:10.3324/haematol.2020.261107

33. Robak T, Korycka A, Kasznicki M, Wrzesien-Kus A, Smolewski P. Purine nucleoside analogues for the treatment of hematological malignancies: Pharmacology and clinical applications. *Curr Cancer Drug Targets*. 2005;5(6):421–444. doi:10.2174/1568009054863618

34. Robak T, Lech-Maranda E, Korycka A, Robak E. Purine nucleoside analogs as immunosuppressive and antineoplastic agents: Mechanism of action and clinical activity. *Curr Med Chem*. 2006;13(26):3165–3189. doi:10.2174/092986706778742918

35. Miyashita T, Harigai M, Hanada M, Reed JC. Identification of a p53-dependent negative response element in the bcl-2 gene. *Cancer Res*. 1994;54(12):3131–3135. PMID:8205530.

36. Miyashita T, Krajewski S, Krajewska M, et al. Tumor suppressor p53 is a regulator of bcl-2 and bax gene expression in vitro and in vivo. *Oncogene*. 1994;9(6):1799-1805. PMID:8183579.

37. Klanova M, Klener P. BCL-2 proteins in pathogenesis and therapy of B-cell non-Hodgkin lymphomas. *Cancers*. 2020;12(4):938. doi:10.3390/cancers12040938

38. Zhang LN, Li JY, Xu W. A review of the role of Puma, Noxa and Bim in the tumorigenesis, therapy and drug resistance of chronic lymphocytic leukemia. *Cancer Gene Ther*. 2013;20(1):1–7. doi:10.1038/cgt.2012.84

39. Chen HC, Kanai M, Inoue-Yamauchi A, et al. An interconnected hierarchical model of cell death regulation by the BCL-2 family. *Nat Cell Biol*. 2015;17(10):1270–1281. doi:10.1038/ncb3236

40. Yu J, Zhang L. PUMA, a potent killer with or without p53. *Oncogene*. 2008;27(S1):S71–S83. doi:10.1038/onc.2009.45

Transient spontaneous osteonecrosis of the knee (SONK) shortly after SARS-CoV-2 infection: A report of 2 cases

Konrad Malinowski[1,2,A–D,F], Paweł Skowronek[3,A–C,E,F], Michael Hirschmann[4,A–C,E,F], Dong Woon Kim[2,A,D–F], Brandon Michael Henry[5,A–C,E,F], Michał Ebisz[1,A,D–F], Marcin Mostowy[6,A,D–F], Przemysław A. Pękala[2,7,A–F]

[1] Artromedical Orthopaedic Clinic, Bełchatów, Poland

[2] International Evidence-Based Anatomy Working Group, Department of Anatomy, Jagiellonian University Medical College, Kraków, Poland

[3] Department of Orthopaedic and Trauma Surgery, S. Żeromski Hospital, Kraków, Poland

[4] Department of Orthopaedic Surgery and Traumatology, Kantonsspital Baselland (Bruderholz, Liestal, Laufen), University of Basel, Switzerland

[5] Clinical Laboratory, Division of Nephrology and Hypertension, Cincinnati Children's Hospital Medical Center, USA

[6] Orthopedic and Trauma Department, Veteran's Memorial Teaching Hospital in Lodz, Medical University of Lodz, Poland

[7] Faculty of Medicine and Health Sciences, Andrzej Frycz Modrzewski Kraków University, Poland

A – research concept and design; B – collection and/or assembly of data; C – data analysis and interpretation;
D – writing the article; E – critical revision of the article; F – final approval of the article

Abstract

Background. This article describes 2 cases of post-coronavirus disease 2019 (COVID-19) transient spontaneous osteonecrosis of the knee (PCT-SONK) observed in patients who had previously recovered from COVID-19 without corticosteroid administration.

Objectives. The possible pathomechanisms by which a recent SARS-CoV-2 infection may contribute as a causative factor for osteonecrosis are reviewed, and the differential diagnosis and treatment are discussed.

Materials and methods. Two patients (males, 45- and 47-year-old) presented with sudden onset knee pain with no trauma history. The pain persisted during rest and at night. On magnetic resonance imaging (MRI), no subchondral bone thickening was observed; bone edema was diffusely distributed in the whole femoral condyle, in contrast to the more focal edema that is typically concentrated mainly around the subchondral region in classic SONK. Both patients were treated nonoperatively with no weight bearing and pharmacological agents, and complete resolution of symptoms was achieved.

Results. A follow-up MRI 10 weeks after presentation revealed a near-complete loss of signal in the medial femoral condyle in both patients.

Conclusions. Orthopedic surgeons should be cautious when sudden knee pain without concurrent trauma or a history of injury occurs shortly after severe acute respiratory syndrome coronavirus 2 (SARS-CoV-2) infection, even with mild COVID-19 illness. While some studies report the development of post-COVID-19 osteonecrosis after lower doses of corticosteroids and sooner after their administration than in comparable non-COVID-19 cases, our study is the first to report 2 cases with no corticosteroid administration at all. Therefore, the authors believe it adds to the body of knowledge on the potential connections between COVID-19 and PCT-SONK. The transient nature of symptoms and radiological findings suggest that aggressive surgical treatment of non-injury local bone edema occurring shortly after SARS-CoV-2 infection should be avoided.

Key words: knee pain, SARS-CoV-2, avascular necrosis, SONK, COVID-19 complications

Background

Severe acute respiratory syndrome coronavirus 2 (SARS-CoV-2) is a positive-sense, single-stranded RNA virus that was first identified in late December 2019 in Wuhan, China.[1] The disease caused by SARS-CoV-2 infection is referred to as coronavirus disease 2019 (COVID-19). The World Health Organization (WHO) officially declared COVID-19 a pandemic in March 2020.[2] By August 2022, the estimated death toll from COVID-19 had risen to 6,446,714.[1] Its typical clinical manifestations include fever, cough and shortness of breath, which can progress to pneumonia. This can further deteriorate into a dysregulated immune state characterized by a hyperinflammatory response and a hypercoagulable state, leading to pulmonary and systemic micro- and macro-immunothrombosis, which ultimately may cause multiple organ failure and death.[3]

Involvement of nearly every organ system has been observed not only during the acute stages of COVID-19 but also after recovery. Recent reports describe post-COVID-19 clinical problems that can extend to affect the knee joint and its function.[4] There are also studies reporting secondary osteonecrosis of the knee after COVID-19 treatment with corticosteroids, but with less than the cumulative dose of corticosteroids reported in the literature for osteonecrosis of the knee.[5,6] Similar studies have been published concerning avascular necrosis of the femoral head occurring with lower doses of corticosteroids and sooner after their administration than in comparable non-COVID-19 cases.[7] Karaarslan et al. recently performed a prospective study on a group of patients discharged after COVID-19 infection and concluded that "92.3%, 72.7% and 56.3% of patients reported any musculoskeletal symptom at hospitalization, 2-week and 1-month, respectively".[8]

Spontaneous osteonecrosis of the knee (SONK) is the most common form of osteonecrosis of the knee joint, but its etiology remains unclear. However, it is believed that SONK might be caused by local blood flow alteration, which leads to subsequent bone ischemia, ultimately resulting in local fluid storage and bone edema that can be visualized on magnetic resonance imaging (MRI).[9] Typically, the subchondral lesion due to SONK is observed unilaterally at the medial femoral condyle (MFC) of the knee (94%). The prevalence of SONK is higher in females, especially those over the age of 55, and typically presents as sudden knee pain without causative trauma or injury.[10]

The COVID-19 has been clearly associated with a hypercoagulable state, referred to as COVID-19-associated coagulopathy (CAC),[11] with evidence strongly suggestive of a secondary microangiopathy phenomenon propagating multiple organ failure.[12] Laboratory hallmarks of CAC, such as decreased platelets and elevated D-dimer, have been shown to persist for several months after recovery, even in mild cases of COVID-19.[13] Therefore, it is possible that SARS-CoV-2 contributes to the development of local blood flow changes and ultimately to post-COVID-19 transient spontaneous osteonecrosis of the knee (PCT-SONK).

This report aims to describe 2 cases of sudden knee pain with radiological features similar to those of SONK that were observed in patients shortly after recovering from COVID-19, and to discuss the possible pathogenesis of this emerging problem for orthopedic surgeons.

Case 1 (K.D.)

A 45-year-old male patient (software engineer, sedentary work) presented with sudden onset right knee pain with no history of trauma. The pain persisted during rest and at night.

On clinical examination, the patient had a full range of motion and a stable knee joint. The patient experienced pain during extension and near-full extension. Palpation of the MFC and medial joint space revealed local tenderness. Additionally, the patient experienced pain when varus stress was applied to the knee in 10° knee flexion. An MRI of the patient's right knee was performed immediately following the orthopedic appointment (7 weeks after the onset of knee symptoms). Magnetic resonance imaging in short tau inversion recovery (STIR) sequence revealed a large area of diffuse increased signal in the MFC and the medial aspect of the intercondylar region (Fig. 1).

Approximately 3 months prior to the onset of knee symptoms, the patient had been diagnosed with COVID-19, which was confirmed by a positive result of a SARS-CoV-2 RT-PCR test. The patient had begun to experience symptoms of acute respiratory infection 5 days prior to diagnosis, which had progressed to severe flu-like symptoms with dyspnea for approximately next 2 weeks. The patient was not hospitalized despite the severity of the respiratory symptoms, and no corticosteroids were administered.

The patient was put on crutches and instructed to bear no weight on the affected leg. Additionally, the patient was prescribed ossein-hydroxyapatite complex (2490 mg/day), calcium (1000 mg/day), vitamin D_3 (150 μg/day), vitamin K_2 (50 μg/day), pentoxifylline (400 mg/day), vitamin C (2,000 mg/day), and acetylsalicylic acid (75 mg/day).

The symptoms subsided completely after approx. 8 weeks of nonoperative treatment. A follow-up MRI scan of the same knee was performed 10 weeks after the first appointment, and showed remission of the radiological findings in the MFC and medial aspect of the intercondylar region (Fig. 2). The next follow-up MRI, which was performed 5 months after the first appointment, showed complete resolution of the bony and soft tissue edema (Fig. 3). There were no adverse or unanticipated events.

Case 2 (K.M.)

A 47-year-old male hotel owner presented with sudden onset of right knee pain without trauma. The pain persisted during rest and at night.
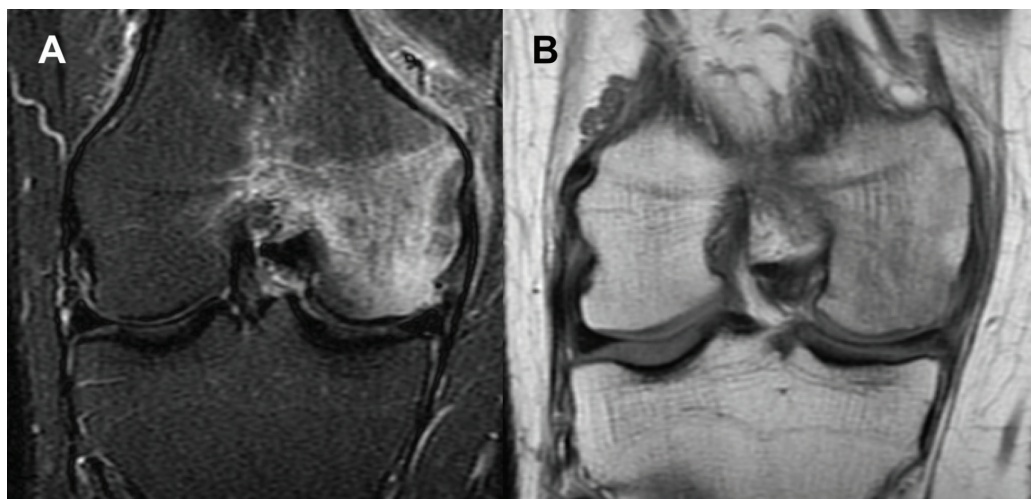
Fig. 1. Magnetic resonance imaging (MRI) coronal view of the right knee (Case 1) performed in the symptomatic period. There is diffuse increase in signal in the medial femoral condyle in both (A) short tau inversion recovery (STIR) fast spin echo (FSE) and (B) proton density (PD) sequences. It is noteworthy that the signal intensity in the subchondral bone is only slightly affected in the (B) PD sequence. Edema of the soft tissues on the medial side of the joint is also clearly visible
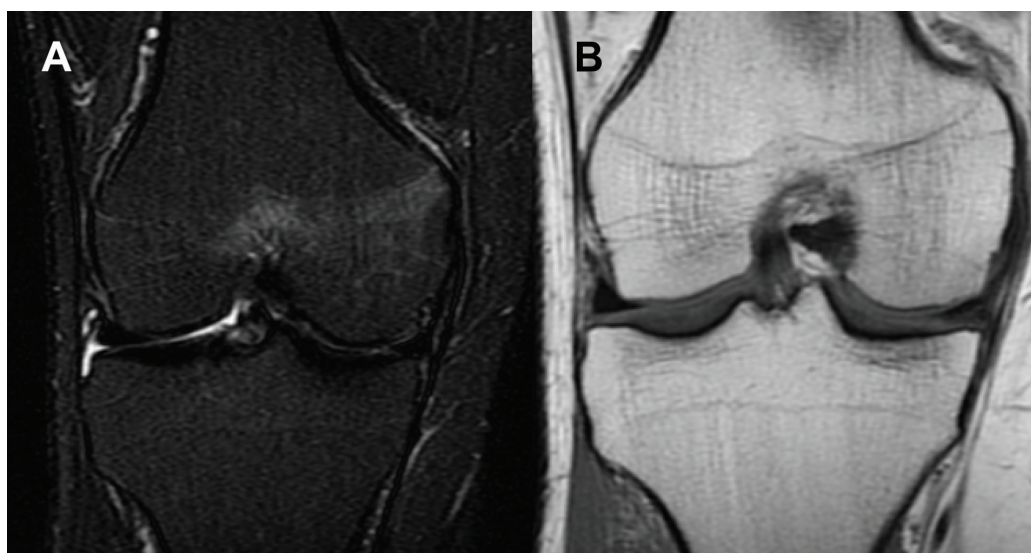

Fig. 2. Follow-up magnetic resonance imaging (MRI) coronal view of the right knee (Case 1) performed after the resolution of symptoms. The signal in the medial femoral condyle in both (A) short tau inversion recovery (STIR) fast spin echo (FSE) and (B) proton density (PD) sequences is almost normal. It is noteworthy that there is no visible soft tissue edema.
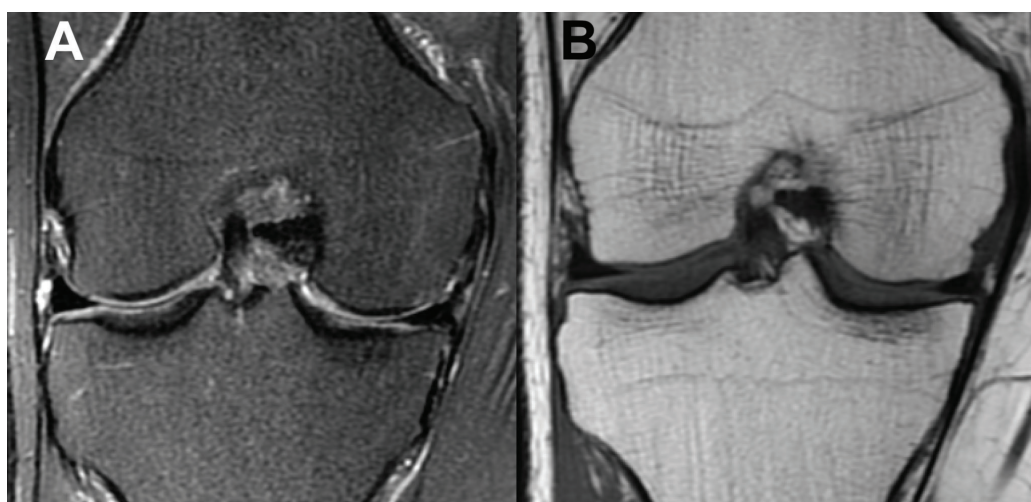

Fig. 3. Second follow-up magnetic resonance imaging (MRI) coronal view of the right knee (Case 1). The signal in the medial femoral condyle in both (A) short tau inversion recovery (STIR) fast spin echo (FSE) and (B) proton density (PD) sequences is normal

On clinical examination, the patient had a full range of motion, with a stable joint, with pain during extension and near full extension. In addition, the patient experienced pain upon palpation of the MFC and joint spaces of the affected knee. Varus stress test applied to the knee with the leg in 10° flexion also elicited pain. The knee axis was recorded as less than 5° of varus. Magnetic resonance imaging of the knee 4 weeks after the onset of symptoms revealed diffuse high signal in the entire MFC, suggesting an accumulation of edema in the bone marrow (Fig. 4).
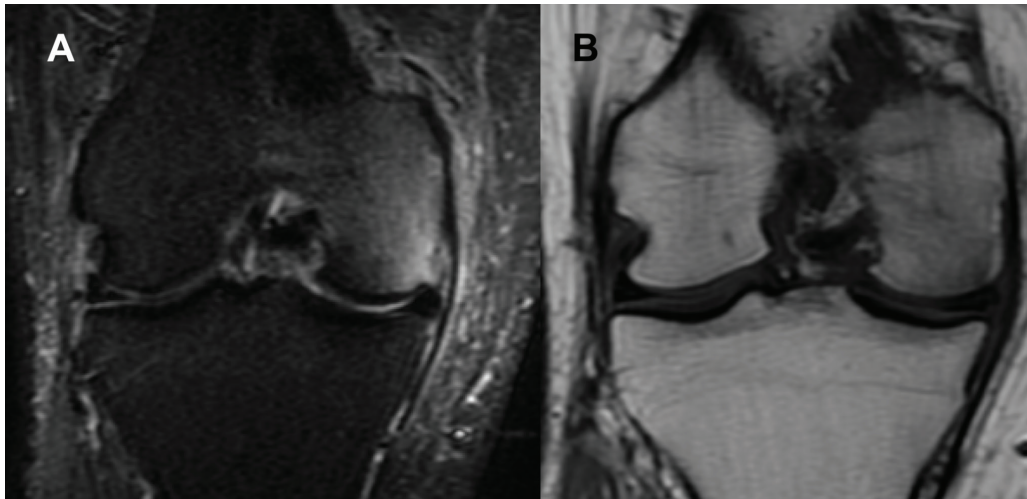
Fig. 4. Magnetic resonance imaging (MRI) coronal view of the right knee (Case 2) performed in the symptomatic period. There is diffuse increase in signal in the medial femoral condyle in both (A) short tau inversion recovery (STIR) fast spin echo (FSE) and (B) longitudinal relaxation time (T1) sequences. It is noteworthy that the signal intensity in the subchondral bone is only slightly affected in the (B) T1 sequence. Edema of the soft tissues on the medial side of the joint is also clearly visible
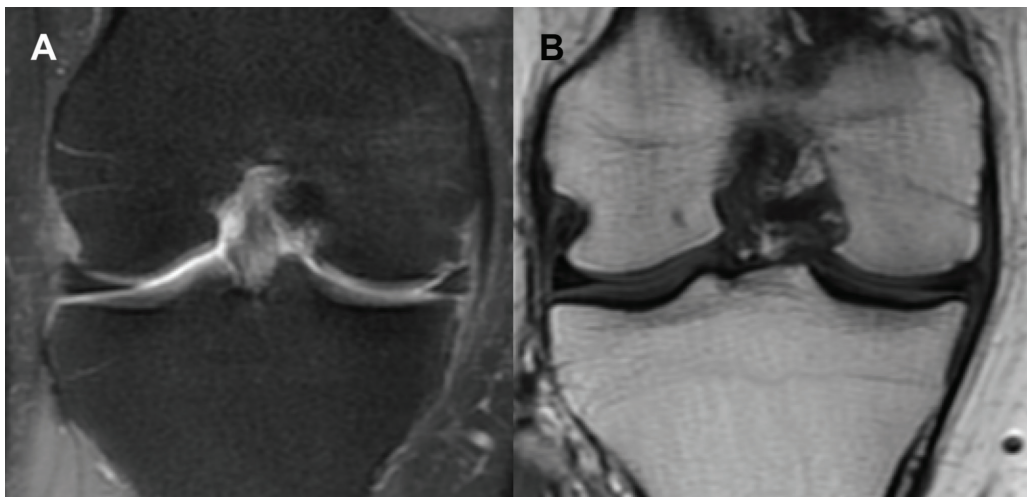

Fig. 5. Follow-up magnetic resonance imaging (MRI) coronal view of the right knee (Case 2) performed after the resolution of symptoms. The signal in the medial femoral condyle in both (A) short tau inversion recovery (STIR) fast spin echo (FSE) and (B) longitudinal relaxation time (T1) sequences is almost normal. It is noteworthy that there is no visible soft tissue edema

Approximately 10 weeks before presentation, the patient had tested positive for SARS-CoV-2 with real-time polymerase chain reaction (RT-PCR) test. He had experienced severe flu-like symptoms, with fever as high as 39.5°C, and pneumonia that lasted 10 days. He was not hospitalized, and corticosteroids were not administered.

The patient was put on crutches and instructed to bear no weight on the affected leg for 6 weeks. Additionally, he was prescribed the same pharmacotherapy as the patient in Case 1.

Full remission of symptoms was achieved after approx. 3 weeks of such conservative treatment. Follow-up MRI 10 weeks after presentation revealed near-complete loss of signal in the MFC (Fig. 5). There were no adverse or unanticipated events.

Discussion

The 2 cases of PCT-SONK presented in this study add to the differential diagnosis of sudden knee pain in un-injured patients during the ongoing pandemic. It is particularly noteworthy that the radiological findings that constitute PCT-SONK, although similar in both cases presented in this study, are radiologically distinct in appearance from classic SONK (Fig. 6). No subchondral bone thickening was observed, and the bone edema was more diffuse in the whole femoral condyle, in contrast to focal edema, which is concentrated mainly around the subchondral region and typically observed in classic SONK (Table 1).

It has been reported that SONK classically occurs in middle-aged females and is caused by excessive stress in the subchondral bone.[14] In previously documented cases of SONK unrelated to COVID-19, high rates of surgical intervention, including total knee replacement, resulted in poor prognoses.[9] However, in the 2 cases presented in this study, nonoperative treatment yielded good results. The transient nature of PCT-SONK suggests that surgical management should be considered only for progressive cases in which conservative management fails to achieve improvement. Thus, it is of utmost importance, particularly during the pandemic, to raise awareness among sports medicine and orthopedic societies to consider microvascular impairment in subchondral bone as a possible source of sudden knee pain in patients without concurrent trauma or a history of recent injury.
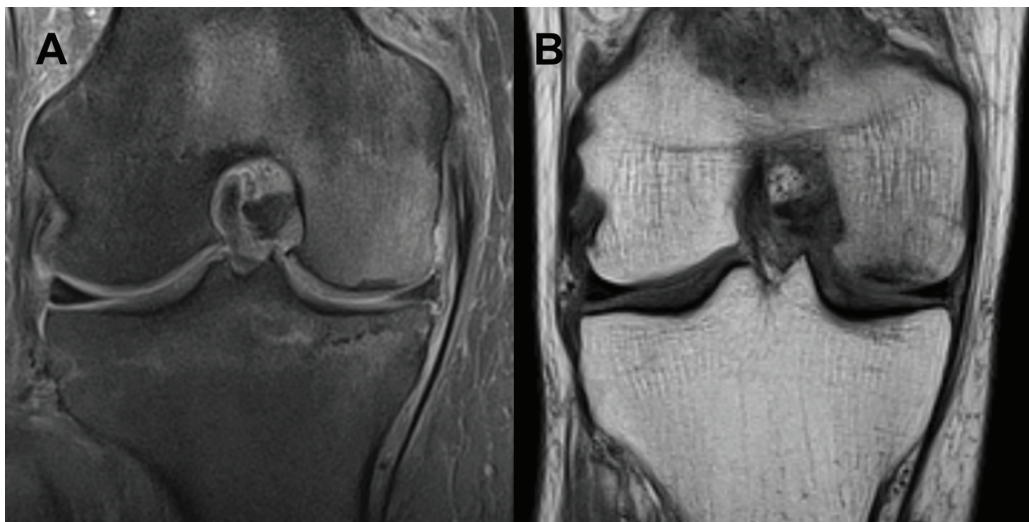
Fig. 6. Radiological (coronal magnetic resonance imaging (MRI) views) appearance of classic spontaneous osteonecrosis of the knee (SONK) in the right knee. There is a focal signal increase in subchondral bone in both (A) short tau inversion recovery (STIR) fast spin echo (FSE) and (B) proton density (PD) magnetic resonance imaging (MRI) sequences

Table 1. Comparison between typical features of SONK and the clinical observations during the 2 reported cases of PCT-SONK

Feature	SONK	PCT-SONK
Subchondral bone thickening with signal intensity increase	yes	no
Bone marrow edema (MRI)	STIR, PD, T1	mostly in STIR
Soft tissue edema (MRI)	no	yes
Tenderness and pain	mostly in the joint line	over the whole medial femoral condyle and surrounding soft tissues
Sudden and unexpected onset of pain	yes	yes
Night pain	yes	yes
Age [years]	>55	~45

SONK – spontaneous osteonecrosis of the knee; PCT-SONK – post-COVID-19 transient spontaneous osteonecrosis of the knee; MRI – magnetic resonance imaging; STIR – short tau inversion recovery; PD – proton density; T1 – relaxation time.

While SONK after COVID-19 in the presented cases may indeed be a coincidence, SARS-CoV-2 infection has been demonstrated to affect nearly every facet of hemostasis. This is likely driven by a combination of a dysfunctional, hyperinflammatory state and direct and indirect endothelial injury, ultimately leading to micro-immunothrombosis both in the lungs and systemic tissues.[11,15] Significant evidence of endotheliopathy and a secondary thrombotic microangiopathy (TMA) or TMA-like phenomenon has emerged. It is often characterized by elevated von Willebrand factor antigen levels and low ADAMTS13 activity,[12,16] overactivation of complement pathways,[17] elevated circulating markers of neutrophil extracellular traps,[18] high serum lactate dehydrogenase levels,[19] and decreased platelet counts,[20,21] as well as the typical clinical manifestations of TMA, such as acute kidney failure.[22] Moreover, evidence of SARS-CoV-2 directly infecting endothelial cells has been presented,[23] and circulating biomarkers of endothelial injury are frequently reported to be elevated in COVID-19 patients.[24] Finally, a TMA-like phenomenon is likely further exacerbated by a state of hypofibrinolysis, impairing the ability to break down newly formed clots in the microcirculation.[25,26]

Given the significant potential for multisystem microvascular injury in COVID-19, it can be hypothesized that there is an increased risk of SONK related to COVID-19 – secondary to damage to blood vessels supplying the MFC regions, leading to impaired microcirculation blood flow and tissue perfusion, and ultimately causing ischemic necrosis of subchondral bone.[27,28] Such phenomenon may occur more often in patients with pre-existing, but clinically silent, excessive subchondral bone stress, with SARS-CoV-2 microvascular flow disturbances exacerbating the underlying knee pathology.

Corticosteroids are widely used, sometimes indiscriminately, for the treatment of COVID-19. They could lead to a reduction in bone mineral density (BMD) in patients and subsequently predispose them to SONK, as low BMD has been shown to be associated with the onset of SONK,[29,30] as well as other orthopedic pathologies, such as steroid-induced avascular necrosis of the femoral head.[31] However, unlike in many other studies reporting post-COVID-19 osteonecrosis,[5–7] corticosteroids were not administered in either of the cases in this study. As stated in a study by Angulo-Ardoy et al., "it is still unclear whether post-COVID SONK is related to the use of corticosteroids or to the virus itself".[6] While some studies report the development of osteonecrosis

1040

K. Malinowski et al. Knee osteonecrosis shortly after SARS-CoV-2

after lower doses of corticosteroids, and sooner after their administration than in comparable non-COVID-19 cases,[5–7] this is the first study to report 2 cases with no corticosteroid administration at all. Therefore, the authors believe it adds to the body of knowledge on the potential connections between COVID-19 and PCT-SONK.

A conservative treatment plan should address all etiologic aspects of PCT-SONK. First, reduction of pressure to the affected subchondral bone is achieved by non-weight bearing; second, supplementation of vitamin D and calcium is implemented to enhance BMD restoration; third, pharmacological agents to improve microvascular circulation (i.e., pentoxyfilline) are administered; and finally, anti-aggregative agents, such as acetylsalicylic acid, to inhibit thrombus formation, are given to the patient.[32] It is important to emphasize that this approach is supported only by limited observations and based on regular SONK treatment algorithms; further studies utilizing evidence-based methods are required. We emphasize a personalized approach in every case, considering a patient's general health status and all possible individual contraindications and risks of given therapies.

This study is limited by a relatively short follow-up, although complete radiological and clinical recovery was obtained during the observation period. While this study has no power to identify any causative relationship with SARS-CoV-2, we hope that it will raise awareness and pave the way for broader studies investigating the PCT-SONK phenomenon.

Conclusions

Orthopedic surgeons should be cautious when sudden knee pain without concurrent trauma or a history of injury occurs shortly after SARS-CoV-2 infection, even when the course of COVID-19 was mild. While there are studies reporting post-COVID-19 osteonecrosis after lower doses of corticosteroids and sooner after their administration than in comparable non-COVID-19 cases, this is the first to report 2 cases with no corticosteroid administration at all. The transient nature of symptoms and radiological findings suggest that aggressive surgical treatment of non-injury local bone edema occurring shortly after SARS-CoV-2 infection should be avoided.

ORCID iDs

Michael Hirschmann https://orcid.org/0000-0002-4014-424X
Dong Woon Kim https://orcid.org/0000-0003-0207-9587
Brandon Michael Henry https://orcid.org/0000-0002-8047-338X
Marcin Mostowy https://orcid.org/0000-0002-8301-164X
Przemysław A. Pękala https://orcid.org/0000-0002-9750-2650

References

1. Worldometer. COVID-19 coronavirus pandemic. https://www.worldometers.info/coronavirus/. Accessed August 11, 2021.
2. Neher RA, Dyrdak R, Druelle V, Hodcroft EB, Albert J. Potential impact of seasonal forcing on a SARS-CoV-2 pandemic. *Swiss Med Wkly*. 2020; 150:w20224. doi:10.4414/smw.2020.20224
3. Datta PK, Liu F, Fischer T, Rappaport J, Qin X. SARS-CoV-2 pandemic and research gaps: Understanding SARS-CoV-2 interaction with the ACE2 receptor and implications for therapy. *Theranostics*. 2020; 10(16):7448–7464. doi:10.7150/thno.48076
4. Hønge BL, Hermansen MLF, Storgaard M. Reactive arthritis after COVID-19. *BMJ Case Rep*. 2021;14(3):e241375. doi:10.1136/bcr-2020-241375
5. Agarwala SR, Vijayvargiya M, Sawant T. Secondary osteonecrosis of the knee as a part of long COVID-19 syndrome: A case series. *BMJ Case Rep*. 2022;15(3):e248583. doi:10.1136/bcr-2021-248583
6. Angulo-Ardoy M, Ureña-Aguilera Á. Knee osteonecrosis after COVID-19. *Family Pract*. 2021;38(Suppl 1):i45–i47. doi:10.1093/fampra/cmab063
7. Agarwala SR, Vijayvargiya M, Pandey P. Avascular necrosis as a part of 'long COVID-19.' *BMJ Case Rep*. 2021;14(7):e242101. doi:10.1136/bcr-2021-242101
8. Karaarslan F, Demircioğlu Güneri F, Kardeş S. Postdischarge rheumatic and musculoskeletal symptoms following hospitalization for COVID-19: Prospective follow-up by phone interviews. *Rheumatol Int*. 2021;41(7):1263–1271. doi:10.1007/s00296-021-04882-8
9. Sibilska A, Góralczyk A, Hermanowicz K, Malinowski K. Spontaneous osteonecrosis of the knee: What do we know so far? A literature review. *Int Orthop*. 2020;44(6):1063–1069. doi:10.1007/s00264-020-04536-7
10. Mears SC, McCarthy EF, Jones LC, Hungerford DS, Mont MA. Characterization and pathological characteristics of spontaneous osteonecrosis of the knee. *Iowa Orthop J*. 2009;29:38–42. PMID:19742083. PMCID:PMC2723690.
11. Lippi G, Sanchis-Gomar F, Favaloro EJ, Lavie CJ, Henry BM. Coronavirus disease 2019-associated coagulopathy. *Mayo Clin Proc*. 2021; 96(1):203–217. doi:10.1016/j.mayocp.2020.10.031
12. Henry BM, Benoit SW, Oliveira MHS, Lippi G, Favaloro EJ, Benoit JL. ADAMTS13 activity to von Willebrand factor antigen ratio predicts acute kidney injury in patients with COVID-19: Evidence of SARS-CoV-2 induced secondary thrombotic microangiopathy. *Int J Lab Hematol*. 2021;43(S1):129–136. doi:10.1111/ijlh.13415
13. Wu X, Luo D, Liu Y, Zeng Y, Gong Y. Continuous thrombocytopenia after SARS-CoV-2 nucleic acid negative in a non-severe COVID-19 patient for several months. *BMC Infect Dis*. 2020;20(1):774. doi:10.1186/s12879-020-05495-5
14. Steinbach L, Suh K. Bone marrow edema pattern around the knee on magnetic resonance imaging excluding acute traumatic lesions. *Semin Musculoskelet Radiol*. 2011;15(3):208–220. doi:10.1055/s-0031-1278421
15. Henry BM, Vikse J, Benoit S, Favaloro EJ, Lippi G. Hyperinflammation and derangement of renin-angiotensin-aldosterone system in COVID-19: A novel hypothesis for clinically suspected hypercoagulopathy and microvascular immunothrombosis. *Clin Chim Acta*. 2020;507:167–173. doi:10.1016/j.cca.2020.04.027
16. Martinelli N, Montagnana M, Pizzolo F, et al. A relative ADAMTS13 deficiency supports the presence of a secondary microangiopathy in COVID 19. *Thromb Res*. 2020;193:170–172. doi:10.1016/j.thromres.2020.07.034
17. Henry BM, Szergyuk I, Oliveira MHS, et al. Complement levels at admission as a reflection of coronavirus disease 2019 (COVID-19) severity state. *J Med Virol*. 2021;93(9):5515–5522. doi:10.1002/jmv.27077
18. Ng H, Havervall S, Rosell A, et al. Circulating markers of neutrophil extracellular traps are of prognostic value in patients with COVID-19. *Arterioscler Thromb Vasc Biol*. 2021;41(2):988–994. doi:10.1161/ATVBAHA.120.315267
19. Henry BM, Aggarwal G, Wong J, et al. Lactate dehydrogenase levels predict coronavirus disease 2019 (COVID-19) severity and mortality: A pooled analysis. *Am J Emerg Med*. 2020;38(9):1722–1726. doi:10.1016/j.ajem.2020.05.073
20. Henry BM, de Oliveira MHS, Benoit S, Plebani M, Lippi G. Hematologic, biochemical and immune biomarker abnormalities associated with severe illness and mortality in coronavirus disease 2019 (COVID-19): A meta-analysis. *Clin Chem Lab Med*. 2020;58(7):1021–1028. doi:10.1515/cclm-2020-0369
21. Lippi G, Plebani M, Henry BM. Thrombocytopenia is associated with severe coronavirus disease 2019 (COVID-19) infections: A meta-analysis. *Clin Chim Acta*. 2020;506:145–148. doi:10.1016/j.cca.2020.03.022

22. Cheruiyot I, Henry B, Lippi G, et al. Acute kidney injury is associated with worse prognosis In COVID-19 patients: A systematic review and meta-analysis. *Acta Biomed.* 2020;91(3):e2020029. doi:10.23750/abm.v91i3.10222

23. Liu F, Han K, Blair R, et al. SARS-CoV-2 infects endothelial cells in vivo and in vitro. *Front Cell Infect Microbiol.* 2021;11:701278. doi:10.3389/fcimb.2021.701278

24. Henry BM, de Oliveira MHS, Cheruiyot I, et al. Circulating level of Angiopoietin-2 is associated with acute kidney injury in coronavirus disease 2019 (COVID-19). *Angiogenesis.* 2021;24(3):403–406. doi:10.1007/s10456-021-09782-w

25. Henry BM, Benoit SW, Hoehn J, Lippi G, Favaloro EJ, Benoit JL. Circulating plasminogen concentration at admission in patients with coronavirus disease 2019 (COVID-19). *Semin Thromb Hemost.* 2020;46(7):859–862. doi:10.1055/s-0040-1715454

26. Henry BM, Cheruiyot I, Benoit JL, et al. Circulating levels of tissue plasminogen activator and plasminogen activator inhibitor-1 are independent predictors of coronavirus disease 2019 severity: A prospective, observational study. *Semin Thromb Hemost.* 2021;47(4):451–455. doi:10.1055/s-0040-1722308

27. Ramani SL, Samet J, Franz CK, et al. Musculoskeletal involvement of COVID-19: Review of imaging. *Skeletal Radiol.* 2021;50(9):1763–1773. doi:10.1007/s00256-021-03734-7

28. Pareek A, Parkes CW, Bernard C, et al. Spontaneous osteonecrosis/subchondral insufficiency fractures of the knee: High rates of conversion to surgical treatment and arthroplasty. *J Bone Joint Surg.* 2020;102(9):821–829. doi:10.2106/JBJS.19.00381

29. Akamatsu Y, Mitsugi N, Hayashi T, Kobayashi H, Saito T. Low bone mineral density is associated with the onset of spontaneous osteonecrosis of the knee. *Acta Orthop.* 2012;83(3):249–255. doi:10.3109/17453674.2012.684139

30. van Niekerk G, Engelbrecht AM. Inflammation-induced metabolic derangements or adaptation: An immunometabolic perspective. *Cytokine Growth Factor Rev.* 2018;43:47–53. doi:10.1016/j.cytogfr.2018.06.003

31. Zhang S, Wang C, Shi L, Xue Q. Beware of steroid-induced avascular necrosis of the femoral head in the treatment of COVID-19: Experience and lessons from the SARS epidemic. *Drug Des Devel Ther.* 2021;15:983–995. doi:10.2147/DDDT.S298691

32. Undas A, Brummel-Ziedins K, Mann KG. Why does aspirin decrease the risk of venous thromboembolism? On old and novel antithrombotic effects of acetyl salicylic acid. *J Thromb Haemost.* 2014;12(11):1776–1787. doi:10.1111/jth.12728

Changes in treatment of aortic valve diseases for acute and elective indications during the COVID-19 pandemic: A retrospective single-center analysis from 2019 to 2020

Katarzyna Cierpiszewska[1,A−D,F], Stanisław Ciechanowicz[1,B−D,F], Maciej Górecki[1,B,D,F], Piotr Kupidłowski[1,B,D,F], Mateusz Puślecki[2,3,A,B,D,F], Bartłomiej Perek[3,D−F]

[1] Faculty of Medicine, Poznan University of Medical Sciences, Poland

[2] Department of Medical Rescue, Poznan University of Medical Sciences, Poland

[3] Department of Cardiac Surgery and Transplantology, Poznan University of Medical Sciences, Poland

A – research concept and design; B – collection and/or assembly of data; C – data analysis and interpretation; D – writing the article; E – critical revision of the article; F – final approval of the article

Abstract

Background. Coronavirus disease 2019 (COVID-19) pandemic had an impact on the quality of healthcare services and led to many changes in the treatment of cardiac pathologies.

Objectives. To assess the differences in the clinical manifestations, management and outcomes of patients with aortic valve diseases (AVDs) treated invasively before and during the pandemic.

Materials and methods. This retrospective single-center study involved patients with AVDs treated by means of balloon aortic valvuloplasty (BAV), transcatheter aortic valve implantation (TAVI) or surgical aortic valve replacement (SAVR) in 2019 and 2020. They were divided into groups with respect to the year of intervention (2019 compared to 2020) and the priority of admission (urgent compared to elective). Preoperative characteristics, early outcomes and probability of annual survival were compared between the groups.

Results. The number of patients admitted urgently increased from 37 in 2019 to 54 in 2020, with a higher prevalence of men in 2020 (83.3% compared to 56.8%, respectively). Elective cases, on the other hand, declined from 279 in 2019 to 256 in 2020. Among the latter, more subjects had manifestations of heart failure (p < 0.001), coronary artery disease (CAD; p = 0.002), hypertension (p = 0.006), as well as had a history of a stroke (p = 0.002). In the meantime, more TAVI and fewer SAVR procedures were performed in 2020 (86 compared to 127 and 192 compared to 125, respectively; p < 0.001). In 2020, TAVI individuals had risk of death (according to the EuroSCORE scale) than in 2019 (p < 0.001). The probability of annual survival was comparable (p = 0.769) among AVD patients treated before and during the coronavirus pandemic (91.3% compared to 88.3%, respectively).

Conclusions. Although during the COVID-19 pandemic more nonelective and higher-risk AVD individuals received interventional treatment, the outcomes were comparable to the pre-pandemic era (2019). Our findings support highly valuable, less invasive therapeutic methods for treating aortic pathologies during the pandemic.

Key words: outcomes, coronavirus, aortic valve replacement, transcatheter aortic valve implantation, aortic valve disease

Background

Coronavirus disease 2019 (COVID-19) pandemic has affected healthcare systems globally. Consequently, the number of admissions to general hospitals[1,2] and cardiology departments in particular decreased markedly.[3,4] Hence, a reduction in the number of cardiology services and procedures, especially elective cases, has been observed.[3,5,6] A marked decline in the majority of cardiac procedures performed at National Health Service (NHS) hospitals (in the UK) was obvious after the pandemic outbreak.[6] A similar trend was also observed in Poland.[7,8]

In the meantime, special attention was paid to minimizing hospitalization times of patients and shifting to minimally invasive procedures, although these were not always considered the method of choice.[9] This trend was observed in many prevalent cardiac diseases such as aortic valve diseases (AVDs), aortic stenosis (AS) and coronary artery disease (CAD) that can be potentially treated by either interventional cardiologists or cardiac surgeons. Patients with AS can be treated surgically with cardiopulmonary bypass (CPB) and surgical aortic valve replacement (SAVR), or by transcatheter aortic valve implantation (TAVI).[10]

Objectives

This study aimed to assess how the COVID-19 pandemic affected the clinical profiles, priority of treatments, form of applied therapeutic methods, and outcomes of patients with AVD, treated at a cardiac surgical center experienced in both SAVR and TAVI procedures.

Materials and methods

Patients

This retrospective study evaluated consecutive patients treated for significant AVD between January 1, 2019, and December 31, 2020, at the Department of Cardiac Surgery and Transplantology in Poznań, Poland. The groups were divided based on the year (2019 – before the coronavirus pandemic outbreak, compared to 2020 – after the outbreak) of admission, the method of treatment (SAVR compared to TAVI) performed, and the priority of the intervention (elective compared to nonelective – urgent/emergent). Medical charts were retrospectively reviewed and baseline data (Table 1,2) were collected and analyzed.

Therapeutic method

Patients were treated with SAVR (218 in 2019 and 168 in 2020) using a complete or upper partial median sternotomy and CPB with cardioplegic arrest. Some patients required additional procedures (see Table 1). Catheter-based methods included TAVI carried out through percutaneous puncture or surgical exposure of the femoral arteries (91 in 2019 and 134 in 2020) and balloon aortic valvuloplasty (BAV; 7 in 2019 and 8 in 2020).

Post-procedural data

Early morbidity and mortality as well as annual survival probability were taken into consideration. Early or in-hospital outcome analysis during the first 30 days after the procedures irrespective of place (hospital, rehabilitation center or home) was performed.

Data analysis

The normality of continuous variables was checked using the Shapiro–Wilk test. Data that met the criteria of normal distribution were shown as means with standard deviations (SDs). Non-normal data were presented using medians with interquartile ranges (IQRs: Q1–Q3). The Levene's test was used to assess the equality of variances between normally distributed data from 2019 and 2020. Student's t-tests were used to compare unpaired continuous variables. The other variables were compared using a nonparametric Mann–Whitney U test and a χ^2 test with or without Yates's correction. Statistical significance

Table 1. Additional invasive procedures among emergency and elective patients

Procedures	Emergency patients					Elective patients				
	2019	Percentage	2020	Percentage	χ^2 test	2019	Percentage	2020	Percentage	χ^2 test
Total number of urgent SAVR procedures	26	100%	43	100%	–	192	100%	125	100%	–
Graft of the aorta	3	11.54%	9	20.93%	p = 0.503	38	19.79%	14	11.20%	p = 0.044
CABG	7	26.92%	8	18.60%	p = 0.417	33	17.19%	17	13.60%	p = 0.392
MVR with/or TVR	2	7.69%	4	9.30%	p = 0.833	8	4.17%	8	6.40%	p = 0.375
Wrapping of the ascending aorta	2	7.69%	1	2.33%	p = 0.653	14	7.29%	8	6.40%	p = 0.760
SAVR isolated	7	26.92%	15	34.88%	p = 0.492	109	56.77%	72	57.60%	p = 0.884

SAVR – surgical aortic valve replacement; CABG – coronary artery bypass grafting; MVR – mitral valve replacement; TVR – tricuspid valve repair.

Table 2. General characteristics and comorbidities of emergency and elective patients in 2019 and 2020

Factors	Emergency patients			Elective patients		
	2019	2020	p-value	2019	2020	p-value
Number of patients	37	54	–	279	256	–
Age, median (IQR)	69 (27–87)	64 (19–82)	p = 0.074	71 (23–92)	71 (20–92)	p = 0.019
Gender W/M	16/21 43.2%/56.8%	9/45 16.7%/83.3%	p = 0.005	125/154 44.8%/55.2%	118/138 46.0%/54.0%	p = 0.765
BMI, mean ±SD	27.85 ±4.79	27.20 ±4.51	p = 0.545	28.25 ±4.65	28.45 ±4.91	p = 0.889
Time of hospitalization, median (IQR)	16.5 (13–28)	15 (10–22)	p = 0.173	SAVR: 14 (11–16) TAVI: 9 (7–10)	SAVR: 12 (10–14) TAVI: 7 (5–10)	SAVR: p = 0.002 TAVI: p = 0.006
Cardiovascular diseases						
Cardiovascular diseases	2019	2020	p-value	2019	2020	p-value
Heart failure	15	23	p = 0.900	104	143	p < 0.001
Myocardial infarction	0	4	–	1	1	p = 0.951
Post-myocardial infarction	2	8	p = 0.159	12	17	p = 0.232
Coronary artery disease	11	18	p = 0.717	60	86	p = 0.002
Aortic aneurysm	4	11	p = 0.227	42	25	p = 0.065
Hypertension	21	35	p = 0.438	176	190	p = 0.006
Atherosclerosis	3	7	p = 0.467	26	28	p = 0.535
Infective endocarditis	7	14	p = 0.436	6	3	p = 0.379
Hyperlipidemia	8	7	p = 0.274	68	56	p = 0.494
Stroke	0	4	–	2	13	p = 0.002
Post-stroke	1	7	p = 0.090	8	12	p = 0.268
Pacemaker	5	2	p = 0.085	9	14	p = 0.201
Other						
Other diseases	2019	2020	p-value	2019	2020	p-value
Diabetes mellitus	10	19	p = 0.412	59	72	p = 0.061
Chronic kidney disease	8	6	p = 0.172	16	19	p = 0.431
Hypothyroidism	8	1	p = 0.002	17	15	p = 0.909
Anemia	3	2	p = 0.365	6	5	p = 0.872
Thrombosis	0	1	–	1	1	p = 0.951
Pulmonary embolism	0	2	–	1	2	p = 0.513
Pulmonary diseases	1	8	p = 0.057	21	22	p = 0.650
Cancer	1	3	p = 0.094	13	7	p = 0.241
EuroSCORE, median (IQR)	1.66 (0.5–44.48)	3.66 (0.5–20.67)	p = 0.086	1.24 (0.61–14.41)	1.96 (0.5–84.83)	p < 0.001

W/M – women/men; IQR – interquartile range; BMI – body mass index; SD – standard deviation; SAVR – surgical aortic valve replacement; TAVI – transcatheter aortic valve implantation.

was defined as $p < 0.05$. The probability of survival was calculated using the Kaplan–Meier method and the differences between the groups were analyzed using a log-rank test. The analysis was performed with Statistica v. 13.3 (TIBCO Software Inc., Palo Alto, USA).

Results

The number of individuals with severe AVD treated invasively remained virtually unchanged between 2019 (n = 316) and 2020 (n = 310). A significant increase in the number of nonelective cases was observed (from 37 in 2019 to 54 in 2020).

Clinical characteristics and procedural details

Nonelective patients

The only difference in the preprocedural clinical presentation (2019 compared to 2020) was the age of the patients (Table 2). The most visible change in nonelective procedures was a marked increase (by 65%) in SAVR cases (26/43) which corresponded with an increase of roughly 10% overall (Fig. 1). The rate of concomitant procedures in the SAVR subset of patients was comparable between years (2019 compared to 2020). More detailed data are outlined in Table 1.

Elective patients

Similar to nonelective patients, there was a difference (2019 compared to 2020) in the age of elective patients (Table 2). In this group, a significant shift from SAVR being the dominant procedure in 2019 to a slight predominance of TAVI in 2020 occurred (Fig. 1). Moreover, some comorbidities such as CAD, arterial hypertension and history of stroke were significantly more common in 2020 (Table 2).

Post-procedural course and one-year probability of survival

Atrial fibrillation was the only early post-procedural adverse event that was found to be more prevalent in 2019 than in 2020 among AVD individuals admitted electively to our department. In the urgent/emergent group of patients, the rates of all in-hospital complications were comparable between the compared years.

A total of 22 patients died during the early post-procedural period. However, the overall mortality in patients undergoing procedures on the aortic valve was almost twice as high in 2020 (4.5%; 14/310) as compared to 2019 (2.5%; 8/316; p = 0.178). In the elective subgroups, in-hospital mortality was 2.2% (n = 6) in 2019 and 3.5% (n = 9) in 2020, whereas among urgently/emergently treated patients, it was 5.4% (n = 2) in 2019 and 5.6% (n = 5) in 2020.

The survival rate for all patients treated invasively for AS was comparable between 2019 and 2020 groups (p = 0.769). Three-month, 6-month and 1-year survival probabilities for patients in 2019 compared to 2020 were calculated using the Kaplan–Meier method and were found to be 95.2% (295 patients at risk) compared to 93.6% (265 patients at risk), 93.4% (273) compared to 90.5% (255), and 91.3% (266) compared to 88.3% (248), respectively. Statistically significant differences were observed among TAVI- and SAVR-treated patients during the consecutive years. In 2020, the annual survival rate was higher among TAVI patients and lower in SAVR patients compared to the survival rates in 2019 (Fig. 2).

Discussion

One of the most important findings of this study was a significant increase in the number of urgently/emergently admitted AVD individuals accompanied by a marked decline in elective admissions. Our observations were not consistent with previously published studies that indicated a reduction in the number of invasive interventions for cardiovascular diseases, irrespective of priority (elective/nonelective), by roughly 50% in the UK.[4–8] A reason for this discrepancy and the increase in the number of nonelective patients in our observational study was the conversion of a second cardiac surgery center in the area, with a similar volume of cases during previous years, into a facility dedicated to the treatment of COVID-19 patients in 2020.

Among elective patients, a significant decrease in the number of SAVR operations and an increase in TAVI procedures were observed. This tendency has been seen for many years.[11] In 2020, the numbers of SAVR and TAVI procedures were almost equal. The shift to less invasive procedures was associated with a decline in the length of hospitalization[12] and may be linked to reduced exposure to medical personnel.[13,14] For these reasons, the TAVI procedure could prove to be more effective during the pandemic.

In elective patients who received SAVR, men remained the prevalent group. Women underwent slightly more TAVI procedures and this tendency was seen in the following years. Besides the typical risk factors for AVD development such as arterial hypertension, hyperlipidemia and smoking (in many countries more prevalent in middle-aged men), women tended to underreport the manifestations of the disease[15] and/or avoid healthcare staff.[16] Moreover, some patients may have developed or aggravated their conditions because of a diagnosis of COVID-19 seen in their medical histories.[17–20]

No statistical differences in the baseline clinical status of patients were found between the compared years in the urgent/emergent group. However, one cannot exclude that this was probably due to the relatively low number of such patients (37 and 54 cases). In the urgent/emergent patients, 6 of them during 2020 only required the replacement
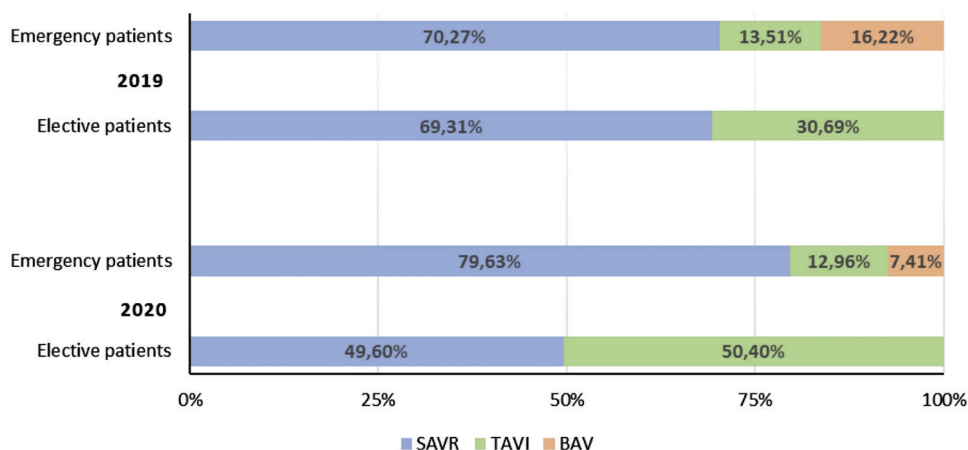

Fig. 1. The structure of procedures among elective and emergency patients in 2019 and 2020

SAVR – surgical aortic valve replacement; TAVI – transcatheter aortic valve implantation; BAV – balloon aortic valvuloplasty.
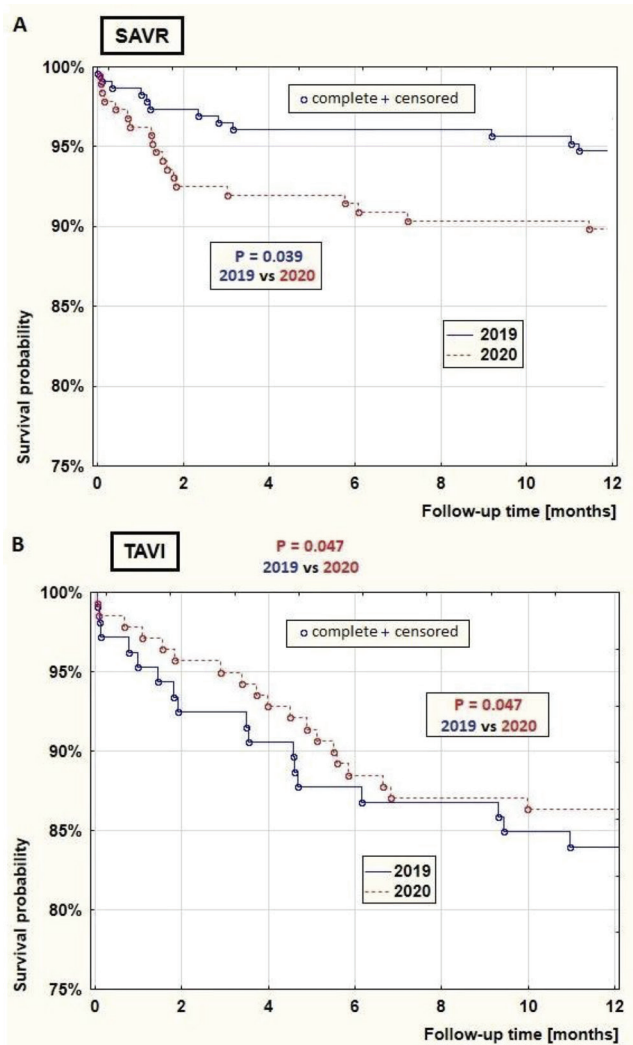
Fig. 2. Annual survival probability in transcatheter aortic valve implantation (TAVI) and surgical aortic valve replacement (SAVR) patients in 2019 and 2020

of a previously implanted aortic valve prosthesis (there were no such cases in 2019). These replacements were mainly due to secondary infective endocarditis and paravalvular leaks.

In our study, some interesting findings regarding the mortality rate were noted, e.g., improved survival after TAVI compared to a worse survival after SAVR procedures. Some research has indicated that the mortality rate of elderly patients after TAVI was similar to that of younger patients.[21] Other publications have shown the survival in elderly patients after TAVI to be similar to the survival in an age-matched general population.[22,23] In our study, we revealed that the experience of our team resulted in a very good survival rate.

Limitations

We are aware of some limitations of our study. First of all, it was a retrospective analysis and the nonelective subgroups were relatively small. Despite the aforementioned facts, some findings were of clinical significance.

Conclusions

Despite the fact that during COVID-19 pandemic more nonelective and high-risk AVD individuals received the interventional treatment, the outcomes were comparable to the pre-pandemic era (2019). Our findings support the value of less invasive therapeutic methods for aortic pathologies during the pandemic.

ORCID IDs

Katarzyna Cierpiszewska ⬤ https://orcid.org/0000-0001-7270-2149
Stanisław Ciechanowicz ⬤ https://orcid.org/0000-0003-0191-1618
Maciej Górecki ⬤ https://orcid.org/0000-0001-6426-1929
Piotr Kupidłowski ⬤ https://orcid.org/0000-0003-1642-6236
Mateusz Puślecki ⬤ https://orcid.org/0000-0003-0015-2808
Bartłomiej Perek ⬤ https://orcid.org/0000-0003-2398-9571

References

1. Rennert-May E, Leal J, Thanh NX, et al. The impact of COVID-19 on hospital admissions and emergency department visits: A population-based study. *PLoS One*. 2021;16(6):e0252441. doi:10.1371/journal.pone.0252441
2. Ojetti V, Covino M, Brigida M, et al. Non-COVID diseases during the pandemic: Where have all other emergencies gone? *Medicina (Kaunas)*. 2020;56(10):512. doi:10.3390/medicina56100512
3. Fersia O, Bryant S, Nicholson R, et al. The impact of the COVID-19 pandemic on cardiology services. *Open Heart*. 2020;7(2):e001359. doi:10.1136/openhrt-2020-001359
4. Ball S, Banerjee A, Berry C, et al. Monitoring indirect impact of COVID-19 pandemic on services for cardiovascular diseases in the UK. *Heart*. 2020;106(24):1890–1897. doi:10.1136/heartjnl-2020-317870
5. Negreira Caamaño M, Piqueras Flores J, Mateo Gómez C. Impact of COVID-19 pandemic in cardiology admissions. *Med Clin (Engl Ed)*. 2020;155(4):179–180. doi:10.1016/j.medcle.2020.05.006
6. Mohamed MO, Banerjee A, Clarke S, et al. Impact of COVID-19 on cardiac procedure activity in England and associated 30-day mortality. *Eur Heart J Qual Care Clin Outcomes*. 2021;7(3):247–256. doi:10.1093/ehjqcco/qcaa079
7. Lackowski P, Piasecki M, Kasprzak M, Kryś J, Niezgoda P, Kubica J. COVID-19 pandemic year in the cardiology department. *Med Res J*. 2021;6(1):40–46. https://journals.viamedica.pl/medical_research_journal/article/view/MRJ.a2021.0009. Accessed April 1, 2022.
8. Sokolski M, Gajewski P, Zymliński R, et al. Impact of coronavirus disease 2019 (COVID-19) outbreak on acute admissions at the emergency and cardiology departments across Europe. *Am J Med*. 2021;134(4):482–489. doi:10.1016/j.amjmed.2020.08.043
9. Juraszek A, Kuriata J, Kołsut P, et al. Literature-based considerations regarding organizing and performing cardiac surgery against the backdrop of the coronavirus pandemic. *J Cardiothorac Surg*. 2021;16(1):73. doi:10.1186/s13019-021-01419-9
10. Kanwar A, Thaden JJ, Nkomo VT. Management of patients with aortic valve stenosis. *Mayo Clin Proc*. 2018;93(4):488–508. doi:10.1016/j.mayocp.2018.01.020
11. Dąbrowski M, Parma R, Huczek Z, et al. The Polish Interventional Cardiology TAVI Survey (PICTS): 10 years of transcatheter aortic valve implantation in Poland. The landscape after the first stage of Valve for Life initiative. *Pol Arch Intern Med*. 2021;131(5):413–420. doi:10.20452/pamw.15887
12. Andra O, Furnică C, Chistol RO, Mitu F, Leon-Constantin MM, Tinică G. Surgical versus transvalvular aortic valve replacement in elderly patients: The impact of frailty. *Diagnostics (Basel)*. 2021;11(10):1861. doi:10.3390/diagnostics11101861
13. Maqbool S, Kumar V, Rastogi V, Seth A. Transcatheter aortic valve implantation under conscious sedation: The first Indian experience. *Indian Heart J*. 2014;66(2):208–210. doi:10.1016/j.ihj.2014.02.004
14. Vendrik J, de Boer J, Zwiers W, et al. Ongoing transcatheter aortic valve implantation (TAVI) practice amidst a global COVID-19 crisis: Nurse-led analgesia for transfemoral TAVI. *Neth Heart J*. 2020;28(7–8):384–386. doi:10.1007/s12471-020-01472-4

15. Nitsche C, Koschutnik M, Kammerlander A, Hengstenberg C, Mascherbauer J. Gender-specific differences in valvular heart disease. *Wien Klin Wochenschr*. 2020;132(3–4):61–68. doi:10.1007/s00508-019-01603-x

16. Lee M, You M. Avoidance of healthcare utilization in South Korea during the coronavirus disease 2019 (COVID-19) pandemic. *Int J Environ Res Public Health*. 2021;18(8):4363. doi:10.3390/ijerph18084363

17. Long B, Brady WJ, Koyfman A, Gottlieb M. Cardiovascular complications in COVID-19. *Am J Emerg Med*. 2020;38(7):1504–1507. doi:10.1016/j.ajem.2020.04.048

18. Babapoor-Farrokhran S, Gill D, Walker J, Rasekhi RT, Bozorgnia B, Amanullah A. Myocardial injury and COVID-19: Possible mechanisms. *Life Sci*. 2020;253:117723. doi:10.1016/j.lfs.2020.117723

19. Nannoni S, de Groot R, Bell S, Markus HS. Stroke in COVID-19: A systematic review and meta-analysis. *Int J Stroke*. 2021;16(2):137–149. doi:10.1177/1747493020972922

20. Chen G, Li X, Gong Z, et al. Hypertension as a sequela in patients of SARS-CoV-2 infection. *PLoS One*. 2021;16(4):e0250815. doi:10.1371/journal.pone.0250815

21. Dąbrowski M, Pyłko A, Chmielak Z, et al. Comparison of transcatheter aortic valve implantation outcomes in patients aged <85 years and ≥85 years: A single-centre study. *Pol Arch Intern Med*. 2021;131(2):145–151. doi:10.20452/pamw.15780

22. Martin GP, Sperrin M, Hulme W, et al. Relative survival after transcatheter aortic valve implantation: How do patients undergoing transcatheter aortic valve implantation fare relative to the general population? *J Am Heart Assoc*. 2017;6(10):e007229. doi:10.1161/JAHA.117.007229

23. Zelis JM, van 't Veer M, Houterman S, Pijls NHJ, Tonino PAL. Survival and quality of life after transcatheter aortic valve implantation relative to the general population. *Int J Cardiol Heart Vasc*. 2020;28:100536. doi:10.1016/j.ijcha.2020.100536

Predicting the chemosensitivity
of pancreatic cancer cells as a personalized therapy

Julia Rudno-Rudzińska[1,A–E], Olga Mitchel[2,B–D], Maciej Płochocki[3,B], Julita Kulbacka[4,A–E]

[1] Department of General and Oncological Surgery, University Hospital in Wrocław, Poland

[2] 2nd Department of Molecular and Cellular Biology, Faculty of Pharmacy with Division of Medical Analytics, Wroclaw Medical University, Poland

[3] Department of Oncology, University Clinical Hospital in Wrocław, Poland

[4] Department of Molecular and Cellular Biology, Faculty of Pharmacy with Division of Medical Analytics, Wroclaw Medical University, Poland

A – research concept and design; B – collection and/or assembly of data; C – data analysis and interpretation;
D – writing the article; E – critical revision of the article; F – final approval of the article

Abstract

Background. Annually, approx. 4000 patients are diagnosed with pancreatic cancer in Poland, and the number of deaths is close to the number of diagnoses. Such a high morbidity/mortality ratio is caused by a high percentage of unresectable lesions (about 80%) and chemoresistance, which, among other things, is due to the specific desmoplastic environment. Currently, there are 2 main systemic treatment regimens for pancreatic cancer: FOLFIRINOX (which is a combination of folic acid, fluorouracil (5-FU), irinotecan, and oxaliplatin) and combined treatment with nab-paclitaxel plus gemcitabine (NPXL+GMC).

Objectives. In order to increase the effectiveness of systemic treatments for individual patients, cell lines derived from resected pancreatic tumors were developed and their chemosensitivity to various agents was examined. The hypothesis was that patients may benefit from individualization of chemotherapy.

Materials and methods. Patients with histopathologically confirmed pancreatic cancer were operated on using irreversible electroporation (IRE) procedure. After isolating and establishing individual cell lines, chemosensitivity to 5-FU, GMC and NPXL was determined using MTT assay in primary and metastatic cell cultures.

Results. Three primary cell lines were isolated for the prediction of chemosensitivity. Gemcitabine was shown to be more effective at lower doses compared to 5-FU, while NPXL was more effective than 5-FU, and both of these were less effective in metastatic cells. Pancreatic cancer cell chemoresistance was confirmed in stage IV.

Conclusions. Determination of chemosensitivity profiles using cell lines may help in the selection of systemic treatments for individual patients. This method can be the basis for a personalized planned chemotherapeutic protocol.

Key words: pancreatic cancer, personalized therapy, chemosensitivity of pancreatic cancer cells

Background

Chemosensitivity of pancreatic cancer cells is a part of the "Personalization of pancreatic cancer treatment" program. The aim of this program is to match the most effective chemotherapy to an individual case to improve outcome for the patients. Patients were operated in the 2nd Department of General and Oncological Surgery of the University Clinical Hospital in Wrocław, Poland.

Objectives

The aim of the study is the personalization of pancreatic cancer treatment. According to treatment guidelines, pancreatic cancer patients receive FOLFIRINOX (a combination of folic acid, fluorouracil (5-FU), irinotecan, and oxaliplatin) or nab-paclitaxel plus gemcitabine (NPXL+GMC), without confirmation of sensitivity. There is a possibility of inadequate chemotherapy. However, matching proper systemic treatment for an individual patient can result in longer overall survival (OS) and progression-free survival (PFS). The question was whether examination of chemosensitivity can influence patient outcome and whether this examination may be mandatory before treatment in future.

Patients were operated on under general and epidural anesthesia. Samples were collected during the operation and delivered immediately to the Department of Molecular and Cellular Biology at the Wroclaw Medical University, Poland, where individual cell lines were isolated.

The patients gave informed consent prior to participation in the study. This study was conducted in accordance with the Declaration of Helsinki and was approved by the Bioethical Committee at Wroclaw Medical University (approval No. KB-330/2018).

Materials and methods

Cell culture

In this study, a primary cell culture technique was used. Fresh tumor samples were acquired from 2 patients during biopsy and the tissue was processed directly after surgery. From the 1st patient, biopsy from a primary pancreatic cancer (PPCC1) was taken, and from the 2nd patient, 2 biopsies were taken: the 1st from the primary tumor (PPCC2) and the 2nd from metastatic tissue (MPCC2). Cells were isolated from tissue samples according to a previously described procedure.[1,2] Briefly, the tissue was gently rinsed with sterile phosphate-buffered saline (PBS; BioShop, Burlington, Canada). Next, samples were minced in Petri dishes (Sigma-Aldrich, St. Louis, USA) using a scalpel and suspended in dedicated culture medium (L-15; Gibco, Life Technologies, Carlsbad, USA). Part of the suspended material was immediately transferred to 25 cm³ culture flasks.

For the first 3 days, the medium was replaced daily and care was taken not to discard any non-attached tissue fragments. Following this, the medium was fully replaced twice a week. The average time to obtain confluence in both the Petri dishes and the culture flasks was 14 days. The cells were cultivated in a modified high-glucose Leibovitz's L-15 medium (Gibco) supplemented with 10% fetal bovine serum (FBS), 1% antibiotics (penicillin and streptomycin), 1.5% sodium bicarbonate (7.5%; Gibco), 1% MEM vitamin solution (Sigma-Aldrich), 0.5% UltraGlutamine™ 1 (Lonza, Basel, Switzerland), 0.1% glucose (45%; Sigma-Aldrich), and 0.7% aprotinin (BioShop). The cells were maintained at 37°C in a humidified 5% CO_2 atmosphere.

MTT assay

Cytotoxicity of the chemotherapeutics was determined using the MTT (3-[4,5-dimethylthiazol-2-yl]-2,5-diphenyltetrazolium bromide; Sigma-Aldrich) assay. This is a colorimetric assay that measures the metabolic rate in viable cells. Cells were seeded at 4×10^3 cells per well in 96-well plates (Greiner, Pleidelsheim, Germany) and left to adhere for 24 h. The cells were then exposed to the chemotherapeutic drugs (GMC, 5-FU, NPXL) for 24 h and 48 h to evaluate short-term and long-term effects on cell viability. The drugs were dissolved in sterile PBS and then with diluted in culture medium at concentrations of 0–1000 µg/mL. Absorbance of the wells was measured using a multi-well scanning spectrophotometer at 570 nm (Glomax; Promega Polska, Pisz, Poland). Absorbance values were expressed as a percentage of treated cells compared to control cells. All experiments were performed in triplicate.

Patient data

Before surgery, a 62-year-old male with diabetes and an ECOG score of 0 received 6 courses of NPXL+GMC. The patient's histopathological results showed a regression of the neoplastic lesions, which was confirmed by a decrease in serum carbohydrate antigen 19-9 (CA 19-9) from 1280.98 U/mL to 18.98 U/mL and radiological regression according to the Response Evaluation Criteria in Solid Tumors (RECIST). This also correlated with the results of the chemosensitivity testing (see below). After the procedure, the patient was treated with 7 courses of FOLFIRINOX according to drug protocols approved in Poland. During chemotherapy, progression of the disease in the retroperitoneal space occurred. Therefore, in line with the results obtained from the chemosensitivity testing, we returned to treatment with NPXL+GMC (8 courses). Unfortunately, this treatment regimen was not eligible for reimbursement because drug programs in Poland do not provide for a return to previous regimens.

Another patient, a 68-year-old female with hypertension and a ECOG score of 1, received 8 cycles of GMC alone and

was qualified for the IRE procedure. Two cell lines were isolated from this patient from the primary and metastatic lesions. In both lines, chemoresistance was viable. Therefore, patient died 2 months after the IRE procedure.

Statistical analyses

As the number of patients was too small to generalize the results of the analysis for the population, our analysis aimed to prove the studied effects. The survival of 3 line cells (PCC1, PCC2 and MPCC2) was analysed for 3 drugs: fluorouracil, gemcitabine and nab-paclitaxel, in addition to exposition time and dose (Fig. 1). Analysis was performed using R-package "nparLD" function (R Foundation for Statistical Computing, Vienna, Austria).[3] This package is a nonparametric rank-based tool for the analysis of variance in repeated measures design, and does not require any assumptions on data distribution.[4] Due to these features it can be used for a small number of replications

(n = 3 in this study). Overall effect was tested with the use of the "nparLD" function, according to a two-way analysis of variance (ANOVA) design. Values of $p \leq 0.05$ were considered statistically significant.

Results

Results indicated higher efficacy of GMC, even at low concentrations, in a cell line derived from a patient diagnosed with pancreatic cancer (PPCC1). This was highlighted by a pronounced effect of time (much lower survival rate after 72 h when compared to 24 h, $p < 0.001$) and a small but marginally statistically significant effect of the dose ($p = 0.041$). The efficacy of the 5-FU in the cell line taken from the 1st patient (PPCC1) increased with both the dose ($p < 0.001$) and time ($p < 0.001$). In the cell line taken from the 2nd patient (PPCC2), cell viability was higher after 48 h for both NPXL and 5-FU. However, there
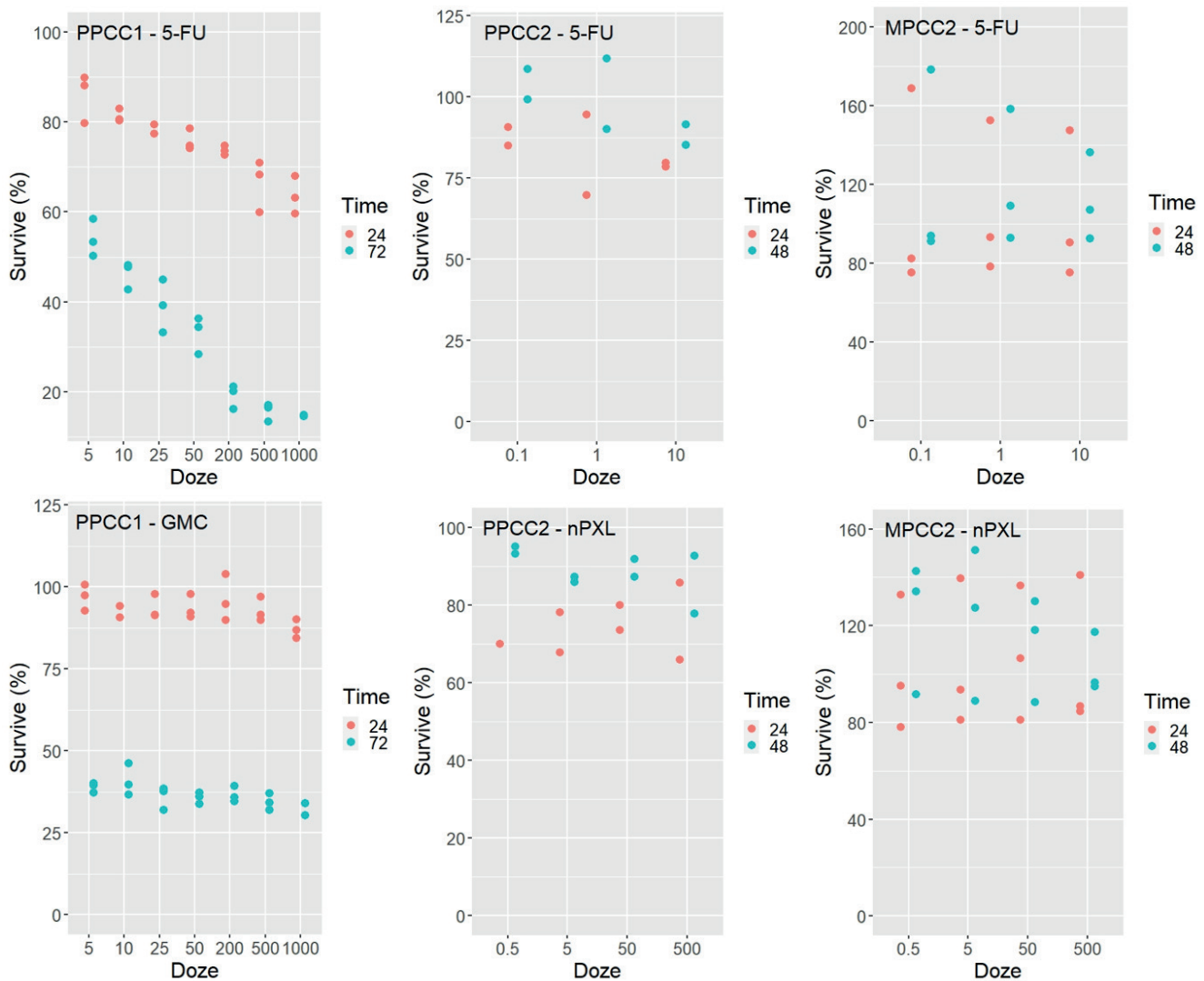

Fig. 1. The effect of the dose and the duration of administering fluorouracil (5-FU), gemcitabine (GMC) and nab-paclitaxel (NPXL) on the survival of cells from the primary pancreatic cancer lesion (biopsy from the 1st patient (PPCC1) and primary tumor biopsy from the 2nd patient (PPCC2)), and from the metastatic lesion (biopsy from the metastatic tissue from the 2nd patient (MPCC2)) after 24 h, 48 h and 72 h

Table 1. The effect of drug dose (dose) and exposition time (time) on cell survival (results of nonparametric analysis of variance (ANOVA))

Drug	Cell origin	Predictor	F	df	p-value
GMC	PPCC1	dose	2.41	4.41	0.0412
		time	448.37	1.00	0.0000
		dose:time	2.25	4.27	0.0564
5-FU	PPCC1	dose	58.62	2.96	0.0000
		time	1404.19	1.00	0.0000
		dose:time	0.38	3.95	0.8185
	PPCC2	dose	0.72	1.15	0.4133
		time	28.17	1.00	0.0000
		dose:time	0.17	1.60	0.7980
	MPCC2	dose	0.08	1.85	0.9092
		time	8.58	1.00	0.0034
		dose:time	0.06	1.77	0.9218
nPXL	PPCC2	dose	0.28	1.36	0.6709
		time	160.19	1.00	0.0000
		dose:time	7.81	1.51	0.0014
	MPCC2	dose	0.05	2.82	0.9812
		time	5.71	1.00	0.0169
		dose:time	0.92	1.66	0.3835

5-FU – fluorouracil; GMC – gemcitabine; NPXL – nab-paclitaxel; PPCC1 – cell line obtained via biopsy from the 1st patient; PPCC2 – cell line obtained via primary tumor biopsy from the 2nd patient; MPCC2 – cell line obtained via biopsy from the metastatic lesion tissue from the 2nd patient.

was no statistically significant effect of the dose (p = 0.671 and p = 0.413, respectively), which was an evidence of chemoresistance (PPCC2).

The same situation occurred in the metastatic cell line (MPCC2). No effect of dose was observed (p = 0.909 and p = 0.981 in 5-FU and nPXL, respectively), though the viability of the cells increased significantly (p = 0.003 and p = 0.017, respectively) after 48 h (Table 1).

Discussion

At present, pancreatic cancer is the 4th most common cause of cancer-related death worldwide, and it is estimated that by 2030, it will be the 2nd most common cause of death after lung cancer.[5] The incidence of pancreatic cancer continues to rise both in Poland and worldwide, and the mortality rate remains at a level almost equal to the incidence rate. Globally, the number of cases in 2018 was 458,918 and the number of deaths was 432,242.[6] The reasons for the high mortality/morbidity ratio are late detection, a lack of sensitive and specific markers for the disease, a lack of novel therapies, and chemoresistance.

The primary treatment modalities for pancreatic cancer are surgical resection and adjuvant chemotherapy. Unfortunately, resection is only possible in 15–20% of cases, and 80% of patients who undergo resection will have a recurrence within a year.[7] Regarding adjuvant treatment, there are 2 treatment regimens available: NPXL+GMC and FOLFIRINOX. Although the differences between OS

and PFS for both regimens are statistically insignificant, NPXL+GMC has been shown to be more effective, with indications of less toxicity.[8–10]

Unfortunately, pancreatic cancer is a chemoresistant disease. This is due to acquired abnormalities in the tumor cell membrane transport protein hENT1,[11] nucleoside enzymes[12,13] and changes in the epithelial–mesenchymal transition.[14,15] One of the key mechanisms of pancreatic cancer chemoresistance is stellate cell activation, which induces a change in tumor bedding to the desmoplastic environment.[16–18] Chemoresistance was confirmed in our study in the 2nd patient with metastatic disease.

Due to the poor prognosis, personalized therapy is being explored for pancreatic cancer patients. Research has been carried out on the benefits of establishing tumor gene profiles[18] and immunotherapy.[19,20] Unfortunately, neither therapy has been shown to be effective to date. Determining the chemosensitivity of tumor cell lines derived from a given patient seems to be a good direction for the personalization of treatment. By comparing the relative effectiveness of 2 lines of treatment with proven efficacies (NPXL+GMC and FOLFIRINOX), we can choose the more effective treatment for an individual patient. The results of one of the patients treated at the University Clinical Hospital indicated a higher chemosensitivity to GMC, which correlated with the clinical course. Clinical and radiographic regression occurred during NPXL+GMC therapy. However, after the conversion into FOLFIRINOX, which was stipulated by the current oncological treatment regimens, tumor progression occurred.

In 2 of the cell lines, we confirmed chemoresistance in metastatic and progressive disease, so the prognosis for the patient was poor. Thus, the determination of chemosensitivity may be important for patient prognosis and requires further studies with a larger number of patients.

Limitations

The main limitation of this study was the low number of examined tissue specimens. Further studies with larger samples and more comprehensive evaluations are necessary. The study was also limited by the determination of chemosensitivity for only a few chemotherapeutics (GMC 5-FU, NPXL). It would be advisable to determine the chemosensitivity for each chemotherapeutic, or for the full NPXL+GMC and FOLFIRINOX regimens, to gather complete data.

Conclusions

Examined cell lines have different biology and different chemosensitivity in every patient, and cancer progression is related to chemoresistance of cancer cells. The determination of chemosensitivity in pancreatic cancer cell lines derived from a given patient may be useful in the selection of a systemic treatment. At present, this is not a standard technique and it is not included in treatment protocols. However, in the future, this procedure may be used as a guideline to select the best systemic treatment for an individual patient and individual stage.

ORCID iDs

Julia Rudno-Rudzińska ● https://orcid.org/0000-0002-4619-7510
Julita Kulbacka ● https://orcid.org/0000-0001-8272-5440
Olga Mitchel ● https://orcid.org/0000-0002-6757-3837
Michał Płochocki ● https://orcid.org/0000-0003-3550-7461

References

1. Saczko J, Dominiak M, Kulbacka J, Chwiłkowska A, Krawczykowska H. A simple and established method of tissue culture of human gingival fibroblasts for gingival augmentation. *Folia Histochem Cytobiol*. 2008;46(1):117–119. doi:10.2478/v10042-008-0017-4
2. Michel O, Kulbacka J, Saczko J, et al. Electroporation with cisplatin against metastatic pancreatic cancer: In vitro study on human primary cell culture. *Biomed Res Int*. 2018;2018:1–12. doi:10.1155/2018/7364539
3. Noguchi K, Gel YR, Brunner E, Konietschke F. nparLD: An R software package for the nonparametric analysis of longitudinal data in factorial experiments. *J Stat Soft*. 2012;50(12):1–23. doi:10.18637/jss.v050.i12
4. Konietschke F, Bathke AC, Hothorn LA, Brunner E. Testing and estimation of purely nonparametric effects in repeated measures designs. *Computational Statistics Data Analysis*. 2010;54(8):1895–1905. doi:10.1016/j.csda.2010.02.019
5. Rahib L, Smith BD, Aizenberg R, Rosenzweig AB, Fleshman JM, Matrisian LM. Projecting cancer incidence and deaths to 2030: The unexpected burden of thyroid, liver, and pancreas cancers in the United States. *Cancer Res*. 2014;74(11):2913–2921. doi:10.1158/0008-5472.CAN-14-0155
6. Siegel RL, Miller KD, Jemal A. Cancer Statistics, 2018. *CA Cancer J Clin*. 2018;68(1):7–30. doi:10.3322/caac.21442
7. Labori KJ, Katz MH, Tzeng CW, et al. Impact of early disease progression and surgical complications on adjuvant chemotherapy completion rates and survival in patients undergoing the surgery first approach for resectable pancreatic ductal adenocarcinoma: A population-based cohort study. *Acta Oncol*. 2016;55(3):265–277. doi:10.3109/0284186X.2015.1068445
8. Pusceddu S, Ghidini M, Torchio M, et al. Comparative effectiveness of gemcitabine plus nab-paclitaxel and FOLFIRINOX in the first-line setting of metastatic pancreatic cancer: A systematic review and meta-analysis. *Cancers (Basel)*. 2019;11(4):484. doi:10.3390/cancers11040484
9. Chen J, Hua Q, Wang H, et al. Meta-analysis and indirect treatment comparison of modified FOLFIRINOX and gemcitabine plus nab-paclitaxel as first-line chemotherapy in advanced pancreatic cancer. *BMC Cancer*. 2021;21(1):853. doi:10.1186/s12885-021-08605-x
10. Muranaka T, Kuwatani M, Komatsu Y, et al. Comparison of efficacy and toxicity of FOLFIRINOX and gemcitabine with nab-paclitaxel in unresectable pancreatic cancer. *J Gastrointest Oncol*. 2017;8(3):566–571. doi:10.21037/jgo.2017.02.02
11. Rauchwerger DR, Firby PS, Hedley DW, Moore MJ. Equilibrative-sensitive nucleoside transporter and its role in gemcitabine sensitivity. *Cancer Res*. 2000;60(21):6075–6079. PMID:11085530.
12. Saiki Y, Yoshino Y, Fujimura H, et al. DCK is frequently inactivated in acquired gemcitabine-resistant human cancer cells. *Biochem Biophys Res Commun*. 2012;421(1):98–104. doi:10.1016/j.bbrc.2012.03.122
13. Han QL, Zhou YH, Lyu Y, Yan H, Dai GH. Effect of ribonucleotide reductase M1 expression on overall survival in patients with pancreatic cancer receiving gemcitabine chemotherapy: A literature-based meta-analysis. *J Clin Pharm Ther*. 2018;43(2):163–169. doi:10.1111/jcpt.12655
14. Du F, Liu H, Lu Y, Zhao X, Fan D. Epithelial-to-mesenchymal transition: Liaison between cancer metastasis and drug resistance. *Crit Rev Oncog*. 2017;22(3–4):275–282. doi:10.1615/CritRevOncog.2018024855
15. Lambies G, Miceli M, Martínez-Guillamon C, et al. TGFβ-activated USP27X deubiquitinase regulates cell migration and chemoresistance via stabilization of Snail1. *Cancer Res*. 2019;79(1):33–46. doi:10.1158/0008-5472.CAN-18-0753
16. Apte MV, Xu Z, Pothula S, Goldstein D, Pirola RC, Wilson JS. Pancreatic cancer: The microenvironment needs attention too! *Pancreatology*. 2015;15(4):S32–S38. doi:10.1016/j.pan.2015.02.013
17. Pothula SP, Xu Z, Goldstein D, Pirola RC, Wilson JS, Apte MV. Key role of pancreatic stellate cells in pancreatic cancer. *Cancer Lett*. 2016;381(1):194–200. doi:10.1016/j.canlet.2015.10.035
18. Zeng S, Pöttler M, Lan B, Grützmann R, Pilarsky C, Yang H. Chemoresistance in pancreatic cancer. *Int J Mol Sci*. 2019;20(18):4504. doi:10.3390/ijms20184504
19. Singhi AD, George B, Greenbowe JR, et al. Real-time targeted genome profile analysis of pancreatic ductal adenocarcinomas identifies genetic alterations that might be targeted with existing drugs or used as biomarkers. *Gastroenterology*. 2019;156(8):2242–2253.e4. doi:10.1053/j.gastro.2019.02.037
20. Miyazawa M, Katsuda M, Kawai M, et al. Advances in immunotherapy for pancreatic ductal adenocarcinoma. *J Hepatobiliary Pancreat Sci*. 2021;28(5):419–430. doi:10.1002/jhbp.944